University of Southampton

An investigation of factors affecting proprioception at the ankle joint complex

Christopher John Monk

Thesis submitted for consideration for Doctor of Philosophy

Department of Medical Physics & Bioengineering

School of Medicine,

Faculty of Medicine, Health & Life Sciences

December 2004

UNIVERSITY OF SOUTHAMPTON

ABSTRACT

FACULTY OF MEDICINE, HEALTH & LIFE SCIENCES

SCHOOL OF MEDICINE

Doctor of Philosophy

AN INVESTIGATION OF FACTORS AFFECTING PROPRIOCEPTION AT THE ANKLE JOINT COMPLEX

by Christopher John Monk

This report details work that has been undertaken in order to complete an investigation of factors that affect proprioception at the ankle joint complex. A thorough literature search revealed that detailed research in the area is notable by its absence; indeed one of the first steps was to adopt and clarify definitions relevant to the scope of this work. After considering the techniques employed in previous work, it was decided that unconstrained joint repositioning would be used to test a subject's proprioception. This was intended to address a fundamental criticism of the majority of the work reviewed regarding the imposition of an unnatural movement pattern, where a subject's foot is constrained to follow rotations about a fixed mechanical axis. In order to measure unconstrained movement, three-dimensional motion analysis techniques were required. Equipment that is capable of measuring the movement of markers in three dimensions is widely commercially available. However, methods of describing movement at the ankle joint vary, and the choice of method will have a direct effect on the interpretation, and clinical significance, of the measurements made. A novel implementation of an existing technique has been developed and is described here. This technique allows the variation of the axis of rotation of the joint to be described throughout the range of motion. Results obtained under different loading conditions are presented for a range of subjects. Although not considered in detail at the outset of the project, the way in which the motion is described is itself a factor that affects the measurement of proprioception. A protocol for the measurement of proprioception, based on the description of patterns of movement of axes, has been developed and is described, and preliminary results obtained using this protocol are presented. Future developments and applications of this work, including applications to investigations of joint pathologies, are discussed.

Contents

1 Introduction **1**

1.1 The Problem 1

1.2 Aims 2

1.3 Focus on three-dimensional motion analysis 4

1.4 Organisation of report 4

2 Background **7**

2.1 Introduction 7

2.2 Proprioception 8

2.2.1 Definition 8

2.2.2 Mechanoreceptors 9

2.2.3 Cutaneous mechanoreceptors 9

2.2.4 Mechanoreceptors in muscle and tendon 10

2.2.5 Capsular mechanoreceptors 17

2.2.6 Central coordination of afferent input 22

2.3 The Ankle Joint Complex 25

2.3.1 The anatomy of the foot and ankle: bones 26

2.3.2 The anatomy of the foot and ankle: ligaments 29

2.3.3 The anatomy of the foot and ankle: muscles 31

2.4 Previous investigations of proprioception 35

2.4.1 Overview 35

2.4.2 Threshold testing 35

2.4.3 Repositioning error 38

2.4.4 Others 43

2.5 The use of three-dimensional motion analysis to assess ankle proprioception 44

2.6 Investigations of joint axes of rotation 45

2.6.1 Overview 45

2.6.2 Previous investigations 46

2.7 Conclusions 48

3 Development of Experimental Protocol **50**

3.1 Introduction 50

3.2 Development of experimental protocol for the assessment of proprioception 51

3.2.1 Overview 51

3.2.2 Proprioceptive assessment technique 51

3.2.3 Isolation of ankle joint proprioception 52

3.2.4 Knee angle 52

3.2.5 Support for the subject 53

3.2.6 Footwear 54

3.2.7 Direction and range of movement 55

3.2.8 Number of attempts 55

3.3 The Protocol Adopted 56

3.4 Experimental protocol for the investigation of axes of rotation of the ankle joint complex 58

3.5 Three-dimensional motion analysis 60

3.5.1 Introduction 60

3.5.2 Embedded Coordinate Systems 60

3.5.3 Transformation Matrices 61

3.5.4 From transformation matrices to rotations and translations . . . 64

3.5.5 Euler and Cardan angles 65

3.5.6 Helical axis approach 65

3.5.7 The Joint Coordinate System 66

3.6 The Polaris System 71

3.6.1 Introduction 71

3.6.2 Polaris Tools and markers 72

3.6.3 Validation 74

3.7 Limitations of conventional 3D motion analysis techniques 79

3.7.1 Investigation of limitations of the helical axis method 79

3.7.2 Constructing and using a digitising pointer 85

3.7.3 Combining the helical axis technique with the JCS 85

3.8 Describing how the axes of rotation vary throughout joint motion . . . 90

3.8.1 Instantaneous Helical Axes 91

3.8.2 Sequential Finite Helical Axes 92
3.8.3 Discussion of technique 92
3.8.4 Application to the ankle joint complex 93
3.8.5 Validation 95
3.9 Conclusions 95

4 Presentation of Results **98**

4.1 Introduction 98
4.1.1 Subject data 99
4.2 Investigation of axes of rotation relative to the intermalleolar line . . . 100
4.2.1 Results 100
4.2.2 Limitations 101
4.3 The Sequential Finite Helical Axis Technique 102
4.3.1 Introduction 102
4.3.2 Subject 1 - unloaded, barefoot measurements 104
4.3.3 Results - validation tool 108
4.4 Comparison of unloaded movements made barefoot and wearing shoes (dorsiflexion movements) 114
4.4.1 Introduction 114
4.4.2 Theta vs time 115
4.4.3 First component of the direction vector, n1 117
4.4.4 Second component of the direction vector, n2 123
4.4.5 Third component of the direction vector, n3 124

4.4.6 y-coordinate of point of intersection 130

4.4.7 z-coordinate of point of intersection 133

4.5 Comparison of unloaded movements made barefoot and wearing shoes (plantarflexion movements) 136

4.5.1 Introduction 136

4.5.2 y-coordinate of point of intersection 137

4.5.3 z-coordinate of point of intersection 137

4.6 Comparison of different loading conditions 141

4.6.1 Introduction 141

4.6.2 Theta vs time 142

4.6.3 First component of the direction vector, n1 149

4.6.4 Second component of the direction vector, n2 149

4.6.5 Third component of the direction vector, n3 150

4.6.6 y-coordinate of point of intersection 156

4.6.7 z-coordinate of point of intersection 164

4.7 Proprioception 168

4.7.1 Overview 168

4.8 Conclusions 174

5 Discussion **175**

5.1 Introduction 175

5.2 The evolution of the project 176

5.3 Definitions 177

5.3.1 Ankle joint complex 177
5.3.2 Proprioception 178
5.4 Protocol for the assessment of proprioception 178
5.5 Choice of 3D motion analysis technique 179
5.6 Limitations of the seqFHA technique 181
5.6.1 Sources of error 182
5.7 Conclusions drawn from axes results 183
5.7.1 Observations 184
5.7.2 Is the variation in the axis important? 186
5.8 Observations on proprioception results 187
5.9 Further work 190
5.9.1 Collection of normative data 190
5.9.2 Investigation of ankle pathologies and neuropathies 191
5.9.3 Calculation and presentation of results 192
5.10 Conclusions 192

List of Tables

2.1 Table of RE results for the right ankle (from Payne et al. (1997), with permission) 42

3.1 Table of mean (SD) of helical axis parameters 81

3.2 Table of means and standard deviations of selected helical axis parameters 81

4.1 Table of summary physical data of the test subjects 100

4.2 Table of average angles in degrees between intermalleolar line and calculated helical axes for all subjects 101

5.1 Table of calculated lengths of intermalleolar line, in mm, for Subject 4 and Subject 5 183

List of Figures

2.1 Cutaneous mechanoreceptors (from Kandel et al. (1991) with permission) . . 10

2.2 Mechanoreceptors in muscle and tendon (from Kandel et al. (1991) with permission) 11

2.3 Muscle spindle (from Kandel et al. (1991) with permission) 12

2.4 Golgi Tendon Organ (GTO) (from Kandel et al. (1991) with permission) . . . 14

2.5 Response of muscle spindles to various stimuli 16

2.6 The use of gamma activation to maintain spindle firing during muscle contraction 18

2.7 Ascending pathway for proprioceptive impulses (from Tortora and Grabowski (1996) with permission) 23

2.8 Shank (from Tortora and Grabowski (1996) with permission) 27

2.9 The bones of the foot (from Donatelli (1996) with permission) 28

2.10 The ligaments in the ankle joint complex (from Donatelli (1996) with permission) 30

2.11 The muscles acting about the ankle joint complex (1)(from Tortora and Grabowski (1996) with permission) 33

2.12 The muscles acting about the ankle joint complex (2) (from Tortora and Grabowski (1996) with permission) 34

3.1 The subject seated on the treatment couch 57

3.2 A Local Coordinate System (O-xyz) rotated and translated relative to a Global Coordinate System (O-XYZ) (From Zatsiorsky (1998) with permission) 61

3.3 Components of unit vector Ox in the GCS O-XYZ 62

3.4 Graphical representation of transformation from one LCS to another (L1 to L2) (From Zatsiorsky (1998) with permission) 63

3.5 ISB proposal for a Joint Coordinate System at the ankle joint complex (from Wu et al. (2002), with permission) 67

3.6 An anatomical reference frame for the shank (from Cappozzo et al. (1995), with permission) 69

3.7 ISB proposal for an anatomical reference frame for the foot and shank (From Wu et al. (2002) with permission) 70

3.8 Polaris in use 73

3.9 A sample ToolViewer screen, illustrating the measurement volume of the Polaris system 75

3.10 The arrangement of the Polaris Global Coordinate System 75

3.11 A Polaris tool with embedded LCS 76

3.12 The shank tool (left) and the foot tool (right) used to measure ankle movements 76

3.13 Graph of measured versus input roll angle with regression line 78

3.14 Graph of measured versus input translation, positive x-axis of tool aligned with direction of movement 78

3.15 The tool used to validate the helical axis approach 80

3.16 Variation in the range of the helical axis direction vector components with angle 83

3.17 Variation in the range of the coordinates of the helical axis intercept with the xy plane with angle 83

3.18 Variation of the error in the components of the direction vector with angle of rotation about the helical axis 84

3.19 Variation of the error in the coordinates of the helical axis intercept with angle of rotation about the helical axis 84

3.20 The pointer used to digitise bony landmarks 86

3.21 The pointer being used to digitise a subject's left lateral malleolus 86

3.22 Movement matching results: Joint rotations described in a JCS based on Helical Axes 90

4.1 Plots of the sequential Finite Helical Axes calculated for Subject 1, for unloaded, barefoot, dorsiflexion movements 104

4.2 Angle vs time: Subject 1, unloaded, barefoot, dorsiflexion movements 106

4.3 n1 values of the seqFHAs: Subject 1, unloaded, barefoot, dorsiflexion movements 106

4.4 n2 values of the seqFHAs: Subject 1, unloaded, barefoot, dorsiflexion movements 107

4.5 n3 values of the seqFHAs: Subject 1, unloaded, barefoot, dorsiflexion movements 107

4.6 y-intercept values of the seqFHAs: Subject 1, unloaded, barefoot, dorsiflexion movements 109

4.7 z-intercept values of the seqFHAs: Subject 1, unloaded, barefoot, dorsiflexion movements 109

4.8 The tool used to validate the helical axis approach 110

4.9 Angle vs time: Validation tool, dorsiflexion movements 111

4.10 n1 values of the seqFHAs: Validation tool, dorsiflexion movements 111

4.11 n2 values of the seqFHAs: Validation tool, dorsiflexion movements 112

4.12 n3 values of the seqFHAs: Validation tool, dorsiflexion movements 112

4.13 y-intercept values of the seqFHAs: Validation tool, dorsiflexion movements . 113

4.14 z-intercept values of the seqFHAs: Validation tool, dorsiflexion movements . . 113

4.15 Angle of rotation about im line (theta) plotted against time for Subject 1. . . 118

4.16 Angle of rotation about im line (theta) plotted against time for Subject 2. . . 118

4.17 Angle of rotation about im line (theta) plotted against time for Subject 3. . . 119

4.18 Angle of rotation about im line (theta) plotted against time for Subject 4. . . 119

4.19 Angle of rotation about im line (theta) plotted against time for Subject 5. . . 120

4.20 First component of direction vector (n1) plotted against angle of rotation about IM line for Subject 1. 120

4.21 First component of direction vector (n1) plotted against angle of rotation about IM line for Subject 2. 121

4.22 First component of direction vector (n1) plotted against angle of rotation about IM line for Subject 3. 121

4.23 First component of direction vector (n1) plotted against angle of rotation about IM line for Subject 4. 122

4.24 First component of direction vector (n1) plotted against angle of rotation about IM line for Subject 5. 122

4.25 Second component of direction vector (n2) plotted against angle of rotation about IM line for Subject 1. 125

4.26 Second component of direction vector (n2) plotted against angle of rotation about IM line for Subject 2. 125

4.27 Second component of direction vector (n2) plotted against angle of rotation about IM line for Subject 3. 126

4.28 Second component of direction vector (n2) plotted against angle of rotation about IM line for Subject 4. 126

4.29 Second component of direction vector (n2) plotted against angle of rotation about IM line for Subject 5. 127

4.30 Third component of direction vector (n3) plotted against angle of rotation about IM line for Subject 1. 127

4.31 Third component of direction vector (n3) plotted against angle of rotation about IM line for Subject 2. 128

4.32 Third component of direction vector (n3) plotted against angle of rotation about IM line for Subject 3. 128

4.33 Third component of direction vector (n3) plotted against angle of rotation about IM line for Subject 4. 129

4.34 Third component of direction vector (n3) plotted against angle of rotation about IM line for Subject 5. 129

4.35 y-coordinate of point of intersection of axis with MM plane plotted against angle of rotation about IM line for Subject 1. 131

4.36 y-coordinate of point of intersection of axis with MM plane plotted against angle of rotation about IM line for Subject 2. 131

4.37 y-coordinate of point of intersection of axis with MM plane plotted against angle of rotation about IM line for Subject 3. 132

4.38 y-coordinate of point of intersection of axis with MM plane plotted against angle of rotation about IM line for Subject 4. 132

4.39 y-coordinate of point of intersection of axis with MM plane plotted against angle of rotation about IM line for Subject 5. 133

4.40 z-coordinate of point of intersection of axis with MM plane plotted against angle of rotation about IM line for Subject 1. 134

4.41 z-coordinate of point of intersection of axis with MM plane plotted against angle of rotation about IM line for Subject 2. 134

4.42 z-coordinate of point of intersection of axis with MM plane plotted against angle of rotation about IM line for Subject 3. 135

4.43 z-coordinate of point of intersection of axis with MM plane plotted against angle of rotation about IM line for Subject 4. 135

4.44 z-coordinate of point of intersection of axis with MM plane plotted against angle of rotation about IM line for Subject 5. 136

4.45 y-coordinate of point of intersection of axis with MM plane plotted against angle of rotation about IM line for Subject 2, plantarflexion movements. . . . 138

4.46 y-coordinate of point of intersection of axis with MM plane plotted against angle of rotation about IM line for Subject 3, plantarflexion movements. . . . 138

4.47 y-coordinate of point of intersection of axis with MM plane plotted against angle of rotation about IM line for Subject 4, plantarflexion movements. . . . 139

4.48 z-coordinate of point of intersection of axis with MM plane plotted against angle of rotation about IM line for Subject 2, plantarflexion movements. . . . 139

4.49 z-coordinate of point of intersection of axis with MM plane plotted against angle of rotation about IM line for Subject 3, plantarflexion movements. . . . 140

4.50 z-coordinate of point of intersection of axis with MM plane plotted against angle of rotation about IM line for Subject 4, plantarflexion movements. . . . 140

4.51 Angle of rotation about IM line (theta) plotted against time for Subject 2 (dorsiflexion movements). 143

4.52 Angle of rotation about IM line (theta) plotted against time for Subject 2 (plantarflexion movements). 143

4.53 Angle of rotation about IM line (theta) plotted against time for Subject 3 (dorsiflexion movements). 144

4.54 Angle of rotation about IM line (theta) plotted against time for Subject 3 (plantarflexion movements). 144

4.55 Angle of rotation about IM line (theta) plotted against time for Subject 6 (dorsiflexion movements). 145

4.56 Angle of rotation about IM line (theta) plotted against time for Subject 6 (plantarflexion movements). 145

4.57 First component of direction vector (n1) plotted against angle of rotation about IM line for Subject 3 (dorsiflexion movements). 146

4.58 First component of direction vector (n1) plotted against angle of rotation about IM line for Subject 3 (plantarflexion movements). 146

4.59 First component of direction vector (n1) plotted against angle of rotation about IM line for Subject 4, Session 2 (dorsiflexion movements). 147

4.60 First component of direction vector (n1) plotted against angle of rotation about IM line for Subject 4, Session 2 (plantarflexion movements). 147

4.61 First component of direction vector (n1) plotted against angle of rotation about IM line for Subject 5, Session 2 (dorsiflexion movements). 148

4.62 First component of direction vector (n1) plotted against angle of rotation about IM line for Subject 5, Session 2 (plantarflexion movements). 148

4.63 Second component of direction vector (n2) plotted against angle of rotation about IM line for Subject 1 (dorsiflexion movements). 151

4.64 Second component of direction vector (n2) plotted against angle of rotation about IM line for Subject 1 (plantarflexion movements). 151

4.65 Second component of direction vector (n2) plotted against angle of rotation about IM line for Subject 2 (dorsiflexion movements). 152

4.66 Second component of direction vector (n2) plotted against angle of rotation about IM line for Subject 2 (plantarflexion movements). 152

4.67 Second component of direction vector (n2) plotted against angle of rotation about IM line for Subject 4, Session 2 (dorsiflexion movements). 153

4.68 Second component of direction vector (n2) plotted against angle of rotation about IM line for Subject 4, Session 2 (plantarflexion movements). 153

4.69 Second component of direction vector (n2) plotted against angle of rotation about IM line for Subject 5, Session 2 (dorsiflexion movements). 154

4.70 Second component of direction vector (n2) plotted against angle of rotation about IM line for Subject 4, Session 1 (plantarflexion movements). 154

4.71 Second component of direction vector (n2) plotted against angle of rotation about IM line for Subject 5 (plantarflexion movements). 155

4.72 Second component of direction vector (n2) plotted against angle of rotation about IM line for Subject 5, Session 2 (plantarflexion movements). 155

4.73 Third component of direction vector (n3) plotted against angle of rotation about IM line for Subject 3 (dorsiflexion results). 157

4.74 Third component of direction vector (n3) plotted against angle of rotation about IM line for Subject 3 (plantarflexion results). 157

4.75 Third component of direction vector (n3) plotted against angle of rotation about IM line for Subject 4, Session 2 (dorsiflexion results). 158

4.76 Third component of direction vector (n3) plotted against angle of rotation about IM line for Subject 4, Session 2 (plantarflexion results). 158

4.77 Third component of direction vector (n3) plotted against angle of rotation about IM line for Subject 5 (dorsiflexion results). 159

4.78 Third component of direction vector (n3) plotted against angle of rotation about IM line for Subject 5, Session 2 (dorsiflexion results). 159

4.79 y-coordinate of point of intersection of axis with MM plane plotted against angle of rotation about IM line for Subject 2 (dorsiflexion movements). 160

4.80 y-coordinate of point of intersection of axis with MM plane plotted against angle of rotation about IM line for Subject 2 (plantarflexion movements). . . 160

4.81 y-coordinate of point of intersection of axis with MM plane plotted against angle of rotation about IM line for Subject 3 (dorsiflexion movements). 161

4.82 y-coordinate of point of intersection of axis with MM plane plotted against angle of rotation about IM line for Subject 3 (plantarflexion movements). . . 161

4.83 y-coordinate of point of intersection of axis with MM plane plotted against angle of rotation about IM line for Subject 5, Session 2 (dorsiflexion movements).162

4.84 y-coordinate of point of intersection of axis with MM plane plotted against angle of rotation about IM line for Subject 5, Session 2 (plantarflexion movements). 162

4.85 y-coordinate of point of intersection of axis with MM plane plotted against angle of rotation about IM line for Subject 4 (plantarflexion movements). . . 163

4.86 y-coordinate of point of intersection of axis with MM plane plotted against angle of rotation about IM line for Subject 4, Session 2 (plantarflexion movements). 163

4.87 y-coordinate of point of intersection of axis with MM plane plotted against angle of rotation about IM line for Subject 5 (dorsiflexion movements). 165

4.88 z-coordinate of point of intersection of axis with MM plane plotted against angle of rotation about IM line for Subject 5 (dorsiflexion movements). 165

4.89 z-coordinate of point of intersection of axis with MM plane plotted against angle of rotation about IM line for Subject 5, Session 2 (dorsiflexion movements).166

4.90 z-coordinate of point of intersection of axis with MM plane plotted against angle of rotation about IM line for Subject 5 (plantarflexion movements). . . 166

4.91 z-coordinate of point of intersection of axis with MM plane plotted against angle of rotation about IM line for Subject 5, Session 2 (plantarflexion movements). 167

4.92 Subject 5 Session 2. Plots of theta vs time for 2 proprioception tests. 170

4.93 Subject 5 Session 2. Plots of theta2 vs time for 2 proprioception tests. 170

4.94 Subject 5 Session 2. Plots of theta3 vs time for 2 proprioception tests. 171

4.95 Subject 5 Session 2. Plots of n1 vs angle of rotation about IM line for 2 proprioception tests. 171

4.96 Subject 5 Session 2. Plots of n2 vs angle of rotation about IM line for 2 proprioception tests. 172

4.97 Subject 5 Session 2. Plots of n3 vs angle of rotation about IM line for 2 proprioception tests. 172

4.98 Subject 5 Session 2. Plots of y intercept vs angle of rotation about IM line for 2 proprioception tests. 173

4.99 Subject 5 Session 2. Plots of z intercept vs angle of rotation about IM line for 2 proprioception tests. 173

5.1 Subject 4, Session 2. Effective moment arms calculated for unloaded, barefoot, dorsiflexion movements 188

5.2 Subject 5, Session 2. Effective moment arms calculated for unloaded, barefoot, dorsiflexion movements 188

DECLARATION OF AUTHORSHIP

I, Christopher John Monk, declare that the thesis entitled

An investigation of factors affecting proprioception at the ankle joint complex

and the work presented in it are my own. I confirm that:

- this work was done wholly or mainly while in candidature for a research degree at this University;
- where any part of this thesis has previously been submitted for a degree or any other qualification at this University or any other institution, this has been clearly stated;
- where I have consulted the published work of others, this is always clearly attributed;
- where I have quoted from the work of others, the source is always given. With the exception of such quotations, this thesis is entirely my own work;
- I have acknowledged all main sources of help;
- where the thesis is based on work done by myself jointly with others, I have made clear exactly what was done by others and what I have contributed myself;
- none of this work has been published before submission.

Signed:..... [redacted] ..... Date: 17/06/05

ACKNOWLEDGEMENTS

This work would not have been possible without the involvement of Dr Hamid Rassoulian, the first supervisor for this work. The author wishes to take this opportunity to thank Dr Rassoulian for his inspiration and tireless nurturing of the project, and his continued support when the author moved to Cambridge before the project was complete. The author also wishes to thank Dr Peter Jackson and Mr Frank Clewlow, who, with Dr Rassoulian, were instrumental in shaping a role in the Department of Medical Physics and Bioengineering at Southampton General Hospital based around a part-time PhD. The support of Dr Chris Callicott and Mrs Karen Goldstone, both of the Department of Medical Physics and Clinical Engineering at Addenbrooke's Hospital in Cambridge, is also gratefully acknowledged; their support minimised the disruption caused by the move. Finally, the author wishes to thank all of the subjects (in particular Miss Angela Darekar who endured the more developmental phases of the data collection) without whose patient co-operation there would have been no data to analyse, Dr Graham Petley for his assistance with data capture and analysis, and the author's sister, Catherine Monk, for her assistance with proof-reading. The progress of the project has been ensured throughout by the support of family and friends that is easily taken for granted but counts for so much.

ABBREVIATIONS USED

AJPS Active Joint Position Sense

ARF Anatomical Reference Frame

AROM Active Range of Movement

BMI Body Mass Index

COM Centre of Mass

ECS Embedded Coordinate System

FHA Finite Helical Axis

GCS Global Coordinate System

GTO Golgi Tendon Organ

HA Helical Axis

IAOR Instantaneous Axis of Rotation

IHA Instantaneous Helical Axis

IM line Intermalleolar line (line connecting the most medial point of the medial malleolus and the most lateral point of the lateral malleolus)

ISB International Society of Biomechanics

JCS Joint Coordinate System

JMPT Joint Movement Perception Threshold

LCS Local Coordinate System

LM Lateral Malleolus

MM Medial Malleolus

MM plane Mid-malleolar plane (plane perpendicular to the intermalleolar line, passing through the midpoint of that line)

n1, n2, n3 x, y and z components of the direction vector of a helical axis, respectively

NDI Northern Digital Incorporated

RE Repositioning Error

RMS Root Mean Squared

ROM Range of Movement

SD Standard Deviation

seqFHA Sequential Finite Helical Axis

TIU Tool Interface Unit

TT Threshold Testing

Chapter 1

Introduction

1.1 The Problem

The original problem that was addressed was the lack of understanding of the clinical significance of ankle proprioception. Specific examples of cases where this might be important are falls in the elderly and recurrent ankle injuries sustained during sporting activities. If ankle proprioception were found to be important, then it might be possible to enhance proprioceptive acuity by controlling one of a number of factors. For example, the way in which factors such as age, ankle support, speed of movement and range of movement affect proprioceptive feedback could be investigated.

The original hypothesis, then, was that for any individual, there exists a set of conditions that will optimise their ankle proprioception. In order to investigate this hypothesis, a robust technique for the assessment of ankle proprioception is required. As discussed in greater detail later, a review of the literature identified a serious lack of consistency in the methods adopted by different investigators. This made a comparison of previous work extremely difficult, and provided no solid foundation on which to

build. Therefore, it was necessary to develop a more complete technique for the assessment of proprioception. The technique developed relied on the comparison of repeated movements; in order to compare physiological movements, three-dimensional motion analysis was required. Although a number of established techniques for the description of three-dimensional movement were identified, a novel approach was investigated.

The Sequential Finite Helical Axis technique that was developed provides information relating to variations in the axis of rotation of a joint (here, the ankle joint complex), throughout the range of movement at that joint. In fact, the development of this novel approach proved to be the major focus for the work described in this thesis. The technique is believed to offer a useful contribution to the field of biomechanics, as it could be used to assess how patterns of variation in the axes of rotation vary with joint laxity, ligament injuries and neuromuscular disorders. It is possible that the description of joint movement that is provided could be used in the diagnosis of pathology and the assessment of progression of pathology, for example during the rehabilitation process. It is of course important to remember the original aim of the work, and this report includes a description of the application of the Sequential Finite Helical Axis technique to the assessment of proprioception.

1.2 Aims

At the outset of the project, five distinct aims were identified in order to achieve the original goal. They were as follows:

Aim 1 - Establish the current state of knowledge This requires an extensive review of the literature to be carried out in order to ascertain details of previous work. The review should include work carried out to investigate proprioception,

but also descriptions of the anatomy and physiology relevant to proprioception at the ankle joint complex. Investigations of proprioception at joints other than the ankle may be helpful in establishing definitions of proprioception, techniques employed, equipment, subjects tested and influencing factors considered. Such a review will also allow the availability of normal data to be established.

Aim 2 - Define what is meant by proprioception In order to proceed with the project, it is essential to define what is meant by ankle proprioception, at least within the scope of this work.

Aim 3 - Establish a test protocol Based on previous protocols employed, and the neurophysiology and biomechanics involved, a test protocol that would allow unconstrained movement should be developed.

Aim 4 - Implement the protocol Having developed the test protocol to be used, it would then be necessary to actually apply it. In order to do this, the following issues would require consideration: how the subject would be supported; what equipment would be used to measure three-dimensional movement; the technique used to describe three-dimensional movement at the ankle joint complex; development of software to acquire and analyse the movement data.

Aim 5 - Use the protocol to assess ankle proprioception In order to use the technique developed to assess ankle proprioception, intra- and inter-rater as well as intra- and inter-subject reliability must be established. Also, the way in which proprioceptive acuity will be quantified from the results obtained must be decided. Investigations of normal subjects and factors such as age and ankle injury could then be carried out.

1.3 Focus on three-dimensional motion analysis

One of the issues identified above under Aim 4, the implementation of the protocol developed, is the selection of a technique for three-dimensional motion analysis. As previously noted in Section 1.1, this area of the project evolved into the development of a novel approach that is of considerable value in its own right. The organisation of the thesis naturally reflects the shift of focus away from the collection of the extensive data that would be required to fully address Aim 5, on to the presentation and discussion of the novel technique.

1.4 Organisation of report

This report is organised into chapters according to the different aspects of the work.

Chapter 2 describes the review of the literature, addressing Aim 1 above. Early in the chapter, definitions of proprioception and of the ankle joint complex adopted for this work are given, so that Aim 2 is also covered. The definition is presented at this stage because any discussion of proprioception is meaningless without it. There is a description of the anatomy and biomechanics of the ankle joint. When considering rotation at the ankle, a knowledge of the axes of rotation and the factors affecting movement of the foot relative to the shank is vital. The neurophysiological structures involved in proprioception are described, and there is a brief discussion of central processing of the afferent information as well as the roles of the different receptors. The chapter continues with a description of previous work on proprioception at the ankle, as well as investigations of other joints including the shoulder, knee, and elbow. The methods and equipment used, and the subjects tested, are described and discussed. Where possible, comparisons are drawn between the results obtained, in order to gain

a clear, overall picture of the established knowledge; this gives valuable pointers for future work. A review of previous investigations of the variation in axes of rotation at a joint is presented, and a general discussion of the background information presented concludes the chapter.

Chapter 3 describes the experimental protocol and its development. The influence of previous work on each aspect of the protocol is discussed in detail; the combination of these influences with consideration of the neurophysiology and biomechanics of the joint are used to justify the approach adopted. A brief description of data collection, both for investigations of proprioception and axes of rotation, is included to illustrate the practical application of the protocol. Considerable attention is devoted to the description and analysis of three-dimensional movement. This includes a general review of the more popular techniques for describing 3D movement, a description of the motion analysis equipment used for this work, and the development of a novel technique specifically suited to an investigation of joint axes of rotation. This Chapter addresses Aims 3 and 4.

The majority of the results presented in **Chapter 4** illustrate the use of the novel motion analysis technique to investigate how the patterns of variation in the axes change with different loading conditions. There are also results from early investigations of the coincidence of the axis of rotation of the ankle joint complex with the intermalleolar line, which formed the basis for the later work. Finally, results from proprioceptive testing are presented, where the motion is analysed using the novel approach developed. The work presented in Chapter 4 goes some way towards addressing Aim 5, although as noted above the volume of subject data is smaller than intended, and extensive assessments of reliability and repeatability have not been possible.

Finally, **Chapter 5** contains a discussion of the work reported in the previous chap-

ters. The value of the approach adopted and the conclusions that can be drawn from the results obtained are considered in detail. There are then suggestions for future developments that would build upon the work presented here in order to increase the body of knowledge relating both to the assessment of proprioception and to axes of rotation of joints.

Chapter 2

Background

2.1 Introduction

This chapter provides background information that is the basis for the work described later in the thesis. To begin with, the definition of proprioception adopted for this project is given, followed by a discussion of the neuroanatomy and neurophysiology of the structures involved in proprioception. Such detail is important when considering how various factors, such as anaesthetic agents or activity, might affect the various mechanoreceptors and therefore proprioception. The majority of assessments of proprioception involve movement of a joint. As joint motion is largely dependent on the anatomy and physiology of the structures involved in the joint, a description of those structures relevant to the ankle joint complex is presented. Having described the structures involved in proprioception, the chapter then moves on with a summary of previous investigations of proprioception. Attention is naturally focused on investigations of proprioception at the ankle joint complex, but assessments of other joints are also considered, where the techniques used and the focus of the investigation are of interest. One of the key observations arising from the review of previous investiga-

tions of the ankle was a tendency to constrain motion, often using a hinged footplate. This allows a simple means of describing the movement, as the angle of rotation of the footplate about its fixed, mechanical axis can be reported. However, as explained in greater detail later, it is believed that natural, unconstrained motion should be allowed when proprioception is assessed. Such complex movement can only be described using three-dimensional motion analysis techniques. Examples of the use of three-dimensional motion analysis for the assessment of proprioception are presented separately, before a review of investigations of joint axes of rotation, both generally and then with specific reference to the ankle joint. The chapter concludes with an overall summary of the literature review.

2.2 Proprioception

2.2.1 Definition

Before considering how to assess proprioception, or what factors may affect it, it is essential to define what is meant by the term proprioception. Various definitions can be found in the literature, but a common agreement is not obvious. The definition that will be used throughout this work is as follows:

Proprioception is the sense of position and movement of parts of the body, based solely on neural input from mechanoreceptors in the joint capsules, ligaments, muscles, tendons and skin.

This borrows from definitions of proprioception given in work by Rowinski (1990), cited in Wilkerson and Nitz (1994), and by Hamer et al. (1992). By combining elements of each, a more complete definition results.

2.2.2 Mechanoreceptors

The term mechanoreceptor is an umbrella descriptor for any physiological transducer that converts mechanical stimuli into neural impulses, so that a proprioceptive mechanoreceptor is any such structure that is involved in proprioception. The precise nature and relative importance of afferent information from the various proprioceptive mechanoreceptors has been the cause of considerable debate for some time, and the situation remains unclear, although the anatomy and physiology of the structures are better established. Proprioceptive mechanoreceptors can be divided into cutaneous, muscular and capsular categories. Cutaneous mechanoreceptors are stimulated when the skin around a joint is stretched as the joint moves. Muscular receptors are stimulated by tension in muscle fibres and tendons, and by any change in length of the muscle fibres. Therefore, afferent impulses from such receptors in the muscles crossing a joint signal position and movement information for that joint. All receptors in the joint capsule, as well as those found in ligaments, are classified as capsular mechanoreceptors. These are stimulated by changes in the loading of the structures in which they lie; such changes will occur as a result of movement, and will depend on whether a joint is loadbearing or not. A discussion of the three categories of mechanoreceptor follows; greater detail is given of the muscular mechanoreceptors because an understanding of their complexity is important when considering how to assess proprioception.

2.2.3 Cutaneous mechanoreceptors

The principal superficial mechanoreceptors in skin are the hair follicle receptor in hairy skin, and the Meissner's corpuscle and Merkel's receptor in glabrous (non-hairy) skin. However, it is primarily the fast-adapting Pacinian corpuscles and slow-adapting Ruffini's corpuscles, both found in the subcutaneous tissue beneath both hairy and

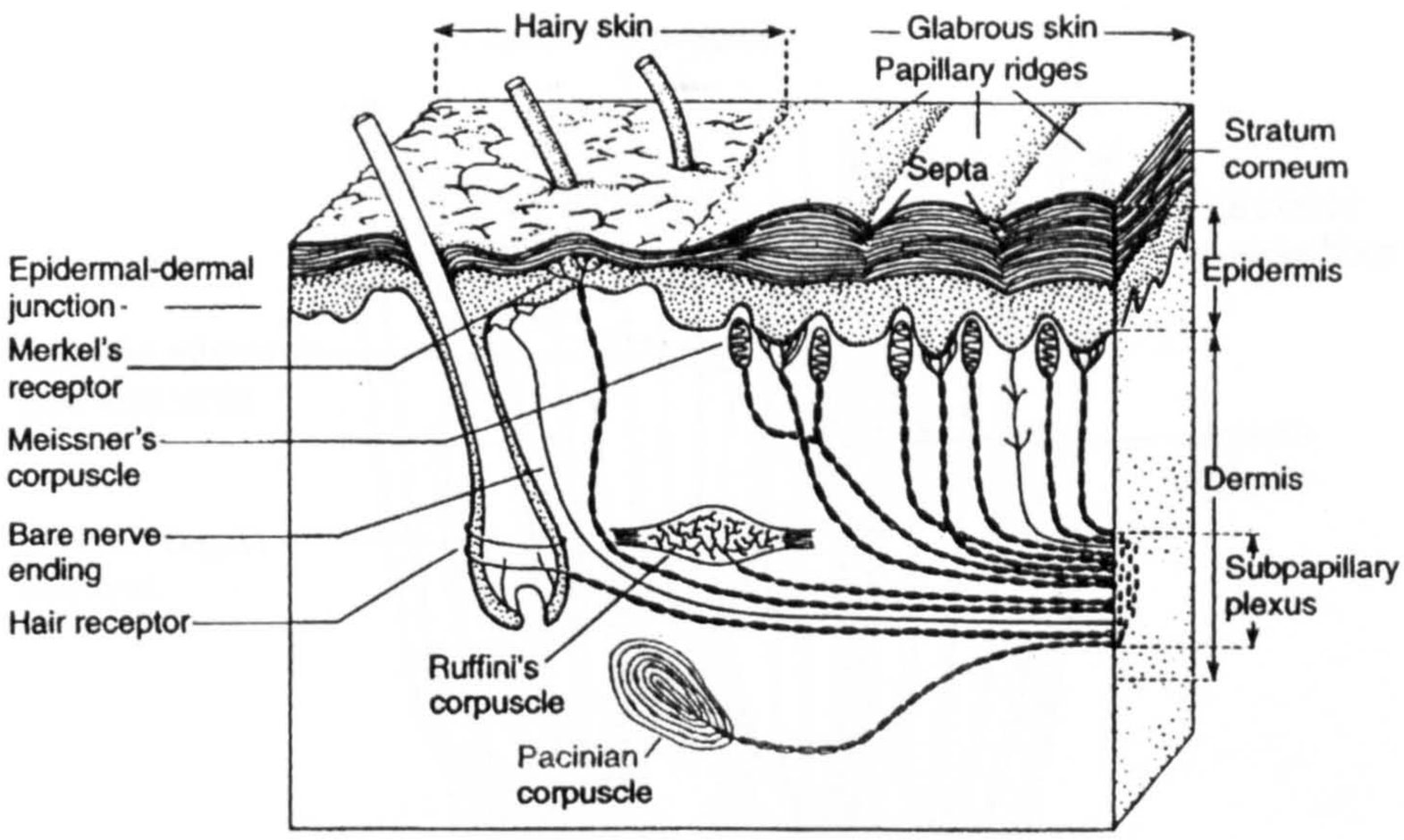

Figure 2.1: Cutaneous mechanoreceptors (from Kandel et al. (1991) with permission)

glabrous skin, which are excited by stretching of the skin. These receptors are illustrated in Figure 2.1.

The location and orientation of the receptors determines their sensitivity to a particular direction of stretch. Therefore, specific receptors will be stimulated by movements which cause the skin to be stretched in a certain way. Although afferent impulses from cutaneous receptors will not arise uniquely from movement at a joint, these impulses may be used to correlate other proprioceptive information to enhance proprioceptive acuity.

2.2.4 Mechanoreceptors in muscle and tendon

As stated above, movement at a joint will be associated with changes in length and tension in muscles, and the associated tendons, crossing the joint concerned. Muscle spindles, the proprioceptive mechanoreceptors in muscle, and Golgi Tendon Organs, the receptors in tendons, signal such changes. The arrangement of mechanoreceptors in muscle and tendon are shown in Figure 2.2.

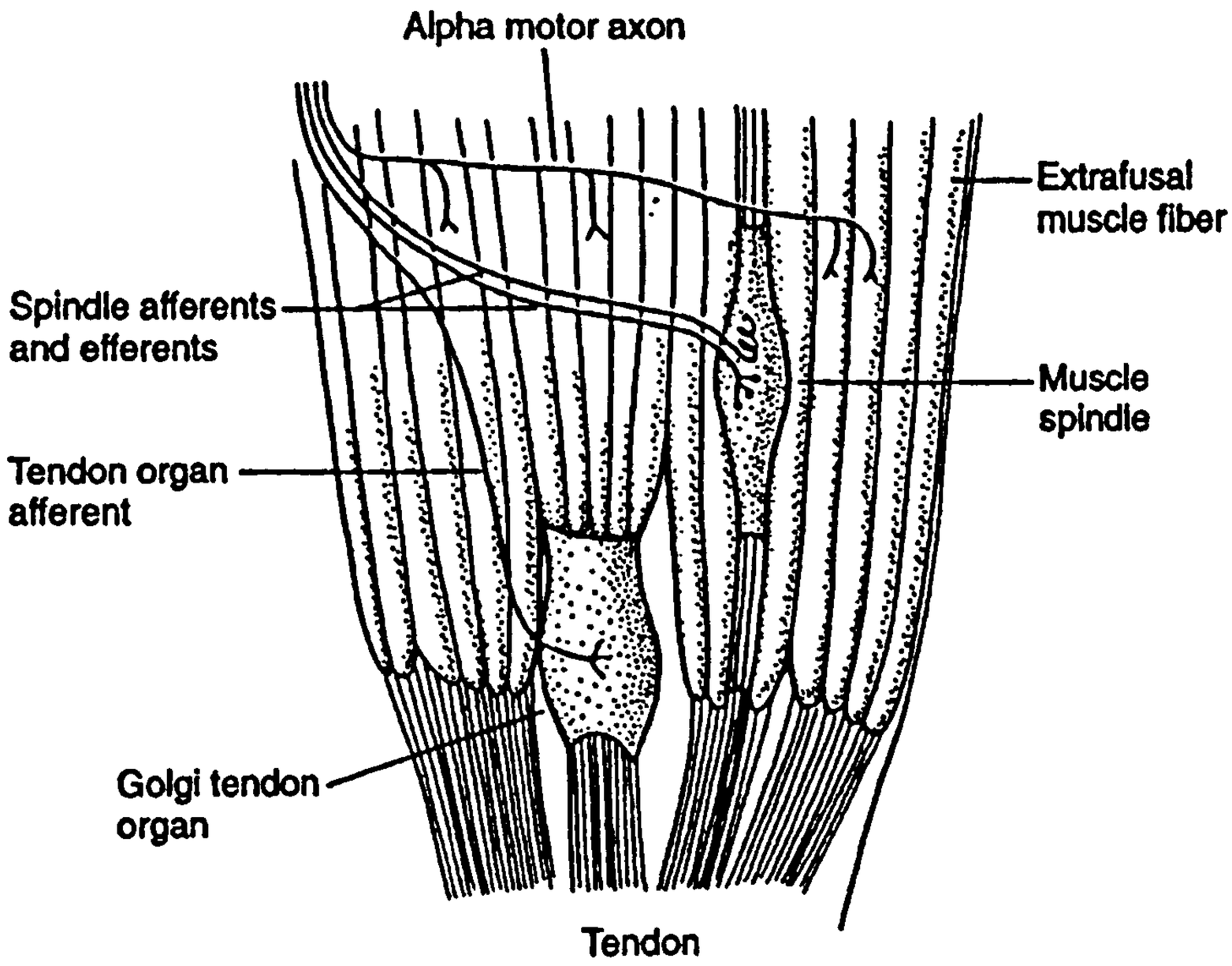

Figure 2.2: Mechanoreceptors in muscle and tendon (from Kandel et al. (1991) with permission)

Muscle spindles are fusiform in appearance, and 4-10 mm long. They consist of three main components: specialised muscle fibres; sensory axons which terminate on those fibres; and motor axons that regulate the sensitivity of the spindle. The centre of the spindle is enclosed by a capsule made of connective tissue that is filled with gelatinous fluid, which facilitates the sliding of the muscle fibres within it. The specialised muscle fibres are referred to as intrafusal fibres, distinguishing them from the larger extrafusal fibres. Intrafusal fibres do not contribute significantly to muscular contractions; the central regions are noncontractile, while the polar regions actively contract. Intrafusal fibres are either nuclear chain or nuclear bag fibres. The former are short and slender, with the nuclei in single file within the fibre. Nuclear bag fibres are thicker, with the nuclei clustered in the central region; they are subdivided into dynamic and static fibres. A typical mammalian muscle spindle contains one dynamic and one static nuclear bag fibre, and approximately five nuclear chain fibres; this can be seen in Figure 2.3.

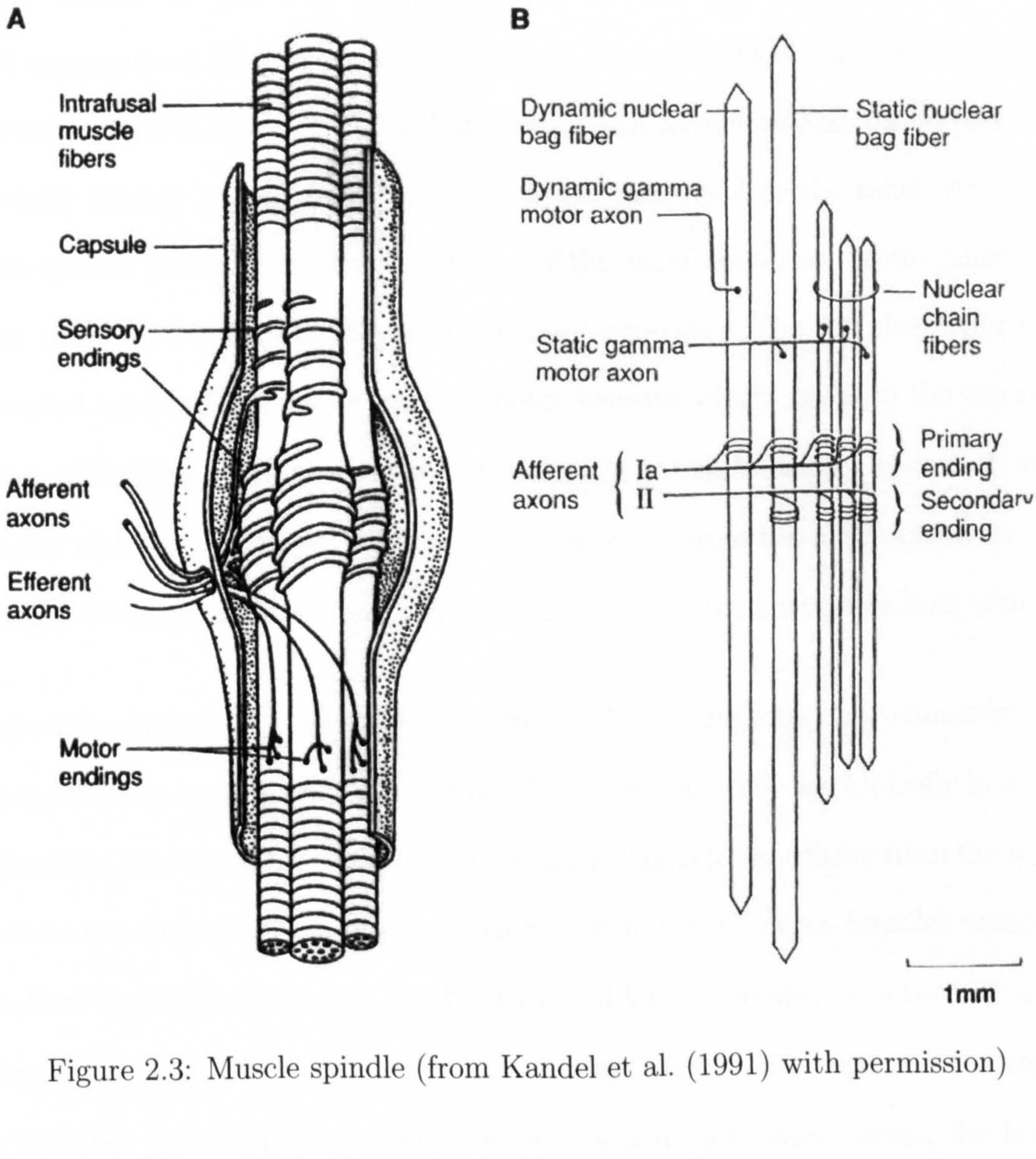

Figure 2.3: Muscle spindle (from Kandel et al. (1991) with permission)

Muscle spindles are innervated by Group Ia (large-diameter myelinated) and Group II (small diameter myelinated) afferents. The myelinated sensory axons enter the spindle capsule in the central region, and terminate on or near the central portions of the intrafusal fibres. Most afferent fibres spiral around individual intrafusal fibres. In each spindle there is a primary sensory ending and a secondary ending. The primary ending contains the terminations of all branches of a single Group Ia afferent axon, which terminate on all three types of intrafusal fibre. The secondary ending contains the terminations of a single Group II afferent, which terminate only on nuclear chain and static nuclear bag fibres. The motor axons that regulate the sensitivity of the muscle spindle terminate on the polar region of the intrafusal fibres. Motor innervation of the intra- and extrafusal fibres is generally separate. The intrafusal fibres are innervated by smaller diameter gamma motor neurons which make up the fusimotor system, while the extrafusal fibres are innervated by the skeletomotor system of larger-diameter alpha motor fibres. Some collateral efferents from the alpha motor neurons innervate intrafusal fibres. These are referred to as skeletofusimotor or beta efferents.

Golgi tendon organs (GTOs) are slender, encapsulated structures approximately 1 mm long and 0.1 mm in diameter, as illustrated in Figure 2.4. They are typically located at the junction between muscle and tendon, where collagen fibres arising from the tendon attach to the ends of groups of extrafusal muscle fibres. Collagen bundles within the capsule of the GTO divide into fine fascicles and form a braided structure. They are innervated by a single Ib axon, that loses its myelination after entering the capsule and branches into many fine endings, each of which intertwines among the braided collagen fascicles.

Muscle spindles and golgi tendon organs convey different and complementary information regarding muscle activity. When a muscle is stretched, spindle afferents increase their discharge rate sharply, whereas the firing rate of GTOs exhibits only a slight,

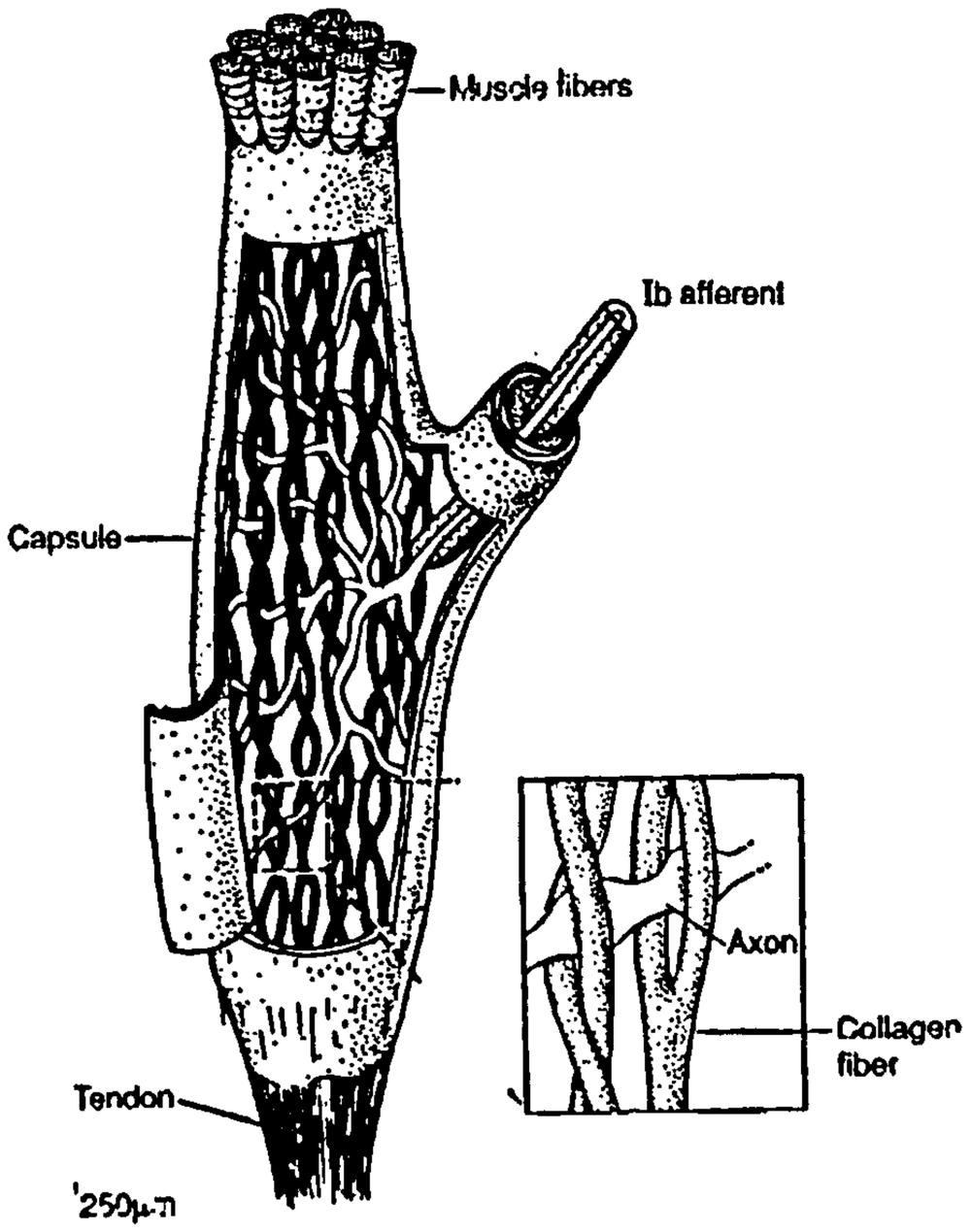

Figure 2.4: Golgi Tendon Organ (GTO) (from Kandel et al. (1991) with permission)

inconsistent increase. However, in a muscle that is contracting as a result of stimulation of the motor nerve, the firing rate of the GTO increases considerably, while that of the spindle decreases or ceases completely (Kandel et al., 1991). The reason for the different behaviour lies partly in the arrangement of the fibres. As mentioned previously, spindles are arranged in parallel with the extrafusal muscle fibres, so stretching the muscle also stretches the muscle spindles, causing the increased firing rate. GTOs are arranged in series with the muscle fibres, and the collagen fibres of the tendon are stiffer than the muscle fibres, so that when a muscle is stretched, the more elastic muscle fibres stretch more than the tendon fibres. A contracting muscle is a different situation. The contracting muscle fibres pull on the collagen fibres, causing the tendon organs to fire. The intrafusal fibres, on the other hand, are shortening, resulting in a decreased spindle firing rate.

Primary and secondary spindle endings respond differently to transient and steady-

state conditions. When a muscle is lengthened, both endings increase their firing rates to a higher rate, and then decrease their firing rate when the muscle is shortened and released from stretch. However, the primary endings fire at a much higher rate during the dynamic than the static phase, whereas the secondary endings only gradually increase their firing rate. This can be seen in Figure 2.5A. The behaviour of the primary endings can be explained by their mechanical characteristics; their central region acts like a spring, extending in response to the stretch, but the polar regions exhibit viscoelastic creep, so that the central region gradually contracts. This behaviour is referred to as intrafusal creep. Primary endings are highly sensitive to the rate of change of muscle length, the firing rate increasing with velocity. This is shown in Figure 2.5B. During rapid shortening, the primary ending shows a pause in its output, and then resumes at a lower rate when the shortening stops. Transient stimulation, such as brief taps or vibration of the muscle elicit bursts of firing from the primary endings, while the secondaries are less affected because the changes are too quick to be reflected in the steady-state output. Primary endings then signal both position and velocity, and as muscle length is related to the angle at a joint, they signal joint angle indirectly. Primary endings are most sensitive to sub-millimetre changes in muscle length; their dynamic sensitivity decreases significantly with large changes in length. Primary endings are also able to reset their responsiveness when they stabilise at a new length.

There are two types of gamma motor neurone that selectively alter the static and dynamic responsiveness of the spindle afferents. Static gamma motor neurones innervate nuclear chain and static bag fibres, and enhance the steady-state discharge of primary and secondary endings. Dynamic gamma motor neurons only innervate dynamic nuclear bag fibres, enhancing their high frequency burst of firing during the dynamic phase. It should be remembered that primary spindle endings terminate on all the

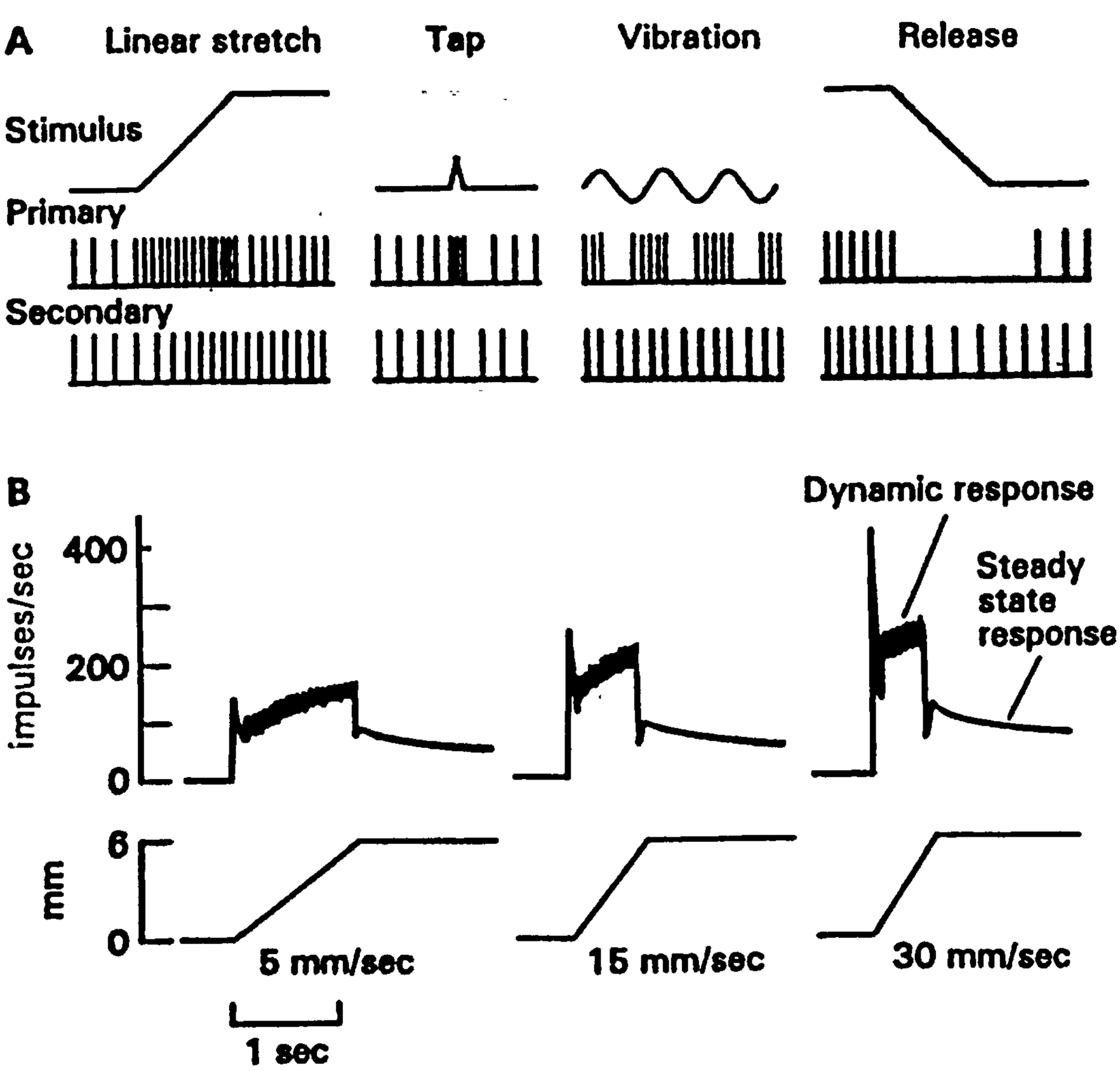

Figure 2.5: A: The responses of primary and secondary endings in muscle spindles to different stimuli. B: Change in response of primary ending with rate of stretch (from Kandel et al. (1991) with permission)

intrafusal fibres within a spindle, whereas the secondary endings terminate only on the nuclear chain fibres and the static bag fibres. Activation of the dynamic bag fibres by the dynamic gamma motor neurons prior to stretch results in stiffening rather than shortening of the polar contractile portions. This increases their viscous resistance to stretch, so that the stretch of the central sensory region is enhanced; in this way they are made more sensitive. The central nervous system controls the sensitivity of the spindles through gamma motor neuron activity. As has already been noted, when a muscle contracts, the spindle fibres are shortened, decreasing their firing rate. However, the contractile regions can be stimulated by the gamma motor neurons so that the fibres will still be stretched, and can fire to relay information about the length of contracting muscles. This is shown in Figure 2.6. The fusimotor output can be adjusted independently of the skeletomotor output, so that the afferent information from the muscle spindles can be optimised for a given task or situation.

In Golgi tendon organs, stretching of the organ results in straightening of the collagen fibres. This compresses and elongates the nerve endings, causing them to fire. As the free nerve endings intertwine among the collagen fibre bundles, even small stretches can deform the nerve endings. The firing rate is very sensitive to changes in tension in the muscle. A twitch contraction of a single motor unit is sufficient to increase the firing rate of a tendon organ afferent (Kandel et al., 1991) .

2.2.5 Capsular mechanoreceptors

In a review article of articular neurology, Wyke (1972) describes the previous use of neurohistological staining techniques (Wyke, 1967) to characterise the dual innervation of synovial joints by primary and accessory articular nerves. The former are independent branches of adjacent peripheral nerves while the latter are branches of

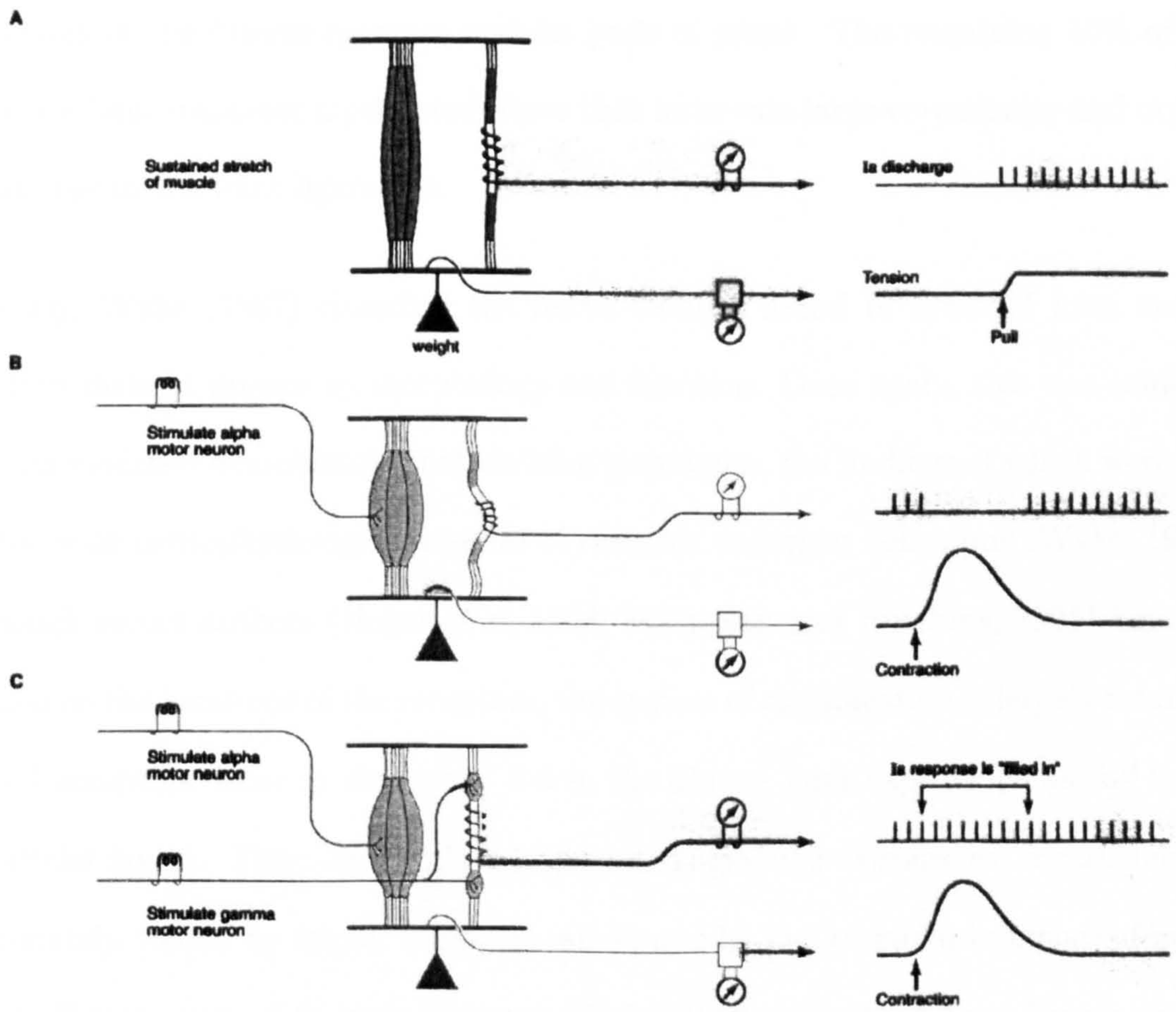

Figure 2.6: The use of gamma activation to maintain spindle firing during muscle contraction. A: The Ia afferent fires steadily in response to sustained tension. B: When the muscle contracts as a result of stimulation of its alpha motor neuron there is a pause in the Ia's firing. C: If a gamma motor neuron is also stimulated, the spindle is not unloaded and there is no pause in discharge (from Kandel et al. (1991) with permission)

related muscle and cutaneous nerves. The articular nerves can be divided into three categories. The majority of the fibres (approximately 45%) have diameters less than 5μm. These include unmyelinated pain afferents and vasomotor efferents, and small myelinated nociceptive afferents. The second group, constituting another 45% of the total, are myelinated mechanoreceptor afferents. These innervate small corpuscular endorgans in the fibrous capsules and fat pads of joints. The remaining 10% of the fibres are large diameter myelinated fibres that innervate large corpuscular end organs found only in the joint ligaments.

Similarly, Wyke (1967) classified the nerve endings found in synovial joint tissues into four distinct groups by morphology and function. Once again, this was achieved through modified neurohistological staining techniques, the findings of which were correlated with neurophysiological studies of receptor endorgan behaviour (Wyke, 1967). Although recent authors (Hogervorst, 1998; Michelson and Hutchins, 1995) have expanded on the locations of the receptors, the system of classification is largely retained. Type I receptors occur in clusters of 3-6 in the fibrous joint capsule, primarily in the superficial layers. They are thinly encapsulated, globular corpuscles, measuring approximately 100μm by 40μm. They are innervated by fine terminal branches of myelinated afferent axons, 6-9μm in diameter. Wyke (1972) notes that Type I receptors are more densely distributed in proximal joints, such as the hip, than in distal joints, such as the ankle. In a given joint, he also describes a higher density of Type I receptors on aspects of a joint that undergo the greatest changes in stress during natural patterns of movement at the joint. Type II receptors are elongated and conical and measure approximately 280μm by 120μm. They have a thick, multi-laminated connective tissue capsule which encloses a single or multi-stranded, unmyelinated nerve terminal that ends in a bulb or a Y-shaped bifurcation near the apex of the corpuscle. Type II receptors are found in varying numbers in the deeper layers of the fibrous capsule of all

joints; contrary to Type I receptors they are more numerous in distal than proximal joints. They are found particularly at the border between the fibrous capsule and sub-synovial fibro-adipose tissue. They often lie alongside, or coil around, articular blood vessels. Clusters containing 2-4 corpuscles are innervated by branches of parent myelinated afferent articular nerve fibres. Similar clusters of Type II receptors are also present on the surfaces of all intra/extra-articular fat pads related to a synovial joint. Type III receptors were found in both extrinsic and intrinsic ligaments. They are the largest of the four receptor types, and are structurally identical to golgi tendon organs (described above). Type III receptors lie in parallel with joint ligaments, usually near bony attachments. They consist of a mass of densely branching nerve filaments derived from large myelinated parent afferent axons up to 17μm in diameter. Type IV receptors are non-corpuscular nerve endings found in the joint tissues. They consist of plexi of small, unmyelinated nerve fibres or free nerve endings, derived from small, thinly-myelinated or small unmyelinated articular nerves. They were described by Wyke (1972) as being prominent in limb joints, distributed throughout the fibrous capsule, adjacent periosteum, articular fat pads and the adventitial sheaths of articular blood vessels. In capsular tissues, free nerve endings were found to be relatively sparse, being confined primarily to extrinsic and intrinsic joint ligaments.

Differences in findings reported in more recent work have concerned primarily the locations of the various receptors. According to Hogervorst (1998), Type I receptors are found not only in the joint capsule, but also in the periosteum, ligaments and tendons, while Type III and Type IV receptors also occur in tendons. Michelson and Hutchins (1995) reports finding primarily Type II and Type III receptors in human ankle ligaments. They used a gold-chloride technique and examined sections every 200μm. This conflicts with Hogervorst (1998) who reports that primarily Ruffini (Type I) receptors and free nerve endings (Type IV receptors) have been found in the

anterior cruciate ligament, with less common reports of Pacini (Type II) receptors. However, the situation is complicated by the fact that traditional gold- and silver-chloride stains are non-specific and stain vascular and other structures containing collagen and elastin (Hogervorst, 1998). Furthermore, Ruffini receptors are described by Hogervorst (1998) as having a variable morphology. Electron microscope images have shown Ruffini receptors of the subsynovial layer of the anterior cruciate ligament to be ovoid in shape, measuring 50 by 500μm. In ligaments with parallel-oriented fibrils, the Ruffini corpuscles resemble Golgi tendon organs, which serves to confuse the situation further.

In terms of function, Wyke (1972) described the Type I receptors as being low-threshold, slowly-adapting mechanoreceptors. He claimed that they respond to the changing mechanical stresses in the tissue in which they lie. Due to stresses created by varying degrees of muscle tone, and the intracapsular pressure being 5-10 mmHg less than atmospheric pressure, some of the lowest threshold Type I receptors are active throughout the joint range of motion, even when the joint is stationary. A resting discharge rate of approximately 20Hz was described. The firing rate changes with any variations in the mechanical stress on the tissue containing the receptors, and clusters of receptors with increasingly high thresholds are recruited with increasing stress. On this basis, Wyke (1972) categorised Type I receptors as static and dynamic mechanoreceptors, capable of signalling static joint position, intra-articular or atmospheric pressure changes and the direction, amplitude and velocity of both active and passive joint movements. Type II receptors were found to behave as low-threshold, rapidly-adapting mechanoreceptors. Inactive in immobile joints, they emit brief (<1 s), high frequency bursts of impulses when sudden changes of stress occur. As they are innervated by large-diameter afferents, the conduction velocity is greater than for Type I afferents. Wyke (1972) regards these as dynamic mechanoreceptors that signal

acceleration at a joint in active or passive movement. Wyke (1972) went on to propose that Type III receptors, which he found only in ligaments, were high-threshold, slowly-adapting mechanoreceptors. Like GTOs, they only become active towards extremes of range of movement, when the tissues containing the receptors are under a high degree of stress. Under such conditions, the receptors fire a stream of impulses that are conducted at high velocity by the large-diameter afferents to the related parts of the central nervous system. If the condition is maintained, the firing rate adapts only very slowly. Type IV endings constitute the pain receptor system of the articular tissues. Under normal conditions, the plexi and free nerve endings are inactive. They are stimulated by extreme mechanical deformation or tension, or direct mechanical or chemical irritation. Agents found in inflammatory exudates produced by damaged or necrosing tissues have been suggested (Wyke, 1972) to be chemical irritants.

2.2.6 Central coordination of afferent input

Nerve impulses for conscious proprioception and most tactile sensations ascend a common pathway to the cortex. First-order neurons, with their cell bodies in the dorsal root ganglia of spinal nerves, extend from the sensory receptors into the spinal cord and on to the ipsilateral portion of the medulla oblongata. In the medulla, the axon terminals synapse with second-order neurons, which decussate to the contralateral medulla and enter the medial leminiscus. This is a projection tract extending from the medulla to the thalamus, where the second-order axons synapse with third-order neurons. These last project their axons onto the somatosensory area of the cortex (Tortora and Grabowski, 1996).

As noted previously, the exact way in which the afferent proprioceptive information is coordinated is not fully understood. Wyke (1972) emphasised the importance of joint

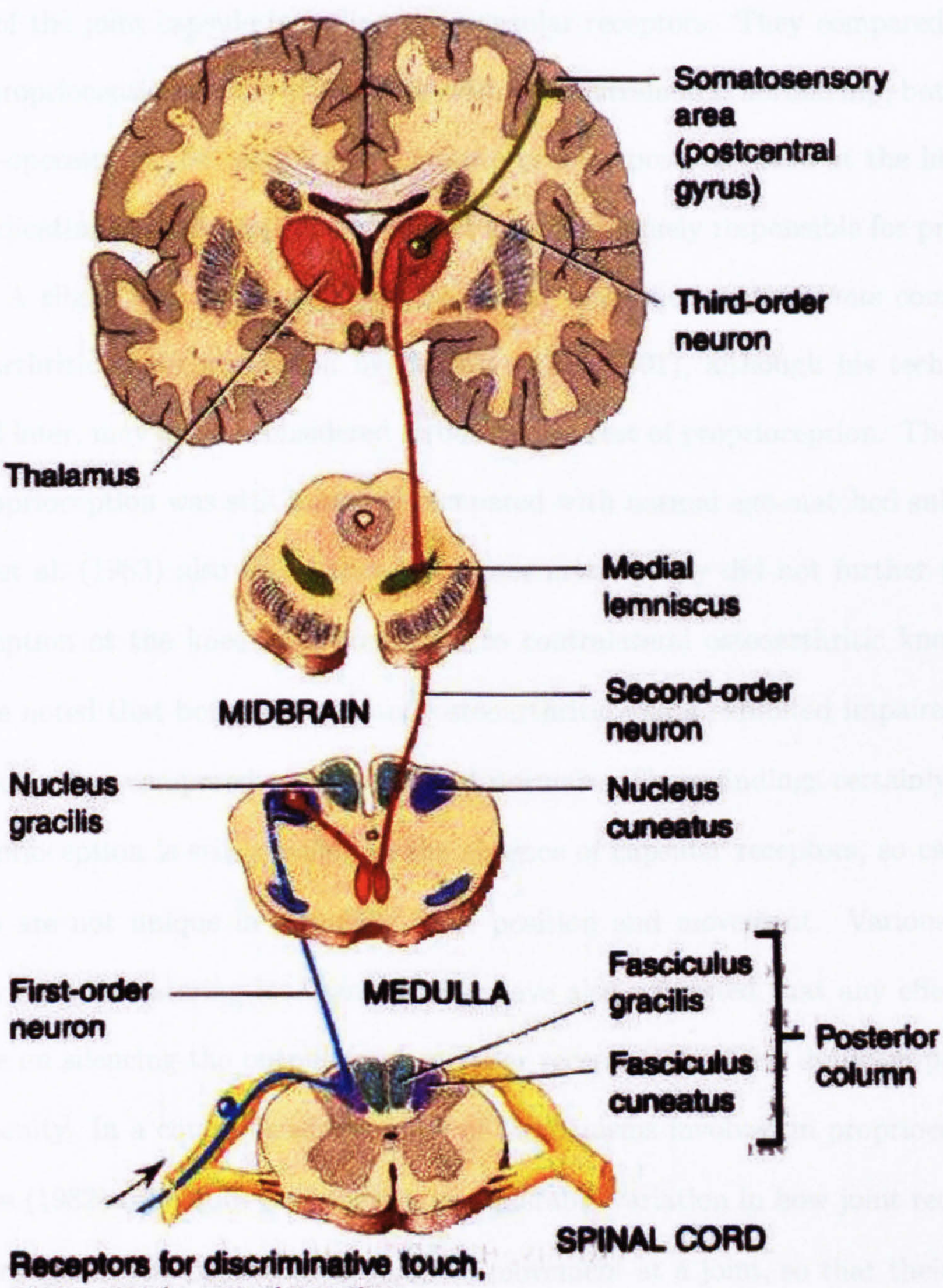

Figure 2.7: Ascending pathway for proprioceptive impulses (from Tortora and Grabowski (1996) with permission)

receptors over that of muscle receptors. However, a number of researchers have found evidence that suggests that the reverse is actually true. Grigg et al. (1973) investigated patients who had undergone unilateral total hip replacement, which involved removal of the joint capsule including any capsular receptors. They compared measures of proprioception for the affected hip with the contralateral normal hip, both pre- and post-operatively. No significant difference in joint position sense at the hip was found, indicating that the capsular receptors are not uniquely responsible for proprioception. A slight improvement of proprioception with knee replacements compared to osteoarthritic knees was found by Barrett et al. (1991), although his technique, described later, may not be considered to be an ideal test of proprioception. The measured proprioception was still impaired compared with normal age-matched subjects. Barrack et al. (1983) also found that total knee arthroplasty did not further impair proprioception at the knee joint compared to contralateral osteoarthritic knees. It should be noted that both replaced and osteoarthritic joints exhibited impaired proprioception when compared to age-matched normals. These findings certainly show that proprioception is still possible in the absence of capsular receptors, so capsular receptors are not unique in signalling joint position and movement. Various studies involving administering local anaesthetic have also suggested that any effect this may have on silencing the output from capsular receptors does not diminish proprioceptive acuity. In a comprehensive review of mechanisms involved in proprioception, Matthews (1982) concludes that there is considerable variation in how joint receptors signal throughout the physiological range of movement at a joint, so that their exact contribution remains difficult to establish.

Various researchers have focused on the role of muscle spindles in proprioception (Goodwin et al., 1972; Matthews, 1982; Burgess et al., 1982). Muscle spindles, as described earlier, can signal both change of length, and therefore joint angle, and rate

of change of length. They can thus contribute to both static and dynamic aspects of proprioception. In order to interpret spindle discharges in terms of muscle length and rate of change of length, the fusimotor activity must also be taken into account (Burgess et al., 1982). Goodwin et al. (1972) produced an illusion of movement by vibrating the tendon of the biceps or triceps at 100 Hz. The movement was in the direction that would occur if the vibrated muscle were being stretched. This was performed under a variety of conditions, including with muscles relaxed and contracting, and the same illusion was found. Goodwin et al. (1972) attributed this to activity in the primary spindle endings, as they have the strongest dynamic response. However, in micro-electrode recordings from human peroneal and tibial nerves, Burke et al. (1976) recorded phase-locked responses from primary and secondary endings and from golgi tendon organs, at frequencies from 20-220 Hz. Matthews (1982) concludes that primary spindle endings in agonist and antagonist muscles are likely to contribute primarily information relating to movement, while the secondaries contribute information relating to position. He suggests that corollary discharges allow distinction between spindle discharges caused by changes in muscle length and those due to fusimotor activity.

2.3 The Ankle Joint Complex

As stated above, the vast majority of techniques for investigating proprioception at any joint involve measuring motion at that joint. Therefore, for this work, considerable attention has been focussed on the characterisation of ankle joint motion, and specifically to the estimation of the axes of rotation of the joint. The pattern of motion at a joint is dependent upon the morphology of the bones that articulate to form the joint, the orientation and mechanical properties of the constraining ligaments,

the lines of action of the muscle forces acting across a joint and the loading of the joint. The anatomical descriptions below are intended to illustrate how these structures inter-relate at the ankle; furthermore, the descriptions indicate how the various mechanoreceptors described in 2.2.2 might contribute to proprioception at the ankle joint complex.

There is a surprising degree of variation in descriptions of the ankle joint in the literature. For the purposes of this work the ankle joint complex is considered to be composed of the articulation between the tibia and the talus, referred to here as the tibio-talar joint, and that between the talus and the calcaneus, referred to as the talo-calcaneal joint. This should ensure clarity and thus avoid confusion. Although not universally adopted, the same or similar definitions have been proposed by van den Bogert et al. (1994) and Demarais et al. (2002), among others. The terms dorsiflexion and plantarflexion will be used to describe rotations about the tibio-talar joint, and inversion and eversion will be used to describe rotations about the talo-calcaneal joint.

2.3.1 The anatomy of the foot and ankle: bones

The medial surface of the distal end of the tibia is described as the medial malleolus; it is this part of the tibia that actually articulates with the talus. Similarly, at the distal end of the fibula is a projection referred to as the lateral malleolus. The tibia and fibula articulate at the fibular notch on the tibia. This arrangement is illustrated in Figure 2.8. The foot can be divided into three sections: the rearfoot, the midfoot and the forefoot. The function and movement of the three sections is inter-related. The rearfoot includes the talus and the calcaneus. The navicular and cuboid bones make up the midfoot; the navicular articulates with the talus while the talus articulates with the calcaneus, as discussed previously. Functionally, the midfoot transmits movement

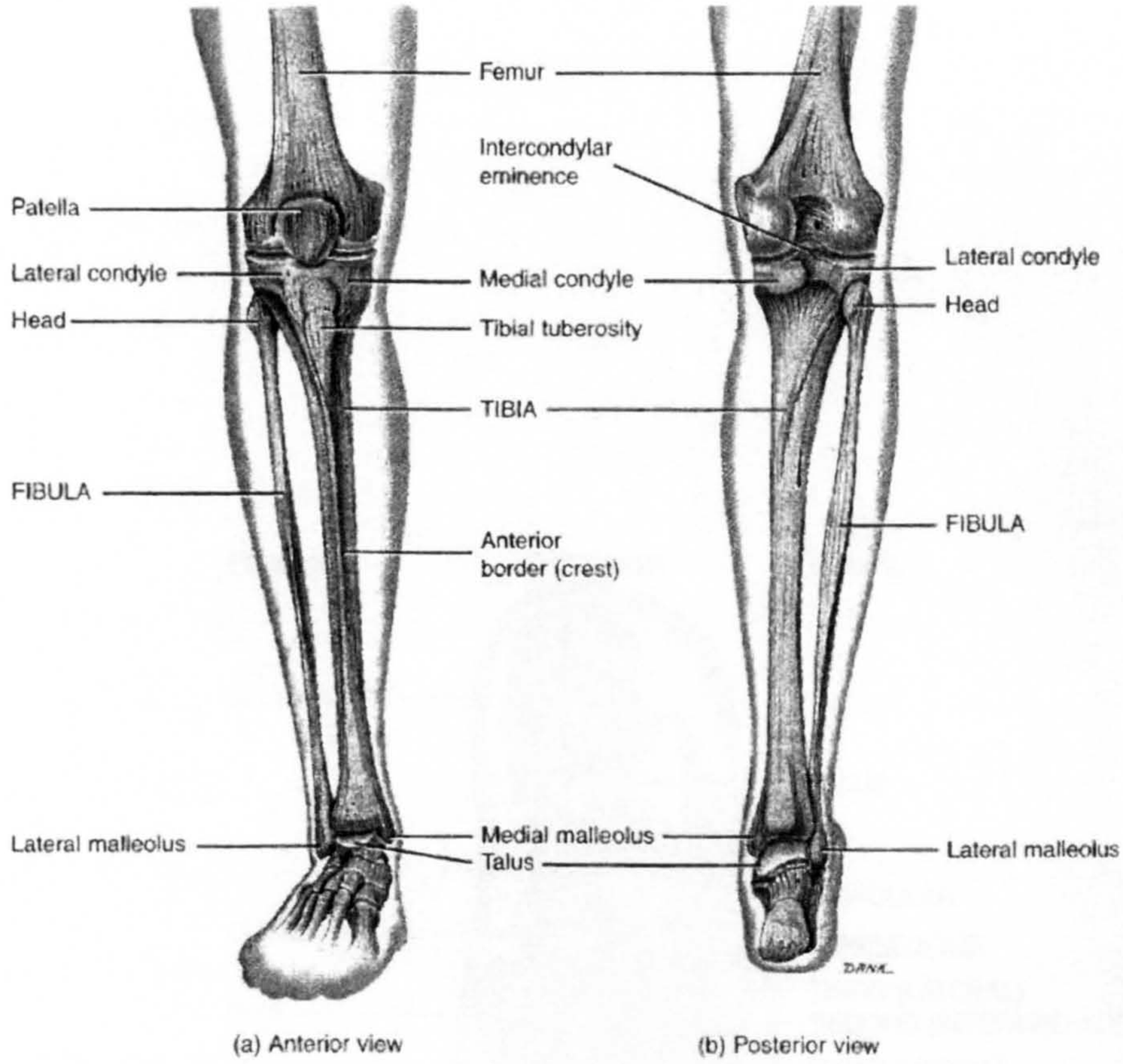

Figure 2.8: Shank (from Tortora and Grabowski (1996) with permission)

from the rearfoot to the forefoot. The cuneiforms, metatarsals and phalanges are collectively referred to as the forefoot. The flexibility afforded by this structure allows adaptation to uneven surfaces. The bones of the foot are illustrated in Figure 2.9.

The superior surface of the talus, the talar trochlea or talar dome, is cone-shaped with a medial apex. It has been suggested that the morphology of the talar dome allows the talus to move into external rotation in dorsiflexion and internal rotation in plantarflexion. Donatelli (1996) reports a normal ankle range of movement of 20^o dorsiflexion and 50^o of plantarflexion. In weight-bearing, inversion and eversion stability is accounted for by the joint articular surfaces.

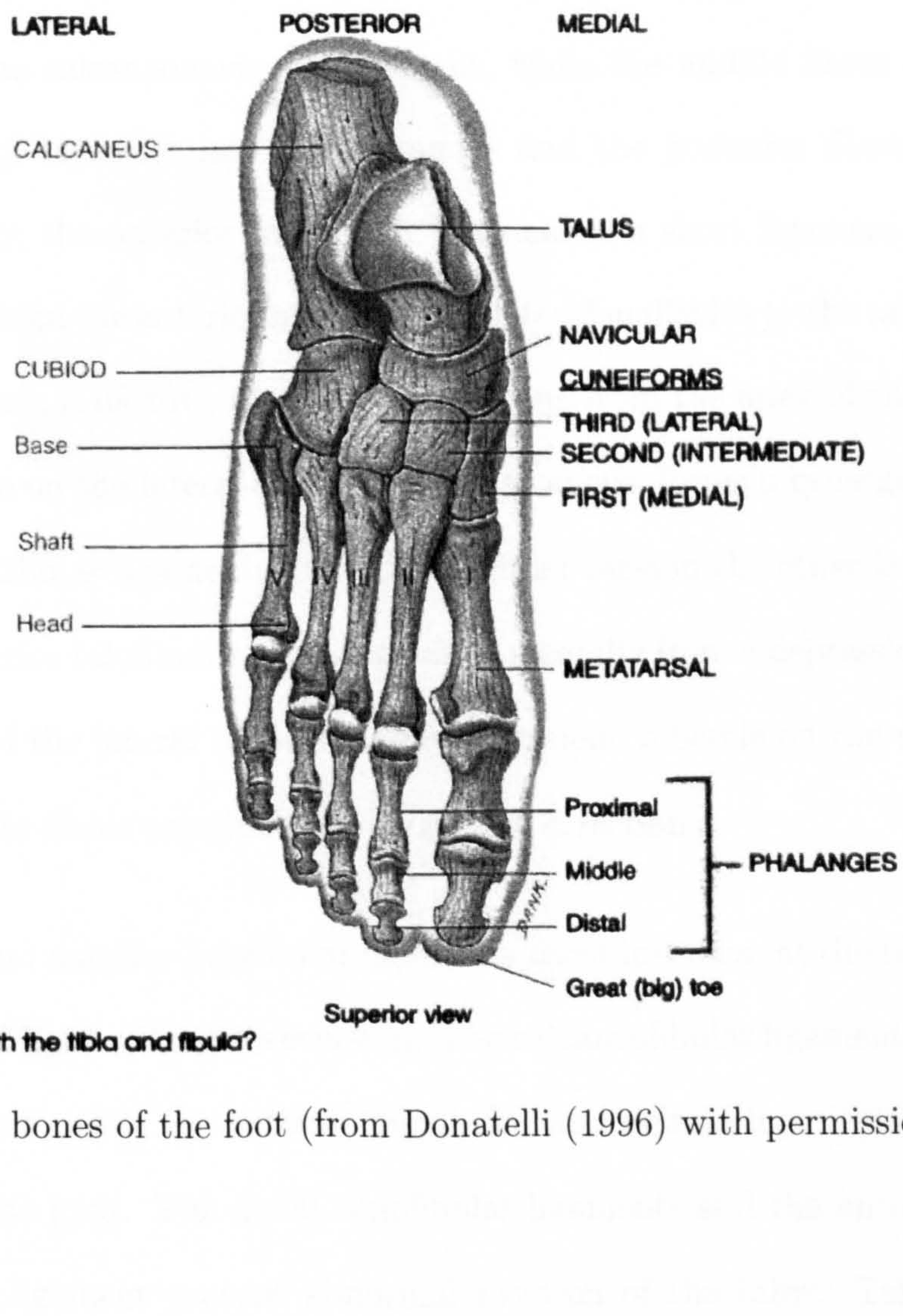

Figure 2.9: The bones of the foot (from Donatelli (1996) with permission)

2.3.2 The anatomy of the foot and ankle: ligaments

The ligaments around the ankle joint play an important role in stabilising the ankle, especially under non-weightbearing conditions. The ligaments are shown in Figure 2.10. The descriptions that follow are based on Gray (1977). Medially, the deltoid ligament is a strong, flat, triangular band. It attaches above to the apex and anterior and posterior borders of the medial malleolus. The most anterior fibres insert into the navicular bone and the calcaneonavicular ligament, while the middle fibres descend almost perpendicularly to insert into the calcaneus and the posterior fibres attach to the talus. Laterally, the anterior talofibular ligament is a short ligament passing forward and medially from the anterior margin of the lateral malleolus to the talus. The calcaneofibular ligament, a narrow, rounded cord passing from the apex of the lateral malleolus to a tubercle on the lateral surface of the calcaneus, forms a synergistic pair with the anterior talofibular ligament; when one is under tension the other is relaxed. The deep-seated posterior talofibular ligament passes medially from a depression at the inner and back part of the lateral malleolus to a prominent tubercle on the posterior surface of the talus. Its fibres are almost horizontal in direction.

The calcaneofibular and anterior talofibular ligaments resist inversion at the tibio-talar joint, while the deltoid ligament resists eversion. The calcaneofibular ligament also stabilises external rotation, while the anterior talofibular and deltoid ligaments stabilise internal rotation at the joint. The distal tibiofibular ligaments and the anterior two-thirds of the deltoid ligament prevent abnormal rotation of the talus. Talar tilt is limited in plantarflexed and neutral positions by the anterior talofibular ligament, and in dorsiflexion by the calcaneofibular and posterior talofibular ligaments.

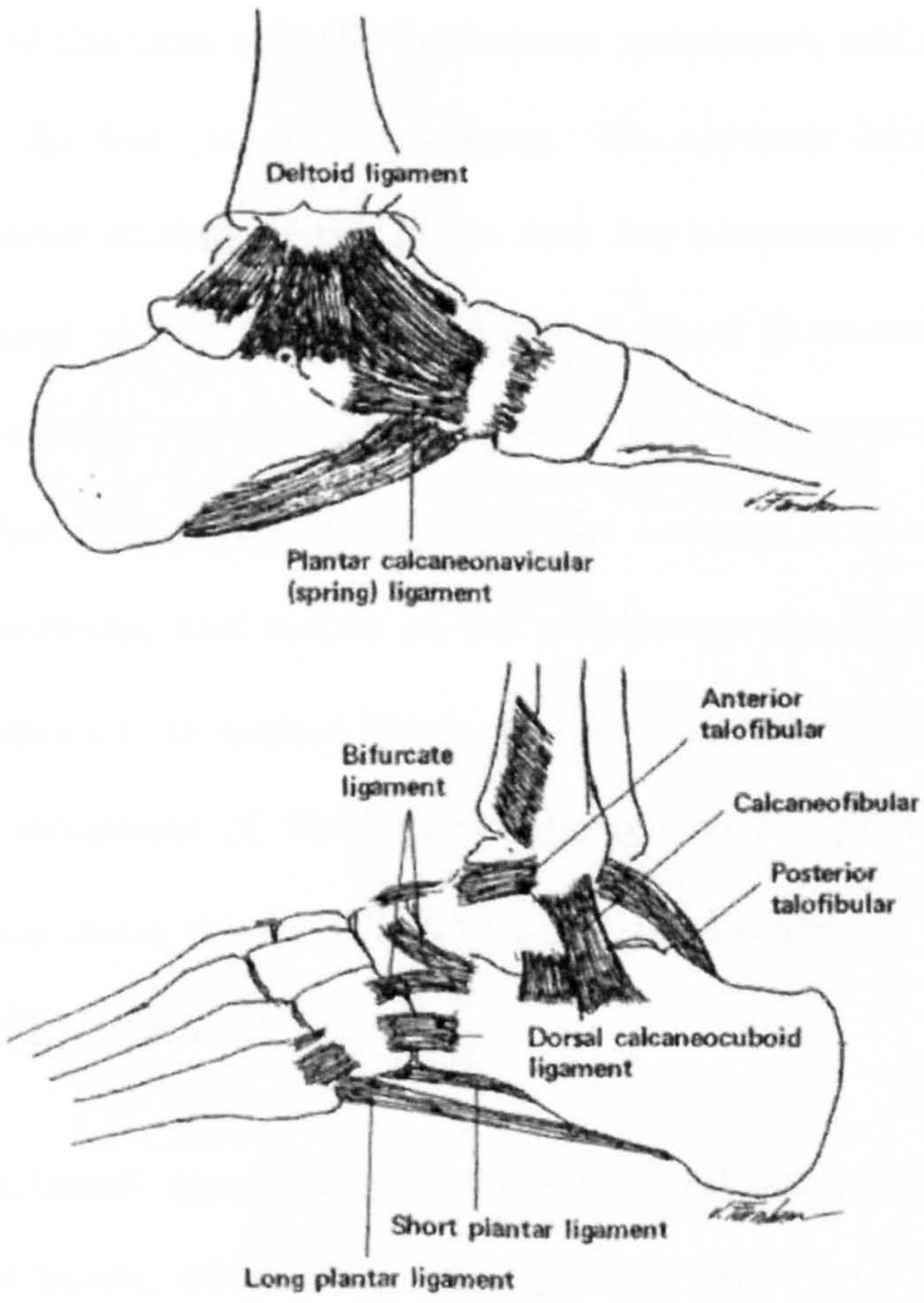

Figure 2.10: The ligaments in the ankle joint complex (from Donatelli (1996) with permission)

2.3.3 The anatomy of the foot and ankle: muscles

The muscles that act about the ankle joint are shown in Figures 2.11 and 2.12. The musculature of the leg is divided into three compartments by deep fascia. The anterior compartment contains muscles that dorsiflex and invert or evert the foot, and are innervated by the deep peroneal nerve. The tibialis anterior originates on the lateral condyle and body of the tibia and the interosseus membrane, and inserts on the first metatarsal and on the first (medial) cuneiform. The extensor hallucis longus has its origins on the anterior surface of the fibula and the interosseus membrane, and its insertion on the distal phalanx of the great toe. Both of these muscles dorsiflex and invert the foot; the latter also extends the great toe. The extensor digitorum longus originates on the lateral condyle of the tibia, the anterior surface of the fibula and the interosseus membrane, and inserts on the middle and distal phalanges of the four outer toes. This allows it to extend the toes in addition to dorsiflexing and everting the foot. Similar movement of the foot is achieved by the peroneus tertius, which has its origin on the distal third of the fibula and the interosseus membrane, and its insertion on the fifth metatarsal.

The lateral compartment, innervated by the superficial peroneal nerve, contains the peronei longus and brevis, which plantarflex and evert the foot. The peroneus longus originates on the head and body of the fibula and inserts on the first metatarsal and the first cuneiform, while brevis has a single origin on the body of the fibula and a single insertion on the fifth metatarsal. Three further plantarflexors, the soleus, gastrocnemius and plantaris, commonly referred to as the calf muscles, make up the superficial posterior compartment. All three insert on the calcaneus via the calcaneal (Achilles) tendon. The gastrocnemius originates on the lateral and medial condyles of the femur and the posterior capsule of the knee; this muscle flexes the knee as well as plantarflexing the ankle. The soleus originates on the head of the fibula and the

medial border of the tibia, while plantaris originates on the femur superior to the lateral condyle. Due to the fact that gastrocnemius and plantaris cross the knee joint as well as the ankle joint, the knee angle will affect the length of these muscles which may in turn influence the afferent proprioceptive signals generated by muscle spindles in the respective muscle fibres. For this reason, it is important to consider the effect of the subject testing arrangement on knee angle when assessing proprioception.The deep posterior compartment, again innervated by the tibial nerve, contains four muscles. The popliteus originates on the lateral femoral condyle and inserts on the proximal tibia, flexing and medially rotating the leg. The flexor hallucis longus originates on the inferior two-thirds of the fibula and inserts on the distal phalanx of the great toe, allowing it to flex the great toe as well as plantarflexing and inverting the foot. The flexor digitorum longus originates on the posterior surface of the tibia and inserts on the distal phalanges of the four outer toes, which it flexes in addition to plantarflexing and inverting the foot. Finally, the tibialis posterior also plantarflexes and inverts the foot, from its origins on the tibia, fibula and interosseus membrane, and insertions on the second, third and fourth metatarsals, the navicular, all three cuneiforms and the cuboid.

The different insertions of the dorsiflexors and plantarflexors are important in terms of considering how moments are applied about the ankle joint, which will influence the resulting movement patterns. Furthermore, the fact that different muscle groups are involved according to the direction of movement leads to possible differences in proprioceptive acuity between plantarflexing and dorsiflexing movements.

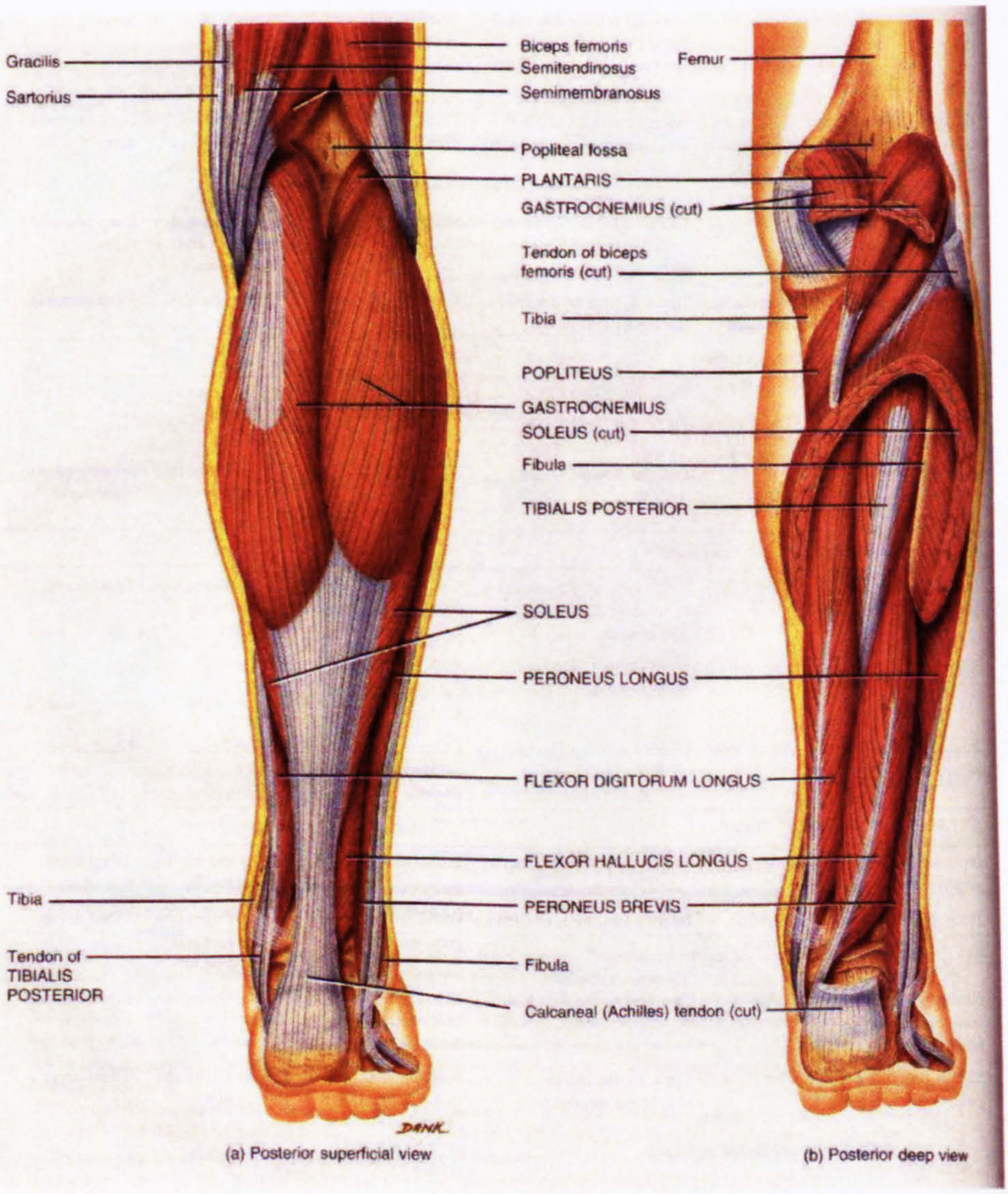

Figure 2.11: The muscles acting about the ankle joint complex (1)(from Tortora and Grabowski (1996) with permission)

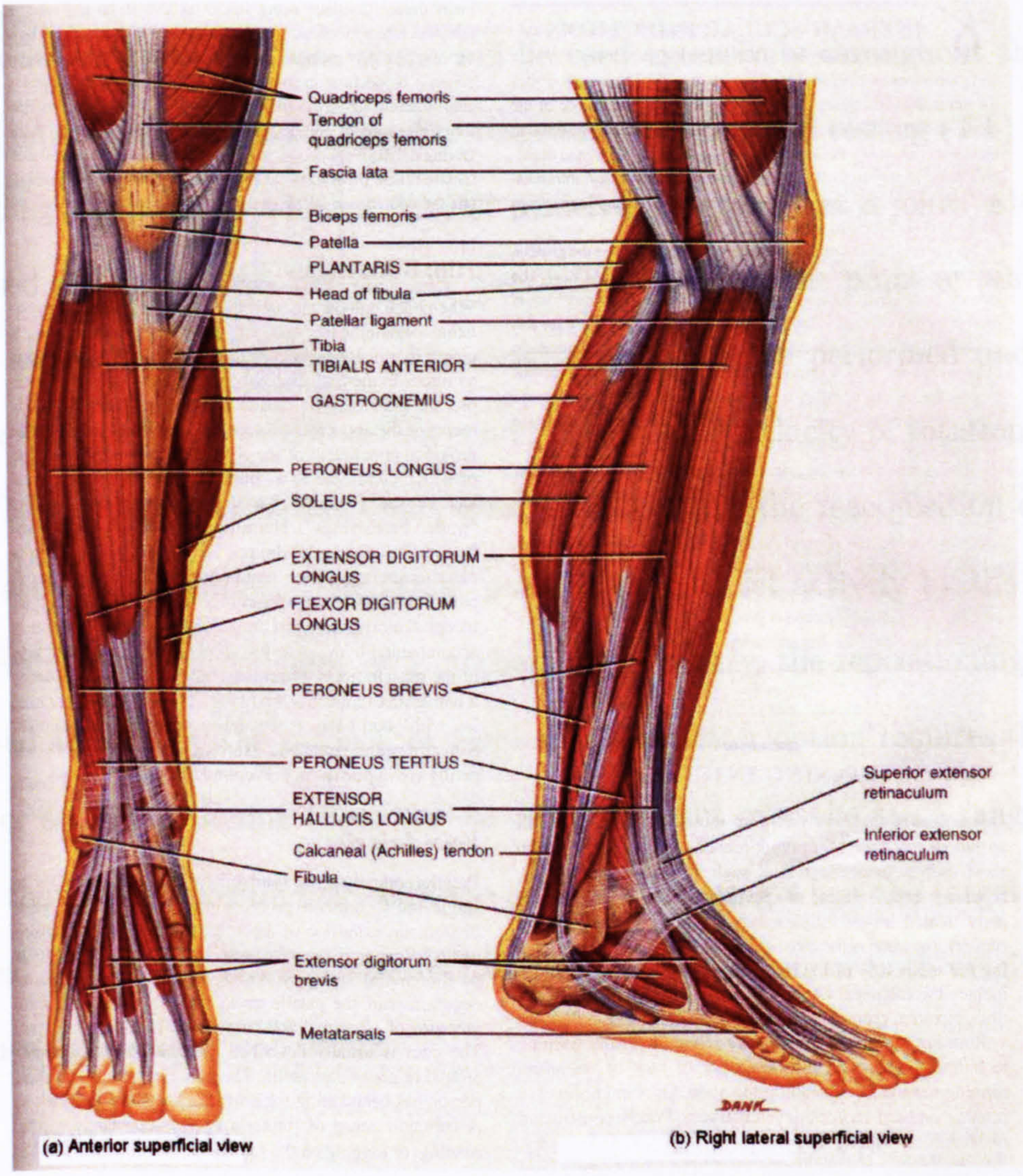

Figure 2.12: The muscles acting about the ankle joint complex (2) (from Tortora and Grabowski (1996) with permission)

2.4 Previous investigations of proprioception

2.4.1 Overview

Two common techniques used in investigations of proprioception are threshold testing and repositioning error. These terms will be used extensively throughout the work, and will be abbreviated to TT and RE, respectively. Threshold testing (TT) involves establishing the point at which a subject perceives movement at a joint. Movement is imposed at a joint, and the subject responds to indicate the point at which they become aware of the movement. Threshold testing may be performed under both weightbearing and non-weightbearing conditions, and the velocity of rotation is often varied. Measurement of repositioning error (RE) involves the reacquisition of a previously set target position. The target position may be set actively by the subject, or passively by the investigator or a mechanism. Similarly, the repositioning may be performed actively by the subject, or passively. This latter option requires the investigator or some positioning apparatus to move the joint over the same range as was used in the original positioning, with the subject indicating when the target position is reached. As for TT, RE assessments have been performed under both weightbearing and non-weightbearing conditions.

2.4.2 Threshold testing

Thelen et al. (1998) investigated twelve young (mean age 22) and twelve elderly (mean age 70) healthy females. The subjects stood on a servo-controlled platform that was used to rotate the dominant foot at three angular velocities (0.1, 0.5 or $2.5^{o}s^{-1}$) to a range of angles (0.05, 0.1, 0.2, 0.4 or 0.8^{o}). The results were presented as success rates of detecting that rotation at the ankle had occurred, and separately as success

rates of detecting the direction of that rotation. Regression was used to estimate the angular threshold to achieve a 75% success rate of detection of direction of rotation for the various speeds. For the young females, the angular thresholds were 0.51, 0.09 and 0.04^o at 0.1, 0.5 and $2.5^o s^{-1}$ respectively in dorsiflexion, compared with 0.36 and 0.11 at 0.5 and $2.5^o s^{-1}$ for the older females; the older subjects did not reach a 75% success rate for any of the angles at the $0.1^o s^{-1}$ velocity. In plantarflexion, the angular thresholds were 0.43, 0.16 and 0.03^o for the younger females, and 0.51 and 0.13^o, again at the higher velocities, for the older females. A similar regression is not presented for the straightforward rotation detection. The results from the tests indicated that performance under TT decreases with increasing age. It was also found that the detection of rotation direction was slightly more reliable in dorsiflexion than in plantarflexion. A similar investigation focussed on inversion and eversion detection thresholds at the ankle in single-leg and two-legged stance (Gilsing et al., 1995). In two-legged stance, it was found that the mean threshold for detecting inversion with a probability of 75% was 0.35^o in the older subjects (mean age 70.3 years) compared with 0.06^o in the younger subjects (mean age 22.6 years). In one-legged stance, inversion thresholds were increased to 0.52^o (older) and 0.35^o (younger); the effect of age was considerably smaller. The cradle was moved at a maximum velocity of $23^o s^{-1}$ in inversion and $19^o s^{-1}$ in eversion. An investigation was carried out into varying the movement velocity from $2^o s^{-1}$ to $200^o s^{-1}$ in a subgroup of 5 subjects. It was found that movements of 0.1-0.2^o were detected with a 20% better reliability, while movements of 0.5^o or over were not affected by velocity. These findings support the decline in proprioceptive acuity with age noted by groups investigating the knee (Skinner et al., 1984; Petrella et al., 1997).

Van den Bosch et al. (1995) found a significant difference in TT results between patients with peripheral neuropathy and normals. The patients were tested in inversion

and eversion. The patients underwent nerve conduction studies to confirm their neuropathy. There were seven patients (five male, two female) with a mean age of 66.7 years. An age and gender matched group of 7 normals was also tested. The neuropathy group had a mean threshold of 1.37^o to detect the presence and direction of an ankle rotation with a 75% rate of success, while mean threshold for the normals was 0.3^o . The difference between the two was highly significant (p=0.0026). Simoneau et al. (1996) investigated dorsiflexion and plantarflexion using TT techniques. In agreement with Van den Bosch et al. (1995), a significant ($p<0.01$) difference between subjects with peripheral neuropathy and those without was found. Vibratory perception threshold, touch-pressure sensation and ankle movement perception were measured in three groups: diabetic patients with neuropathy (DM-NP); diabetic patients without neuropathy (DM-nonNP); and normal subjects (nonDM). There were thirteen men and four women in each group, and the average age within each group was approximately 55 years. Both right and left ankles were tested for dorsiflexion and plantarflexion at two angular velocities (0.25 and $0.75^o s^{-1}$), under weight-bearing conditions. The angular velocities were chosen to reflect those occurring at the ankle during quiet stance. Two protocols were used; in the first, the subject stopped the movement of the platform once they knew which direction the platform was moving in. This was referred to as the Method of Limits. In the second, the investigator controlled the platform, which was moved a fixed distance before the subject was asked to determine whether the movement was dorsiflexion or plantarflexion. This method was described as the Forced Choice Protocol. The average of three correct answers was then used to establish the threshold. No significant difference was found between dorsiflexion and plantarflexion, so the results for each were added. As stated above, the DM-NP group demonstrated an increased threshold compared to the other groups under all conditions. They performed significantly better at the forced choice protocol at $0.75^o s^{-1}$ than under the other three conditions. The nonDM group also performed best at this

test. No significant differences were found between the DM-nonNP and the nonDM groups. Interestingly, the measurements of vibration perception and touch-pressure sensation only partially (less than 50%) accounted for the increased joint movement perception threshold (JMPT), indicating that other mechanisms were being investigated. Simoneau et al. (1997) investigated the effect of applying athletic tape over the skin using TT. Taping was not found to significantly affect joint movement perception thresholds. Twenty normal males (average age 20.3 years, SD 1.5 years) took part in the investigation. An angular velocity of $0.25^{o}s^{-1}$ was used, and the subject controlled the movement of the platform with a stop button. Subjects were tested both under weight-bearing and seated conditions.

2.4.3 Repositioning error

An investigation of the effect of anaesthesia on ankle proprioception was conducted by Konradesen et al. (1993). Anaesthesia was used in an attempt to simulate a loss of proprioceptive input from ligamentous mechanoreceptors following ligament rupture. Seven active men between the ages of 27 and 38 years with normal ankles were the subjects. The median passive repositioning error increased from 1.8 to 5.8^{o} following anaesthesia, which was significant at p=0.02, while the median active positioning error only increased from 1.7 to 1.8^{o} , which was not significant (p=0.40). For testing of active and passive joint repositioning, subjects lay supine with their legs supported on splints and their knees flexed to 20-30^{o} , with the foot padded and strapped to a goniometer footplate, and out of sight. The goniometer pivot was aligned to an inversion/eversion axis, 25^{o} medial to the longitudinal axis of the foot and 40^{o} to the horizontal plane; this was chosen based on Inman (1976). Carbocain was injected into two distal veins of the foot after three minutes of elevation and application of a tourniquet, just above the ankle, inflated to a minimum pressure of 350mmHg. Under

anaesthesia, all subjects were unable to feel tension in the lateral ligaments when the foot was stressed into maximum inversion. For passive testing, the investigator moved the ankle to 5, 10, 15, 20 or 25° of inversion, at random. The movement took 1s and was held for 5s. The ankle was then returned to neutral, before being inverted at $2^{o}s^{-1}$, until the subject verbally indicated that the target position had been reached. For active testing, the subject was instructed to move his foot at $15^{o}s^{-1}$. It was then held at one of the five test positions by the investigator before the subject moved his foot back to neutral and then attempted to reproduce the position.

Moving on to the effects of cooling, Hopper et al. (1997) used a pedal goniometer to investigate RE at the ankle before and after 15 minutes of ice immersion. Although the difference in RE was statistically significant, due to the magnitude ($<0.5^{o}$) the results were not considered clinically significant. Active repositioning was employed on 49 normals between the ages of 17 and 28 years. The ankle joint was immersed in ice to a level 5cm above the medial malleolus and the skin temperature was measured with a thermocouple device. The subjects were blindfolded, and the operator moved the foot to the target position and held it for 3s. The foot was returned to the start position and the subject then actively reproduced the reference position. No significant difference between mid- and outer-range was found.

Konradsen et al. (1998) found the mean RE to be significantly greater in injured ankles compared to contralateral non-injured ankles. They also reported that the RE at 12 weeks was significantly less than at 1 week, for the injured ankle. Forty-four patients with clinical grade II (partial ligament rupture) or grade III (complete ligament rupture) first time ankle inversion sprains were assessed. Repositioning error was measured at 1, 3, 6 and 12 weeks after injury. The patient was supine and rested the leg under investigation on a splint, with the knee flexed at 20-30° . The foot was padded and strapped to a goniometer footplate, whose axis was aligned approximately

with the axis of inversion and eversion. It is not clear how this axis was identified. The ankle was passively moved from 0^o to 10, 15 or 20^o of inversion, returned to the neutral position and then mechanically inverted at an angular velocity of $2^o s^{-1}$, until the patient indicated that their foot had reached the target position. Tests on 20 healthy subjects had shown the 95% confidence limits for test-retest to be $\pm 1.5^o$.

Boyle and Negus (1998) conducted a similar investigation and found significant differences between RE measured in recurrently sprained and uninjured ankles. Under active repositioning conditions, the difference between injured and uninjured was only significant for positions up to 30% of the range of movement. Like Konradsen et al. (1998), a goniometer was used, although Boyle and Negus (1998) used a pedal goniometer based on the design described by Gordan (1988). There was a difference compared to the previous two investigations in that normals were used rather than contralateral limbs in unilaterally injured patients. Inversion to 30, 60 and 90% of the range of movement was imposed, with the foot angled at 42^o of plantarflexion. The foot was manually moved to each position, held for 3*s*, returned to the start position and then passively returned towards the target position until the subject indicated verbally that the position had been reached. They were allowed to correct the position if they believed they were mistaken. The process was repeated with the subject actively reproducing the test position. The range of movement (ROM) was measured and found to vary from $25\text{-}58^o$ in the uninjured subjects, and from $31\text{-}49^o$ in the recurrently sprained subjects. In all cases, the repositioning errors were greater for active than passive repositioning. For passive repositioning, there was no significant difference between the three positions, while for active repositioning there was a significant difference between the results at 30% of ROM and those at 90% of ROM.

Similarly, Hertel et al. (1996) found no significant difference in RE measured at the ankle under anaesthesia of the anterior talofibular ligament. They used an isokinetic

dynamometer to assess eight males and eight females (average age 22.6±1.9 years) before and after a lidocaine injection. The subjects lay supine, with their knees flexed at 90° and their ankles plantarflexed at 90° and in what was described as subtalar neutral position. The dynamometer footplate was used to passively invert and evert the foot at $3^o s^{-1}$. The subjects had their eyes closed and were barefoot. Three positions were used: 10° of eversion and 20° and 30° of inversion. Each position was held for 15s before the foot was passively moved to the end of the range of movement, returned to the test position for a further 15s, and finally returned to the start position. The foot was then moved towards the reference position and the subject was instructed to provide resistance to the passive movement when they reached the reference position.

Gross (1987) did not find any significant difference between injured and contralateral uninjured ankles using passive positioning and repositioning, and passive positioning with active repositioning RE techniques. They assessed 14 patients and 7 normals. The subjects were all in the age range 18-35 years (mean age 20.8); the patients all had recurrent lateral sprains. Inversion and eversion were assessed using a Cybex II isokinetic dynamometer, with the subjects blindfolded and lying supine. The ankle was moved into 10° of eversion, 10° of inversion and 20° of inversion. Each test position was maintained for 15s and the ankle was then moved from one extreme of the passive range of motion to the other. As the ankle was moved back towards the test position, the subject gave the instruction to stop. The movement was at $5^o s^{-1}$. The active protocol was the same, but the subject actively reproduced the position. Passive AJPS was found to be more accurate than active, and the sprain was not found to be significant.

Payne et al. (1997) investigated the use of a measurement of RE to predict ankle injury in college basketball players. Seven women and one man suffered an ankle

injury during the season, and it was found that proprioceptive deficits correlated with injury to the left ankle in all subjects ($p \leq 0.05$), and with injuries to both left and right ankles in female subjects ($p \leq 0.05$). It was concluded that a measure of proprioception could be used to indicate increased likelihood of injury. Subjects were assessed at the start of a 9-week season, at which point they had no history of injury; details of any initial injury during the season were recorded. An isokinetic dynamometer was used to measure RE in dorsiflexion, plantarflexion, inversion and eversion. The results of RE's for left and right ankles, for men and women in inversion, eversion, dorsiflexion and plantarflexion are presented in Table 2.1.

Table 2.1: Table of RE results for the right ankle (from Payne et al. (1997), with permission)

	inv	ev	df	pf
Women	$2.7^o \pm 2.4^o$	$2.7^o \pm 2.8^o$	$2.1^o \pm 1.4^o$	$2.6^o \pm 2.4^o$
Men	$2.1^o \pm 1.8^o$	$5.4^o \pm 2.6^o$	$2.6^o \pm 1.5^o$	$3.4^o \pm 3.0^o$

A Cybex II isokinetic dynamometer was used by Heit et al. (1996) to assess the effects of ankle taping and bracing. With no taping or bracing, the mean repositioning errors (SD in brackets) were found to be 5.93^o (1.91) for plantarflexion and 5.38^o (2.12) for inversion. There was a significant reduction in the repositioning error for bracing (4.68^o (1.52) in plantarflexion and 4.94^o (1.52) in inversion) and for taping (3.90^o (1.80) in plantarflexion and 4.06^o (1.41) in inversion). The subject group consisted of 26 (10 male, 16 female) physically active college-age individuals. The target positions were 30^o of plantarflexion and 15^o of inversion. For plantarflexion, the knee was held in 90^o of flexion. For inversion, the knee was held in 45^o of flexion.

Bernier and Perrin (1998) found that the repositioning errors measured in inversion and eversion in passive tests were significantly lower than those in the active tests. This finding agreed with previous work by Gross (1987), but may have been due to the slow

speed used and the fact that there was movement of the foot on the footplate which was not a problem in passive testing, although it was in active testing. The six-week training programme had no significant effect on ankle proprioception as measured, although improvements in postural sway were noted. An isokinetic dynamometer was used to investigate proprioception in ankle inversion and eversion. They used both active and passive repositioning, and also measured postural sway. Three positions were tested: 15^o of inversion, 0^o or neutral and 10^o of eversion. Each of these was tested at both 0^o and 25^o of plantarflexion. Maximum eversion, defined as 5^o less than each individual's maximum eversion range of movement, was also tested in 25^o of plantarflexion. An angular velocity of $5^o s^{-1}$ was used throughout. In the passive testing, the operator moved the foot through the complete inversion/eversion range of movement, then moved the foot to the test position and held it for $15s$. The foot was then moved to the opposite extreme of the range of movement before being returned towards the target position. The subject indicated with a muscle contraction, that registered on the dynamometer, when the target position was reached. The active repositioning procedure was identical, with the subject actively moving the foot back to the target position.

2.4.4 Others

Robbins et al. (1995) used a sloping box to investigate effects of age and footwear on awareness of foot position. It was found that the effect of age was greater with the athletic footwear than barefoot. Box angles between 0-25^o were used, and the box was rotated to investigate dorsiflexion/plantarflexion and inversion/eversion. Fifteen men over the age of 65 years (mean age 73) were compared with 36 men below the age of 40 (mean age 30). Subjects were tested barefoot and wearing athletic footwear.

Hamer et al. (1992) used an instrumented wobbleboard to assess subjects' ankle proprioception with and without ankle strapping. No significant differences were seen in the subjects' wobbleboard performance with and without strapping. They investigated 24 uninjured females with no previous history of serious (partial or complete ligament rupture) ankle injuries or known vestibular deficiencies. The subjects shaved their legs and underwent an exercise programme that involved jogging round a figure of eight course and then a rectangular circuit. The route was continued for 15 minutes, and wobbleboard trials were conducted at 5, 10 and 15 minutes. The selection for strapping or no strapping was randomised. The instrumented wobbleboard allowed the investigators to record number and duration of contacts with the ground.

2.5 The use of three-dimensional motion analysis to assess ankle proprioception

Feuerbach et al. (1994) also investigated the effect of anaesthesia on RE at the ankle joint in seated subjects. They injected the anterior talofibular and calcaneofibular ligaments, as well as investigating the effect of a rigid ankle orthosis (Aircast Air-Stirrup). No significant differences in RE were found with the ligaments anaesthetised. There were however significant reductions in error when the Aircast splint was worn. The mean (SD in brackets) of the absolute error was as follows: Plantarflexion/dorsiflexion 4.8^o (3.6); inversion/eversion 3.5^o (2.6); internal/external rotation 2.7^o (2.3). The RE was decomposed into these three rotations in the sagittal, frontal and transverse planes respectively; this work was unusual in that the movement was not artificially constrained to rotation about a single axis. It was found that the absolute error did not depend on the position within the range of movement, and that subjects did not demonstrate a tendency towards either under- or over-estimation of the angles. There were twelve healthy subjects between the ages of 21 and 41 years. The subjects' eyes

were closed and shoes were worn. The experimenter manually moved the foot at approximately $30^o s^{-1}$ to a reference position which the subject maintained for $5s$; how the experimenter achieved this velocity is not explained. The experimenter then manually moved the foot back to the rest position and instructed the subject to match the reference position. Nine reference positions were chosen throughout the functional range of movement of the ankle. The above testing procedure was repeated after injection of anaesthesia. In six subjects the anterior talofibular ligament was injected with lidocaine, while in the other six both the anterior talofibular and the calcaneofibular ligaments were injected. Deep pressure was applied manually to assess the degree of anaesthesia achieved. In all cases there was a loss of deep pressure sensation.

Abboud et al. (1999) also used three-dimensional motion analysis to investigate ankle proprioception. They employed an electromagnetic system to investigate the effects of age, knee angle and active and passive positioning and repositioning. Rotations were described using Euler angles with orthogonal axes aligned with the body planes. The findings were described as a comparison of mean repositioning errors for passive and active measurements. This limits the conclusions that can be drawn from the results presented. However, the overall approach described has much to recommend it, as it allows natural movement patterns to be fully described.

2.6 Investigations of joint axes of rotation

2.6.1 Overview

The use of three-dimensional motion analysis in the assessment of proprioception is a central component of the work presented here. The literature contains extensive discussions of the relative merits of various 3D motion analysis techniques. These will

not be discussed here. What follows is a review of previous attempts to describe how the axes of rotation at a joint vary, due to the particular relevance to the Sequential Finite Helical Axis approach developed as part of this work. Axes of joint rotation are of interest due to their application in calculation of joint kinetics, in particular joint moments, and their impact on the design of prostheses, in addition to the contribution to the characterisation of joint movement that they provide.

2.6.2 Previous investigations

A number of authors have investigated joint axes of rotation with various objectives. Blankevoort et al. (1990) used roentgen stereophotogrammetry to record three-dimensional motion data for cadaveric knee specimens. Tantalum pellets were used as markers to reconstruct the movement of the tibia and the fibula which were mounted in a rig allowing variable degrees of flexion to be imposed. The aim was to investigate the consistency and reproducibility of the Finite Helical Axis (FHA) approach for the description of movements recorded under these conditions (this approach is described in more detail in Section 3.5.6). Their conclusions were that, given accurate measurement techniques and reproducible motion patterns, reproducible FHAs can be found for passive knee joint motions. These FHAs were found to depend on particular motion pathways.

Woltring (1994) described the calculation of Instantaneous Helical Axes (IHAs). The application in this paper was an investigation of the rehabilitation of whiplash injuries. In one subject, the IHAs were found to be considerably more dispersed and of varying orientation in a subject who had suffered a whiplash injury than a normal subject. After chiropractic intervention, however, the axes are less dispersed and more parallel even than the normal subject. The calculation of instantaneous helical axes is highly

desirable as the variation throughout movement can then be described. However, the calculations presented require an estimation of velocities from noisy landmark data, which can only be achieved with complex filtering. The results presented were for very slow movements, and the authors admitted uncertainty as to the effect of using the technique for a variety of speeds of movement. A further drawback was also highlighted in that the complex filtering process needs to be optimised for a particular movement.

Instantaneous Helical Axes have been described by Stokdijk et al. (1999) and Stokdijk et al. (2000) for the elbow joint. The objectives were to achieve a standardised method for describing motion at the joint and to determine the optimal axis of rotation for an elbow prosthesis. Results are presented from *in vivo* studies of active movements, but no details are given regarding the filtering of the data required. Leardini et al. (1999) used IHAs to investigate motion at the ankle joint complex. The aim of this work was to develop a method that could inform surgical techniques for joint replacement and ligament reconstruction such that an individual's original range and pattern of motion could be restored. The results of *in vitro* measurements on a skeleto-ligamentous preparation including the intact tibia, fibula, talus and calcaneus were presented. Again, no details of the filtering techniques applied are given, although it is noted that IHAs were only calculated for movements where the angular velocity was greater than $15^{o}s^{-1}$, due to the fact that the axes are ill-defined for measurements that do not meet this condition. A continuous moving path of IHA motion was described that varied from specimen to specimen. Similar work that focussed on the subtalar joint is described in Leardini et al. (2001). Although the use of IHAs is admirable, observations based on results obtained from *in vitro* investigations cannot be assumed to be directly applicable to movements made under a subject's voluntary control.

There have also been investigations of the axes of rotation of the ankle joint complex based on *in vivo* measurements. Lundberg et al. (1989b) used roentgen stereopho-

togrammetry, with tantalum marker beads introduced into the bones of subjects, to record ankle joint motion. The subjects were tested standing with one foot on a footplate that could be set in increments of 10^o . Measurements were made of helical axes between discrete positions; these axes were found to vary through the range of motion. The stated aims of the work were to identify the axis of rotation of the ankle joint complex for use in calculation of kinetic parameters such as joint forces and moments, as well as to improve the design of ankle prostheses. The value of this work is limited by the fact that the results were not obtained from continuous movements; furthermore, the use of a footplate with a fixed axis will influence the patterns of motion. Similar objectives, in addition to the desire to better understand normal ankle joint movement and the aetiology of injuries at the joint, have also led to the use of mathematical modelling techniques to describe ankle motion. For example, van den Bogert et al. (1994) used optimisation techniques to define parameters describing a two-axis system based on kinematic data recorded from subjects, while Demarais et al. (2002) calculated a best-fit plane and a best-fit sphere on the basis of a trajectory of data points, which then allowed the calculation of a mean instantaneous axis of rotation (IAOR). Both of these modelling approaches make certain assumptions about the nature of the motion under consideration, and then find the best description of the true situation within whatever constraints those assumptions impose. Although they allow descriptions of motion to be tailored to an individual, they both aim to identify average static axes.

2.7 Conclusions

There are several conclusions that can be drawn from the information presented in this chapter. The first is that the way in which the afferent proprioceptive information from the various types of mechanoreceptors contributes to proprioception is not

thoroughly established, although the indications are that there is some redundancy in the system. Secondly, there is no standardised protocol for assessing an individual's proprioceptive acuity. For example, in joint repositioning studies, different authors use various combinations of passive and active positioning and repositioning, with little or no justification of the approach adopted. The general lack of standardisation renders comparison of results from different studies, and therefore identification of a logical starting point for a new investigation, impossible. There is little or no evidence that of the factors that might affect proprioception, the way in which it is measured has been considered as a vitally important factor. One aspect of the work reviewed that is common to many investigations is the restriction of motion at the ankle joint, and the simplified description of the motion as a two-dimensional rotation. The work reviewed that has attempted to identify the axes of rotation of the ankle joint complex indicates that not only might the axes of rotation be impossible to determine from the anatomy, but it is likely that they vary throughout the range of motion as well as between individuals. The implications of imposing constrained motion at the ankle joint complex for the measurement of proprioception can only be hypothesised. However, it would appear desirable that where such limitations can be avoided, they should be.

This work must therefore address the development of a technique for the assessment of proprioception at the ankle joint complex that does not constrain the natural motion of the ankle. In parallel with, and complementary to, this development, a detailed investigation of the axes of rotation of the ankle joint complex is also required, which will involve three-dimensional motion analysis. Finally, these two threads must be brought together to allow the three-dimensional motion analysis techniques developed to be used for the assessment of proprioception. The way in which these objectives have been achieved is described in detail in the following chapter.

Chapter 3

Development of Experimental Protocol

3.1 Introduction

This chapter includes a description of the development of the various aspects of the experimental protocol used to obtain the results presented in Chapter 4. This includes the development of the protocol to assess proprioception and the protocol used to investigate axes of rotation. The motion analysis system is described in some detail, and results from validation of the system are presented. There is a general discussion of three-dimensional motion analysis, including the limitations of the various techniques, before the possibility of combining two of these, the Joint Coordinate System and the Helical Axis technique, is explored. Finally, the novel approach to the description of three-dimensional joint movement that was developed is presented and discussed.

3.2 Development of experimental protocol for the assessment of proprioception

3.2.1 Overview

There are a number of factors to consider in terms of developing a protocol for the assessment of proprioception. The previous chapter included a review of the literature relating to previous investigations of proprioception, each of which employed a slightly different protocol. The most important elements are presented below, along with a discussion of how various authors have addressed them; this leads to a description of the protocol used for the work described here.

3.2.2 Proprioceptive assessment technique

The most significant decision is which generic proprioceptive technique to employ. As noted in Section 2.4, the two primary techniques are threshold testing and repositioning error. One of the primary aims of this work was to allow unconstrained movement; this is not possible in threshold testing (TT) techniques, because some movement must be externally imposed. Abboud et al. (1999) describe the assessment of repositioning error using an active positioning, active repositioning protocol, with unconstrained motion measured using three-dimensional motion analysis equipment. This protocol is considered attractive as it allows voluntary, physiological movements and because proprioceptive input from muscle spindles will be the same for repeated movements. This is not true in the case of mixed passive and active movements. In order to use RE to assess proprioception, positioning and repositioning movements must be compared. Although such a comparison could include the trajectory and velocity of the entire movements, the majority of the studies reviewed have only considered the endpoints

of the positioning and repositioning movements. Only Thieme et al. (1996) considered the time taken to complete movements.

3.2.3 Isolation of ankle joint proprioception

All of the repositioning tests that will be discussed were performed under non-weightbearing conditions. This prevents the contribution of afferent signals from the vestibular system and from other joints; such signals may provide additional cues that increase proprioceptive acuity, equally they may have a negative effect by disrupting a subject's concentration. It is desirable to minimise this input, an objective that is most easily achieved by testing seated subjects. Visual input must also be eliminated. Some authors (Bernier and Perrin, 1998; Heit et al., 1996; Steele et al., 1993; Boyle and Negus, 1998; Hopper et al., 1997; Gross, 1987) have used a blindfold, while others (Feuerbach et al., 1994; Payne et al., 1997; Hertel et al., 1996) have simply asked subjects to close their eyes. Berenberg et al. (1987) used a blanket to cover the legs, while Konradesen et al. (1993) positioned the subject so that the ankle was not visible. In order to allow maximum flexibility in positioning subjects and to allow the use of an optical motion analysis system, these latter two options must be discarded. Compared with asking a subject to keep their eyes closed, blindfolding them reduces to a minimum the risk that they will inadvertently open their eyes and removes any obligation to concentrate on keeping their eyes closed, which could distract them from the task of repositioning their ankle.

3.2.4 Knee angle

The knee angle set when testing subjects' ankle proprioception must be considered. The knee angle affects muscles which also control and cross the ankle joint (see Section

2.3.3. Of the literature reviewed, three authors (Bernier and Perrin, 1998; Boyle and Negus, 1998; Gross, 1987) do not specify the knee angle used during testing. A popular solution is to seat the subject with the shank hanging vertically; this is sometimes assumed to give a knee angle of 90^o , although the angle will vary from subject to subject. Such an approach was adopted by Hertel et al. (1996), while Heit et al. (1996) used different knee angles to test dorsi/plantarflexion (90^o) and inversion/eversion (45^o). Feuerbach et al. (1994) did not state the knee angle used, but allowed the shank to hang vertically in seated subjects; this would result in a knee angle of approximately 90^o . Steele et al. (1993) tested subjects using knee angles of 0^o and 90^o . Konradesen et al. (1993); Konradsen et al. (1998) specified a knee angle of 20-30^o , and Berenberg et al. (1987) angled subjects' knees at 55^o . Abboud et al. (1999) measured differences between active and passive repositioning at knee angles of 0 and 30^o . Finally, Payne et al. (1997) used a knee angle of 100^o . Allowing the shank to hang vertically avoids the problem of cutaneous input arising from any support required to achieve a specific, set angle, and is comfortable for subjects.

3.2.5 Support for the subject

The effect of the way in which subjects are supported on the knee angle requires consideration. Berenberg et al. (1987) used an adjustable chair and leg rest, with both feet secured in identical cradles. Bernier and Perrin (1998) tested subjects supine on an examination table with the ankle positioned on the footplate of a dynamometer, but as noted above did not report the knee angle used. Konradsen et al. (1998) used a splint to position the knee at 20-30^o ; again, they tested subjects supine. Payne et al. (1997) seated their subjects upright, with the knee and the hip flexed to 100^o , and the foot secured to the foot pedal on a dynamometer. Both Hertel et al. (1996) and Heit et al. (1996) again used a dynamometer, with patients supine and a knee angle

of 90° . Steele et al. (1993) seated subjects on a dynamometer, but this time with the knee at 0° of flexion. Although they do not describe testing with the knee flexed to 90° , results are given for both positions. The results for the normal contralateral limb are an angular error of 2.6±2.3° with the knee extended, and 3.0±1.8° with the knee in 90° of flexion. Without performing a statistical analysis, the difference between these results does not appear to be particularly marked; there is clearly a considerable degree of overlap. Abboud et al. (1999) seated subjects on an adjustable chiropodist's chair with leg rests that could be used to adjust the knee angle. The key requirements of a method of supporting subjects include a back support that can be raised so that it is near-vertical, leg supports that can be individually adjusted, if the knee angle is to be varied, armrests so that a subject can be seated comfortably and securely, and height adjustment. Ideally the seat length would also be adjustable, in order to ensure that subjects can be positioned with the shank hanging freely irrespective of their leg length, with no contact between the shank and any support surface or covering to minimise cutaneous stimulation. However, this can be achieved by moving subjects forwards on the couch by the addition of pillows or foam cushions.

3.2.6 Footwear

The effect of footwear is an important consideration. The presence or absence of footwear will modify the stimulation of cutaneous mechanoreceptors, and may therefore have an effect on proprioceptive acuity (Robbins et al., 1995). As such, it should be considered by investigators, and at the very least the presence or absence of footwear should be reported, but this is not always the case. Feuerbach et al. (1994) asked subjects to wear low-top athletic shoes, because their study required an ankle brace to be worn that was designed to be worn with such shoes. In their investigation of factors that can be used to predict injury in basketball players, Payne et al. (1997)

also tested subjects wearing low-cut court shoes although they gave no rationale for doing so.

3.2.7 Direction and range of movement

In some cases, the direction of movement is chosen according to the nature of the investigation. For example, in investigations of subjects with inversion injuries, inversion and eversion are generally the movements studied. In other cases the choice may have been somewhat random. It is interesting to note that both groups (Feuerbach et al., 1994; Abboud et al., 1999) using 3D motion analysis investigated movements in all directions. Boyle and Negus (1998); Hopper et al. (1997) related all movements made to the subjects' active ranges of motion (AROM). The former group used test positions of 30, 60 and 90% of a subject's inversion AROM, while the latter investigated 40 and 80%. These two groups were both based in Curtin University in Perth, Australia. Bernier and Perrin (1998) used test positions of 15, 0 and -10^o of inversion at 0 and 25^o of plantarflexion; they also made a further measurement at the subject's maximum inversion AROM minus 5^o , with the foot in 25^o of plantarflexion. Where possible, it would seem appropriate to consider movements made for proprioceptive testing relative to normal movements made by a given subject.

3.2.8 Number of attempts

The number of attempts that a subject is allowed and the length of time for which positions are held should be carefully considered and the presence of learning effects investigated. Many investigators used only two to five repetitions without explanation or justification. Hopper et al. (1997) piloted their protocol for the assessment of the effect of ice on 49 healthy young (17-28 years) subjects with five repetitions. Finding

no significant difference between attempts, their final protocol used only three repetitions. Berenberg et al. (1987) reported no learning effect in twenty-two 21-50 year-old subjects who were given feedback by displaying the output of the potentiometers used to measure angular position on an oscilloscope.

3.3 The Protocol Adopted

Having reviewed the approaches adopted by other investigators, and considered the underlying rationales, a specific experimental protocol was developed for this work. The protocol described here was refined during early subject trials which are not reported in any detail here.

Figure 3.1 shows a subject during a typical measurement session. The subject was seated on a treatment couch that provides an adjustable backrest and height adjustment as discussed in Section 3.2.5. The couch was raised and pillows were placed behind the back so that the shank was hanging freely in space, and the subject was blindfolded. Any visual, vestibular or proprioceptive input from joints other than the ankle was therefore excluded. Only dorsiflexion movements were performed. The subject was asked to relax his foot; this was taken as the neutral position. He was then instructed to move his foot up (into dorsiflexion) to a new, self-selected position, and to hold the position until prompted after 5 s by the investigator to return the foot to the neutral position. The subject relaxed for a further 5 s before he was instructed to repeat the original movement, again holding the final position for 5 s. It is considered important that subjects were asked to repeat the original movement, rather than reacquire the final position. The task of matching the entire movement is more detailed than simply reacquiring a position, and may therefore offer a more sensitive assessment of a subject's proprioceptive acuity. Four further pairs of repeated movements were

Figure 3.1: The subject seated on the treatment couch

made in the same manner as that described above. In each case, the subject was free to select the dorsiflexed position to which they moved their foot. It is clear that this protocol could be extended to include movements in different directions. Furthermore, any 3D motion analysis technique could be used to analyse the measurements made during a session following the protocol described.

3.4 Experimental protocol for the investigation of axes of rotation of the ankle joint complex

The majority of the investigations of ankle proprioception reviewed in Section 2.4 employed a footplate with a fixed mechanical axis. Many three-dimensional motion analysis techniques are also based on fixed axes of rotation, referenced to the anatomy. The morphology of the joint is such that a static mechanical axis of rotation seems unlikely; this is supported by investigations in the literature. These factors, in addition to the close interrelationship between neuromuscular control, joint moments and axes of rotation, led to the decision to investigate how the location and orientation of the axis of rotation of the ankle joint complex varies throughout movement. The analysis technique is described later, but a brief description of the protocol for data collection is included here.

Subject data were recorded in three separate series of measurements. For the first series, the objective was to describe the angle between the axes of rotation and the intermalleolar (IM) line. The testing arrangement was as described in Section 3.3, although no blindfold was used. Movements were performed as sequences of five cycles of dorsiflexion-plantarflexion. The second and third series of measurements were very similar; the second series will be described first and in greater detail. In addition to the investigation of unloaded movements, it was decided that the way in which the axes vary depending on the loading of the joint would also be assessed. Therefore, it

was decided that subjects would be asked to perform a variety of tasks. The first was to make separate, directed movements of the foot relative to the shank in dorsiflexion and plantarflexion, with the subject barefoot, seated and the foot hanging off the floor, again using the testing arrangement described in Section 3.3 but omitting the blindfold. The fact that individual movements in different directions were performed and recorded separately facilitated comparisons according to the direction of movement. The unloaded measurements were then repeated wearing shoes. In order to investigate the effect of loading on the joint axes, two further tasks were performed, shoes were worn in both cases. The subject was first asked to descend into a squat, hold the position and then return to a standing position. As for the unloaded measurements, descent and ascent were recorded separately. Subjects were instructed only to squat as far as was comfortable. In descending into a squat, subjects performed a loaded, dorsiflexion movement. In order to investigate loaded, plantarflexion movements, subjects were asked to perform a toe raise, rising up so that they were standing on the balls of their feet. They were again instructed to hold this position briefly before descending to a standing position. Subjects naturally found greater difficulty in balancing at the highest position; if necessary they touched a wall to aid in balancing. Subjects were instructed to perform all movements at a comfortable speed. The third series of testing varied only in that all movements were performed barefoot. The results from the tests are presented in Chapter 4.

3.5 Three-dimensional motion analysis

3.5.1 Introduction

The protocol developed for the assessment of proprioception requires the comparison of unconstrained positioning and repositioning movements. In order to compare such movements, the movements must be measured and described completely in three dimensions; a method of representation that is suited to the application must be selected. Ideally, the method selected will allow the motion to be described in an intuitive, meaningful way with clear reference to the anatomy. It is important to consider how movements were recorded and analysed in order to arrive at the results presented in the following Chapter. This section is intended to give a brief introduction to 3D motion analysis in general and the various analysis techniques.

3.5.2 Embedded Coordinate Systems

Three-dimensional motion analysis is based on describing the relative positions of two or more rigid bodies. In order to achieve this, the rigid bodies are assigned Embedded Coordinate Systems (ECSs). In general, there will be one ECS that is attached to a reference volume in space. This is referred to as the Global Coordinate System (GCS). For human motion analysis, each body segment that is described has an ECS that is described as the Local Coordinate System (LCS). In order to describe movements of a given segment, the relevant LCS must be described relative to the GCS. Figure 3.2 depicts a Local Coordinate System (Cartesian reference system $O - xyz$) that is translated and rotated relative to a Global Coordinate System (Cartesian reference system $O - XYZ$). This translation and rotation can be described in a number of different ways. Transformation matrices are a particularly powerful and versatile

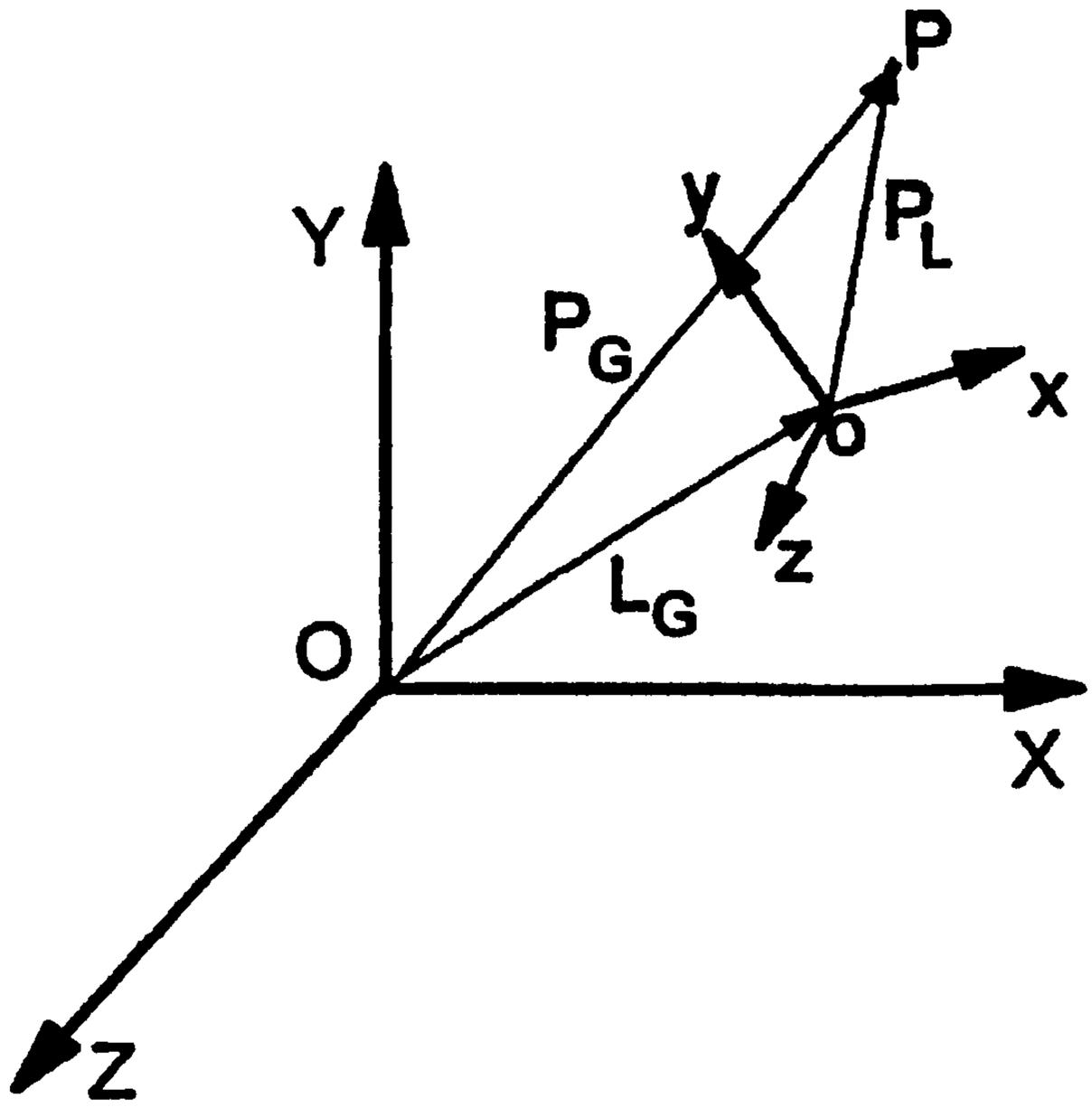

Figure 3.2: A Local Coordinate System (O-xyz) rotated and translated relative to a Global Coordinate System (O-XYZ) (From Zatsiorsky (1998) with permission)

method of describing ECSs relative to each other; these will be considered first.

3.5.3 Transformation Matrices

Transformation matrices are 4x4 matrices that completely describe position and orientation in three dimensions. A transformation matrix T is composed of a 3x3 rotation matrix R, three translational components and a fourth row [0 0 0 1] (see below). This final row is included for mathematical convenience, allowing inversion of the matrices. This is an important property, as the ability to perform matrix multiplication and inversion makes transformation matrices very useful despite relative computational inefficiency and the fact that they cannot be immediately interpreted.

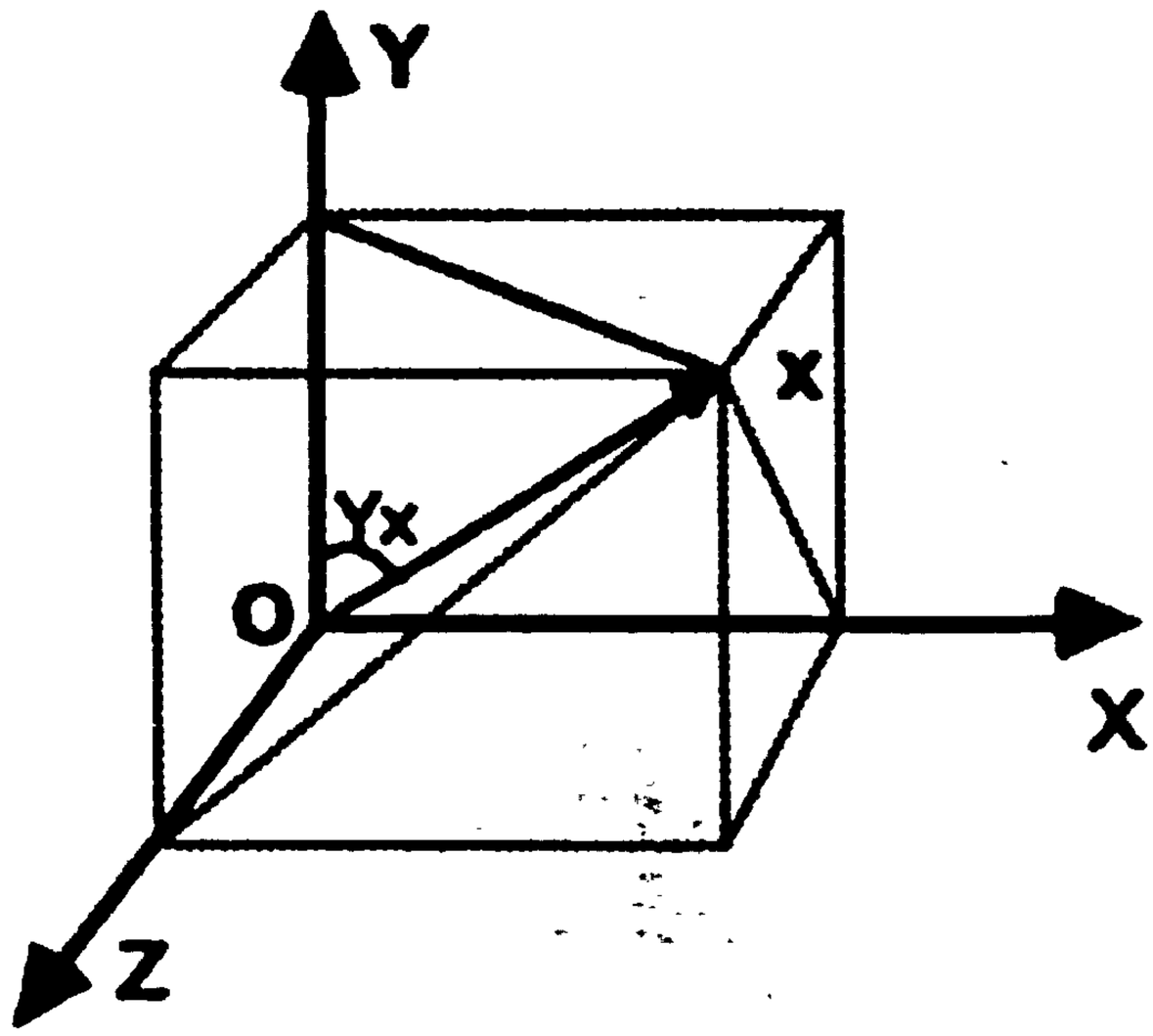

Figure 3.3: Components of unit vector Ox in the GCS O-XYZ. These components, divided by the length of the vector, give the cosines of the angles that the vector makes with the coordinate axes (the direction angles). For instance, angle Yx is made by the vector Ox and the Y axis. Because the vector under consideration is a unit vector (its length equals one), the direction cosines equal the components of the vector. (From Zatsiorsky (1998) with permission)

$$\mathbf{R} = \begin{pmatrix} R_{11} & R_{12} & R_{13} & T_x \\ R_{21} & R_{22} & R_{23} & T_y \\ R_{31} & R_{32} & R_{33} & T_z \\ 0 & 0 & 0 & 1 \end{pmatrix} \tag{3.1}$$

The rotation matrix R describes the orientation of one cartesian coordinate system relative to another. The three translational components $[TxTyTz]$ constitute a vector that connects the origins of these two coordinate systems. R is in fact a matrix of the direction cosines of the LCS within the GCS. When the axes of the LCS are described as unit vectors, the components of those unit vectors in the GCS are identical to the direction cosines. This can be seen from Figure 3.3 where the adjacent is the component and the hypoteneuse (the magnitude of the unit vector) is 1.

Subscripts and superscripts will be used to denote coordinate systems and positions

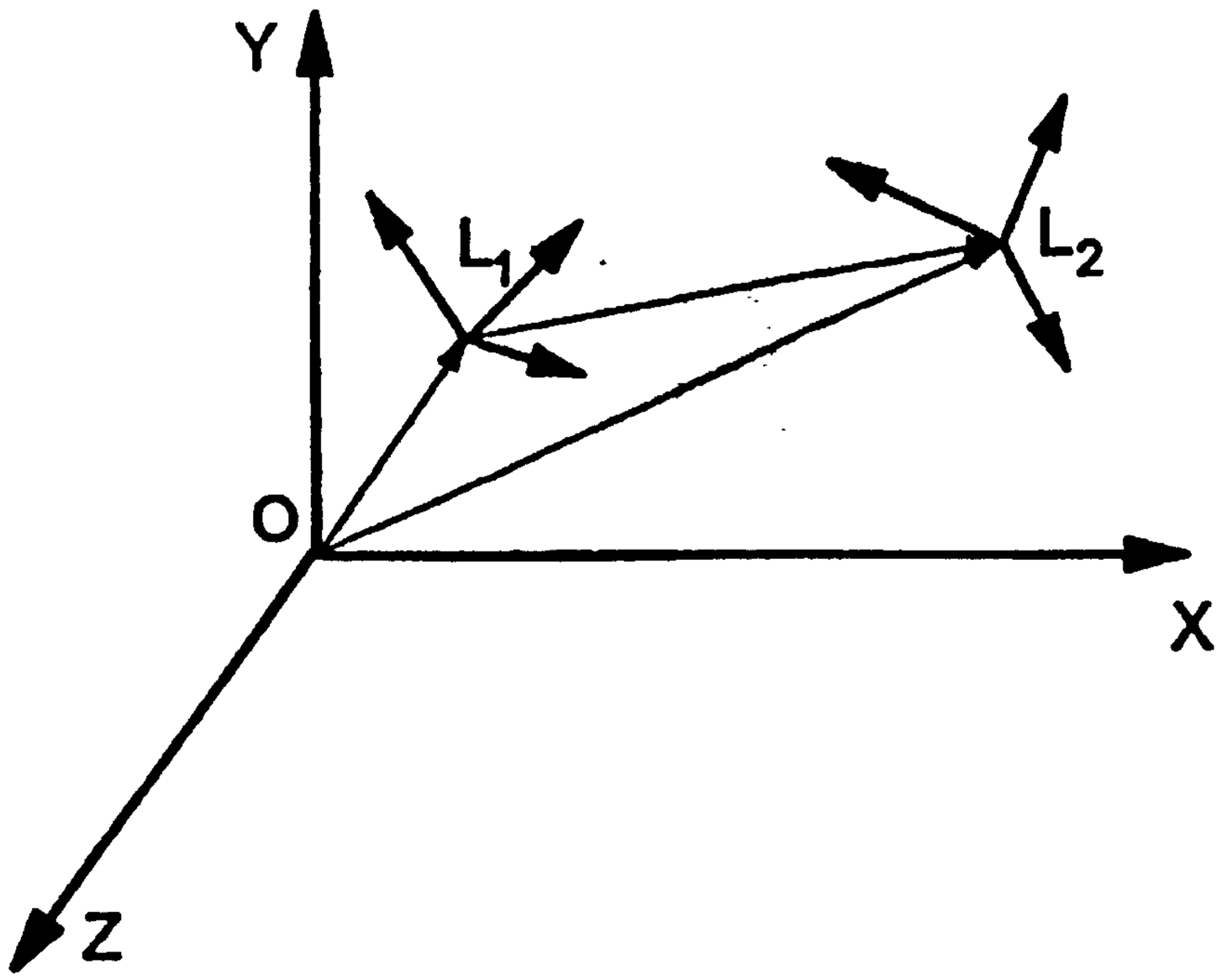

Figure 3.4: Graphical representation of transformation from one LCS to another (L1 to L2) (From Zatsiorsky (1998) with permission)

that transformation matrices refer to. Subscripts and superscripts immediately following T denote coordinate systems, while sub-subscripts separated by a hyphen refer to positions. The Polaris GCS will be denoted by G, while tool-embedded local coordinate systems will be identified according to the tool in which they are embedded. Therefore, $T^{G}_{B_{1-2}}$ signifies the transformation matrix describing the movement of Tool B's LCS in the Polaris GCS from position 1 to position 2.

In order to determine the transformation from one position to another, the transformation matrices can be combined as follows. If the transformation returned by Polaris for Tool A in one position is T_{A_1}, and the transformation returned for the next position is T_{A_2}, then the transformation matrix that describes the movement is:

$$T_{A_{1-2}} = {T_{A_1}}^{-1} \times T_{A_2} \tag{3.2}$$

Similarly, to describe the position of Tool A, with transformation matrix T_{A_1} relative

to Tool B (transformation matrix T_{B_1}),

$$T_{A_1}^{B} = T_{A_1}^{P\,-1} \times T_{B_1}^{P} \tag{3.3}$$

For this work, the movement of the foot relative to the shank was of primary interest. If T_{F_1} and T_{S_1} are the transformations describing the positions of the tools on the foot and shank at one point in time, and T_{F_2} and T_{S_2} are the transformations at another point in time, then the change in the position of the foot relative to the shank is given by:

$$T_{F_{1-2}}^{S} = \left(T_{S_1}^{P\,-1} \times T_{F_1}^{P}\right)^{-1} \times \left(T_{S_2}^{P\,-1} \times T_{F_2}^{P}\right) \tag{3.4}$$

This will give the movement at the ankle joint complex irrespective of movement of the shank.

3.5.4 From transformation matrices to rotations and translations

Transformation matrices are useful because they are easily manipulated in order to transform between coordinate systems. However, as stated above, they do not lend themselves to intuitive interpretation, so that they are not an ideal way of reporting final results. The most common techniques for reporting movement are based either on Euler's theorem or Rodrigues' theorem. Euler's theorem states that any rotation in 3D space can be described as a series of three rotations about distinct axes. Rodrigues' theorem states that any three-dimensional movement can be described as a rotation around and translation along a fixed axis in space; the axis may be referred to as the screw or helical axis.

3.5.5 Euler and Cardan angles

Euler and Cardan angles are slight variations of a common technique based on Euler's theorem. Three axes are defined, and rotations about these axes describe the 3D rotation completely, while translation is described by a translation vector $[T]$ as described in Section 3.5.3. Although the terms Euler angles and Cardan angles are sometimes interchanged, the sequences of rotations in each case are different. Euler angles are combined rotations where the first and third axes of rotation are the same. For example, the first rotation might be about the x-axis, the second about the y-axis and the third about the displaced x-axis again. When Cardan angles are employed, each of the three rotations is about a different axis. When either Euler or Cardan angles are employed, there are six possible sequences of component rotations. For a given 3D rotation, the values of the component rotations will vary according to the sequence used. This is a considerable drawback of Euler and Cardan angles; it is imperative that the order of rotations adopted is specified, in order to meaningfully interpret and compare any results. The investigations of proprioception using 3D motion analysis by Feuerbach et al. (1994) and Abboud et al. (1999) both used Cardan angles. The axes used were orthogonal and aligned with the anatomical planes; this is commonly the case. As physiological rotations do not occur about orthogonal axes, it does not seem that this is an optimal approach.

3.5.6 Helical axis approach

Although it is not widely encountered in the literature, the helical axis (HA) approach does have some attractive features. The technique is particularly suited to describing hinge-like motion, such as dorsi/plantarflexion. There are eight parameters returned when describing motion using the helical axis technique. These describe the orientation

$(n1, n2, n3)$ and intersection with a plane in one of the coordinate systems (x, y, z) of the axis, the rotation about the axis (θ) and translation along the axis (t). The movement of the helical axis may be of interest, providing valuable information in itself. The location and orientation of the axis will be independent of the locations of the Polaris tools, although as discussed below it is useful to relate the axis of rotation to the anatomy. The ability of this technique to identify a real axis of rotation rather than one identified by the anatomy is very valuable. However, the HA is ill-defined for small angular rotations; it is therefore unsuitable for the description of digitised continuous movement. Furthermore, care is required when comparing movements, as both the rotation around and translation along the axis must be considered, as well as motion of the axis itself. This consideration becomes even more of an issue if velocities and accelerations are of interest.

3.5.7 The Joint Coordinate System

The Joint Coordinate System proposed by Grood and Suntay (1983) has been widely adopted. This technique involves the identification of a proximal and a distal segment either side of a joint. A body-fixed axis is identified in each one; the segment is considered to rotate about this axis. These axes are referred to as e_1 and e_3, respectively. A third axis, e_2, is then calculated as the vector product of the two body-fixed axes such that it is perpendicular to both of them. An LCS is defined in each segment based on anatomical landmarks; one of the axes is normally taken to be the body-fixed JCS axis, while the means of identifying the other two axes for each LCS varies. A Joint Coordinate System for the ankle proposed by the International Society of Biomechanics (ISB) is shown in Figure 3.5.

For the ankle joint the two segments are the shank and the foot. Cappozzo et al.

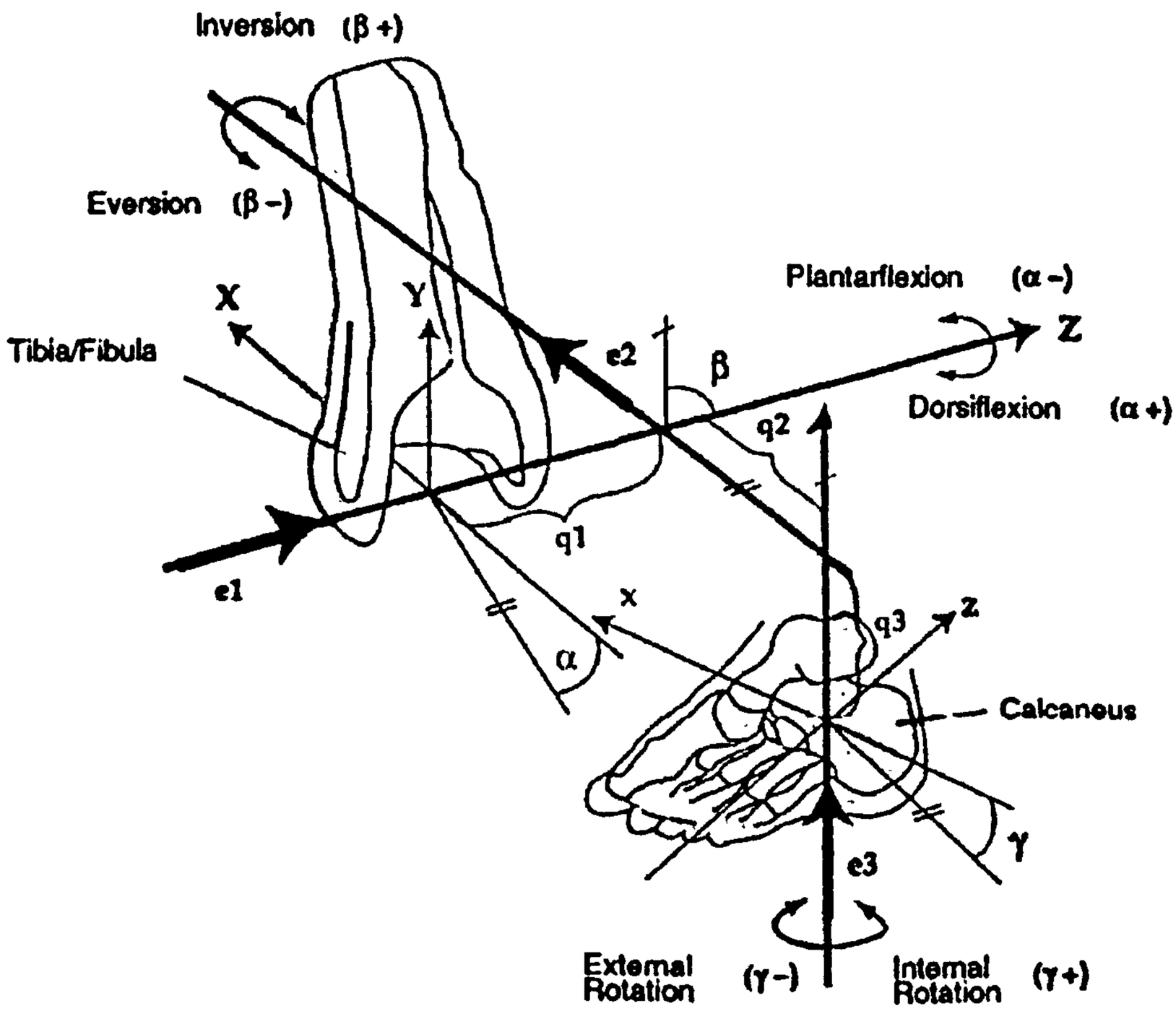

Figure 3.5: ISB proposal for a Joint Coordinate System at the ankle joint complex (from Wu et al. (2002), with permission)

(1995) proposed a local coordinate system, or anatomical reference frame (ARF) for the shank as follows. A quasi-frontal plane is defined as the plane that passes through the head of the fibula, the medial malleolus and the lateral malleolus. The quasi-sagittal plane passes through the inter-malleolar point and the tibial tuberosity and is orthogonal to the quasi-frontal plane. The coordinate system then has its origin at the inter-malleolar point. The y-axis is defined as the line of intersection of the quasi-frontal and quasi-sagittal planes, positive distal to proximal. The z-axis, the axis of dorsi/plantarflexion, lies in the quasi-frontal plane with its positive direction from left to right, while the x-axis is orthogonal to the yz plane, positive posterior to anterior. This can be seen in Figure 3.6. This approach is recommended by Zatsiorsky (1998).

There is also an International Society of Biomechanics (ISB) recommendation for an LCS in the shank (Wu et al., 2002). In the ISB proposal for a definition of the standard anatomical planes of the tibia/fibula, a frontal plane is defined by the inter-malleolar point, the medial tibial condyle and the lateral tibial condyle. A torsional plane contains the inter-condylar point and the medial and lateral malleoli; a sagittal plane is perpendicular to the frontal plane and contains the intercondylar and intermalleolar points. The line connecting these two points is taken to define the long axis of the tibia/fibula. The tibial/fibial coordinate system is then described as follows. The origin is the intermalleolar point. The z-axis lies on the intermalleolar line, and points to the right; as in the above description, this is assumed to be the dorsi/plantarflexion axis. The x-axis is the line perpendicular to the torsional plane of the tibia/fibula, and points anteriorly, so the y-axis is the line perpendicular to both the x- and z- axes. This system can be seen in Figure 3.7.

In both of these anatomical reference frames, the axis of dorsi/plantarflexion is assumed to be coincident with the intermalleolar line in all subjects. There is no flexi-

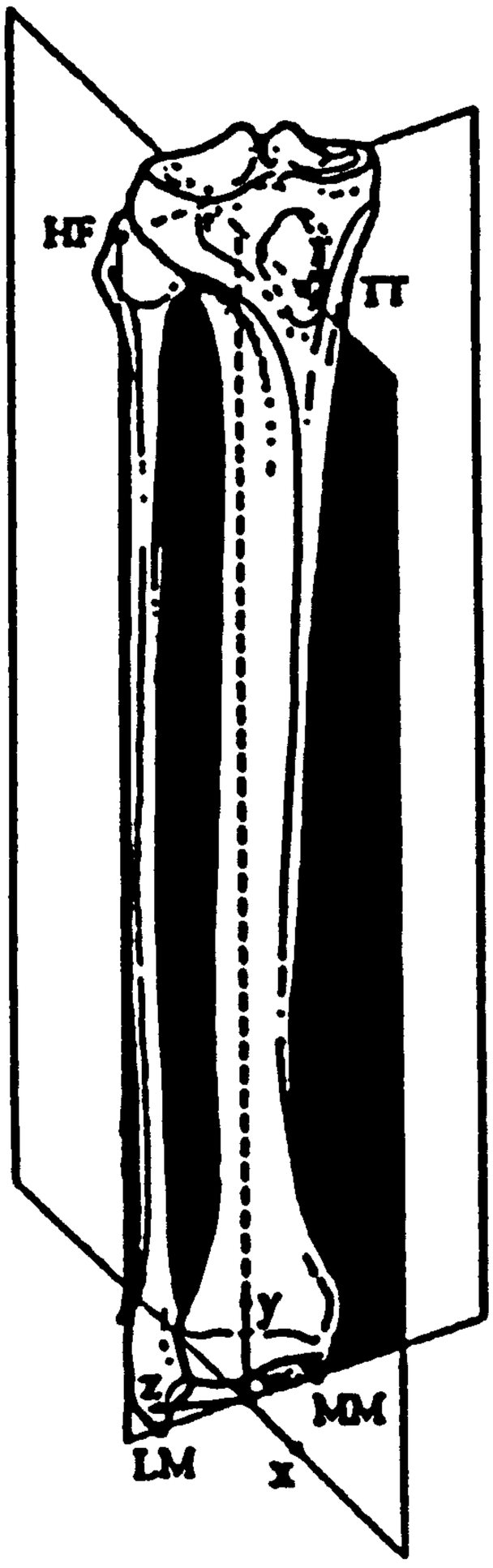

Figure 3.6: An anatomical reference frame for the shank (from Cappozzo et al. (1995), with permission)

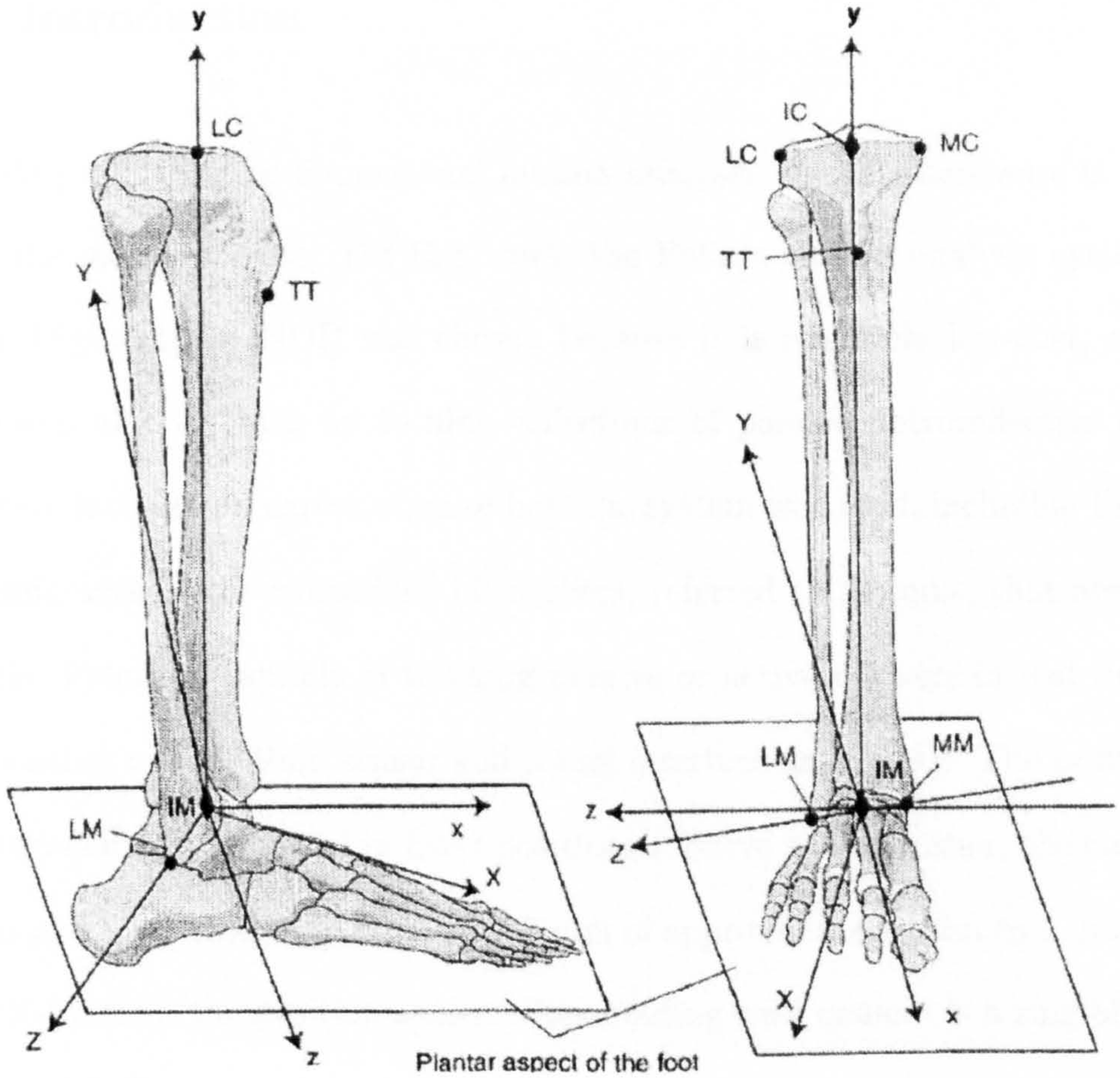

Figure 3.7: ISB proposal for an anatomical reference frame for the foot and shank (From Wu et al. (2002) with permission)

bility to identify an axis that is specific to an individual. Furthermore, it is assumed that the axis is stationary throughout movement.

3.6 The Polaris System

3.6.1 Introduction

In order to perform three-dimensional motion analysis, suitable hardware is required to make the measurements. For this work, the Polaris motion analysis system from Northern Digital Inc. (NDI) was chosen because it is relatively low-cost, accurate, portable and able to track up to nine collections of passive, retroreflective markers. This section includes an explanation of how the system was used, including the design and manufacture of the collections of markers, referred to as tools, that are tracked by Polaris. Polaris is capable of tracking passive or active markers in real time. The system consists of a position sensor and a tool interface unit (TIU). The position sensor has two cameras mounted in fixed positions relative to each other; the calibration volume is pyramidal, extending to a maximum of approximately 1.2m by 1.2m at a distance of 2.4m from the position sensor. Surrounding each camera is a ring of infrared emitters which illuminate the retro-reflective markers. The calibration volume can be seen outlined on the ToolViewer screen in Figure 3.9 on page 75. The reflections from these markers are recorded by the cameras so that they can be tracked by the system. The processing electronics relating to the 3D positioning are contained within the position sensor. The position sensor can be seen in use in Figure 3.8. The Polaris system uses quaternions to describe rotations of tools. Quaternions are non-traditional mathematical objects; a description of these is beyond the scope of this work. Fortunately, however, there are simple formulae for the conversion of quaternions to transformation

matrices; these are applied to all data recorded.

The TIU is used to control the firing sequence of active markers, which are hardwired to the unit. When tracking passive markers only, the TIU serves simply as a power supply for the position sensor. Polaris communicates with a PC over an RS-232 serial communications link; no proprietary interface card is required. Polaris is capable of a theoretical maximum sample rate of 60 Hz. Initially, this was limited by the speed at which ASCII data could be transmitted over the serial link. However, a firmware update was then released that allowed the data to be transmitted using binary coding, so that the full sample rate of 60 Hz was achieved. The Polaris system has a specified accuracy of 0.35 mm RMS. The position sensor and TIU have a combined mass of approximately 6 kg. Bespoke communication software was written in VeePro from Agilent; this was adapted and tailored to specific data collection applications as required. All analysis software was written in Matlab.

3.6.2 Polaris Tools and markers

Polaris works with rigid-body collections of markers referred to as tools. A tool may have a minimum of three and a maximum of six non-colinear markers. The results that are returned by Polaris are the three-dimensional co-ordinates of the origin of the tool's local co-ordinate system (LCS) within the global (Polaris) co-ordinate system (GCS), and the orientation of the tool's co-ordinate system relative to the orientation of the global co-ordinate system. The Polaris GCS is defined with its origin at the centrepoint of a line drawn between the centres of the two cameras. The x-axis extends vertically from the origin, perpendicular to the y-axis that joins the centres of the two cameras. The z-axis extends out from the Polaris, orthogonal to the other two axes. The x-axis is positive upwards, the y-axis is positive to the right (looking out from the

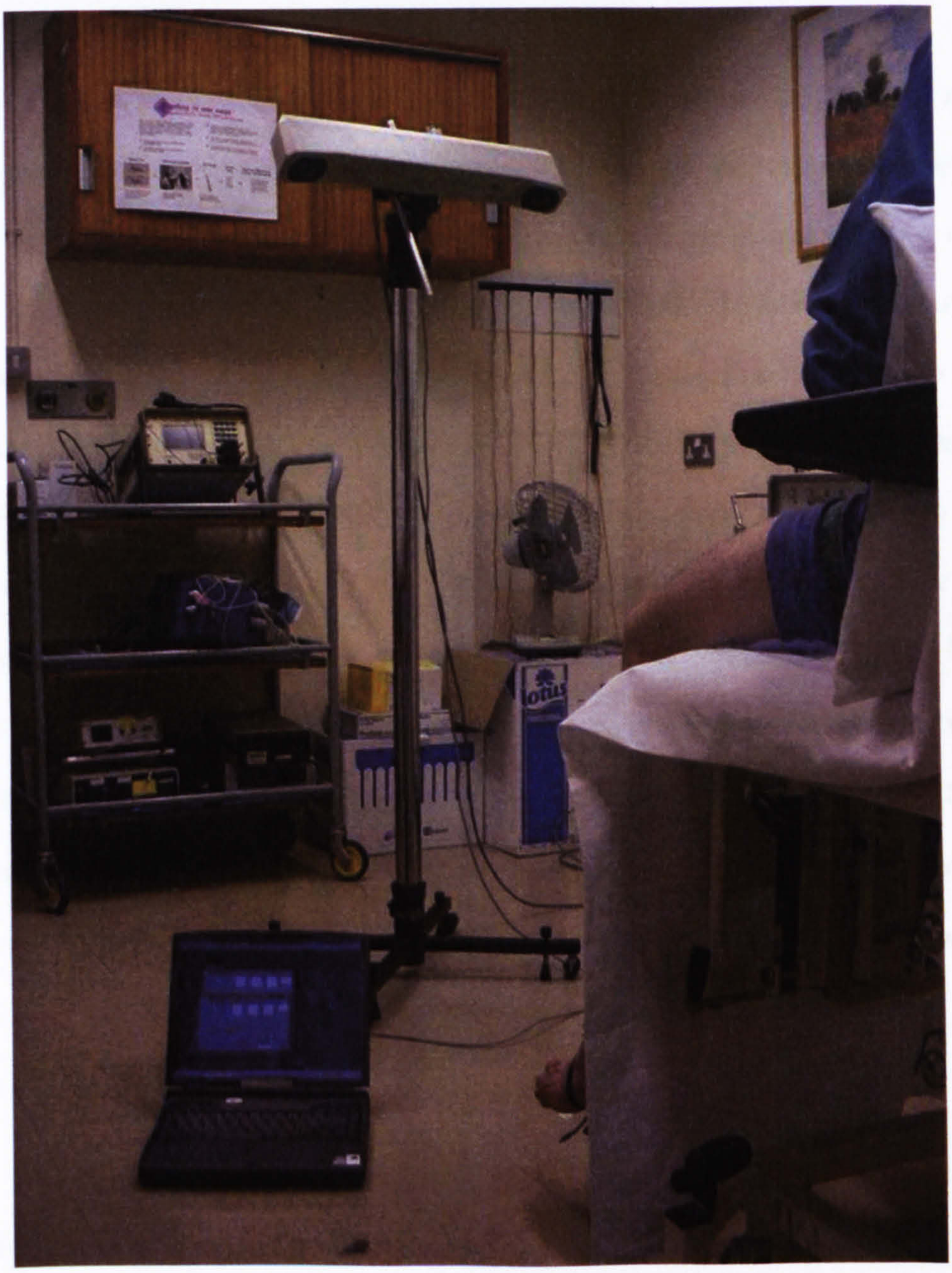

Figure 3.8: Polaris in use

Polaris measurement head), and the z-axis is negative out from the Polaris. This can be seen in Figure 3.10. The local coordinate system embedded in a tool is defined by the manufacturer of the tool, when the tool is characterised; an example can be seen in 3.11.

In order to accurately track a passive tool, the geometric arrangement of the markers must be such that the relative positions of the markers are unique in any orientation. In order to ensure this, there exist certain design rules. The distance between any two markers must be a minimum of 50 mm, and inter-marker distances must vary by at least 5 mm for a tool. The angles between lines connecting markers must also vary by five degrees. These design rules place constraints on the minimum size of a passive tool and force the tool designer to carefully consider the geometry specified. Up to nine passive tools, with different geometrical arrangements of the markers, can be tracked at a maximum sample rate of 60 Hz; no hardwired connection is required between the tool and the TIU. The actual tools used to track movements are illustrated in Figure 3.12. The shank tool was placed over the tibial plateau to minimise the effect of movement of the skin over underlying bone, while the foot tool was located on the dorsum of the foot, or in a similar location on the shoe, if shoes were being worn.

3.6.3 Validation

When interpreting data obtained using the Polaris system, it is important to appreciate how any measurement error due to the system affects those results. The validation of the equipment aimed to quantify that measurement error, and assess the suitability of the Polaris system for the proposed application. Under static conditions the accuracy and precision were extremely impressive.

Errors may be either random or systematic in nature. An example of a random error is

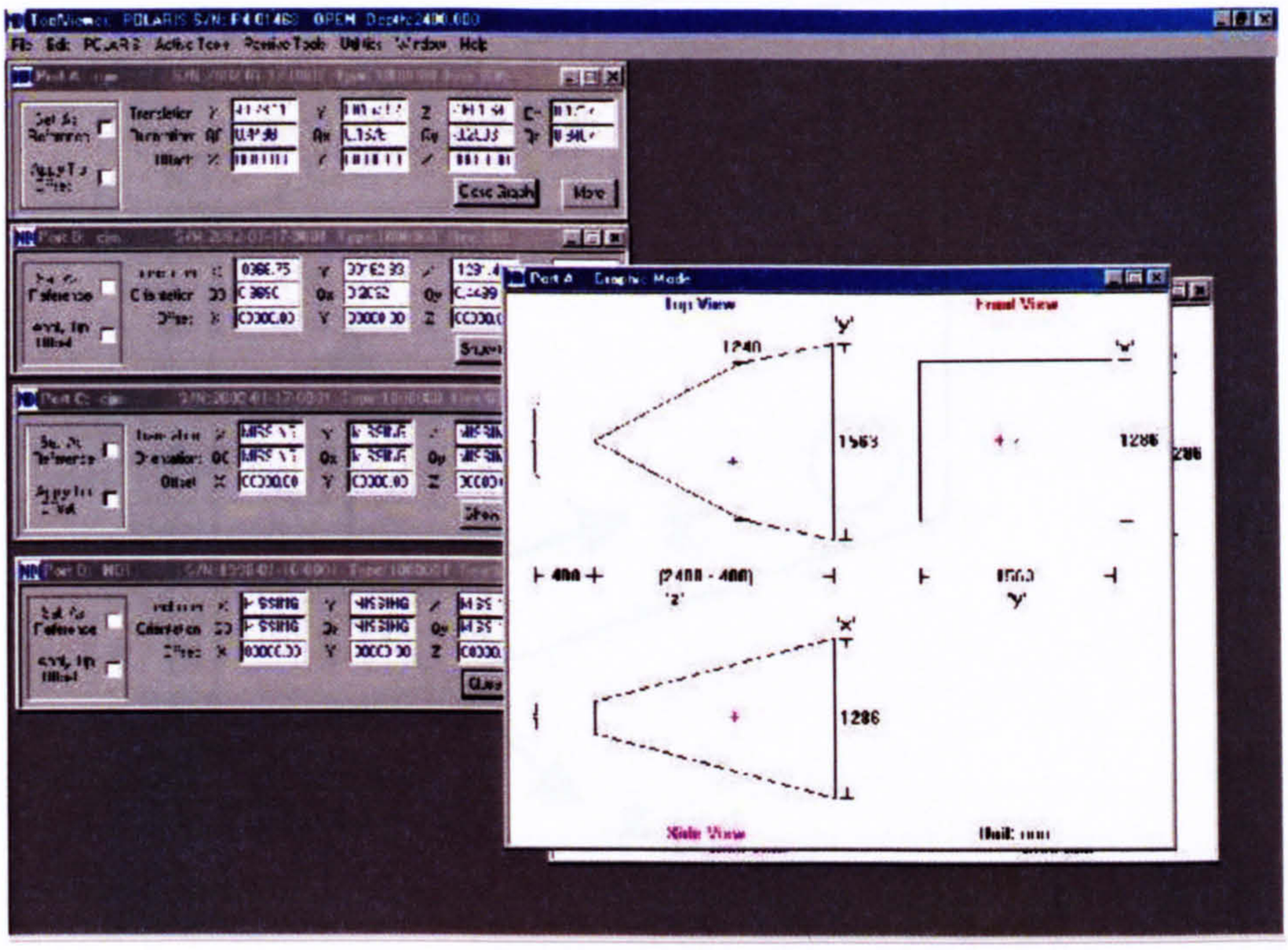

Figure 3.9: A sample ToolViewer screen, illustrating the measurement volume of the Polaris system

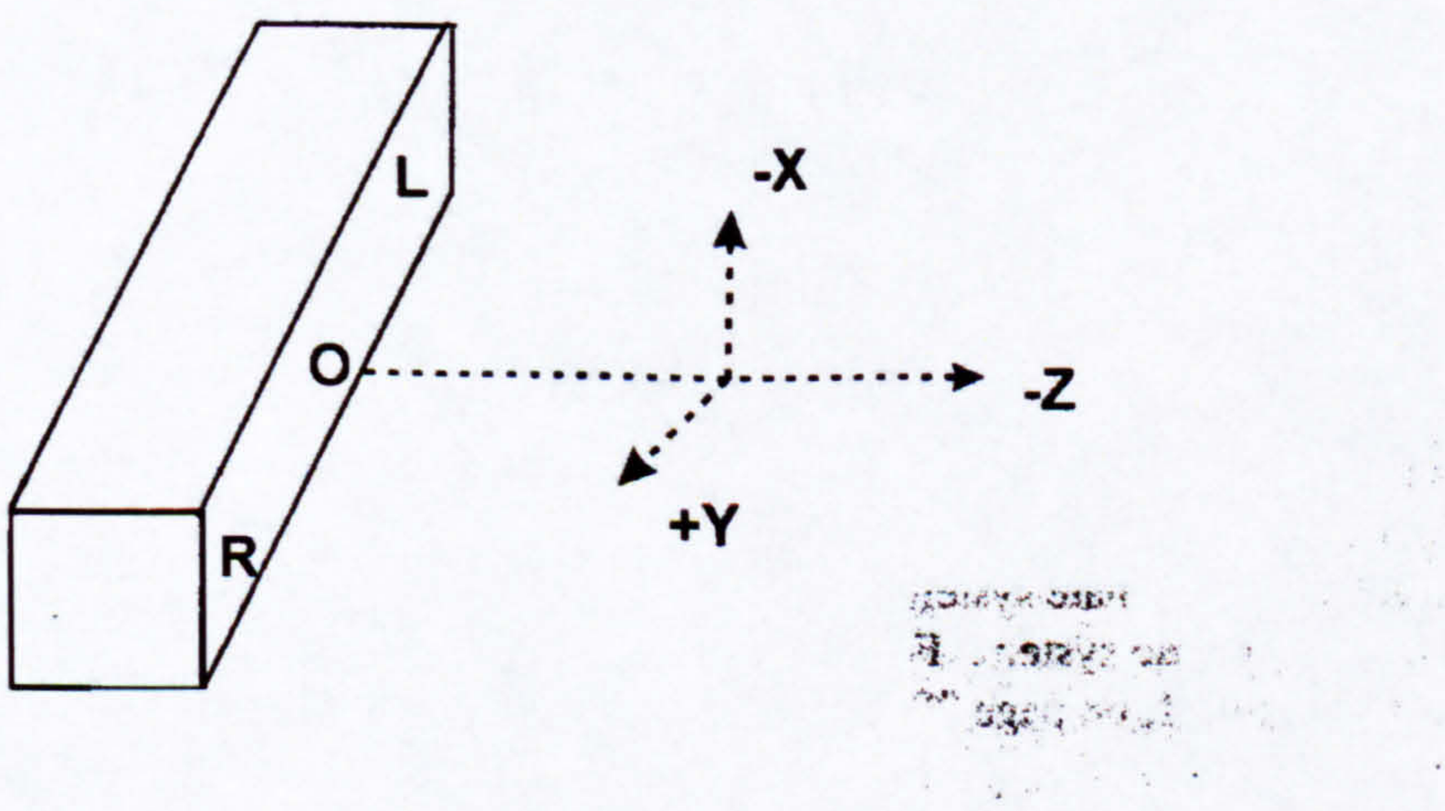

Figure 3.10: The arrangement of the Polaris Global Coordinate System

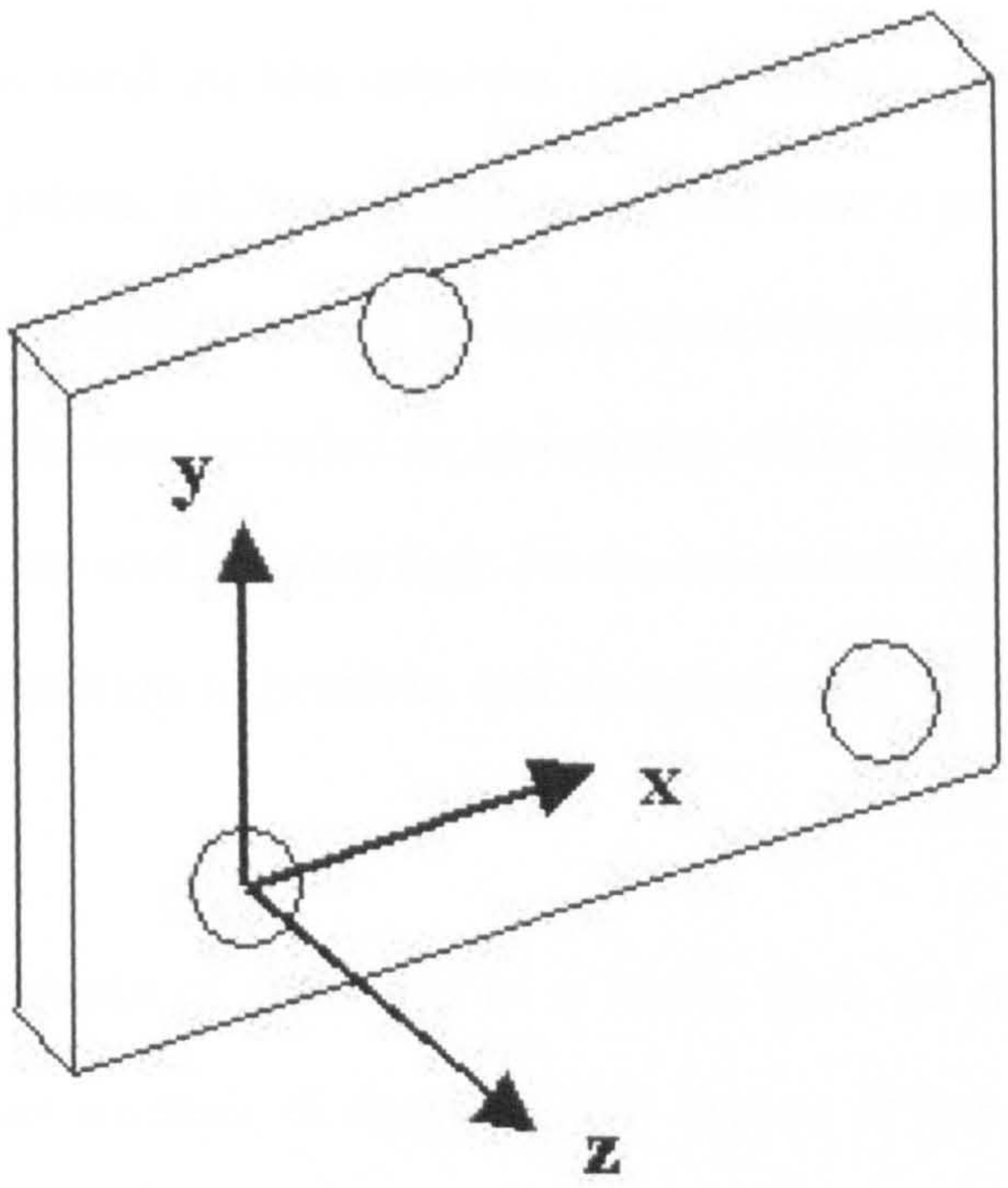

Figure 3.11: A Polaris tool with embedded LCS

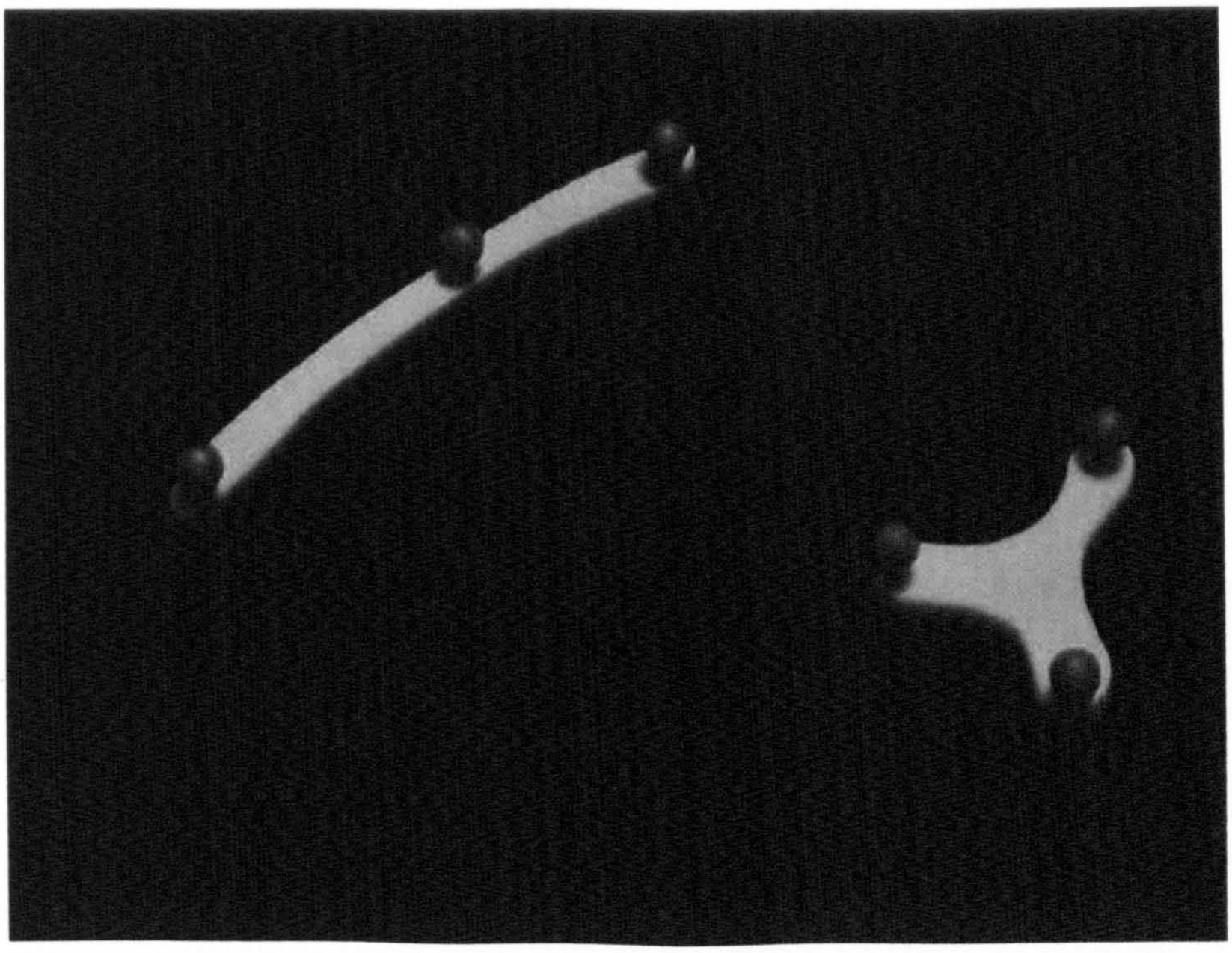

Figure 3.12: The shank tool (left) and the foot tool (right) used to measure ankle movements

electronic noise that affects the system. A systematic error might be optical distortion due to the lenses used on the cameras. A systematic error will tend to affect the accuracy of the system, while a random error will have a greater effect on the precision of the system. Both precision and accuracy were considered throughout the validation process. The validations included an assessment of the effect of environmental variables such as temperature and ambient light levels, measurements on static tools rotated and translated from position to position and an assessment of the dynamic performance of Polaris.

For the measurements of rotations of a static tool, an indexing head was used to rotate a tool a set number of degrees. Ten frames of data were recorded from each new position, and Cardan angles were calculated for each position relative to the first; these angles were then averaged. Figure 3.13 shows the rotation about the z-axis, set in 30^o steps using the indexing head, plotted against the rotation measured using Polaris. The relationship is almost exactly linear, as evidenced by the regression equation. A similar procedure was undertaken for linear movements, using the numerical readout from an $X - Y$ axis milling machine to position the tool in 10 mm steps, again recording 10 frames of data from each position and averaging. A graph of measured versus input translation along the x-axis of the tool is presented in Figure 3.14. Once again, a near-ideal linear relationship can be observed.

The results presented above are only two examples of results obtained as part of the validation process. Although they are impressive, it is important to remember that they only concern static measurements. When data were recorded from two tools fixed relative to each other on a plate as it was moved manually about the measurement volume, greater variations were observed, particularly in the z-coordinate. The mean value of z was 0.48 and the standard deviation was 0.52. It is important to note that any motion analysis system would be expected to perform better for static than

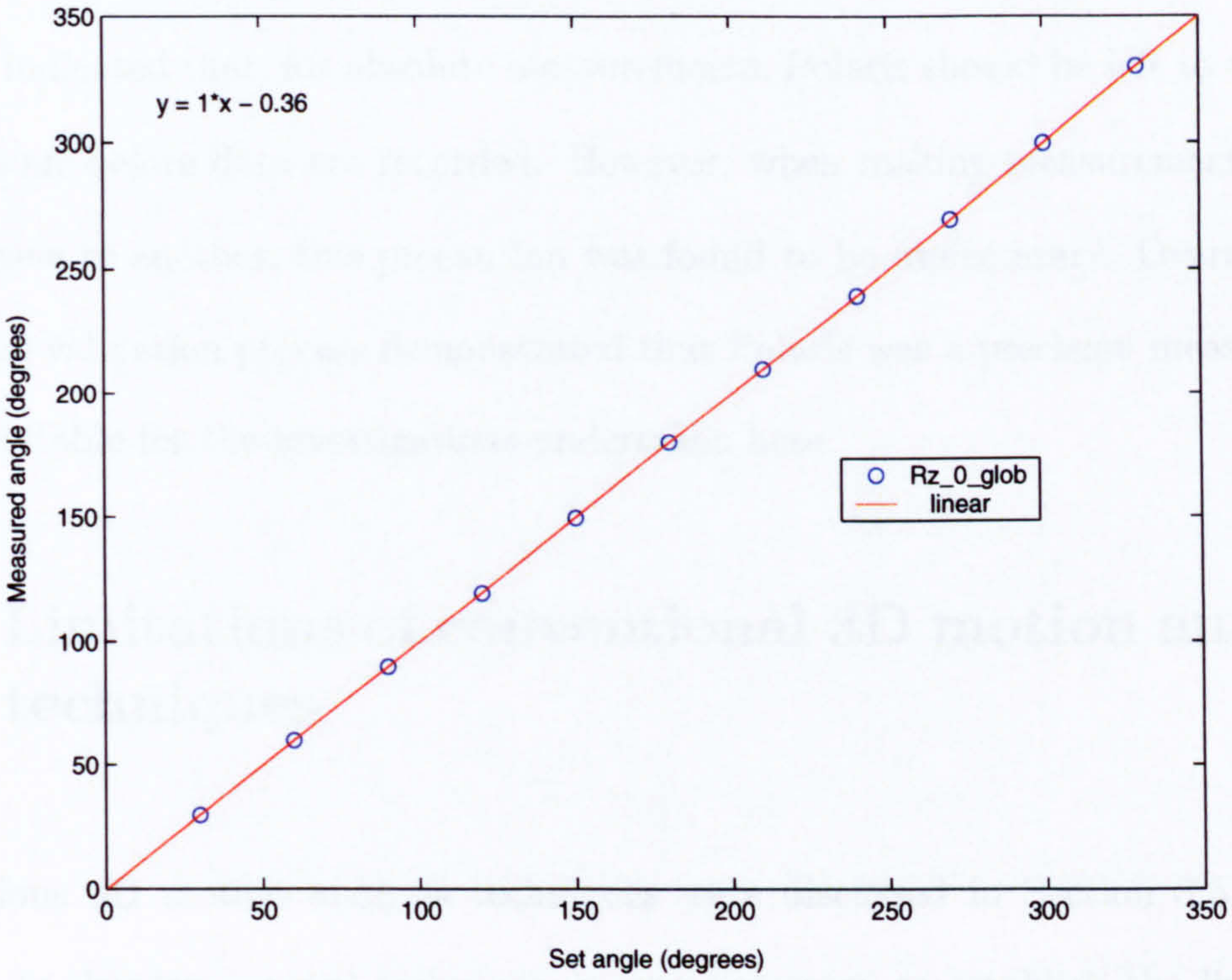

Figure 3.13: Graph of measured versus input roll angle with regression line

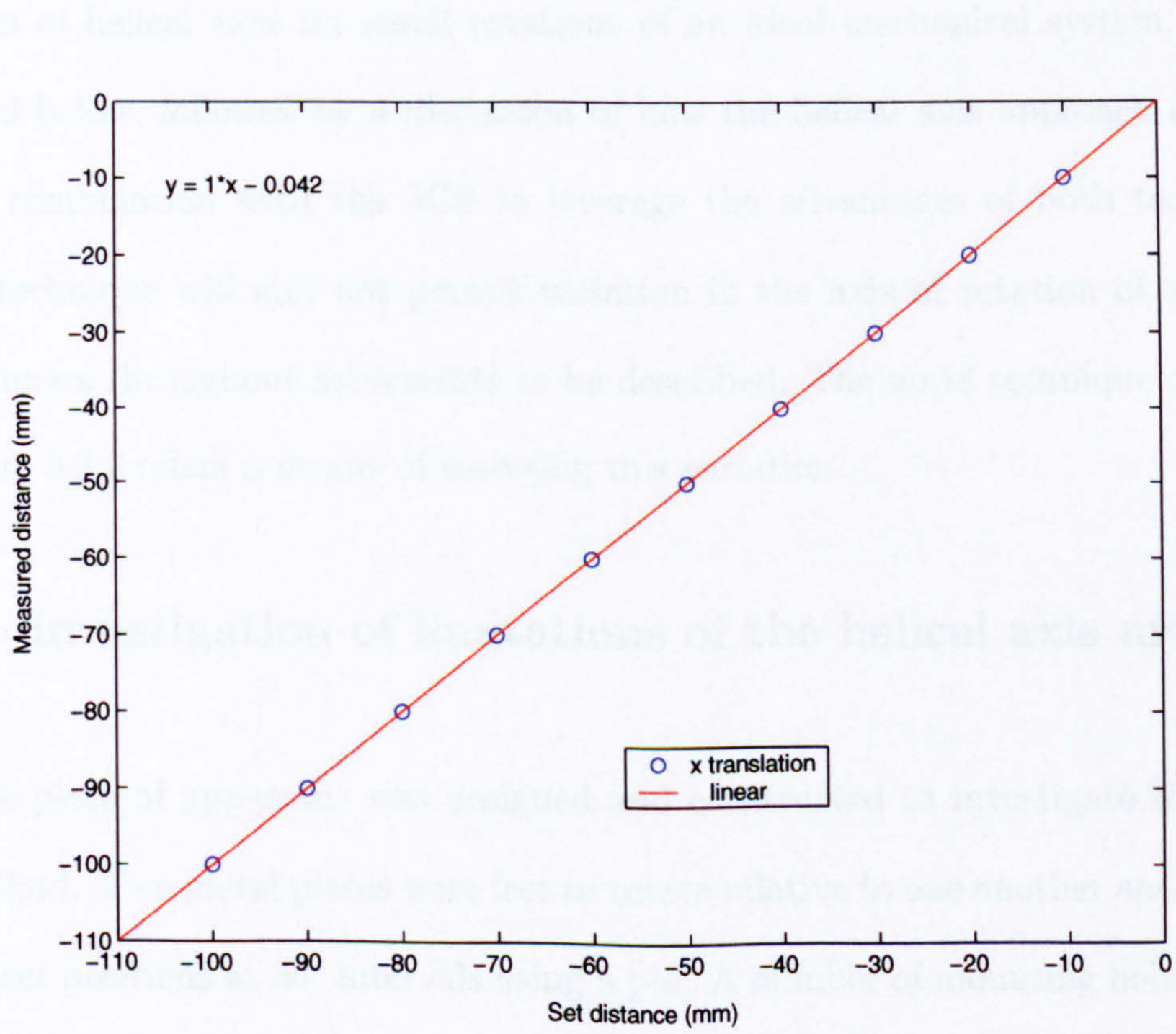

Figure 3.14: Graph of measured versus input translation, positive x-axis of tool aligned with direction of movement

dynamic measurements. It is perhaps worth noting that the investigations of thermal stability indicated that, for absolute measurements, Polaris should be left to warm up for one hour before data are recorded. However, when making measurements of one tool relative to another, this precaution was found to be unnecessary. Overall, then, this initial validation process demonstrated that Polaris was a precision measurement system suitable for the investigations undertaken here.

3.7 Limitations of conventional 3D motion analysis techniques

The various 3D motion analysis techniques were discussed in Section 3.5. Before deciding to develop a novel technique, it was necessary to establish the limitations of these existing methods. A logical point of departure was an investigation of the definition of helical axes for small rotations of an ideal mechanical system. This is described below, followed by a discussion of how the helical axis approach might be used in combination with the JCS to leverage the advantages of both techniques. Such a technique will still not permit variation in the axis of rotation of the ankle joint complex throughout movements to be described. The novel technique described in Section 3.8.2 offers a means of assessing this variation.

3.7.1 Investigation of limitations of the helical axis method

A simple piece of apparatus was designed and constructed to investigate the helical axis method. Two metal plates were free to rotate relative to one another and could be fixed in set positions at 36° intervals using a pin. A number of mounting holes allowed markers to be arranged in a variety of ways, making up tools with different geometries. Tracking one tool on each plate allowed the rotations to be measured. The mounting

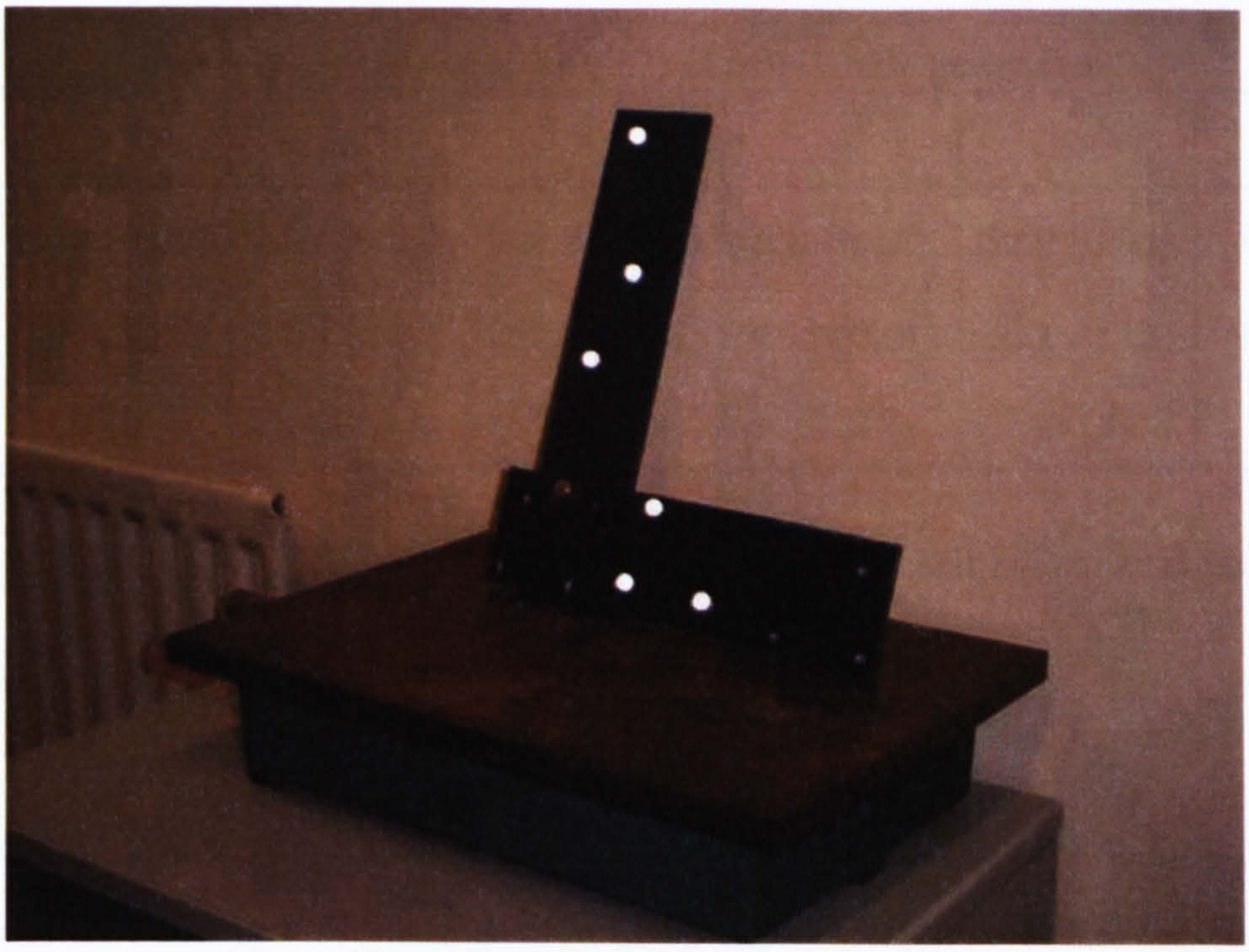

Figure 3.15: The tool used to validate the helical axis approach

holes were drilled using a numerical readout milling machine, so that the location of the axis of rotation relative to origin markers was known. The equipment is shown in Figure 3.15.

Throughout this work, the Matlab routine written by Christoph Reinschmidt based on Spoor and Veldpaus (1980) was used to calculate helical axis parameters. This routine is freely available on the ISB website. The input arguments required are a 4x4 transformation matrix describing the transformation that is of interest, and a number to identify which plane will be used to describe the point of intersection of the axis. The routine returns the direction vector, n, of the helical axis, the point p on the helical axis where it intersects the chosen plane, the angle of rotation about the helical axis (ϕ) and the translation along the axis (t).

Measurements were made of two tool configurations on one plate relative to a fixed tool on the other plate. Measurements were made at the fixed positions, for increasing and decreasing angles. This was done in order to prove that the measurement equipment

Table 3.1: Table of mean (SD) of helical axis parameters

	n1	n2	x	y	theta	t
Pos 1	0.01 (0.01)	0.03 (0.02)	269.9 (0.37)	9.9 (0.16)	36.0 (0.05)	-0.15 (1.1)
Pos 2	0.02 (0.02)	0.03 (0.02)	269.9 (0.23)	9.94 (0.21)	36.1 (0.11)	-0.21 (0.86)
Ideal	0 (0)	0 (0)	270 (0)	10 (0)	36 (0)	0 (0)

Table 3.2: Table of means and standard deviations of selected helical axis parameters

	n1	n2	n3	x	y
Ideal	0.0	0.0	(-)1.0	270.0	10.0
Mean	0.02	0	-0.06	237.8	32.6
Standard Deviation	0.59	0.36	0.72	530.2	530.3

and software were performing satisfactorily. The means and standard deviations of the helical axis parameters calculated from the measurements are presented in Table 3.1. As can be seen by comparison with the ideal values in the third row of figures, the performance of the system for static measurements of large rotations was very good.

The next step was to investigate how well the helical axis approach described sampled continuous motion. The two plates of the testing tool were rotated relative to one another and the movement was recorded; helical axis parameters were calculated from the results describing the relative rotations. The means and standard deviations of the three components of the helical axis direction vector ($n1$, $n2$ and $n3$) and the x and y co-ordinates of the point of intersection of the axis with the z=0 plane are tabulated in Table 3.2. These parameters were chosen because their values should all be constant and are known for the simple mechanical system. As can be seen, the values calculated from the measurements do not correspond to the expected values, and the standard deviations indicate massive fluctuations. It is clear that the helical axis approach is not suited to the description of continuous movement.

The results from the continuous movement are consistent with previous observations that the HA is ill-defined for small rotations (Woltring, 1994; Cheze et al., 1998; Veldpaus et al., 1988). In order to investigate more closely how the definition of the axis varies with angle an engineering protractor was used to set the angle between the two rotating plates in one degree steps. It was estimated that a positioning accuracy better than 0.5^o was achieved. There was a total of 46 readings. This allowed the helical axis parameters for 45 one-degree intervals, 44 two-degree intervals, 43 three-degree intervals and so on to be calculated. The mean and standard deviation for all of the parameters were calculated using Minitab v.13, so that the stability of the parameters with angle could be plotted.

The most striking results were the variation in the range of the components of the HA direction vector and the intercept with the $y = 0$ plane with angle. As can be seen in Figures 3.16 and 3.17 the range only levelled out at rotations of 10-15^o .

These results demonstrate that, even for an ideal mechanical system with a fixed axis, the helical axis is ill-defined for small angles. For the mechanical system, the parameters stabilise between 10 and 15^o ; Cheze et al. (1998) reported that, for physiological measurements, rotations of greater than 25^o were required in order to achieve reliable results. The relationship between angle of rotation and stability of the helical axis was also investigated for the measurements of continuous motion described above. Figures 3.18 and 3.19 show how the errors in the components of the direction vector and the coordinates of the point of intersection of the axis with the $y-z$ plane vary with helical angle, respectively. These results provide further support for the use of a minimum separation angle of 10^o .

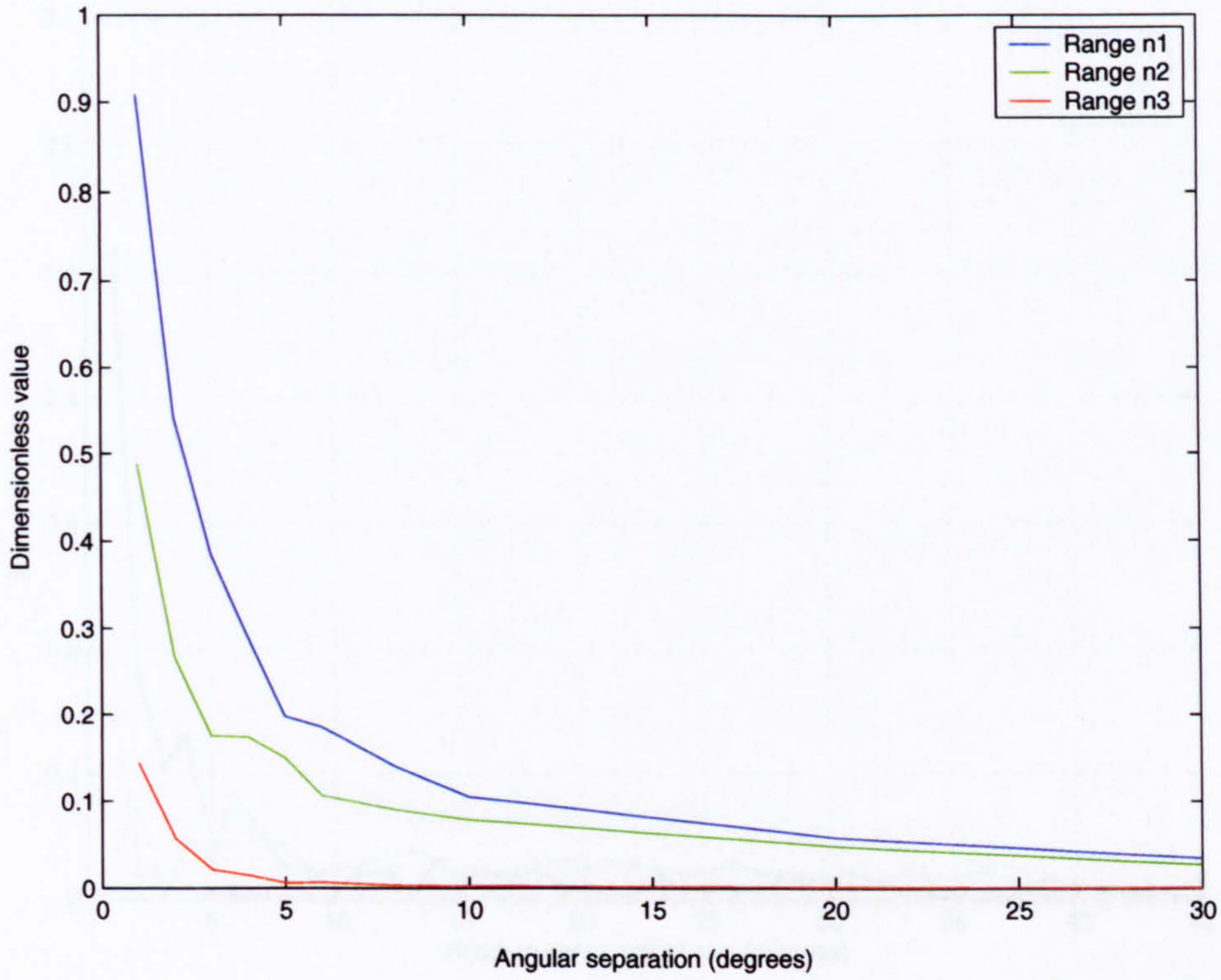

Figure 3.16: Variation in the range of the helical axis direction vector components with angle

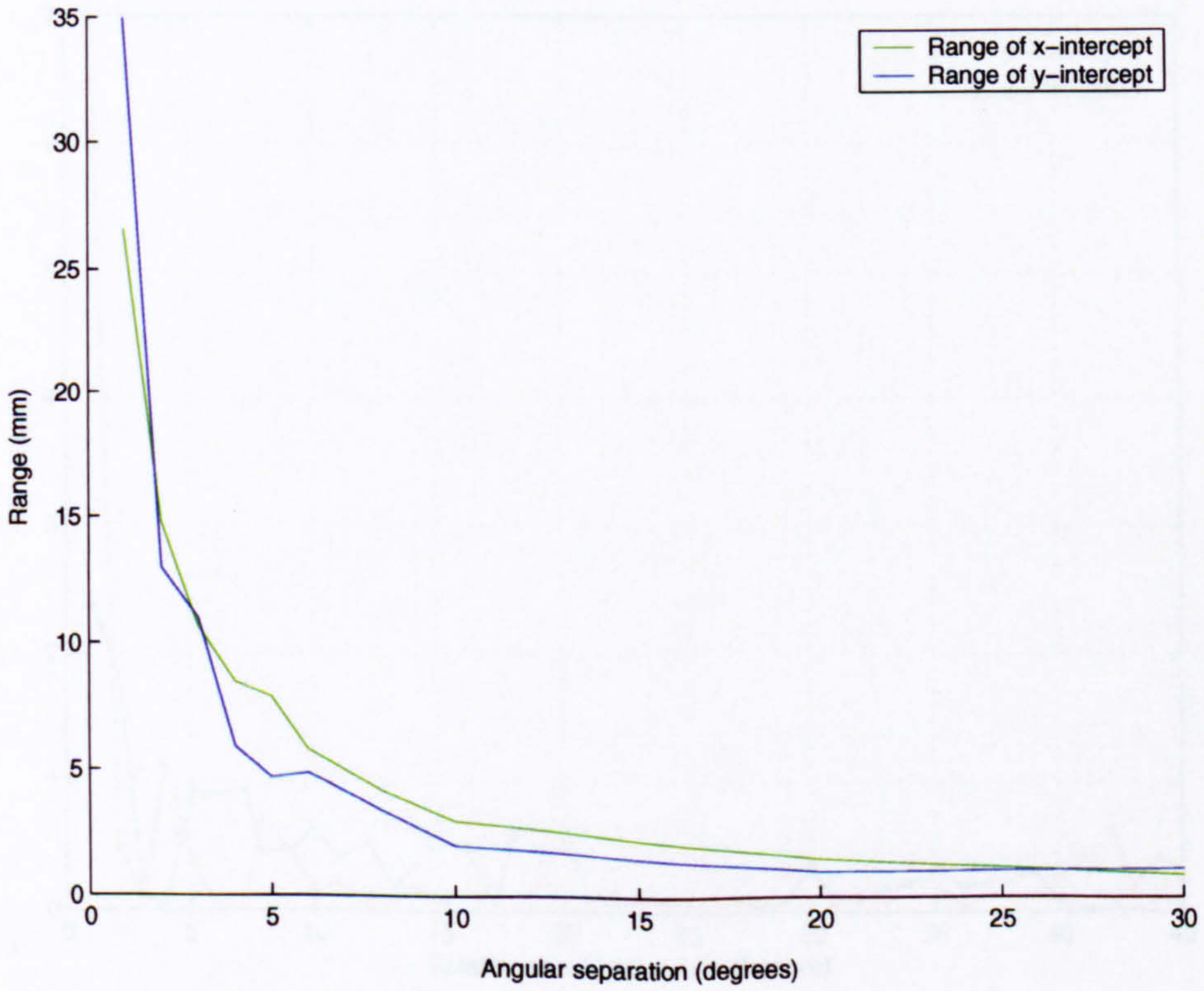

Figure 3.17: Variation in the range of the coordinates of the helical axis intercept with the xy plane with angle

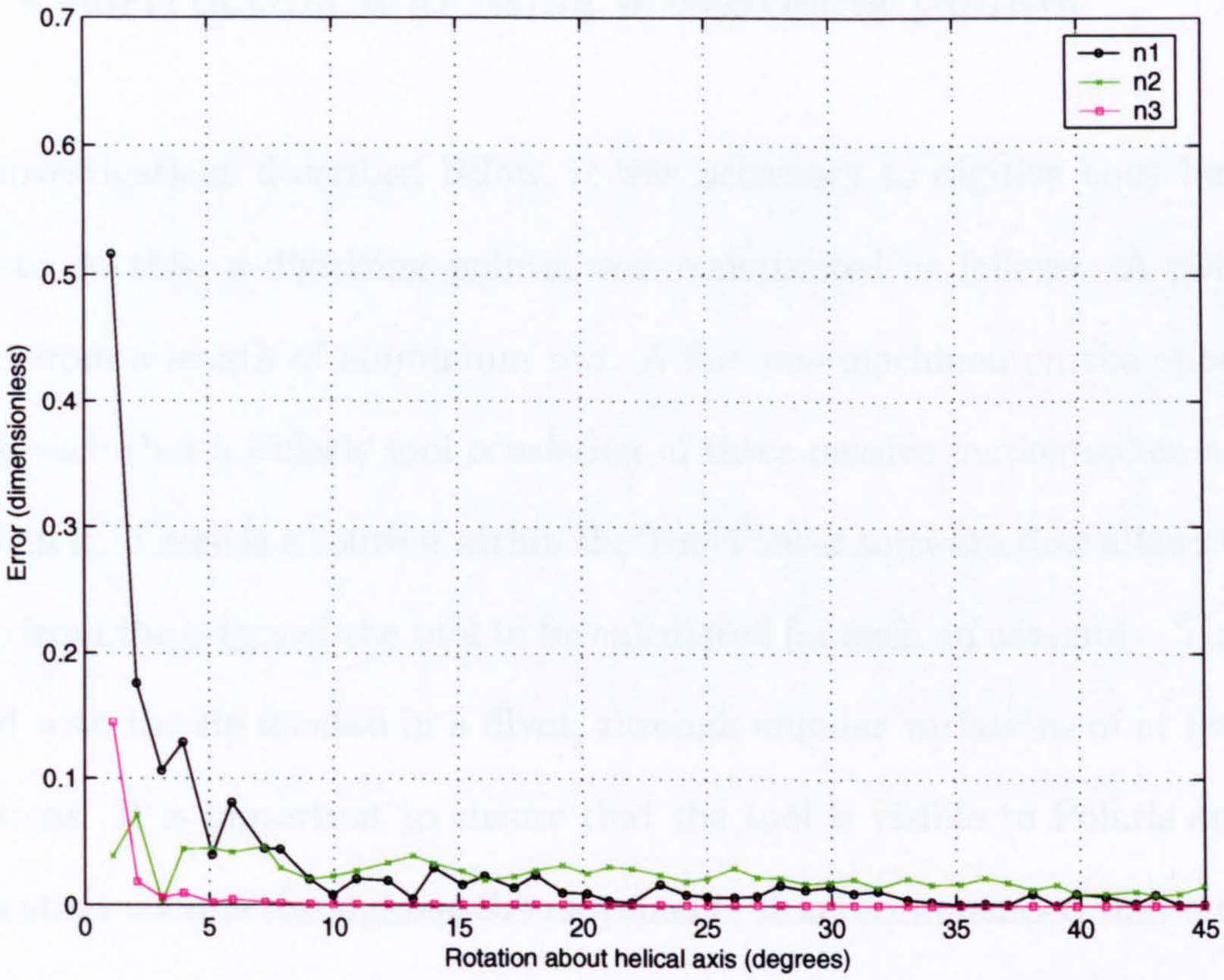

Figure 3.18: Variation of the error in the components of the direction vector with angle of rotation about the helical axis

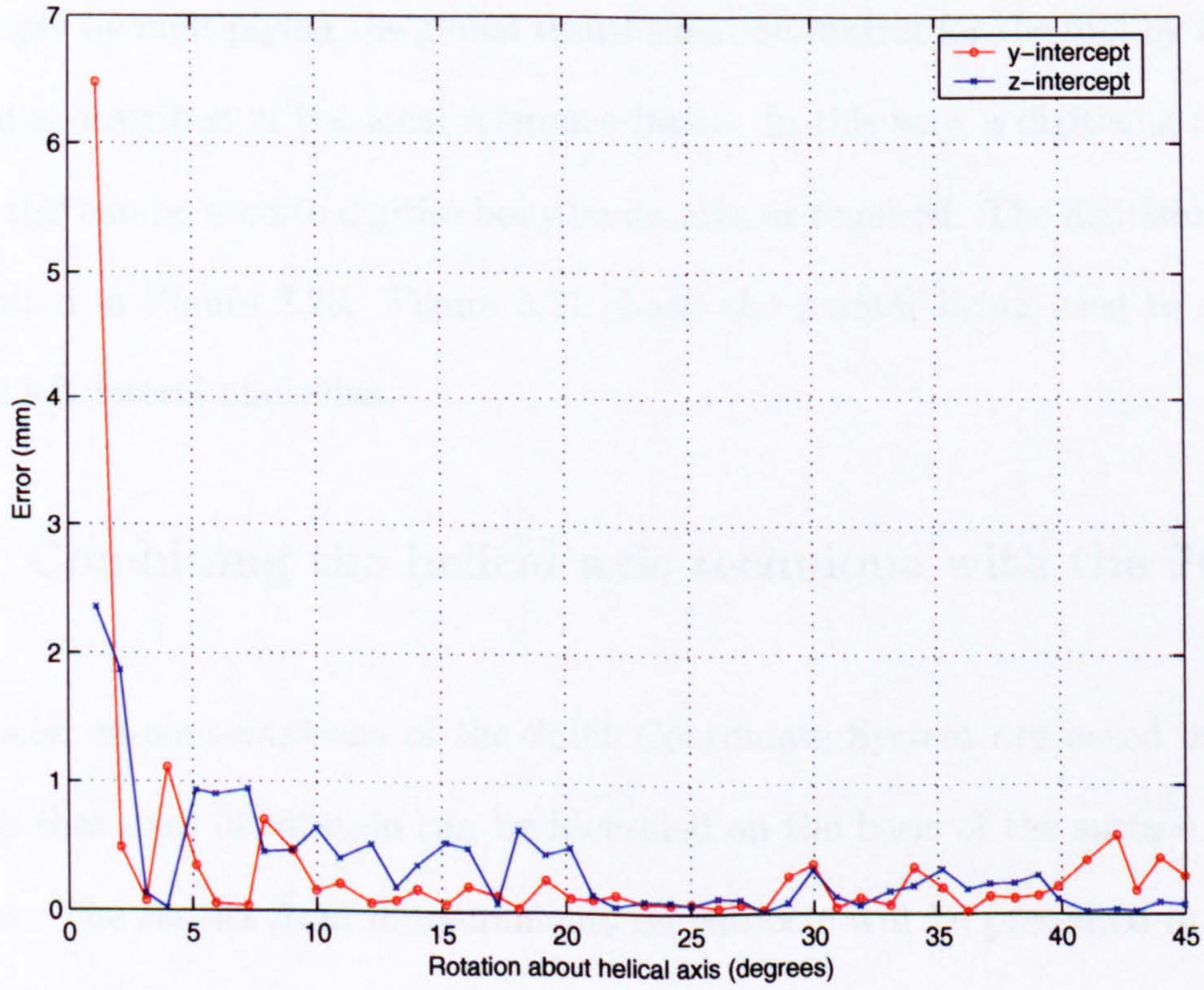

Figure 3.19: Variation of the error in the coordinates of the helical axis intercept with angle of rotation about the helical axis

3.7.2 Constructing and using a digitising pointer

For the investigations described below, it was necessary to digitise bony landmarks. In order to do this, a digitising pointer was constructed as follows. A pointer was machined from a length of aluminium rod. A flat was machined on the opposite end to the tip such that a Polaris tool consisting of three passive marker spheres could be mounted on it. There is a routine within the ToolViewer software that allows the offset of the tip from the origin of the tool to be calculated for such an assembly. The pointer is rotated with the tip located in a divot, through angular variations of at least 30^o in all directions. It is important to ensure that the tool is visible to Polaris and within the calibration volume throughout the movement. It is recommended that a minimum of 400 frames are collected, after which the tip offset is calculated. The software then gives the user the option of applying the tip offset, such that the three-dimensional co-ordinates of the tip are reported rather than the origin of the tool. This is done quite simply by multiplying the global transformation matrix for the tool by the offset coordinates described in the local reference frame. In this way, a digitising pointer is created; this can be used to digitise bony landmarks as required. The digitising pointer is illustrated in Figure 3.20. Figure 3.21 shows the pointer being used to digitise a subject's left lateral malleolus.

3.7.3 Combining the helical axis technique with the JCS

The popular implementations of the Joint Coordinate System are based on the assumption that axes of rotation can be identified on the basis of the surface anatomy of a joint. The results from measurements on subjects will be presented in the next chapter (Section 4.2). They indicate that axes of rotation are not coincident with the IM line and vary from movement to movement. Such variations may be exaggerated in

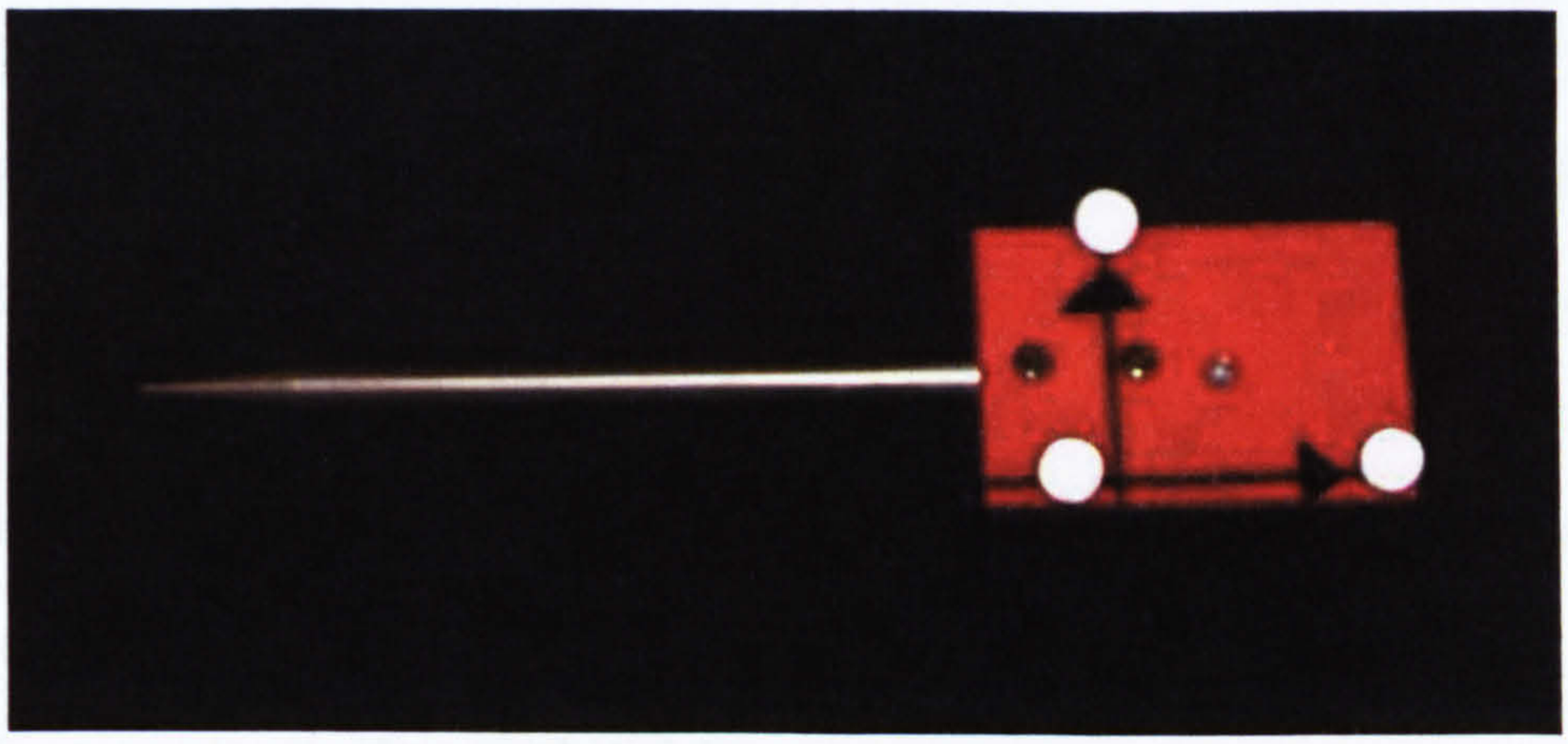

Figure 3.20: The pointer used to digitise bony landmarks

Figure 3.21: The pointer being used to digitise a subject's left lateral malleolus

subjects with ankle pathologies, for example increased joint laxity due to ligamentous damage. In order to tailor motion analysis to an individual, Cheze et al. (1998) suggested that the helical axis technique be used to identify approximate axes of rotation which could be used as the basis for a Joint Coordinate System. Considerable effort went into implementing this hybrid approach for one subject. Although the technique was not used in the rest of the work, the steps taken are described here in some detail, as the ability to customise the JCS to an individual using measured axes has considerable merit. The results used here were collected from one subject during the first series of measurements described in 3.4.

There are five steps in the application of the hybrid method. They are as follows:

1. Determine the talotibial and talocalcaneal joint axes
2. Define the reference frames (LCS's) for the shank and foot
3. Calculate the transformations from the reference frames to the shank and foot tool LCS's
4. Calculate the transformation matrix relating the foot reference frame to the shank reference frame for each sample point
5. Calculate the JCS values

The subject undertook a series of five dorsiflexion-plantarflexion cycles and five inversion-eversion cycles. The two separate axes of rotation for these movements were identified based on the calculation of helical axis parameters between the maxima and minima of the respective cycles. The tibio-talar joint axis was described relative to the shank tool while the talo-calcaneal joint axis was described relative to the foot tool. Having determined these axes (e_1 and e_3 of the JCS, respectively), the floating axis,

e_2, could be calculated. For convenience and generality, the direction vectors of e_1 and e_2 were both transformed to the global coordinate system, before e_2 was calculated as the cross-product of the other two axes. The transformations referred to were achieved by multiplying the direction vectors by the transformation matrices of the tools in the GCS.

The shank and foot reference frames were then defined. Upper case letters denote the axes of the shank reference frame, lower case letters denote those of the foot reference frame. The shank reference frame was described relative to the shank tool, while the foot reference frame was described relative to the foot tool. This facilitated transformation between the coordinate systems. In order to define the reference frames, the locations of the medial and lateral malleoli and the tibial tuberosity were required. These were digitised using the pointer described in 3.7.2 relative to the shank tool and the foot tool at the start of the session. For the shank, the X-axis was taken as the tibio-talar joint axis. A plane was then defined that included this axis and the tibial tuberosity. In practice, the easiest way to do this was to calculate the direction vector of the line from the point of intersection of the df-pf axis with the z=0 plane of the shank tool to the tibial tuberosity (described relative to the shank tool, i.e. in the shank tool LCS). The cross product of this direction vector and the talotibial axis direction vector could then be computed. This defined the Y-axis. The Z-axis was defined as the cross product of the X-axis and the Y-axis, and the origin was taken as the midpoint of the intermalleolar (IM) line.

For the foot, a similar approach was taken. The inversion/eversion axis was the y-axis; the x-axis was calculated as the normal to a plane containing the y-axis and the intermalleolar point, and the z-axis is the cross product of the x- and y-axes. As for the shank, the origin was taken as the midpoint of the intermalleolar line. As the foot and shank reference frames were defined relative to the foot and shank tools,

respectively, the transformation matrices relating the foot reference frame to the foot tool and the shank reference frame to the shank tool were easy to derive. Tx, Ty and Tz are the coordinates of the mid-malleolar point in the shank tool LCS and foot tool LCS, respectively. The rotation matrices are made up of the x, y and z components of each unit vector component in the foot and shank tool LCSs.

Having determined these transformation matrices, they can be multiplied by the recorded transformations of the foot and shank tools. This gives the transformation matrices of the foot and shank reference frames - they are essentially being tracked as virtual tools. The transformation matrices of the reference frames in the GCS can then be combined to obtain the transformation matrix of the foot reference system relative to the shank reference system from one time point to another.

Having obtained this series of transformation matrices, the parameters desired can be calculated from the elements as per Grood and Suntay (1983). The mathematical justification is included in that paper as an appendix; it will not be repeated here. The parameters can be derived in this way because the choice of axes was based on those chosen by Grood and Suntay (1983). It should be noted that the translations described are along the axes of the shank reference system. An example of the results obtained from this subject is presented in Figure 3.22. It is clear how the combinations of angles could be used to compare matched movements. It is also interesting to note that the third angle about the floating axis is small, indicating that the ankle joint complex approximates reasonably well to a two-axis system, and that these axes are well identified using the approach adopted.

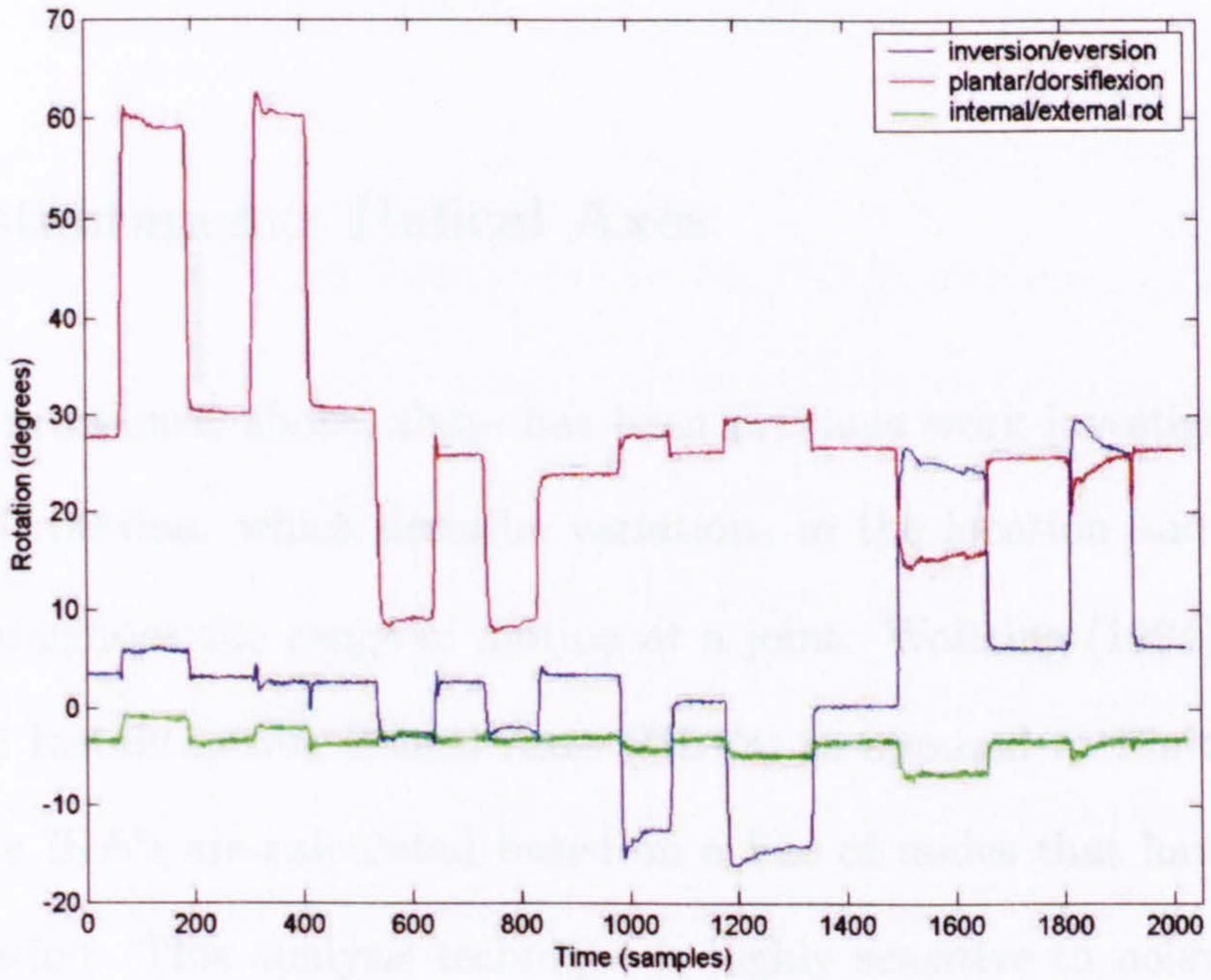

Figure 3.22: Movement matching results: Joint rotations described in a JCS based on Helical Axes

3.8 Describing how the axes of rotation vary throughout joint motion

The combination of the helical axis technique and the Joint Coordinate System described above offers the ability to incorporate an individual's physiology. However, there are still shortcomings. No insight is offered into how the axes of rotation vary throughout motion. Therefore, although this technique might allow us to investigate variations between individuals' approximated axes, as well as the variations in approximated axes between different movements, it does not allow us to investigate any nonstationary characteristics. It is important to remember exactly what the axes calculated represent. They are the helical axis parameters calculated to describe the rotation from the maximally plantarflexed to the maximally dorsiflexed positions. Therefore, that rotation is described as rotation about and translation along a helical axis. However, that axis is a mathematical abstraction, based on the movement

described, rather than a precise, actual axis of rotation.

3.8.1 Instantaneous Helical Axes

As has been mentioned above, there has been previous work investigating instantaneous axes of rotation, which describe variations in the location and orientation of joint axes throughout the range of motion at a joint. Woltring (1994) described the calculation of Instantaneous Helical Axes (IHA's) as opposed to Finite Helical Axes (FHA's). The IHA's are calculated based on a line of nodes that have zero velocity during a rotation. This analysis technique is highly sensitive to noisy data, and requires complex filtering and smoothing in order to achieve meaningful results. The results for the neck in whiplash victims are presented before and after rehabilitation, and a clear difference can be seen in terms of the parallel nature of the axes post rehabilitation. The findings are only from one subject, so no statistical significance is claimed; although the potential utility of such a technique is demonstrated. The IHA approach has also been used by other groups, including Veeger (2000) who calculated instantaneous helical axes for the glenohumeral joint in order to assist in the design of prostheses; Stokdijk et al. (1999) attempted to do the same for the elbow joint. For the glenohumeral joint, the point of intersection of the axes was located as the joint centre of rotation. Modelling techniques have also been used to estimate instantaneous axes of rotation for the ankle joint (Demarais et al., 2002; van den Bogert et al., 1994). None of these techniques is without drawbacks, and all involve a considerable degree of complexity. The proposals that follow outline an alternative method that allows the variation in an axis to be assessed in a relatively simple manner.

3.8.2 Sequential Finite Helical Axes

It has been demonstrated (Section 3.7.1) that a large amplitude of rotation is required in order for finite helical axis parameters to be well-defined. By satisfying this requirement, any information about what happens between the sample points separated by the appropriate number of degrees is lost. The alterative approach that will be discussed here is the calculation of sequential Finite Helical Axes (seqFHAs). This involves calculating the helical axis parameters describing the relative rotation between two tools (sets of markers) between the first frame and successive frames until a suitable rotation is achieved. This is explained in greater detail below.

3.8.3 Discussion of technique

Polaris records frames of data. For each frame, the transformations of all tools (collections of markers) that are within the measurement volume and are visible are calculated. As has been discussed previously, although these transformations are reported in Polaris' native quaternion format, the conversion to transformation matrices is straightforward. Therefore, considering the scenario of two tools, which will be referred to as Tool A and Tool B, one located either side of a joint, for each frame two transformation matrices are recorded. The transformation matrices for Tools A and B describe the orientation and location of the tools relative to the Polaris GCS. Using the matrix manipulations explained in Section 3.5.3, the transformation matrix describing the transformation from Tool A to Tool B can be derived. Then, a similar technique allows a transformation matrix that describes the transformation of A rel B in frame 1 to A rel B in frame 2. Helical axis parameters for that transformation can then be calculated according to Spoor and Veldpaus (1980).

In order to calculate sequential Finite Helical Axes, the helical axis parameters describing the transformation from A rel B in frame 1 to A rel B in frame 2 are calculated. If the rotation angle about the helical axis is 10^o or greater, then that axis is associated with the first frame. If it is less than 10^o , then the helical axis parameters describing the transformation from A rel B in frame 1 to A rel B in frame 3 are calculated, and so on until an angle of rotation about the helical axis greater than 10^o is calculated, and that axis associated with the first frame. The procedure is then repeated for each of the frames recorded in turn.

Although the axes calculated using this technique are still approximations, and indeed mathematical abstractions, some more information regarding how the axis changes throughout the range of motion is provided. Furthermore, the technique can be used without any filtering of the data, and involves simply repeated application of a well-established, existing method.

3.8.4 Application to the ankle joint complex

The sequential FHA technique can be applied to dorsiflexion/plantarflexion and inversion/eversion at the ankle joint complex. This work focuses only on dorsiflexion/plantarflexion, in order to demonstrate the technique for that movement. Extending this to cover inversion/eversion is an obvious area for further work. Movement of the foot and shank are tracked using Polaris with one tool attached to the foot and one to the shank, as before. The helical axes calculated will therefore be described relative to one of the tools. As the tools will not be placed in identical positions each time, it is necessary and useful to describe the axes relative to the anatomy. Therefore, an anatomical reference frame is constructed for the shank. The positions of the lateral and medial malleoli and the tibial tuberosity are digitised as described previously. The position and orientation of the direction vector of the intermalleolar

line (IM) is calculated from the three-dimensional coordinates of the bony landmarks. This defines the x-axis. The direction vector of a line connecting either of the malleoli to the tibial tuberosity is then calculated (imtt), and a direction vector (p) perpendicular to the plane containing the intermalleolar line and the line connecting the chosen malleolus with the tibial tuberosity is calculated as the cross product of these two. This defines the y-axis. Finally, the z-axis is defined as the cross product of the x and y axes. The origin of the shank anatomical reference frame (ARF) is then taken as the mid-malleolar point.

For future calculations, the transformation matrix that describes the position and orientation of the shank ARF in the Polaris GCS is required. This is easily derived, as the digitisation of the bony landmarks, and therefore the direction vectors describing the axes, are given in the Polaris GCS. As the direction vectors are unit vectors, their magnitude is, by definition, 1. Therefore, the x_{GCS}, y_{GCS} and z_{GCS} components of the x, y and z axes give the direction cosines required to construct the rotation matrix R. These will be referred to as x_1, y_1 and z_1 for the x-axis, with the subscripts 2 and 3 used to identify the corresponding components of the y- and z-axes. The coordinates of the intermalleolar point in the Polaris GCS, calculated from the digitised coordinates of the medial and lateral malleoli, give Tx, Ty, and Tz. The transformation matrix, then, is as follows:

$$\mathbf{T} = \begin{pmatrix} x_1 & x_2 & x_3 & T_x \\ y_1 & y_2 & y_3 & T_y \\ z_1 & z_2 & z_3 & T_z \\ 0 & 0 & 0 & 1 \end{pmatrix} \tag{3.5}$$

Having defined the shank ARF, the movements of the foot tool relative to the shank ARF can be calculated. The seqFHA approach can then be applied to the resulting

transformation matrices.

3.8.5 Validation

The software used to implement seqFHAs was written in Matlab. In order to demonstrate that the complete measurement system, i.e. Polaris, the communication/data acquisition software and the analysis software achieved what it set out to do, a simple validation procedure was followed. The plates that were free to rotate about a fixed axis described in 3.7.1 and illustrated in 3.15 were pressed into service again. A long bolt was passed through the pivot and the ends of this were digitised in order to ensure that the calculation of the angle between the measured axis and the digitised IM line was calculated correctly. Data was recorded while the plates were manually rotated, as the foot might rotate relative to the shank during a measurement session. The data was then analysed and the variations in the helical axis parameters calculated were noted. Results from this validation are presented in Section 4.3.3.

3.9 Conclusions

As explained in the introduction to this chapter, the work described here has many different components. An experimental protocol for assessing proprioception at the ankle joint complex is presented. Each aspect of that protocol is justified by comparison with previous work or by reference to the background information presented in Chapter 2. A pilot data collection session with a single subject is described in order to demonstrate the practical application of the protocol, although the results are not presented or discussed, except to specify that the motion of the foot and the motion of the shank must be recorded relative to a common GCS in three dimensions. At

this point, then, any technique for the description of three-dimensional motion could be used in order to compare the initial and position-matching movements made by a subject. Therefore, this is an endpoint in itself. Furthermore, the protocol described could be easily adapted to investigate proprioception at other joints.

The next consideration was which method of describing three dimensional movement would best suit this application. One of the principal criticisms of previous investigations was the restriction of motion to a fixed-pivot, single degree of freedom system. The JCS approach, while providing full three-dimensional description of the movement, also assumes fixed axes of rotation, and for the ankle joint the intermalleolar line is commonly taken to be the dorsiflexion/plantarflexion axis of rotation. A summary of results from a series of subjects indicates that the axis of rotation and the intermalleolar line are not coincident for the subjects investigated, and therefore should not be generalised to be so. The results from these investigations are presented in greater detail in Chapter 4. An alternative technique, the helical axis approach, is then considered, and the inability of the technique to cope with small angular rotations is demonstrated using a simple mechanical system. The possibility of combining the two techniques, using the helical axis approach to define the axes of a joint coordinate system is then considered. This has been suggested before (Cheze et al., 1998), but no description of its implementation was presented. To the author's knowledge, such a technique has not previously been proposed to describe ankle motion. The detail of how this can be done is included and preliminary results from a proprioception testing session are presented. Although this work moves on to consider ways of describing how the axes of rotation vary, the ability to construct a Joint Coordinate System based on measured axes is significant in itself.

In accordance with Lundberg et al. (1989a), initial results from subject testing (see Section 4.2) indicated that the axis of rotation should not be assumed to be coincident

with the intermalleolar line for all subjects and all movements. The work described in this chapter moved on to consider how the axes might vary throughout motion. Although there are existing techniques that could be employed, they are not without complication, and a novel approach is described. The results of implementing this technique to investigate how axes vary in dorsiflexion/plantarflexion under different loading conditions are presented in the next chapter, as well as preliminary results obtained by employing this approach to describe positioning and repositioning movements for proprioceptive testing.

Chapter 4

Presentation of Results

4.1 Introduction

The original focus of this work was the investigation of factors that affect proprioception at the ankle joint complex. In order to comprehensively assess proprioception, it was concluded that three-dimensional motion analysis was required. The existing motion analysis techniques were evaluated, and it was decided that a variation on the helical axis technique would be investigated. The variation, termed the Sequential Finite Helical Axis (seqFHA) technique, was described in some detail in the previous Chapter. The justification for developing this technique was based on the fact that movement at the ankle joint complex, as at all other joints in the body, is a result of joint moments generated by muscles acting across a joint. Moments are associated with an axis of rotation, so that a technique that estimates how the axis of rotation of a joint varies is clearly of value.

The Joint Coordinate System (JCS) is frequently used in motion analysis. For the ankle joint complex, the intermalleolar (IM) line is commonly used as one of the

the axes about which the JCS is constructed. When considering this approach, the question naturally arose as to how close an approximation the IM line is to the dorsiflexion/plantarflexion axis of rotation. The first results presented in this chapter are from a series of experiments conducted to answer this question. Having established a method of calculating an axis of rotation based on an individual's movement patterns rather than on their anatomy, one possibility was to construct a JCS based on these physiological axes. However, the value of such an approach is dependent on the degree of variation in axes of rotation throughout movement. The seqFHA technique allows this variation to be estimated. The remainder of the chapter is devoted to the analysis of a variety of results using this approach. A set of results from one subject is presented to illustrate the technique. This is followed by a similar analysis for the validation tool, a hinged mechanical system with a known axis of rotation, to demonstrate the validity of the measurement system and analysis software. A series of results comparing measurements made from the same subjects tested barefoot and then wearing shoes gives an indication of the importance of how markers are attached to the foot, as well as a more complete assessment of the variation of axes. There is then a further series of measurements made to compare different loading conditions and different directions of rotation of the joint, before a section that describes how seqFHAs can be used in the assessment of proprioception at the ankle joint complex.

4.1.1 Subject data

Summary physical data of the test subjects are presented in Table 4.1 below. It should be noted that the subjects were chosen for convenience, in order to develop the techniques described.

Table 4.1: Table of summary physical data of the test subjects

	Gender	Age (years)	Height (m)	Weight (kg)	BMI (kgm^{-2})
Subject 1	Female	24	1.65	56	20.6
Subject 2	Male	39	1.70	79	27.3
Subject 3	Female	34	1.69	57	20.0
Subject 4	Male	39	1.88	93	26.3
Subject 5	Female	29	1.57	70	28.4
Subject 6	Female	37	1.63	64	24.1

4.2 Investigation of axes of rotation relative to the intermalleolar line

In order to investigate the assumption that the dorsi-/plantarflexion axis is coincident with the IM line, data were recorded from three subjects. In a measurement session, subjects performed two series of five cycles of movement from a fully plantarflexed to a fully dorsiflexed position. For subjects 2 and 3, two sessions were recorded on two different days. The minima and maxima of the five cycles (corresponding to the points of maximum dorsiflexion and maximum plantarflexion) were identified manually, and helical axis parameters were calculated between these extremes. The positions of the lateral and medial malleoli were digitised, allowing the direction vector of the intermalleolar line to be calculated. The scalar product of this direction vector and the direction vector of the calculated axis was computed. It was then a trivial exercise to calculate the angle between the calculated axis and the intermalleolar line.

4.2.1 Results

A summary of the results from these experiments is presented in Table 4.2. There was no second session recorded for Subject 1, hence the X's in the table. It is evident that all results are non-zero, indicating that the calculated axes are not coincident with the IM line, and that there is variation between subjects and between attempts. The

Table 4.2: Table of average angles in degrees between intermalleolar line and calculated helical axes for all subjects

	Subject 1	Subject 2	Subject 3
Session 1 Attempt 1	14.2	15.6	8.6
Session 1 Attempt 2	9.6	18.5	15.4
Session 2 Attempt 1	X	11.5	22.7
Session 2 Attempt 2	X	18.0	4.3

variations could be ascribed to the way in which the intermalleolar line was digitised. However, although only summary data is included here, variations between results from individual cycles observed (ranges up to 10^o) within the same series indicate that this is not the sole source of variation. Differences between subjects support the argument for a more personalised assessment of joint axes than an anatomical generalisation. However, the overall conclusions that can be drawn from these results are limited for reasons that are discussed below.

4.2.2 Limitations

There are three significant limitations to a description of axes based on an interpretation of the above results. The first is that the axes are calculated based on only two frames of data, one at the point of maximum dorsiflexion and one at the point of maximum plantarflexion. Therefore, there is no information regarding what happens between these points. The axes thus calculated are too crude an approximation to draw any useful conclusions regarding the coincidence or otherwise of the calculated axis of rotation and the intermalleolar line. Furthermore, even relatively small variations in the endpoints of movement can significantly alter the calculated axes, although the movement between the extremes may be repeatable.

The second limitation is that the calculated axes are not completely defined relative to the anatomy. The shank tool is not located with respect to any part of the anatomy,

which limits the usefulness of the results. Until now, we have discussed only the angle between the calculated axes and the intermalleolar line. However, also of interest is the location of the axes in space relative to the intermalleolar line. The helical axis parameters include the direction vectors of the axis and the point of intersection of the axis with a plane - for these results that plane is the $x = 0$ plane of the shank tool. This can be addressed by defining an anatomical reference frame (ARF) as described previously. The ARF is based on the lateral and medial malleoli and the tibial tuberosity. The three axes of the Anatomical Reference Frame (ARF) are then defined as follows: the x-axis is the intermalleolar line (directed medially), the y-axis is perpendicular to the plane defined by the intermalleolar line and a line connecting the lateral malleolus and the tibial tuberosity (directed anteriorly), the z-axis is then calculated as being perpendicular to the x and y-axes and directed superiorly. The z-axis therefore lies in the plane previously defined. The origin of the ARF is defined to be the midpoint of the intermalleolar line. This will be used in subsequent descriptions of axes.

The third and final limitation is that so far, only the magnitude of the angle between calculated axes and the IM line has been considered. Although attractive for reasons of simplicity and ease of visualisation, this approach does not give a unique description of the orientation of the calculated axis.

4.3 The Sequential Finite Helical Axis Technique

4.3.1 Introduction

The Sequential Finite Helical Axis (seqFHA) technique has been described previously. The technique calculates the first stable helical axis parameters associated with each

frame of data, or sample point, in turn. This provides a more detailed picture of variations in the axis of rotation throughout the movement. The locations and orientations of the axes calculated are described relative to the anatomical reference frame for a given subject. The orientation of each helical axis is described by three components of a direction vector, along the x, y and z axes of the ARF, the x-axis being the intermalleolar line. These components will be used in preference to the angle between helical axes and the IM line for the remainder of this chapter. Helical axes are located in space by two coordinates (y and z) of the point of intersection of the helical axis with the mid-malleolar (MM) plane, which is perpendicular to the IM line and passes through the mid-malleolar point. Euler parameters are also calculated for the movement of the shank ARF relative to the foot tool, referenced to the standing position, which allows classic rotation about the IM line to be measured. For any set of measurements, this is plotted against time to give a representation of the movement under investigation, and the various parameters discussed above are plotted relative to this angle. This facilitates comparison between results better than would plotting the results against time.

The first set of results is from barefoot, unloaded, dorsiflexion movements for Subject 1. These illustrate how the various parameters are presented. A series of similar measurements made using a validation tool are then presented; these are included to demonstrate the validity of the technique and the measurement system, including the software. Results from measurements made on five subjects first barefeoot and then wearing shoes are discussed, before a more extensive comparison of measurements recorded from a total of six subjects to compare the effect of different loading conditions (unloaded, squatting and toe raise movements). Finally, the seqFHA technique is used to describe movements recorded from proprioception testing.

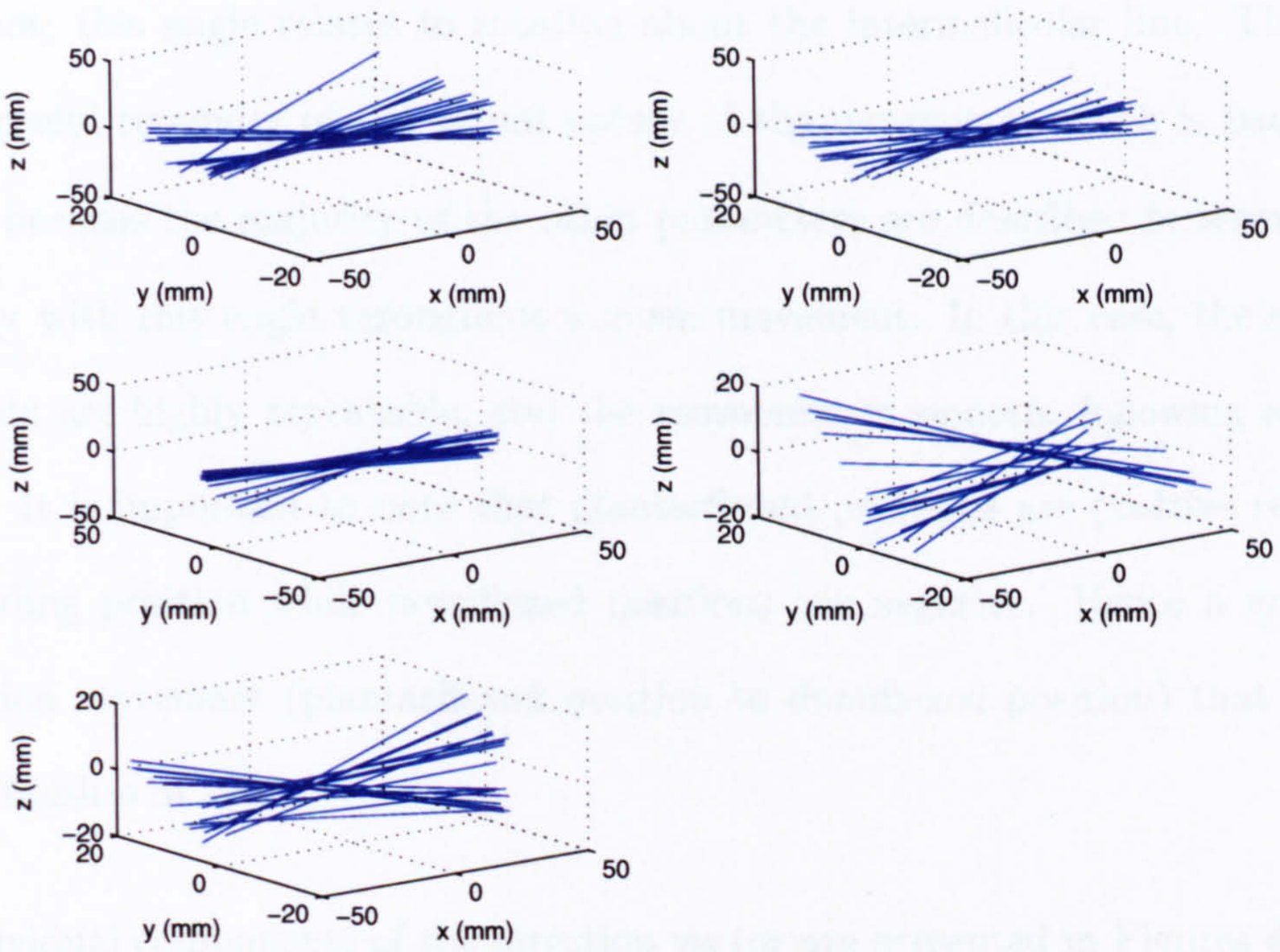

Figure 4.1: Plots of the sequential Finite Helical Axes calculated for Subject 1, for unloaded, barefoot, dorsiflexion movements

4.3.2 Subject 1 - unloaded, barefoot measurements

The results presented here relate to five unloaded dorsiflexion movements made by Subject 1. A summary of the variations in the calculated axes is given by the three-dimensional plots of lines representing the calculated seqFHAs presented in Figure 4.1. The endpoints of these lines are calculated by adding and subtracting arbitrary multiples of the direction vector parameters to the coordinates of the point of intersection. It is very difficult to read useful information from these plots, partly because of the problems of representing a three-dimensional relationship in two dimensions, so that the perspective chosen has a significant effect on the appearance. However, the representation allows a quick eyeballing of the results, and has some value as an overview.

Figure 4.2 shows the graph of angle vs time for the five dorsiflexion movements. The angle is the first of the three Euler angles describing the rotation of the ARF relative

to the foot; this angle relates to rotation about the intermalleolar line. This graph offers a useful reminder of the actual nature of the movement, which is particularly relevant because the majority of the other parameters are described in terms of how they vary with this angle throughout a given movement. In this case, the start and end points are highly repeatable, and the movement is smooth, following a sigmoid pattern. It is important to note that plantarflexed positions are positive relative to the standing position while dorsiflexed positions are negative. Hence a graph of a dorsiflexion movement (plantarflexed position to dorsiflexed position) that starts at 55^o and finishes at -20^o .

The individual components of the direction vector are presented in Figures 4.3 to 4.5. As discussed above, the individual parameters are plotted against angle of rotation about the IM line. There are no helical axes calculated beyond -10^o , although Figure 4.2 shows the dorsiflexion continuing to -20^o , because a minimum rotation of 10^o is required to calculate a stable axis. The vertical scale has been allowed to vary in order to maximise the visibility of any variations. This must be taken into account when interpreting the graphs; for example, the variations in n1 are much smaller than those for n2 and n3. In all five measurements, both n2 and n3 switch from negative to positive, which supports the fanning out seen in the three-dimensional plot of the axes in Figure 4.6. The variations in n1, n2 and n3 are consistent with this pattern; it is interesting to note that there is little or no apparent relationship between these parameters and the position in the movement. Many of the results that will be presented in this chapter vary significantly at the extremes of movements. This is to be expected, as there is a tendency for combined rotations to occur at these extremes. For these results, this effect is most apparent in n1, y and z.

Figures 4.6 and 4.7 show the variations in the y and z values of the intercepts with angle of rotation about the intermalleolar line. A slight downwards trend is seen in the

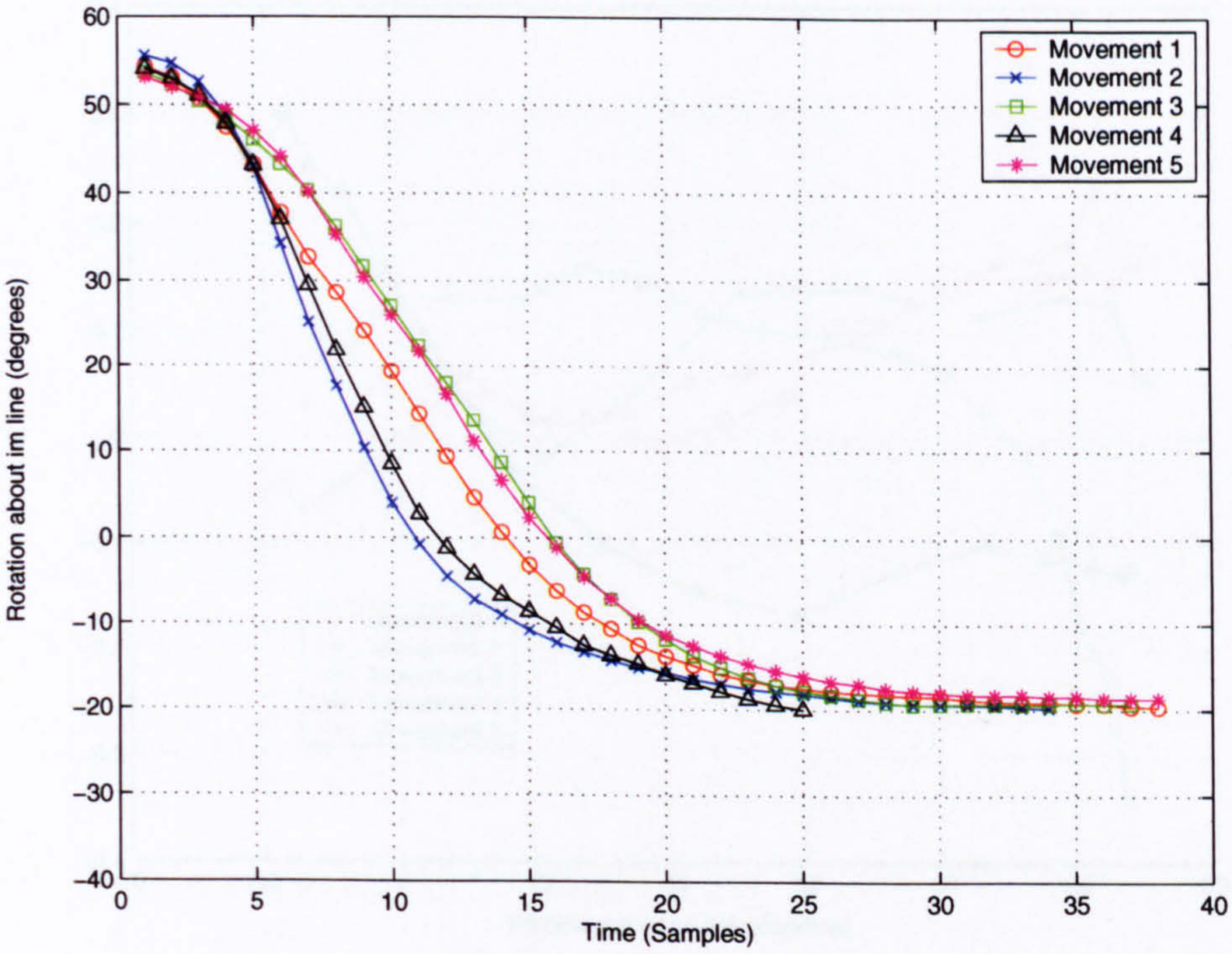

Figure 4.2: Angle vs time: Subject 1, unloaded, barefoot, dorsiflexion movements

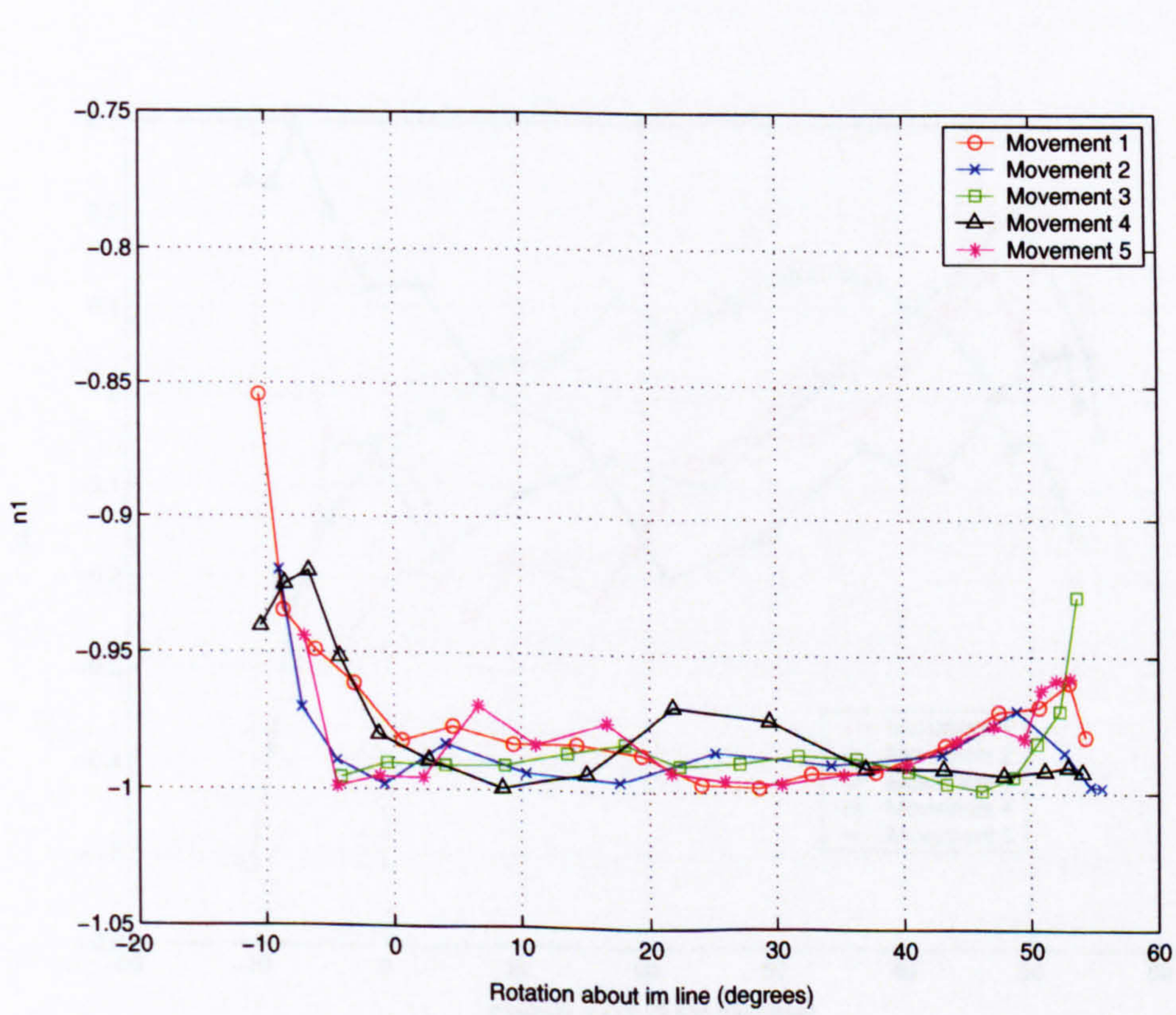

Figure 4.3: n1 values of the seqFHAs: Subject 1, unloaded, barefoot, dorsiflexion movements

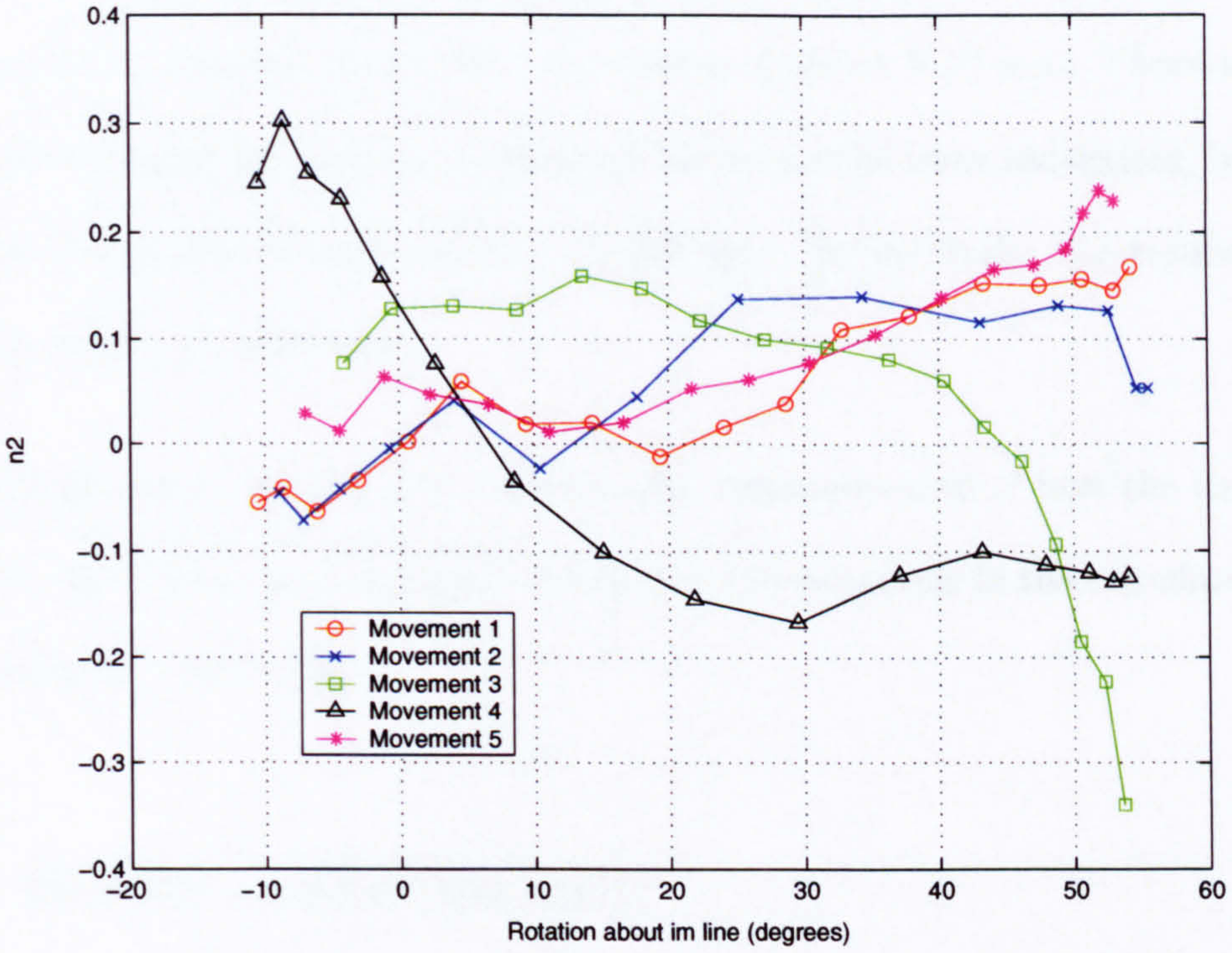

Figure 4.4: n2 values of the seqFHAs: Subject 1, unloaded, barefoot, dorsiflexion movements

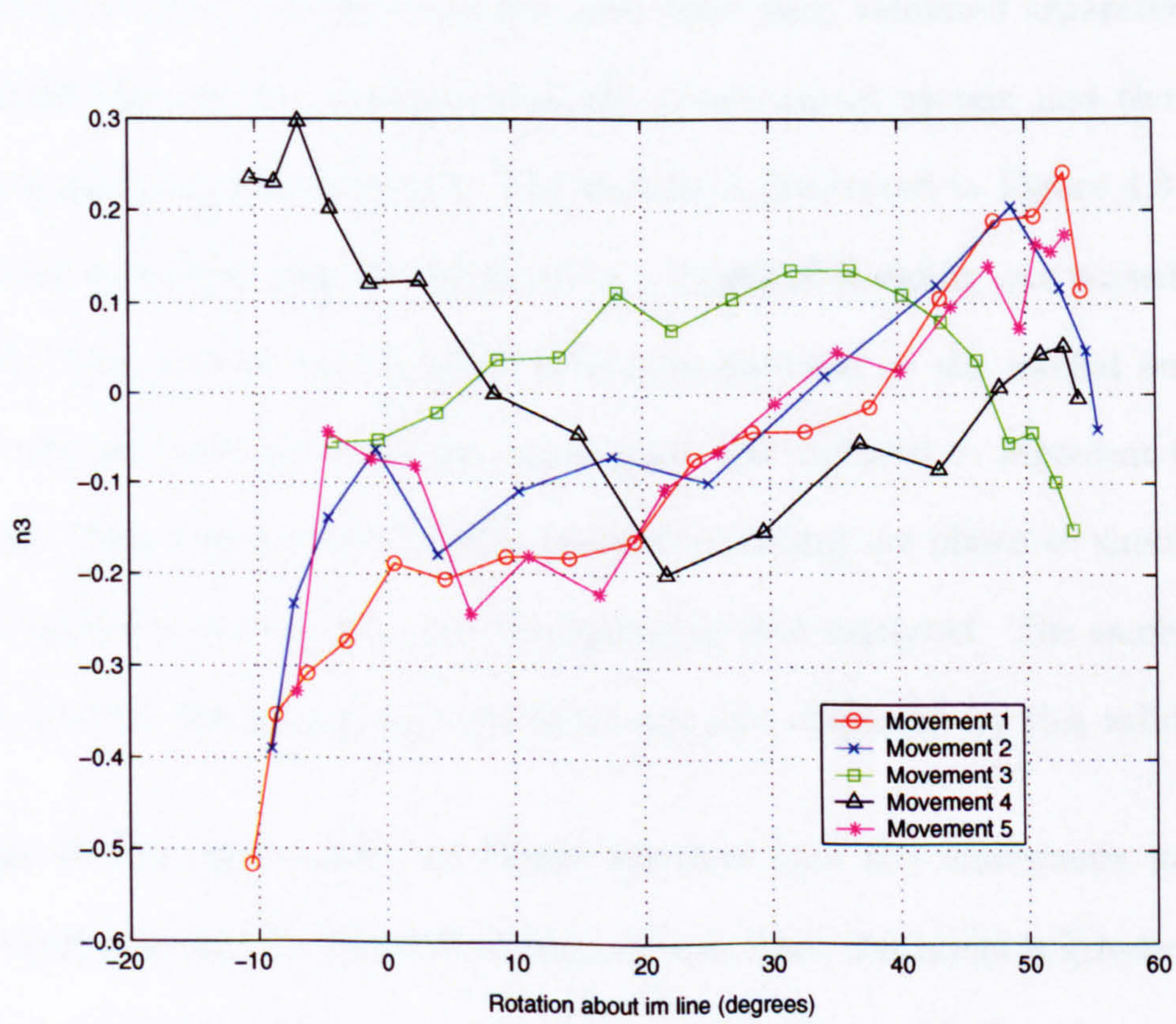

Figure 4.5: n3 values of the seqFHAs: Subject 1, unloaded, barefoot, dorsiflexion movements

y-intercept values moving from plantarflexion (positive angles) to dorsiflexion, relating to an anterior translation of the axis of rotation of about 5-10 mm. There is a more pronounced upwards trend in the z-intercept values for the same movement, indicating a superior translation of approximately 15-20 mm. Subjectively, the results show a reasonable degree of agreement.

The results presented for Subject 1 are a useful demonstration of how the parameters calculated can be presented and used to describe the variations in the calculated helical axis throughout a movement.

4.3.3 Results - validation tool

It seems appropriate at this stage to consider the performance of the system we are using. Various aspects of the technique used have been validated separately, but it is important that we are confident that the measurement system and the analysis software is performing as expected. The apparatus illustrated in Figure 4.8 has previously been described. For this application, a length of studding was passed through the pivot. The ends of the studding were then digitised as the medial and lateral malleoli. An arbitrary point on the upper plate was digitised to represent the tibial tuberosity. Data were recorded whilst manually rotating the plates to simulate individual dorsiflexion movements, and the data were then analysed. The same software that was used for the subject measurements was also employed for this validation.

The angle vs time plots shown in Figure 4.9 show that the movements were made slowly, which accounts for the lack of smoothness. Also, the range is greater than for the subject movements. However, neither of these factors should affect the performance of the system. The components of the direction vector (Figures 4.10 to 4.12) show only very small variations. The axis scaling is the same as that used for the subject

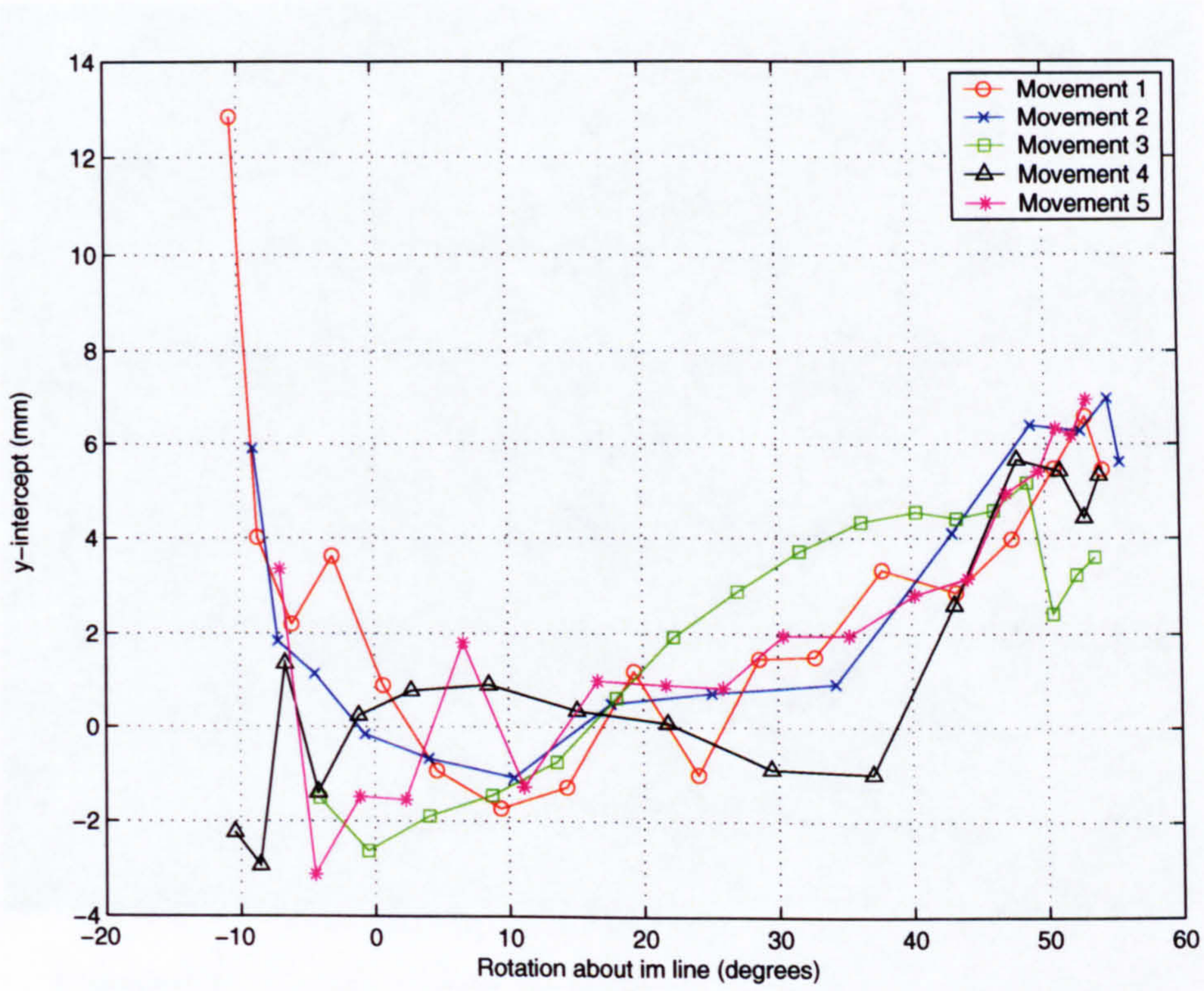

Figure 4.6: y-intercept values of the seqFHAs: Subject 1, unloaded, barefoot, dorsiflexion movements

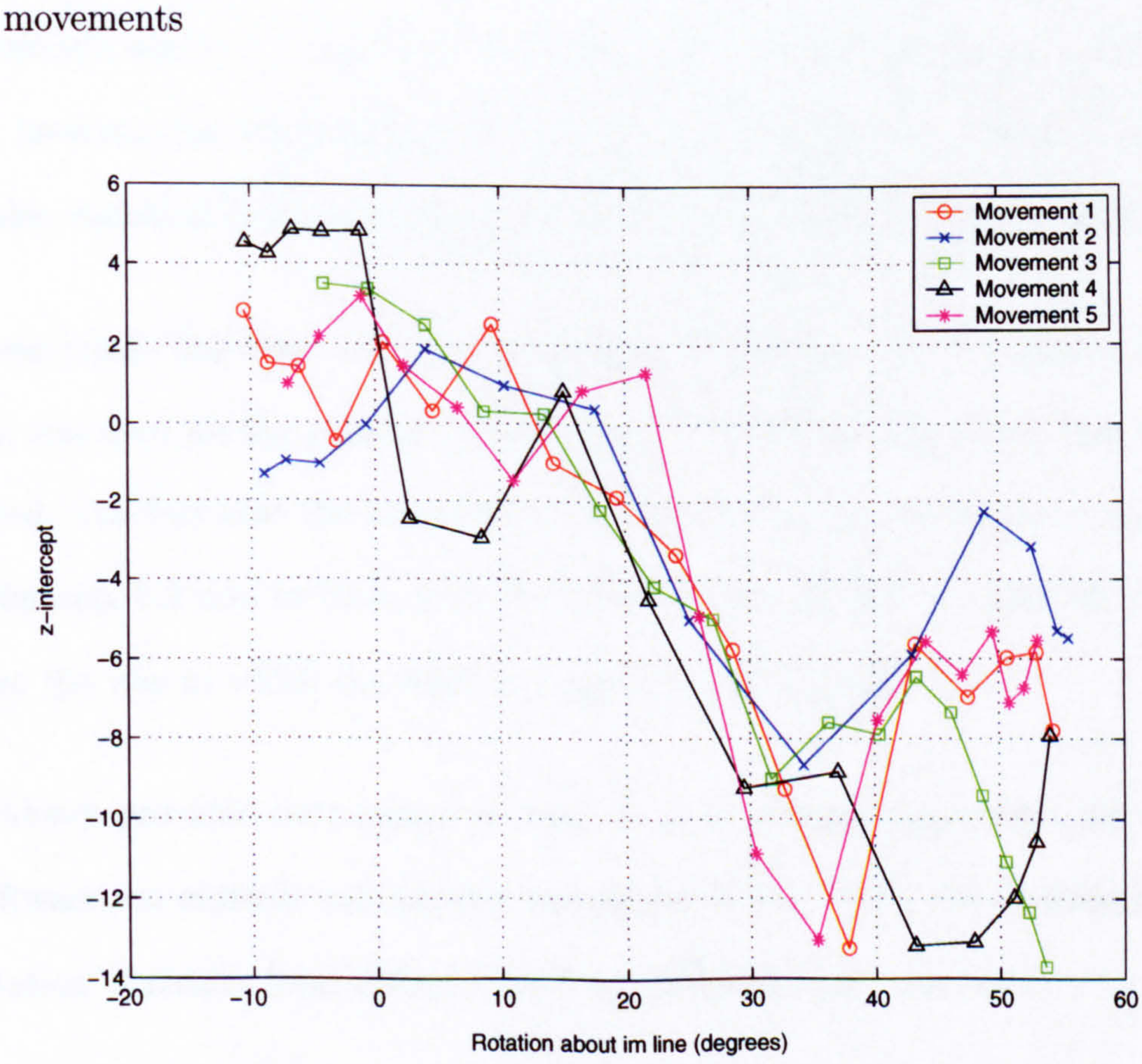

Figure 4.7: z-intercept values of the seqFHAs: Subject 1, unloaded, barefoot, dorsiflexion movements

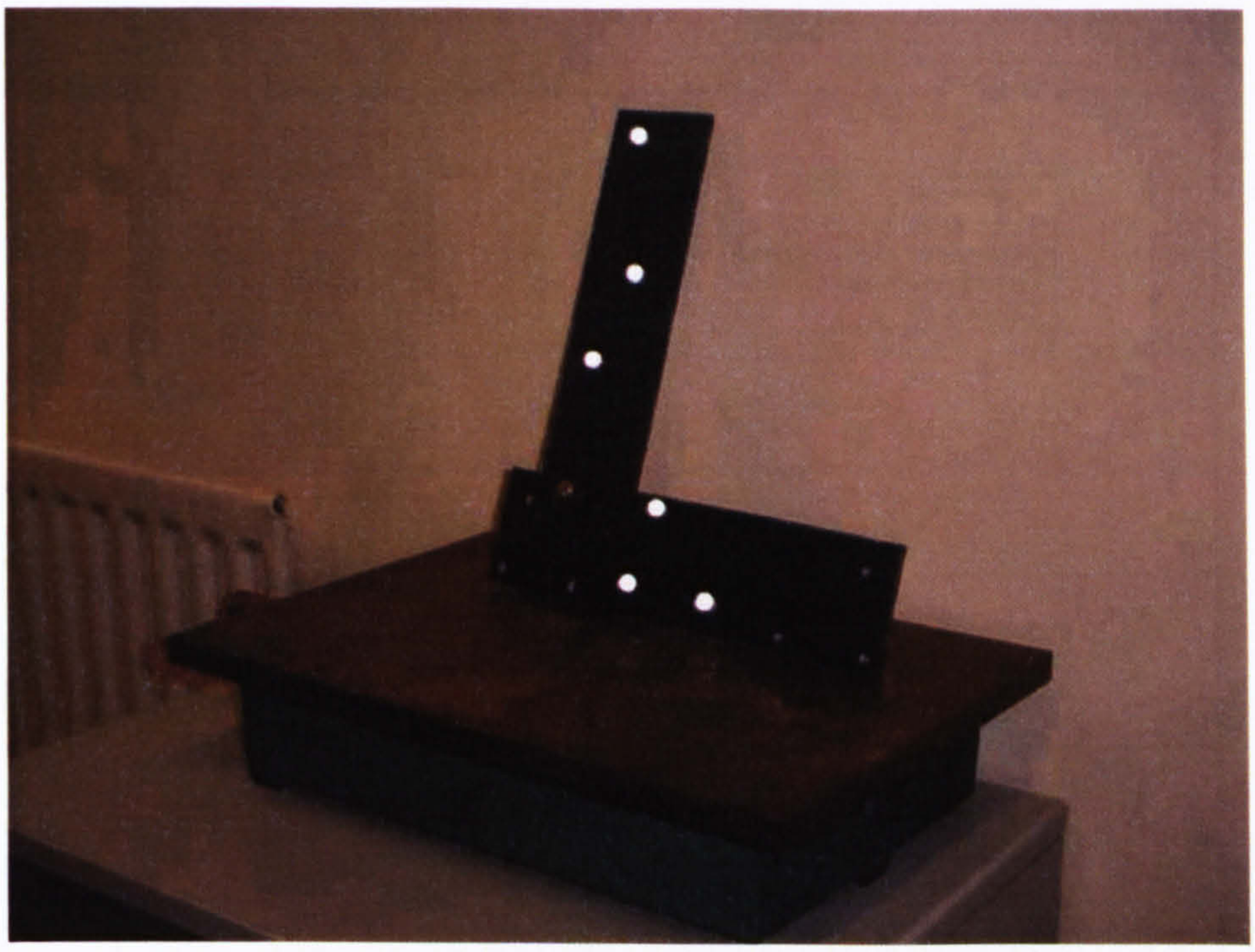

Figure 4.8: The tool used to validate the helical axis approach

measurements above, to emphasise the differences between the results. It is worth noting, however, the slight trends in n2 and n3, which almost certainly relate to a repeatable variation in the alignment of the plates through the range of motion.

The same range has been used for the y and z intercept values (Figures 4.13 and 4.14) as was used for the subject measurements, so that the variations may be easily compared. The fact that the intercepts are very close to zero and exhibit variations of approximately 1-2 mm indicate that the system is performing as expected. This also validates the way in which the ARF is constructed in software.

The evidence provided here indicates that the measurement apparatus and the analysis software are entirely suitable for the intended use. With that reassurance, the presentation of results from different loading conditions can continue.

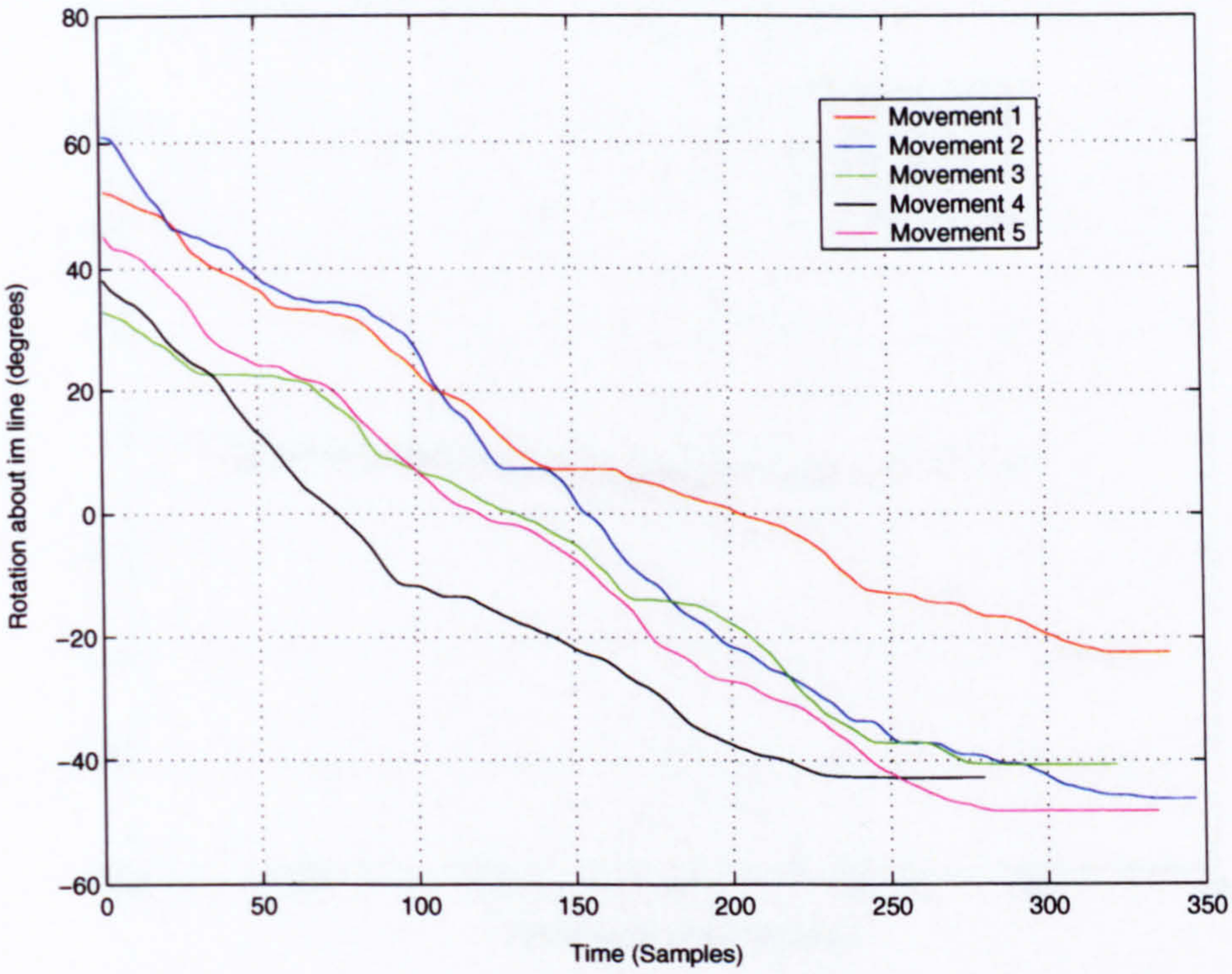

Figure 4.9: Angle vs time: Validation tool, dorsiflexion movements

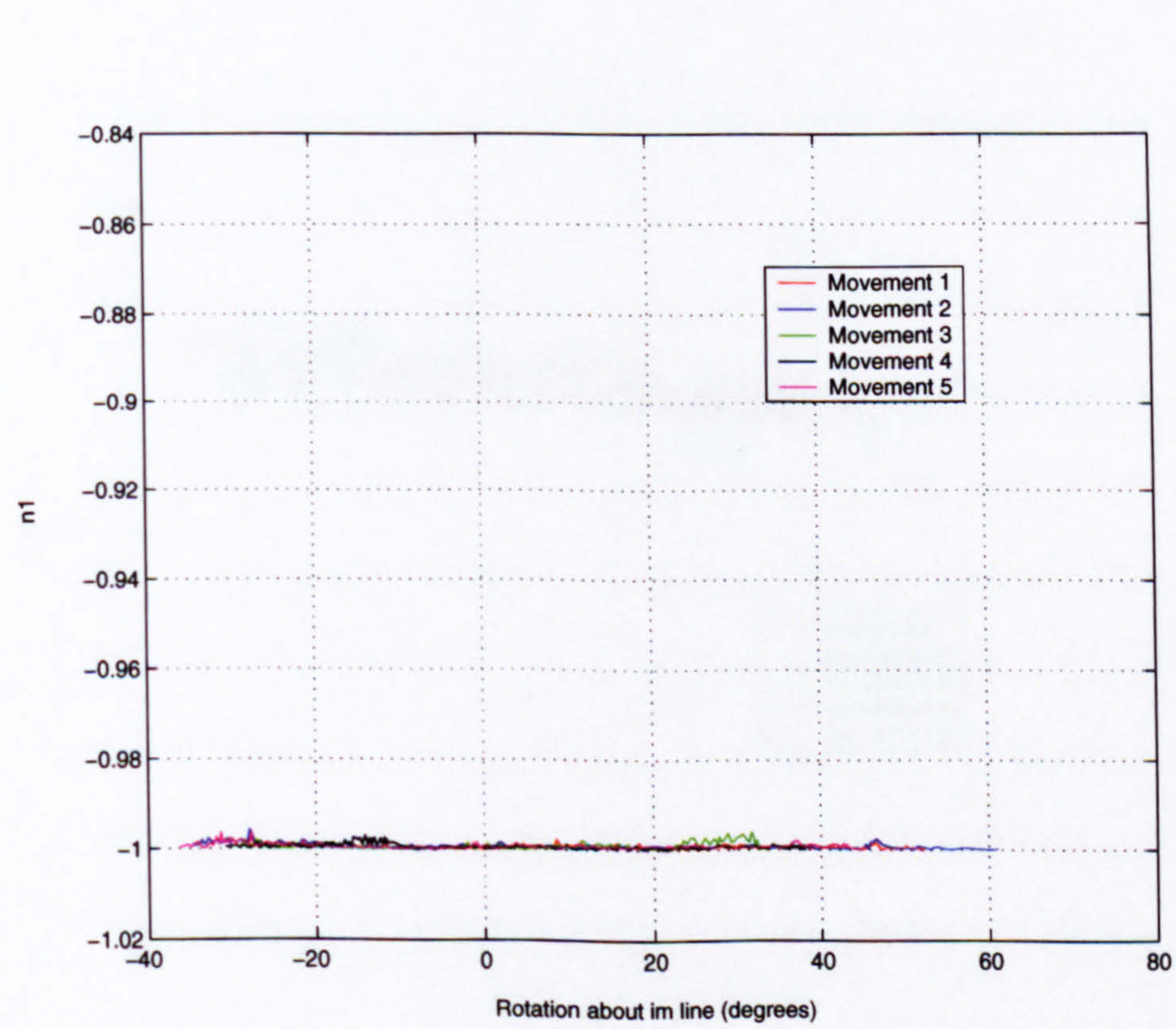

Figure 4.10: n1 values of the seqFHAs: Validation tool, dorsiflexion movements

UNIVERSITY OF SOUTHAMPTON LIBRARY

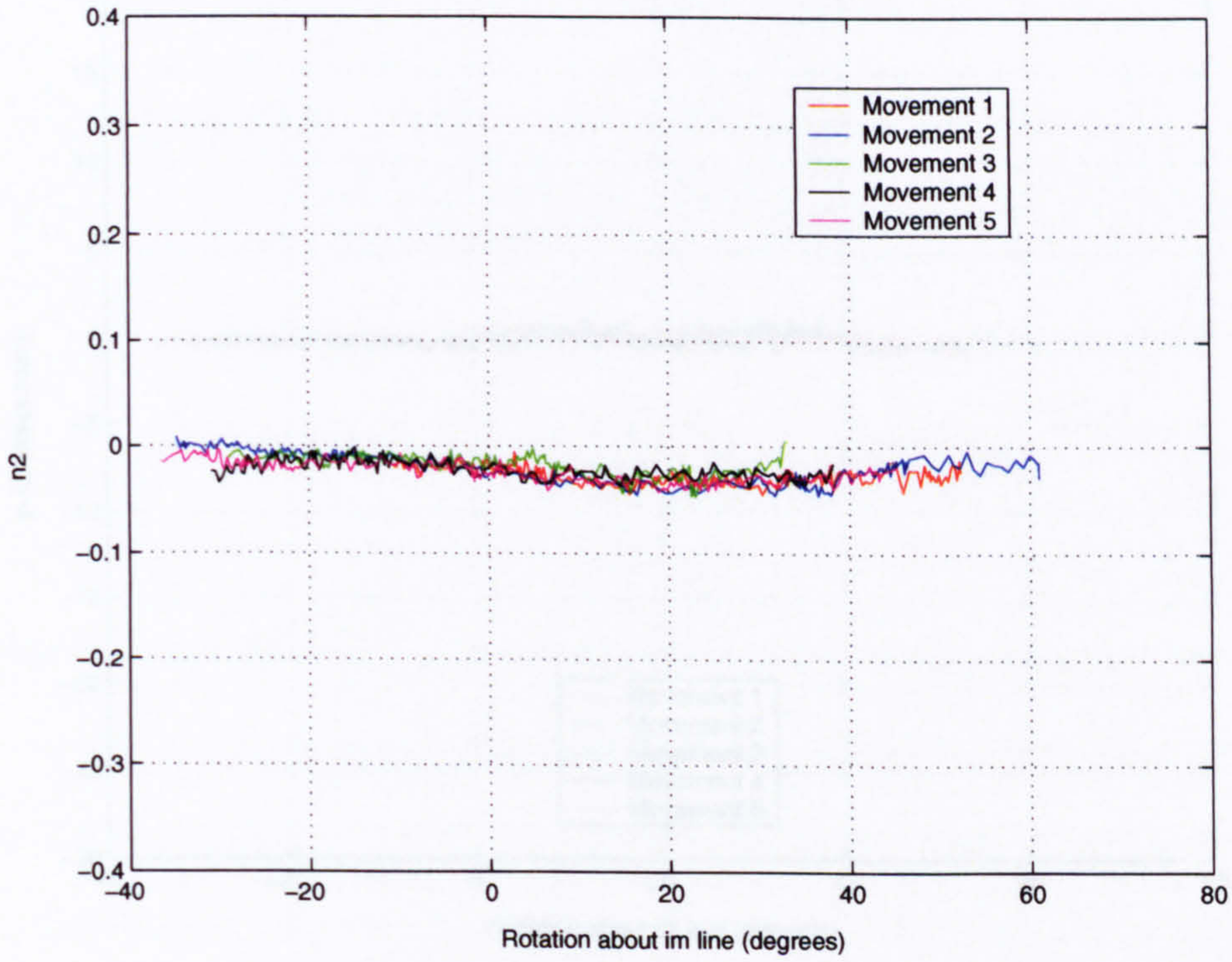

Figure 4.11: n2 values of the seqFHAs: Validation tool, dorsiflexion movements

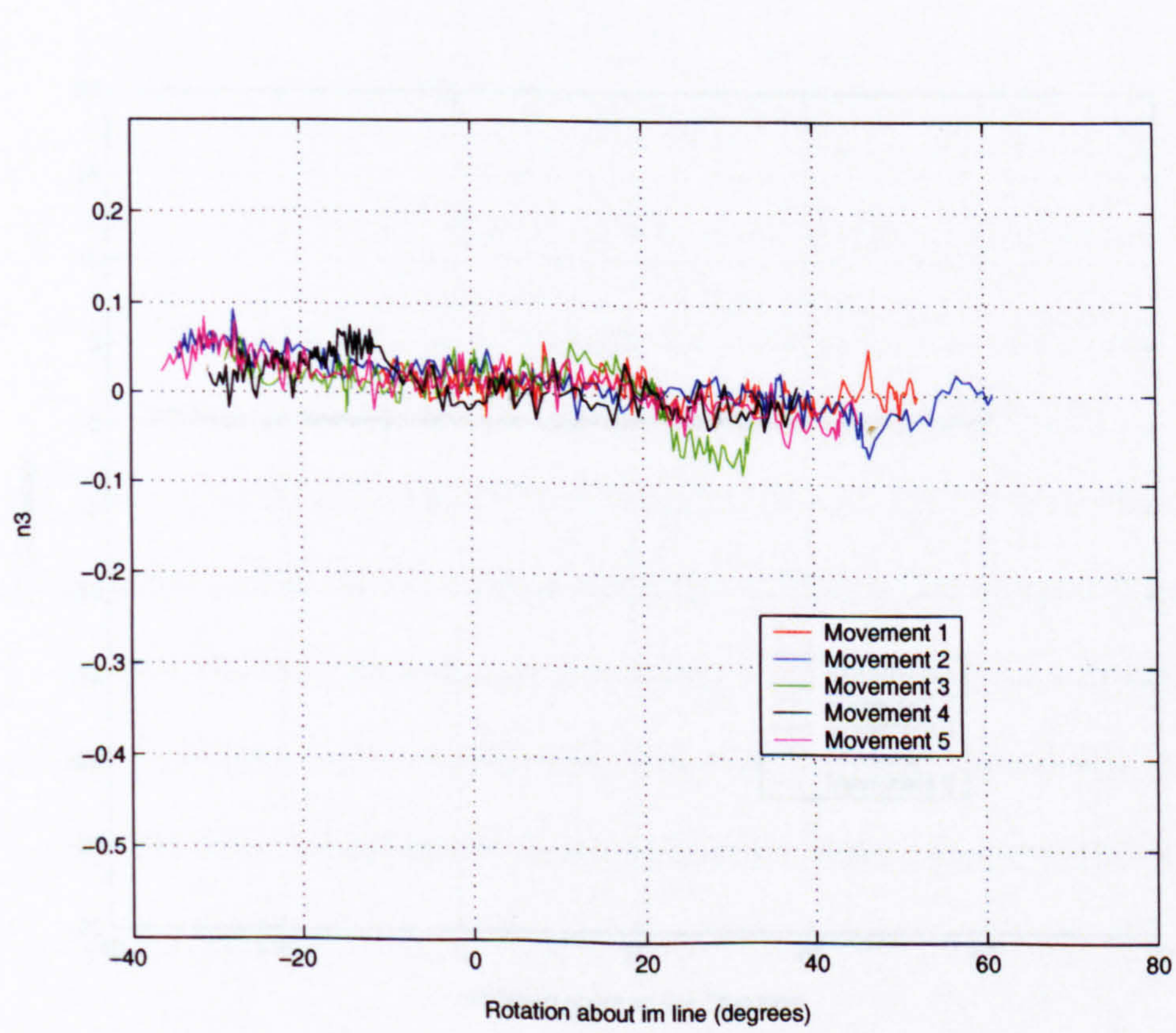

Figure 4.12: n3 values of the seqFHAs: Validation tool, dorsiflexion movements

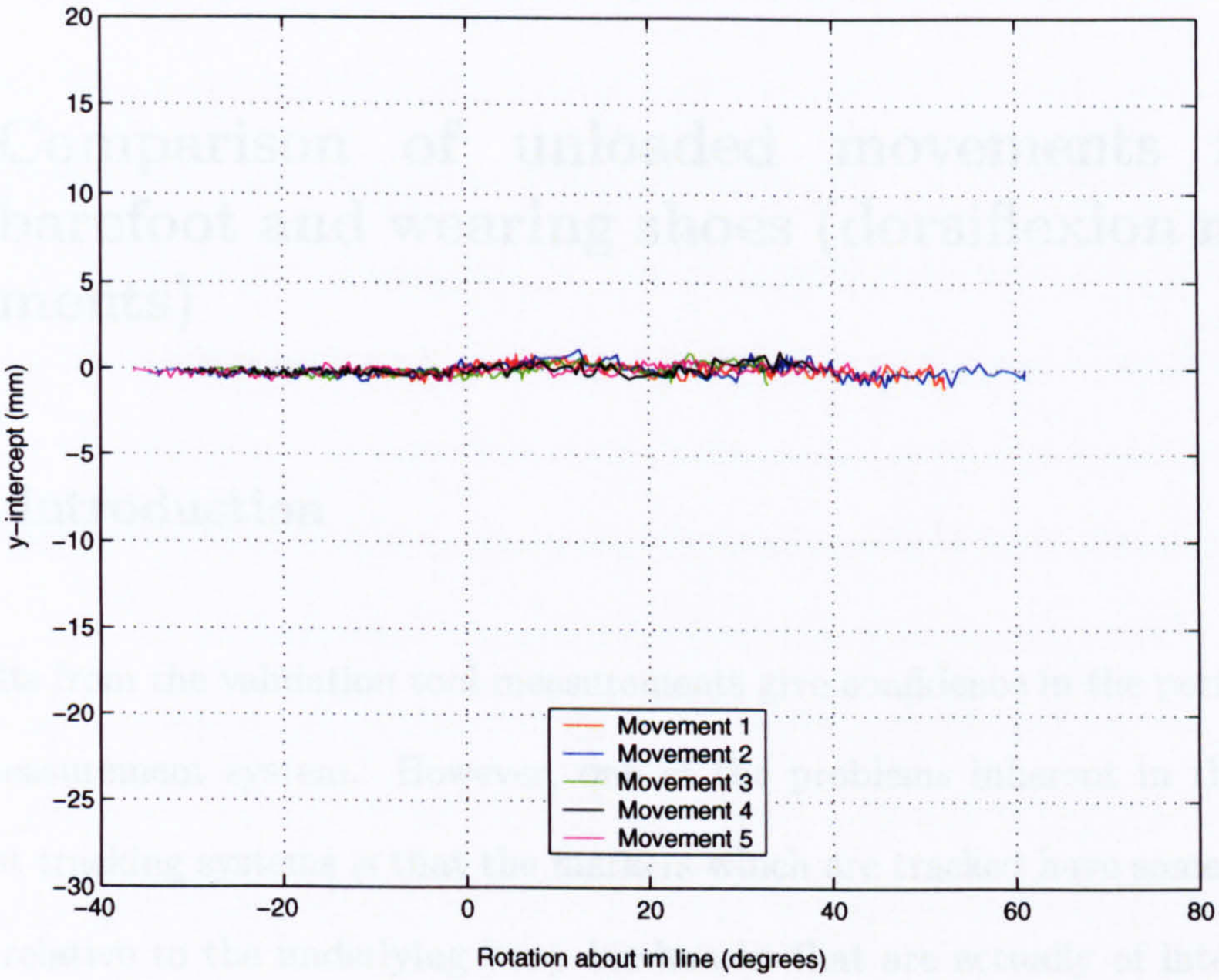

Figure 4.13: y-intercept values of the seqFHAs: Validation tool, dorsiflexion movements

Figure 4.14: z-intercept values of the seqFHAs: Validation tool, dorsiflexion movements

4.4 Comparison of unloaded movements made barefoot and wearing shoes (dorsiflexion movements)

4.4.1 Introduction

The results from the validation tool measurements give confidence in the performance of the measurement system. However, one of the problems inherent in the use of movement tracking systems is that the markers which are tracked have some freedom to move relative to the underlying bony landmarks that are actually of interest. As has already been discussed, one measurement session was recorded for Subjects 1 to 5 which included unloaded barefoot movements, unloaded movements wearing shoes, squatting movements wearing shoes and toe raise movements wearing shoes. The results presented in this section will be graphs of the various parameters for both the unloaded barefoot and unloaded wearing shoes measurements, plotted on the same axes, for the results from these measurement sessions. This will allow comparisons between subjects and between these two conditions. It seems logical to assume that movement of the markers relative to the bony landmarks will vary according to whether the markers are applied in direct contact with the skin or on to a shoe. Therefore, if the axis parameters calculated are significantly affected by movement of the markers relative to the bony landmarks, then it would be reasonable to expect that this would be reflected in differences between the parameters calculated for movements performed wearing shoes and barefoot.

The results presented will focus on dorsiflexion movements, with reference to plantarflexion results where this adds useful information. It is important to remember that in

this work, dorsiflexion and plantarflexion refer to direction rather than range of movement. Dorsiflexion movements start from a maximally plantarflexed position and end at a maximally dorsiflexed position, while plantarflexion movements are the reverse of this. The subjects were instructed to stop at comfortable endpoints, rather than aiming to achieve forced extremes. The sign of the components of the direction vector will change according to the direction of the movement. Although it is a little cumbersome, the parameters will be presented individually, as this facilitates comparison. The angle of rotation about the intermalleolar (IM) line is plotted against time, while the x, y and z components of the axis direction vector (n1, n2 and n3, respectively) and the y and z coordinates of the point of intersection with the MM plane are plotted against angle of rotation about the IM line. Results relating to barefoot movements are plotted as solid red lines, while those relating to movements wearing shoes are plotted as dashed blue lines. Ideally, there should be five plots for each condition for each subject (i.e. a total of ten plots for each figure). However, there are some instances where markers were not visible throughout the movement, so some plots may be missing.

4.4.2 Theta vs time

Let us first consider the angle-time graphs. These plots are a useful starting point as they illustrate the time course of the movements. As discussed previously, the angle that is plotted here is the first of three Cardan angles calculated for movement of the shank-embedded anatomical reference frame (ARF) relative to the foot tool. The Cardan sequence used is zyx, with the IM line defined as the z-axis; the first Cardan angle therefore relates to rotation about the IM line. For clarity, this is simply referred to as rotation about the IM line, or θ. It is important to remember that the values for θ are calculated relative to the standing position. Negative values indicate an

orientation of the shank ARF to the foot that is dorsiflexed relative to the orientation in standing, while positive values indicate an orientation that is plantarflexed relative to the standing position.

The plots of θ against time for Subjects 1 to 5 are presented in Figures 4.15 to 4.19, respectively. The first point to note is the overall similarity between barefoot and shod results. The total range of movement varies between subjects, from about 55° for Subjects 2 and 4 to 75° for Subject 1. However, for the majority of subjects, the range of movement was very similar for barefoot and shod measurements, although Subject 3 exhibits a range of movement about 5-10° greater with shoes compared to barefoot. The offset between barefoot and shod measurements is believed to be due to the effect of wearing shoes on the orientation of the shank ARF to the foot in comfortable standing. It was necessary to record a new standing reference position once the subjects had put on their shoes, due to the movement of the collections of markers. In terms of the time taken, there was a considerable variation between Subjects 1, 2 and 4, who all completed the movements in less than 1 s, and Subjects 3 and 5 who took between 2.5 and 5 seconds to complete the movements. The rate of movement, which was selected by the subjects in response to an instruction to move at a comfortable speed, also seems to affect the trajectory. The trajectories for Subjects 1, 2 and 4 have a sigmoid form, while those for Subjects 3 and 5 are closer to straight lines. This would be expected as accelerations are less pronounced for these longer movements. Subject 3 in particular demonstrates greater jerkiness in the motion as a result of restricting the speed of movement. It is also interesting to note the variations in trajectory, particularly for Subjects 2 and 4 for both conditions and to a lesser extent for Subject 3 when wearing shoes.

There are a few other observations worth making. Both Subject 2 (barefoot and wearing shoes) and Subject 4 (barefoot only) demonstrate one movement that starts

at a position about 15° less plantarflexed than the others. It would appear that these are due simply to inconsistencies in the way the subjects make the movements. Although not presented here, it is worth noting that the results from the plantarflexion movements do not show such an inconsistency for either subject. The apparently rogue result for Subject 5 is a result of the subject starting the movement before the measuring started - this is borne out by the time course and the trajectory of the movement. The gaps in the graphs for Subjects 4 and 5 are due to the markers being obscured, while the irregularities in the results for Subjects 3 and 5 are believed to be due to real irregularities in the movements.

4.4.3 First component of the direction vector, n1

The first component of the direction vector, n1, is the component directed along the x-axis of the shank ARF, which is coincident with the intermalleolar line. Therefore, if a calculated axis were coincident with the intermalleolar line, n1 would be 1 (or -1, depending on direction of rotation), and n2 and n3 would be zero. Therefore, the variation in n1 gives an indication of the degree of deviation of the axis direction vector from the IM line. As a component of a unit direction vector, n1 is dimensionless. The local coordinate systems for the shank ARF and the foot tool are defined in such a way that for dorsiflexion movements, n1 is negative. The following figures are plots of n1 against angle of rotation about the IM line. For a given subject, the range of angles for which values of n1 are plotted is approximately 10° less than the range of movement identified above (Section 4.4.2). This results from the requirement of the sequential FHA technique for a minimum rotation of 10° in order to calculate the helical axis parameters. The plots of n1 against time for Subjects 1 to 5 are presented in Figures 4.20 to 4.24, respectively.

Considering first the difference between results from barefoot and shod measurements,

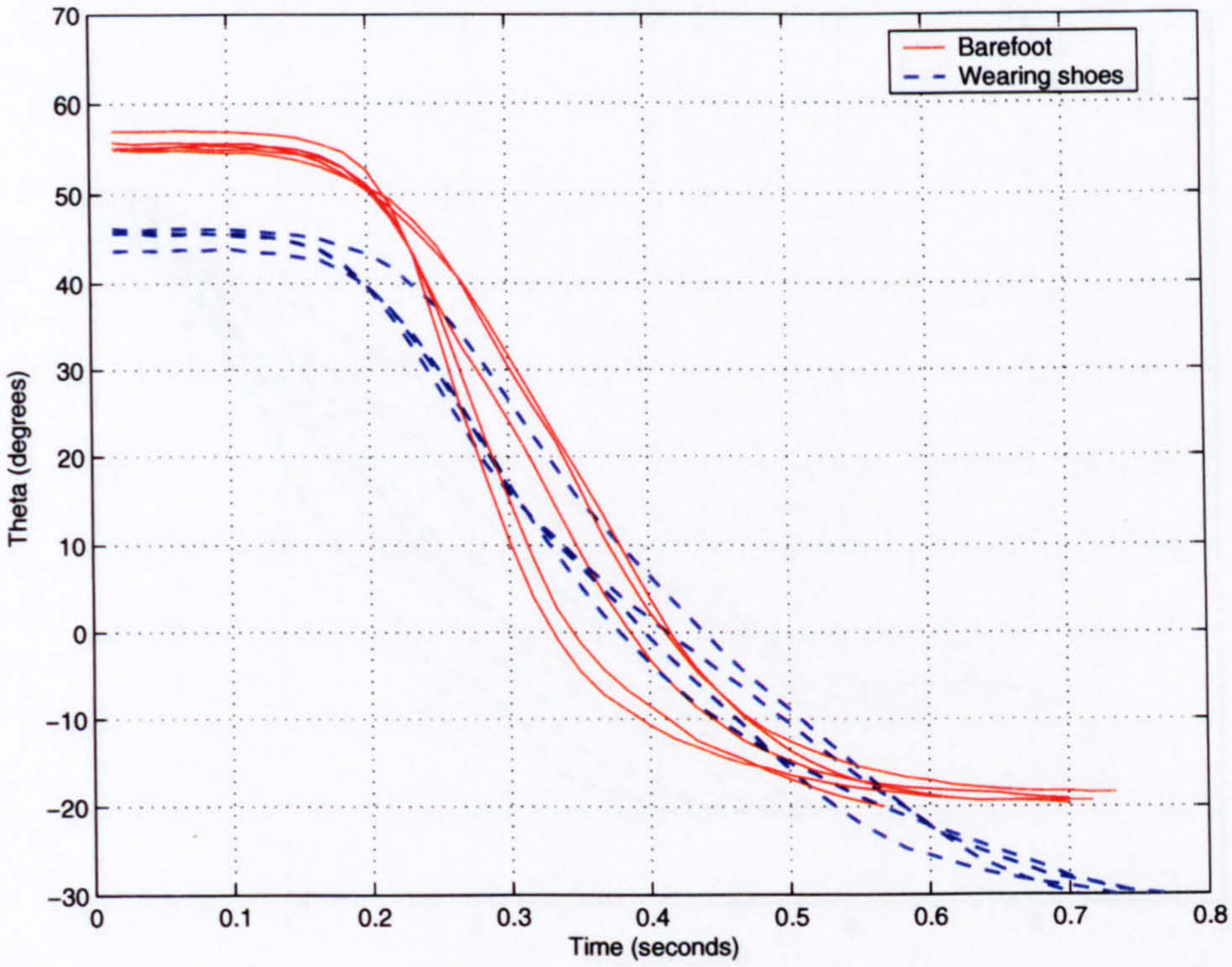

Figure 4.15: Angle of rotation about im line (theta) plotted against time for Subject 1.

Figure 4.16: Angle of rotation about im line (theta) plotted against time for Subject 2.

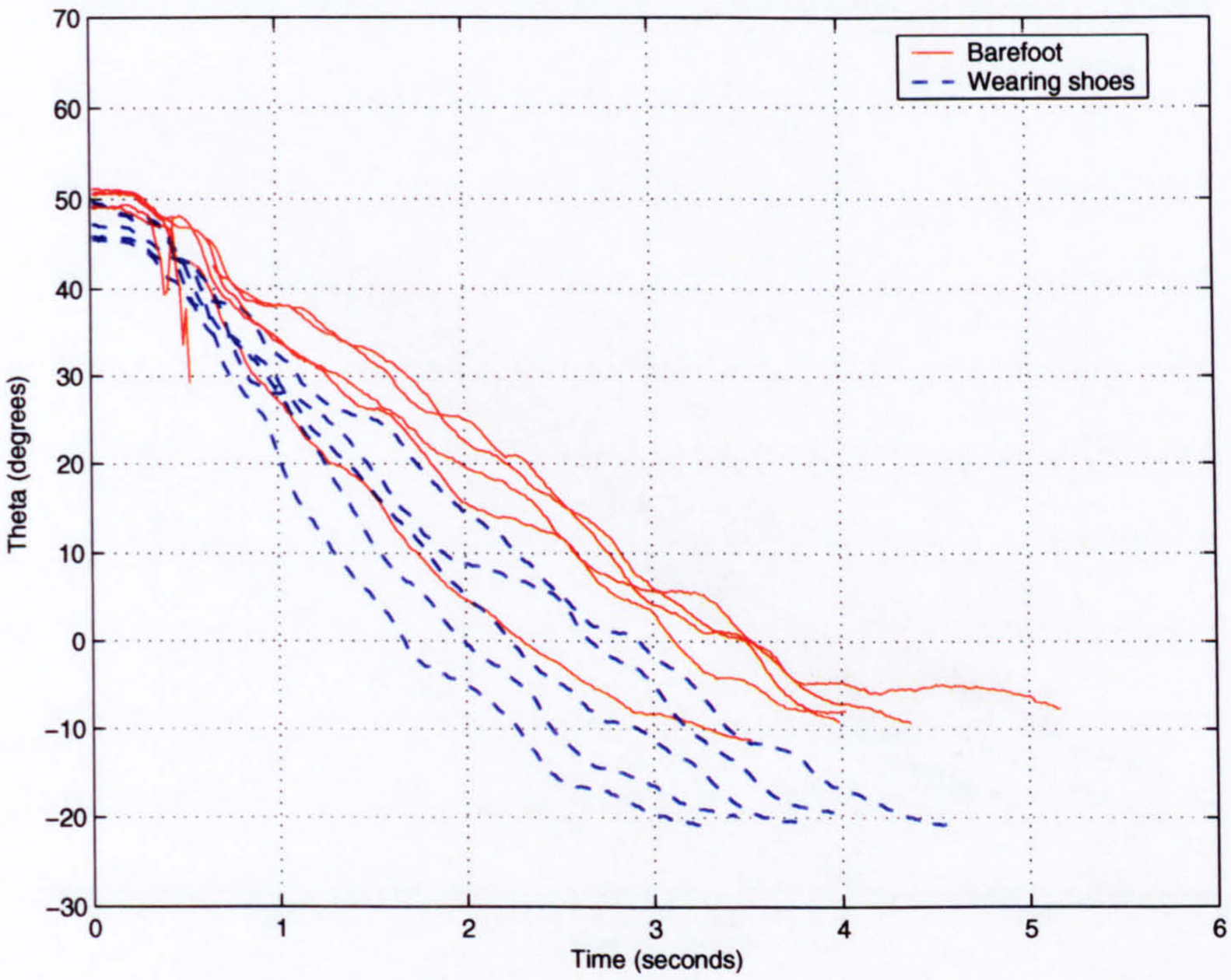

Figure 4.17: Angle of rotation about im line (theta) plotted against time for Subject 3.

Figure 4.18: Angle of rotation about im line (theta) plotted against time for Subject 4.

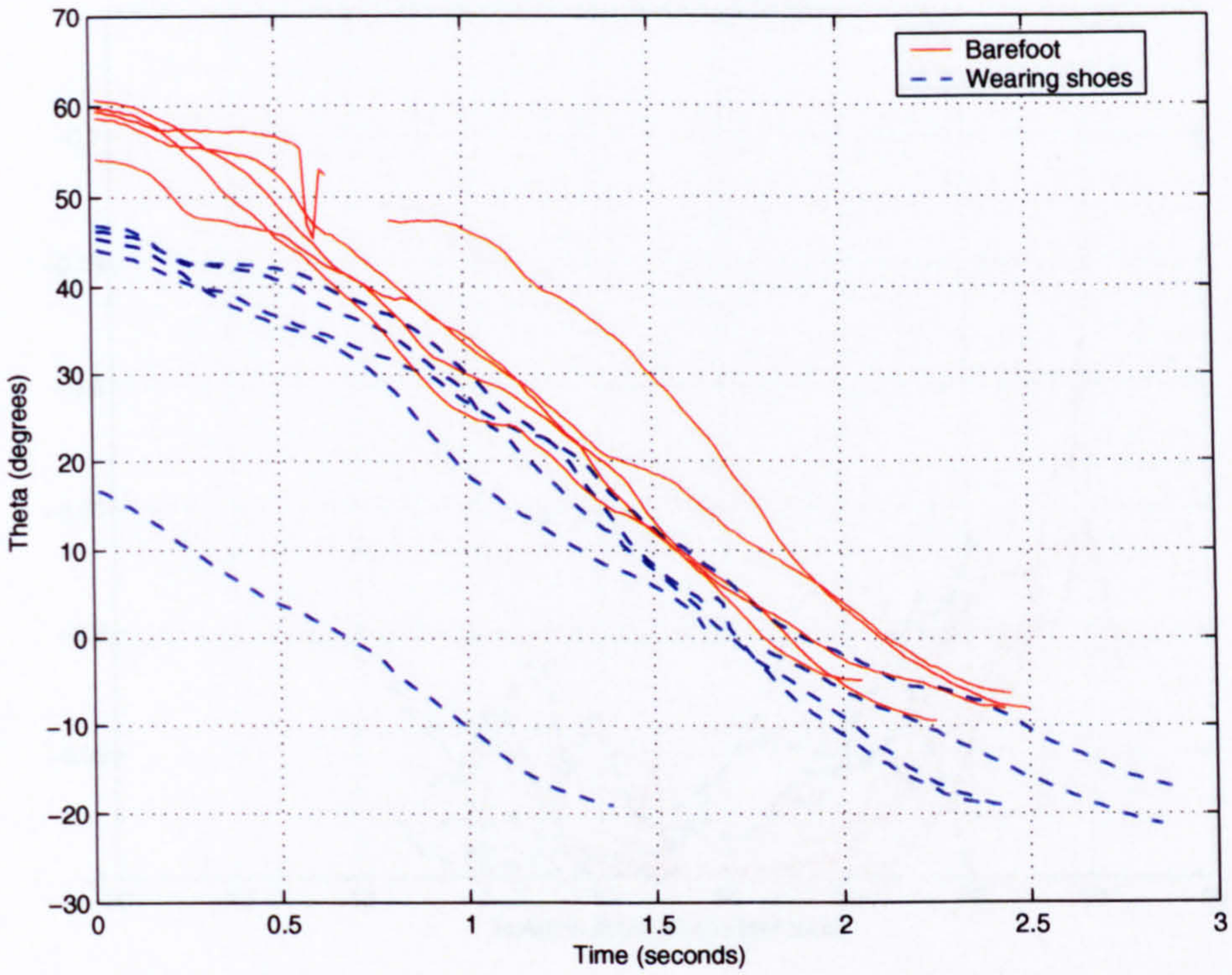

Figure 4.19: Angle of rotation about im line (theta) plotted against time for Subject 5.

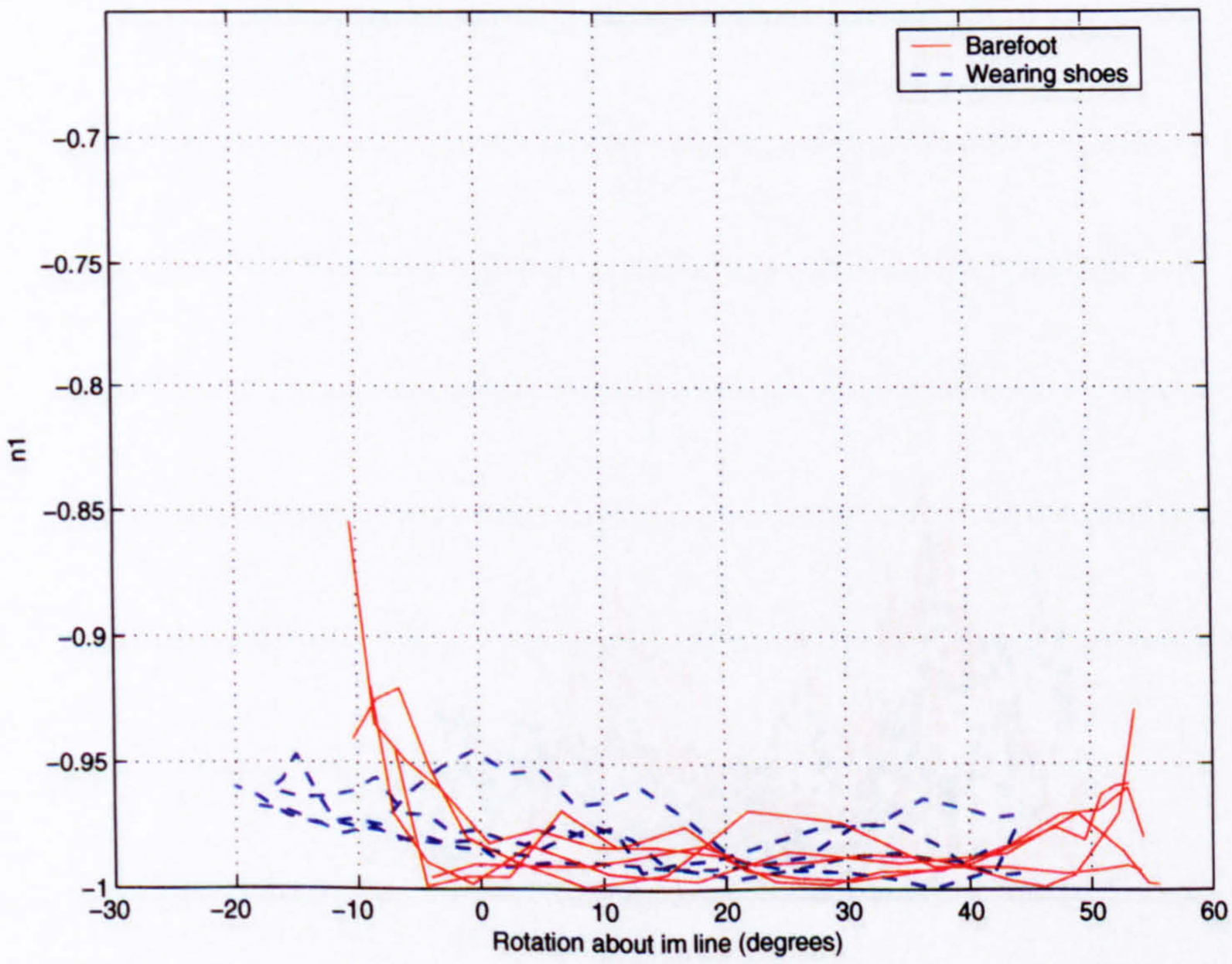

Figure 4.20: First component of direction vector (n1) plotted against angle of rotation about IM line for Subject 1.

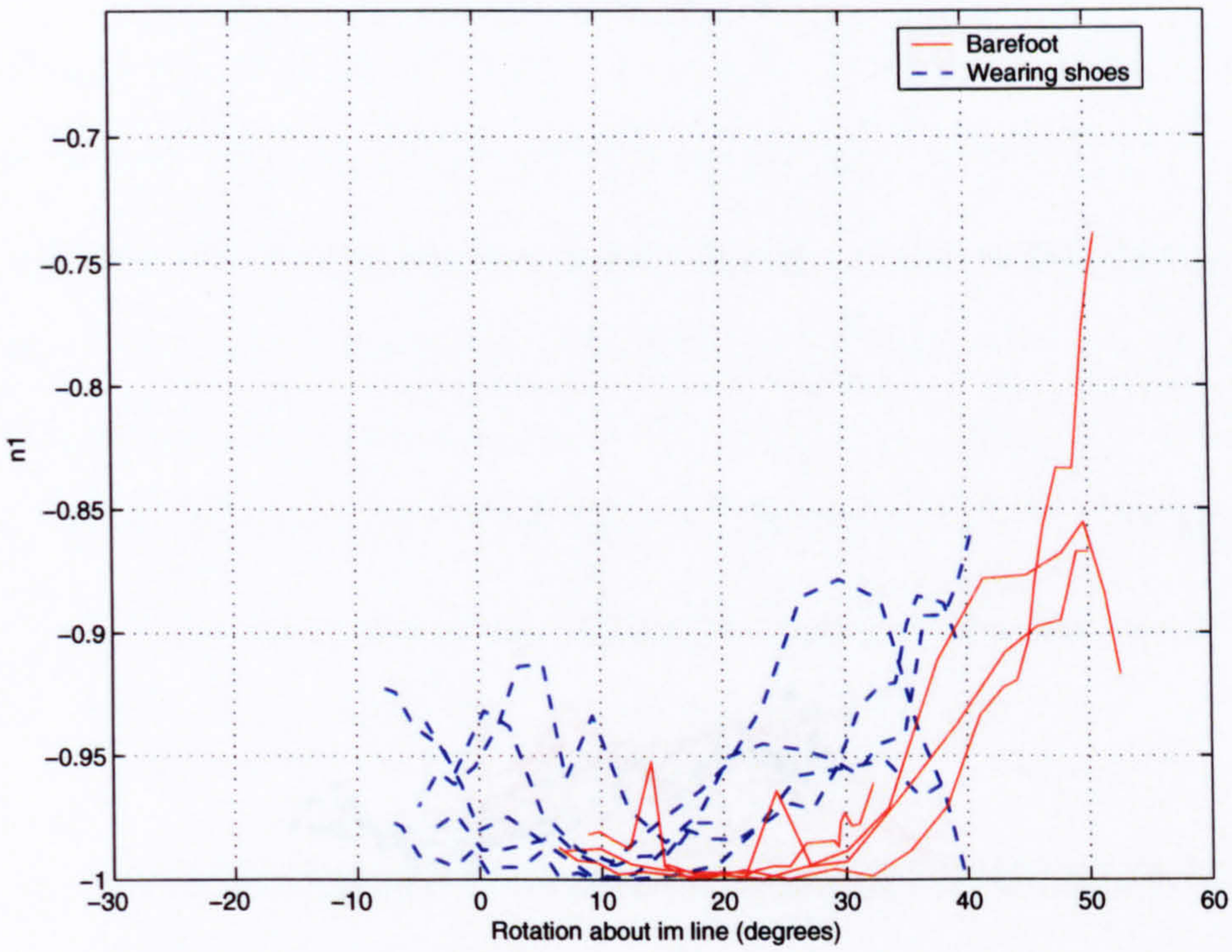

Figure 4.21: First component of direction vector (n1) plotted against angle of rotation about IM line for Subject 2.

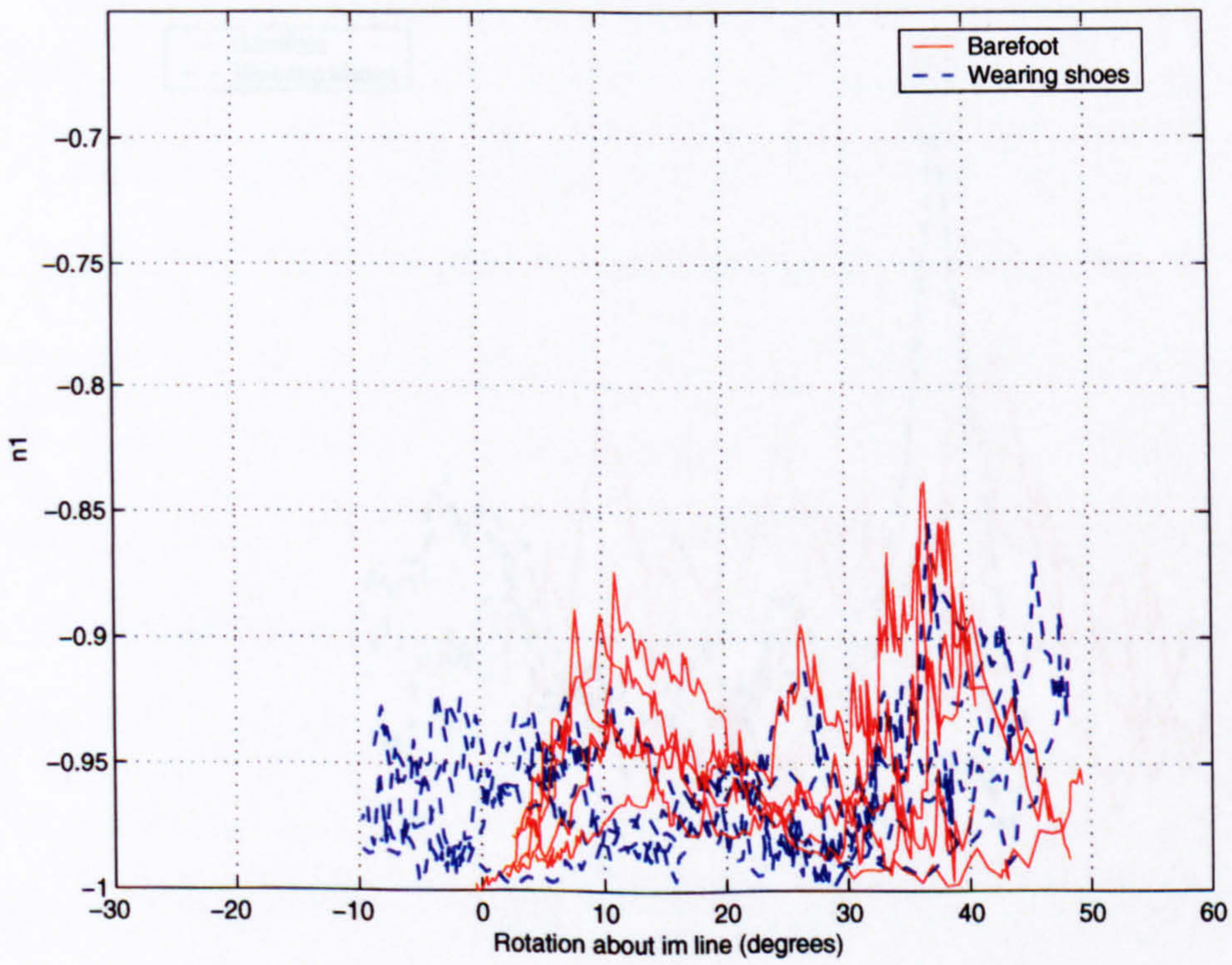

Figure 4.22: First component of direction vector (n1) plotted against angle of rotation about IM line for Subject 3.

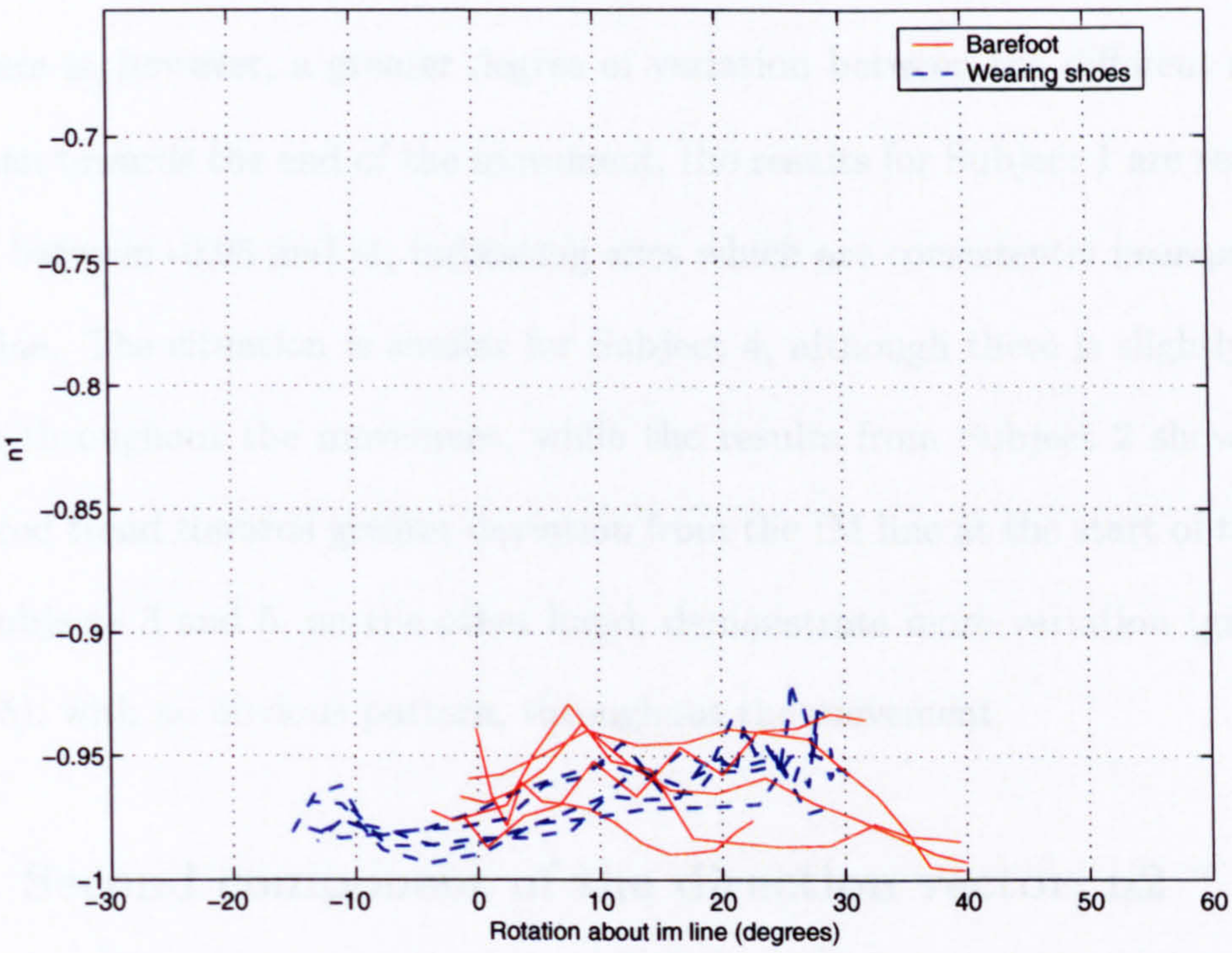

Figure 4.23: First component of direction vector (n1) plotted against angle of rotation about IM line for Subject 4.

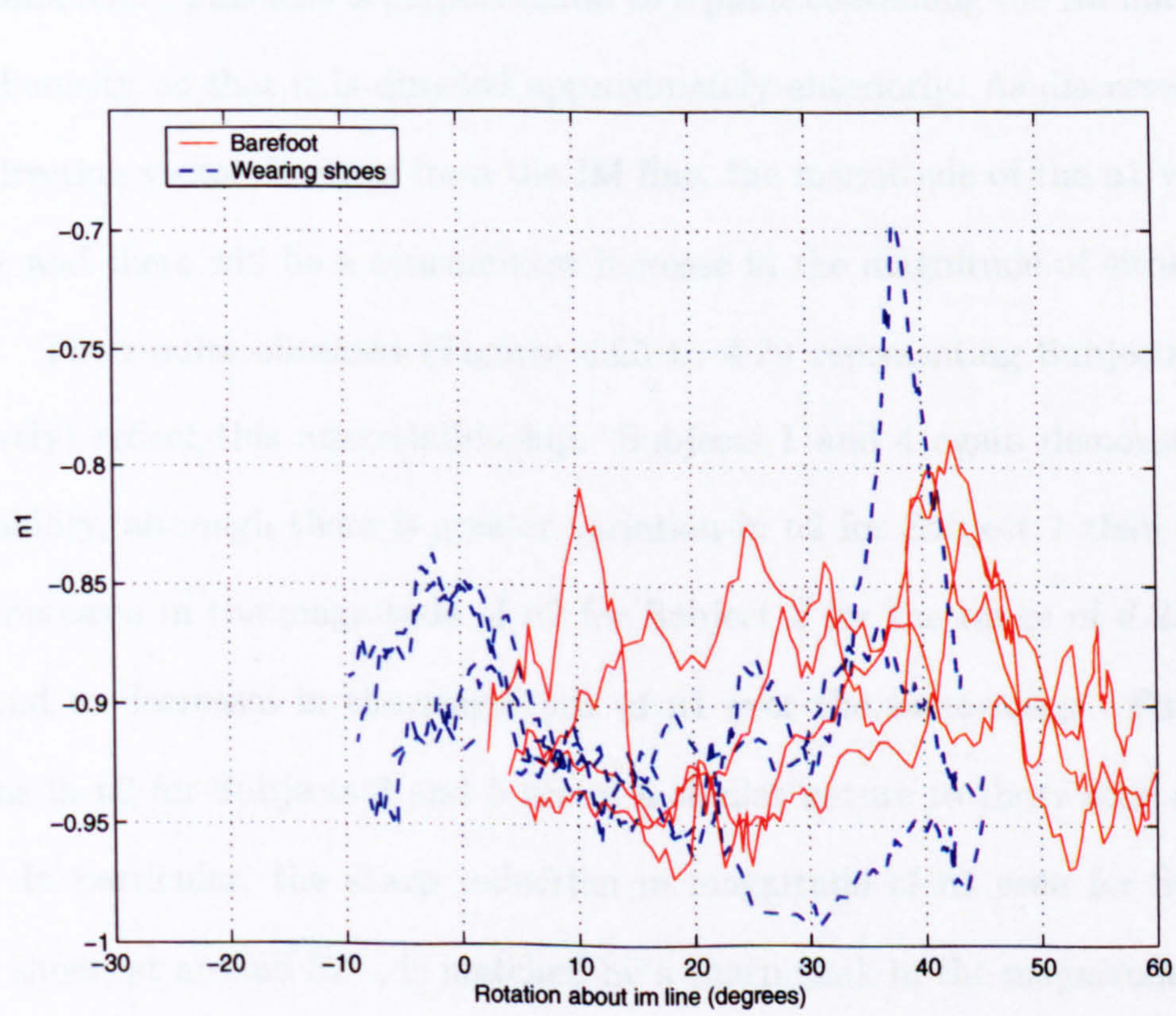

Figure 4.24: First component of direction vector (n1) plotted against angle of rotation about IM line for Subject 5.

it is apparent that there is reasonable agreement between the two for any given subject. There is, however, a greater degree of variation between the different subjects. Other than towards the end of the movement, the results for Subject 1 are reasonably constant between -0.95 and -1, indicating axes which are consistently near-parallel to the IM line. The situation is similar for Subject 4, although there is slightly greater variation throughout the movement, while the results from Subject 2 show a fairly pronounced trend towards greater deviation from the IM line at the start of the movement. Subjects 3 and 5, on the other hand, demonstrate more variation (greater for Subject 5), with no obvious pattern, throughout the movement.

4.4.4 Second component of the direction vector, n2

The second component of the direction vector, n2, is the component along the y-axis of the shank ARF. This axis is perpendicular to a plane containing the IM line and the tibial tuberosity, so that it is directed approximately anteriorly. As discussed above, as the direction vector deviates from the IM line, the magnitude of the n1 value will decrease, and there will be a concomitant increase in the magnitude of either n2, n3 or both. The results obtained (Figures 4.25 to 4.29 representing Subjects 1 to 5, respectively) reflect this interrelationship. Subjects 1 and 4 again demonstrate the most stability, although there is greater variation in n2 for Subject 1 than was seen in n1. Increases in the magnitude of n2 for Subject 2 for the range of θ 25^o to 55^o correspond to decreases in the magnitude of n1 over the same range. Finally, the variations in n2 for Subjects 3 and 5 are of a similar nature to those seen in the n1 results. In particular, the sharp reduction in magnitude of n1 seen for Subject 5, wearing shoes, at around 37^o , is matched by a sharp peak in the magnitude of n2 at the same point. In terms of a comparison between barefoot and shoe measurements, there is again generally fairly close agreement. The results for Subject 2 show very

similar patterns for barefoot and shod movements, although they are shifted relative to each other along the x-axis.

4.4.5 Third component of the direction vector, n3

The z-axis of the shank ARF is by definition perpendicular to both the x-axis and the y-axis, so that it lies in the plane defined by the IM line and the tibial tuberosity and is perpendicular to the IM line, directed superiorly. The third component of the axis direction vector, n3, lies along this axis. On an initial inspection, the plots of n3 for Subjects 1, 2 and 4 (Figures 4.30, 4.31 and 4.33, respectively) indicate greater variations than were seen in n1 and n2, which is inconsistent with the interrelationship between the three parameters previously described. However, much of this variation is due to the change in sign throughout the range of movement, so that variations in the magnitude of n3 are in fact closer to the expected values. For Subjects 2 and 4 there is again a slight shift along the x-axis of similar patterns between barefoot and shod measurements. Subject 3 (Figure 4.32) exhibits considerable variation in n3, although there is a clearer pattern than for n1 and n2, which is apparently consistent across different footwear conditions. Given the fact that the results for Subject 5 (Figure 4.32) change sign in similar fashion to those for Subjects 1, 2 and 4), there is less variation in the magnitude of n3 for this subject than was observed in n1 and n2. Looking at the plots of n1, n2 and n3 for Subject 5, it is useful to continue the analysis of the peaks in the results to illustrate the interrelationship between these parameters. The peak in the n1 trace, which is actually a reduction in magnitude, at 10^o corresponds to a sharp increase in the magnitude of n3 at that angle; the sharp reduction in the magnitude of n2 at about 22^o is mirrored by an increase by a similar value in the magnitude of n3, while the corresponding trough and peak in n1 and n2, respectively, at 37^o has already been described.

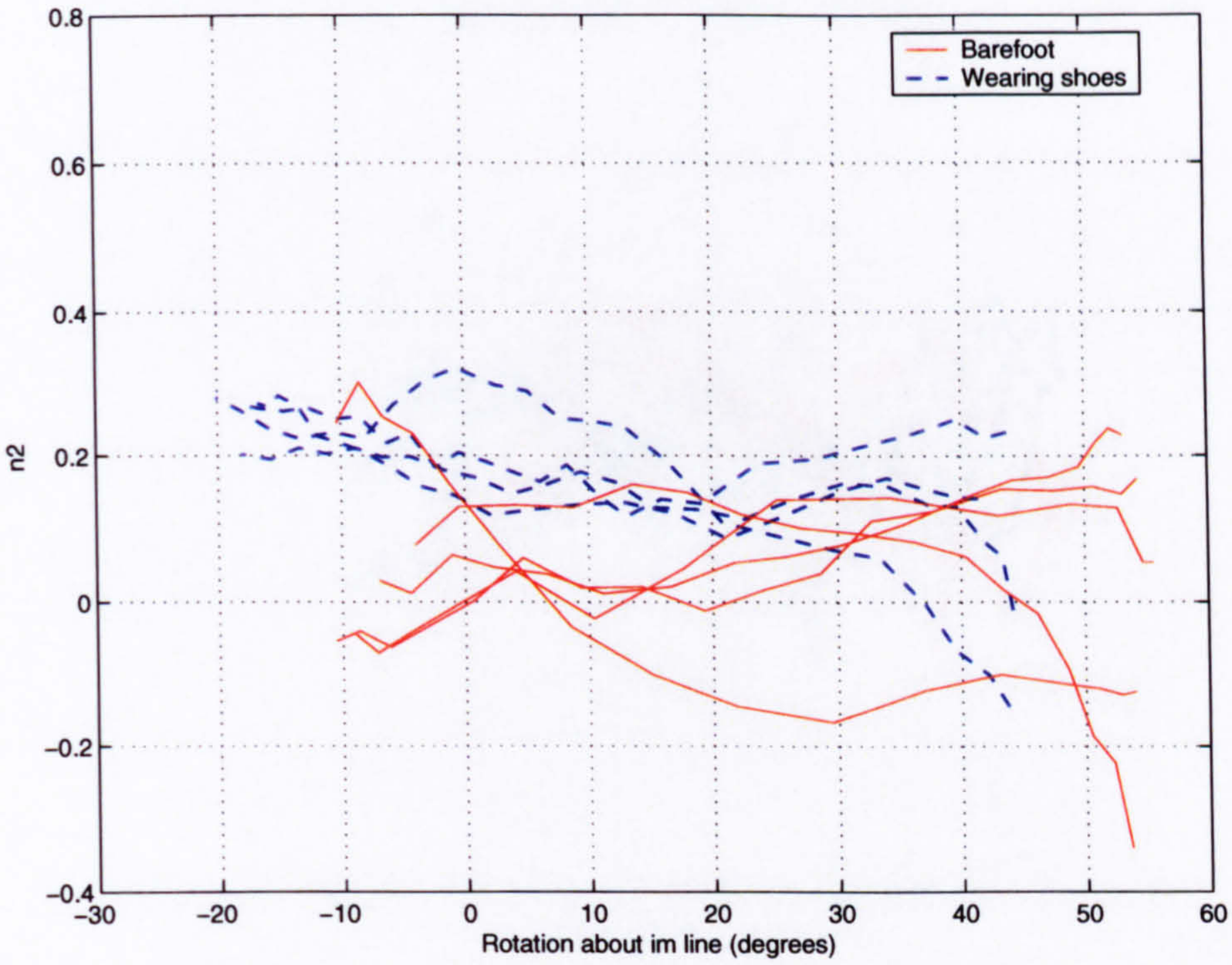

Figure 4.25: Second component of direction vector (n2) plotted against angle of rotation about IM line for Subject 1.

Figure 4.26: Second component of direction vector (n2) plotted against angle of rotation about IM line for Subject 2.

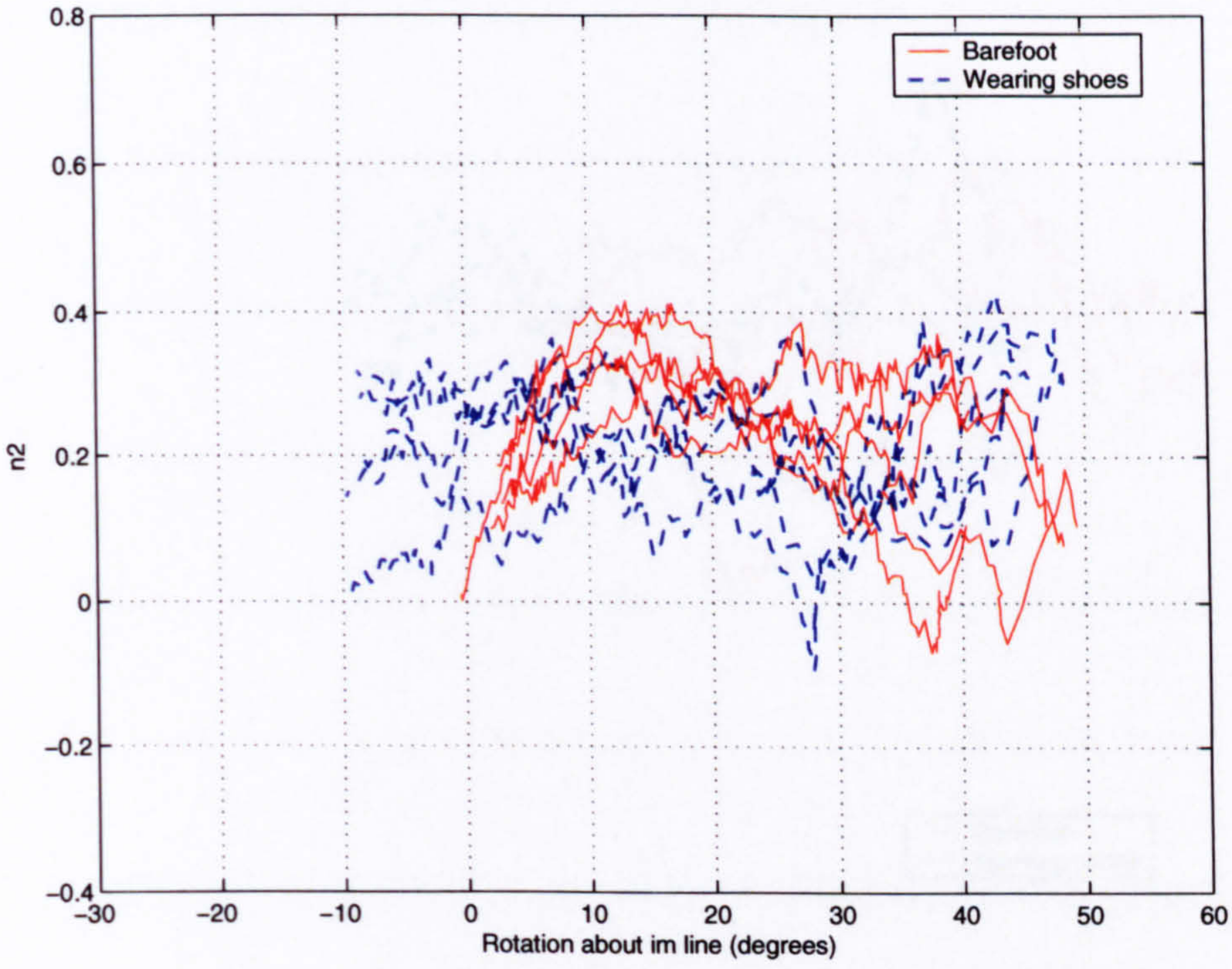

Figure 4.27: Second component of direction vector (n2) plotted against angle of rotation about IM line for Subject 3.

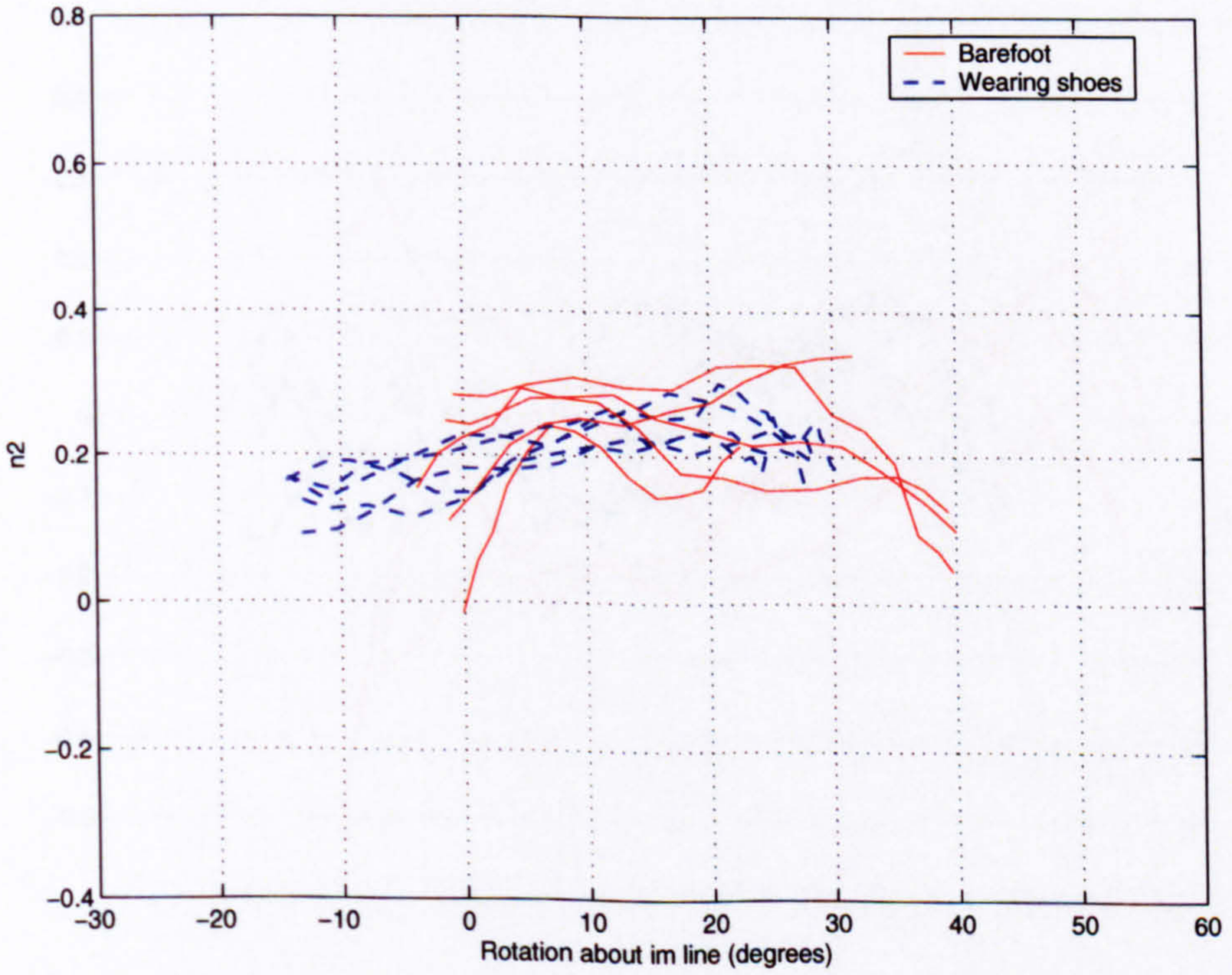

Figure 4.28: Second component of direction vector (n2) plotted against angle of rotation about IM line for Subject 4.

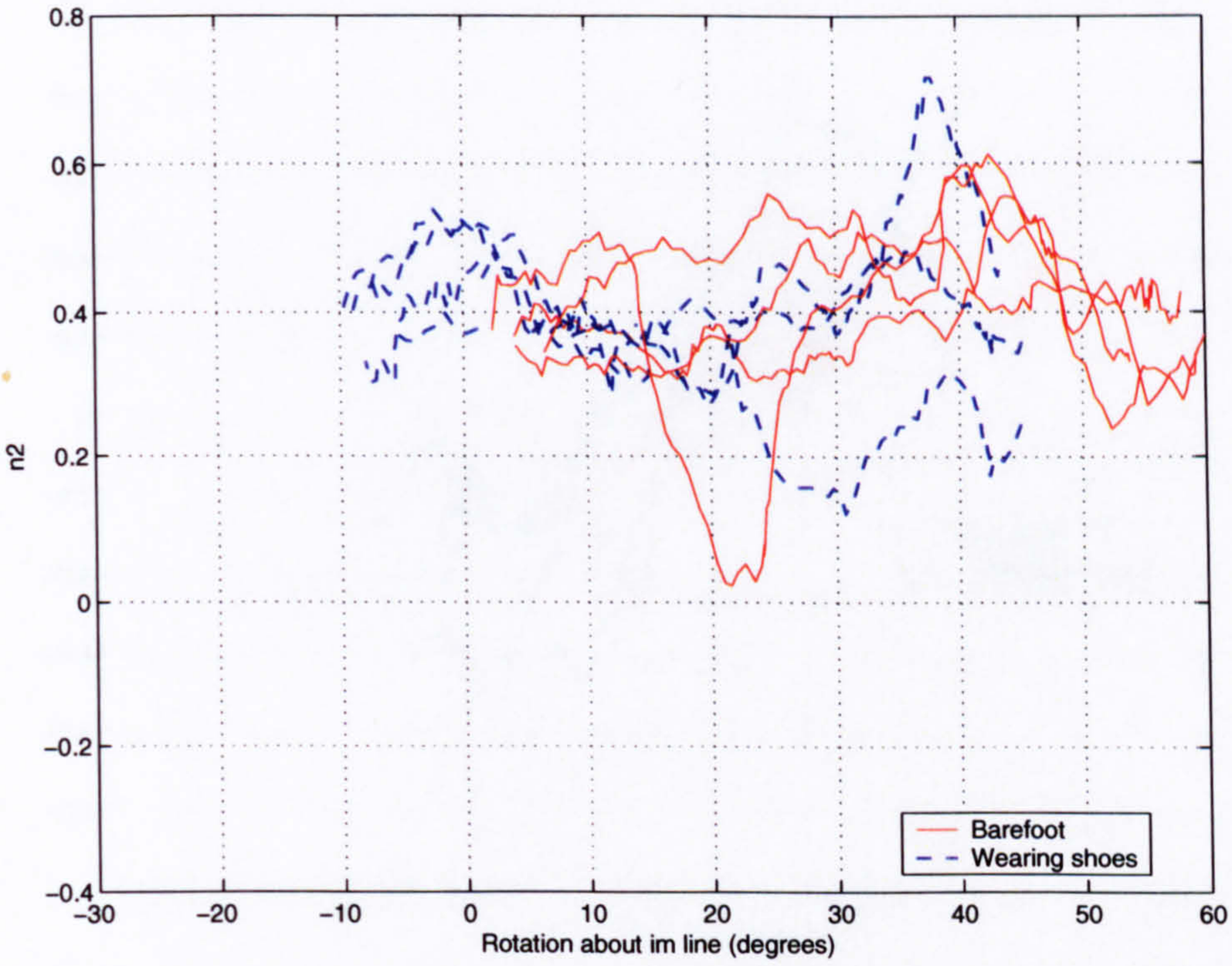

Figure 4.29: Second component of direction vector (n2) plotted against angle of rotation about IM line for Subject 5.

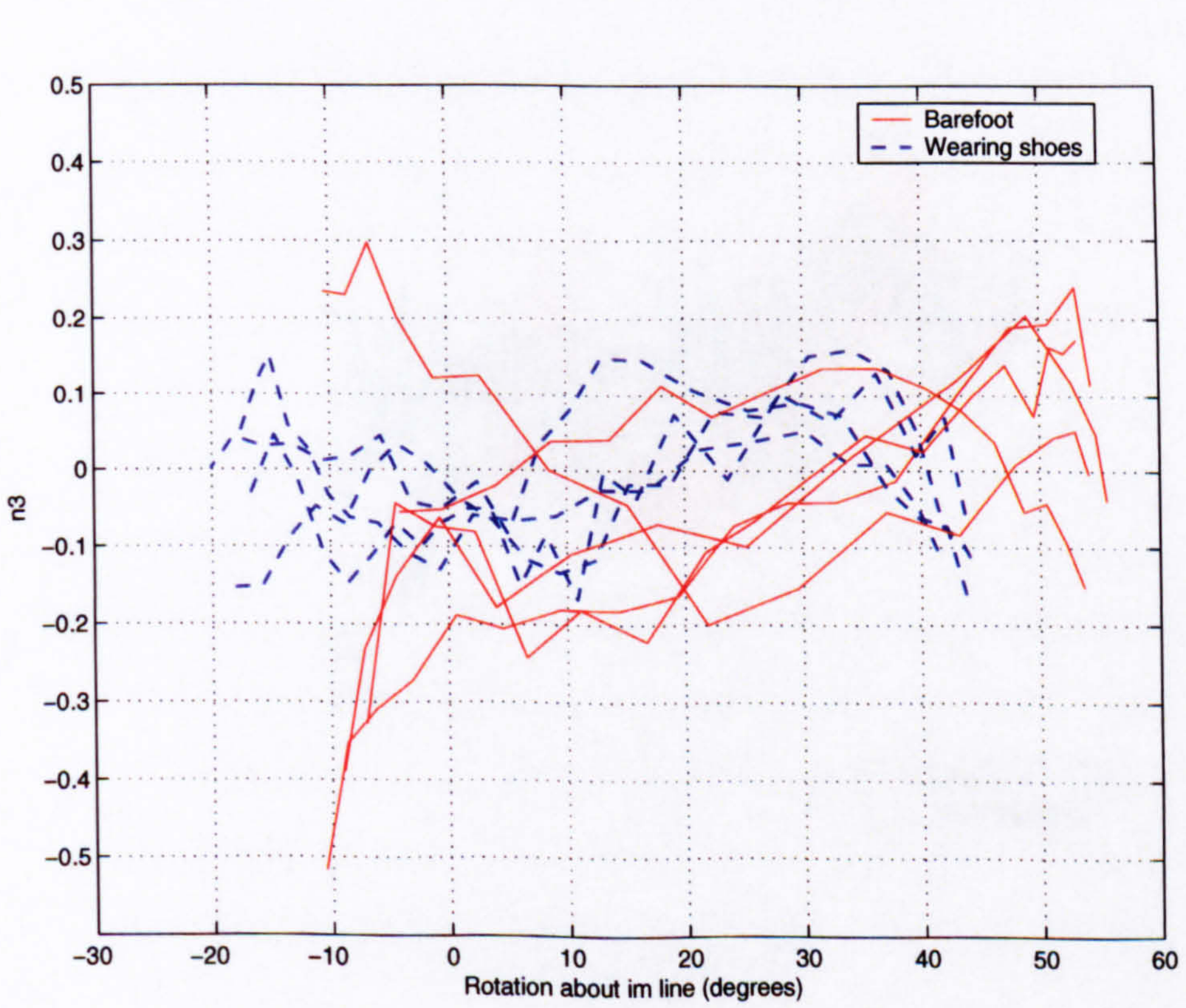

Figure 4.30: Third component of direction vector (n3) plotted against angle of rotation about IM line for Subject 1.

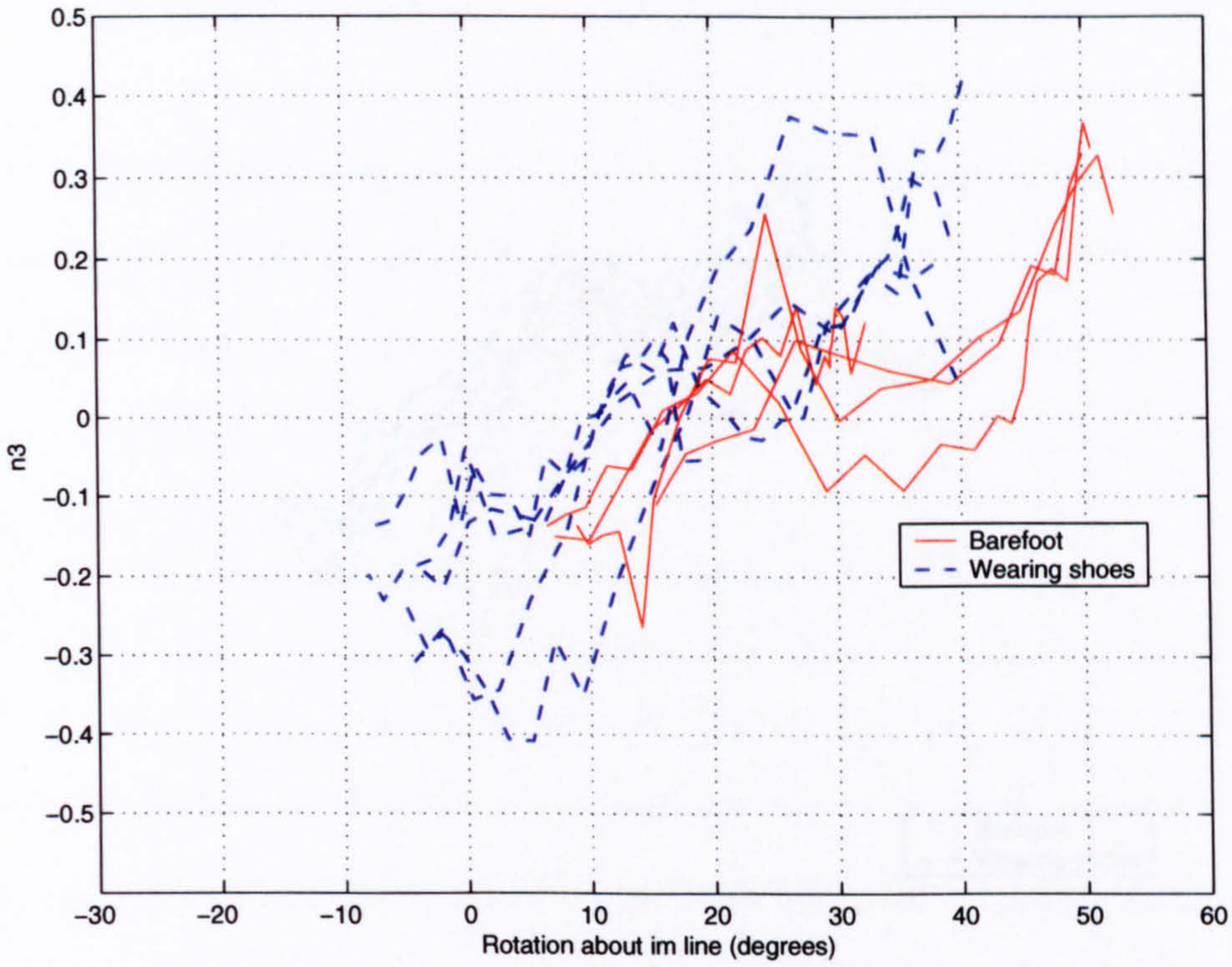

Figure 4.31: Third component of direction vector (n3) plotted against angle of rotation about IM line for Subject 2.

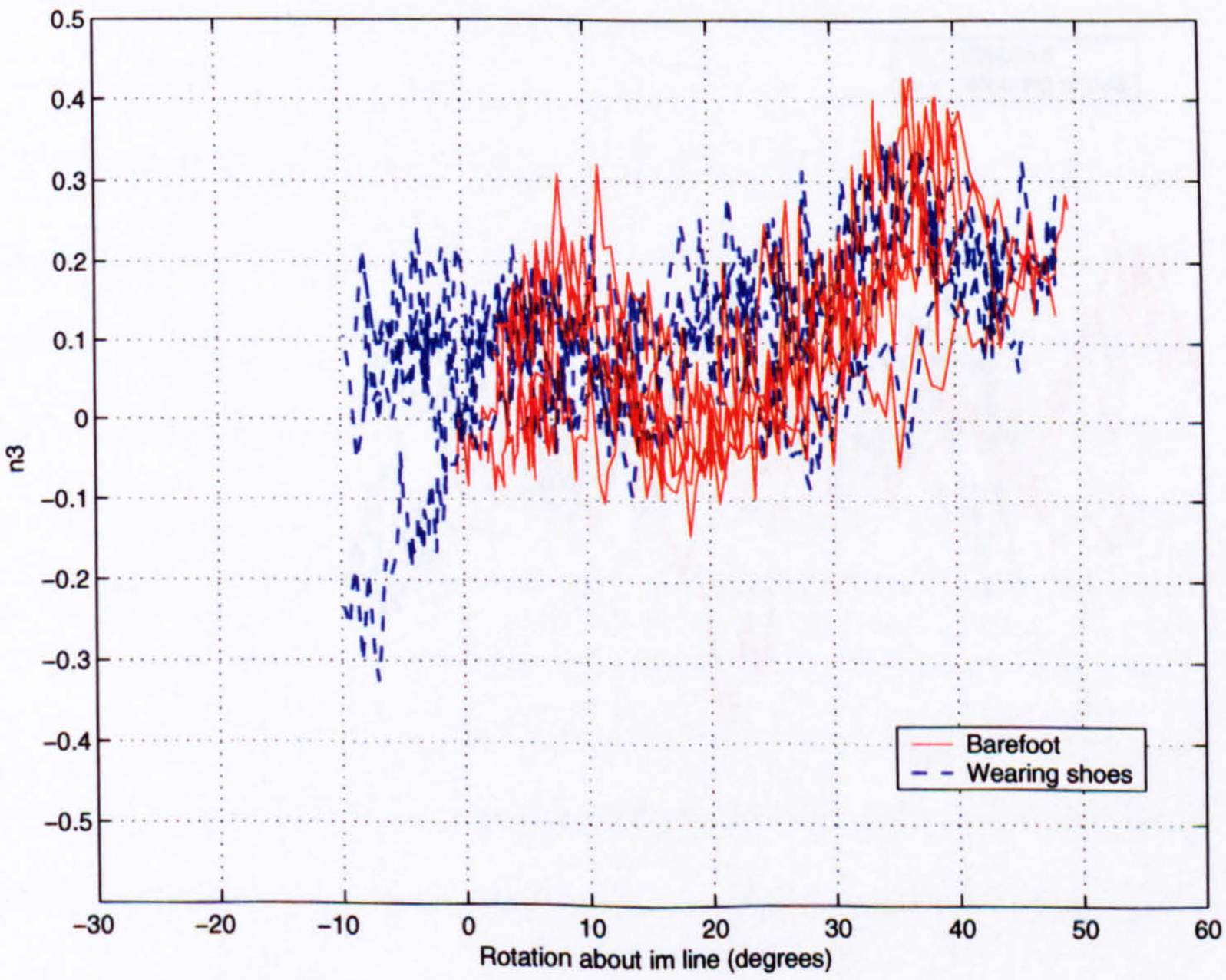

Figure 4.32: Third component of direction vector (n3) plotted against angle of rotation about IM line for Subject 3.

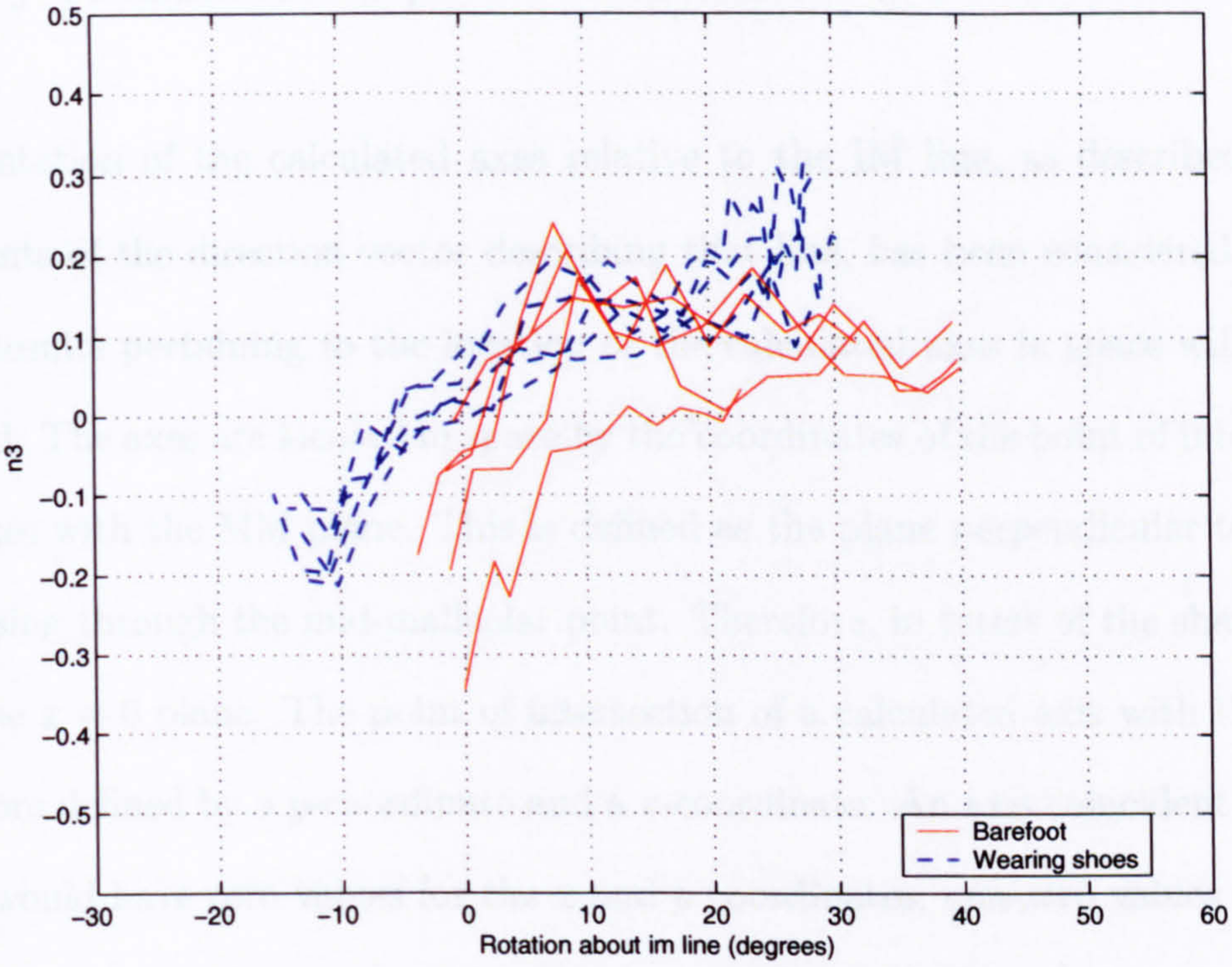

Figure 4.33: Third component of direction vector (n3) plotted against angle of rotation about IM line for Subject 4.

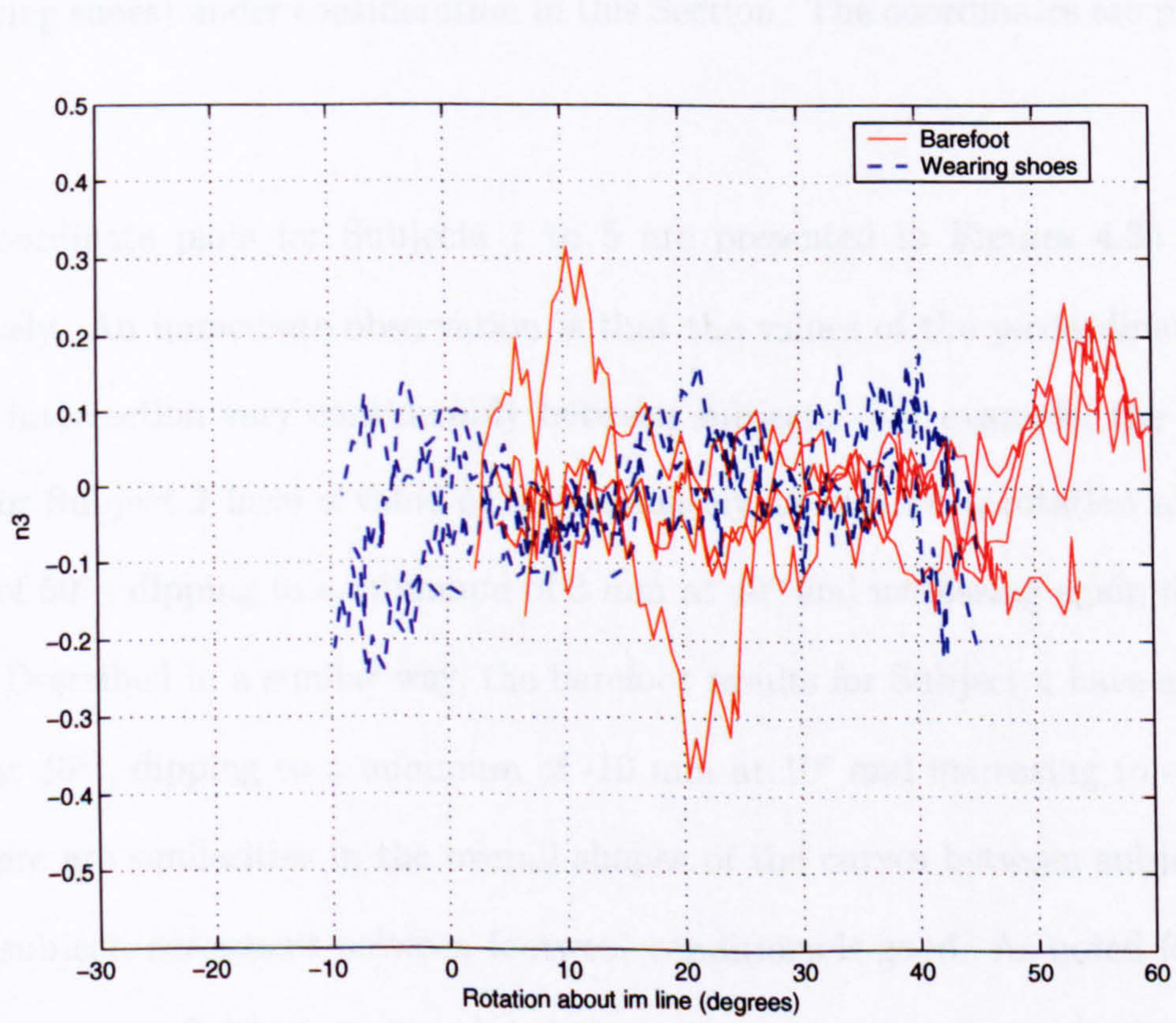

Figure 4.34: Third component of direction vector (n3) plotted against angle of rotation about IM line for Subject 5.

4.4.6 y-coordinate of point of intersection

The orientation of the calculated axes relative to the IM line, as described by the components of the direction vector describing that line, has been considered in some detail. Results pertaining to the location of the calculated axes in space will now be presented. The axes are located in space by the coordinates of the point of intersection of the axes with the MM plane. This is defined as the plane perpendicular to the IM line, passing through the mid-malleolar point. Therefore, in terms of the shank ARF, this is the $x = 0$ plane. The point of intersection of a calculated axis with this plane is therefore defined by a y-coordinate and a z-coordinate. An axis coincident with the IM line would have zero values for the x and y coordinates; non-zero values therefore indicate an axis displaced in space relative to the IM line. Plots of the variation of these coordinates with θ will be presented for the two footwear conditions (barefoot and wearing shoes) under consideration in this Section. The coordinates are presented in mm.

The y-coordinate plots for Subjects 1 to 5 are presented in Figures 4.35 to 4.39, respectively. An immediate observation is that the values of the y-coordinate of the point of intersection vary considerably between subjects. For example, the barefoot results for Subject 2 have a value of approximately 18 mm for a rotation about the IM line of 50^o , dipping to a minimum of 3 mm at 40^o and increasing again to 12 mm at 10^o . Described in a similar way, the barefoot results for Subject 4 have a value of -5 mm at 40^o , dipping to a minimum of -10 mm at 10^o and increasing to -3 mm at 0^o . There are similarities in the overall shapes of the curves between subjects. For a given subject, agreement between footwear conditions is good. As noted for the n2 and n3 results, in Subjects 1, 2 and 4 there is clear agreement between the patterns of the results although the curves are translated relative to each other on the axes.

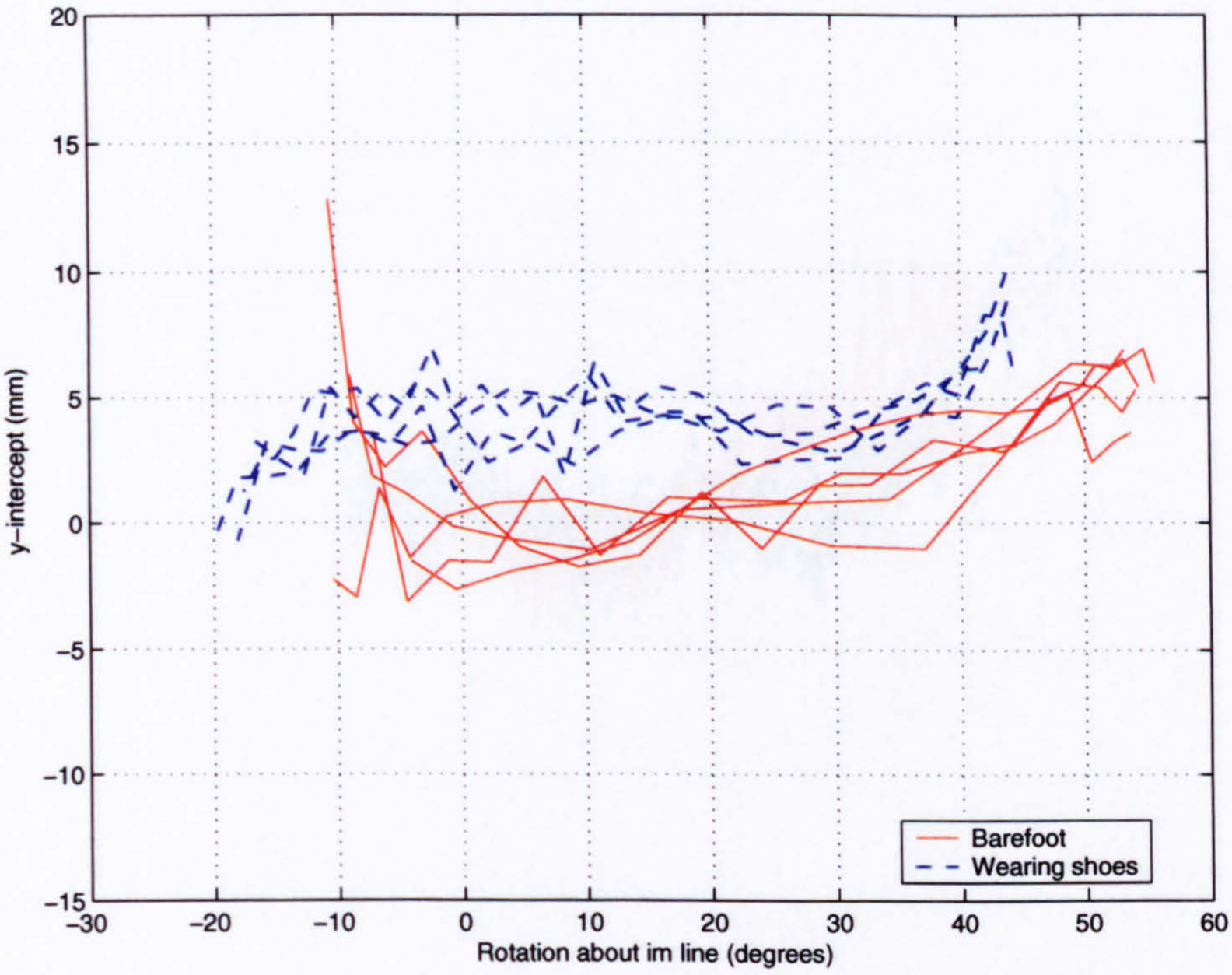

Figure 4.35: y-coordinate of point of intersection of axis with MM plane plotted against angle of rotation about IM line for Subject 1.

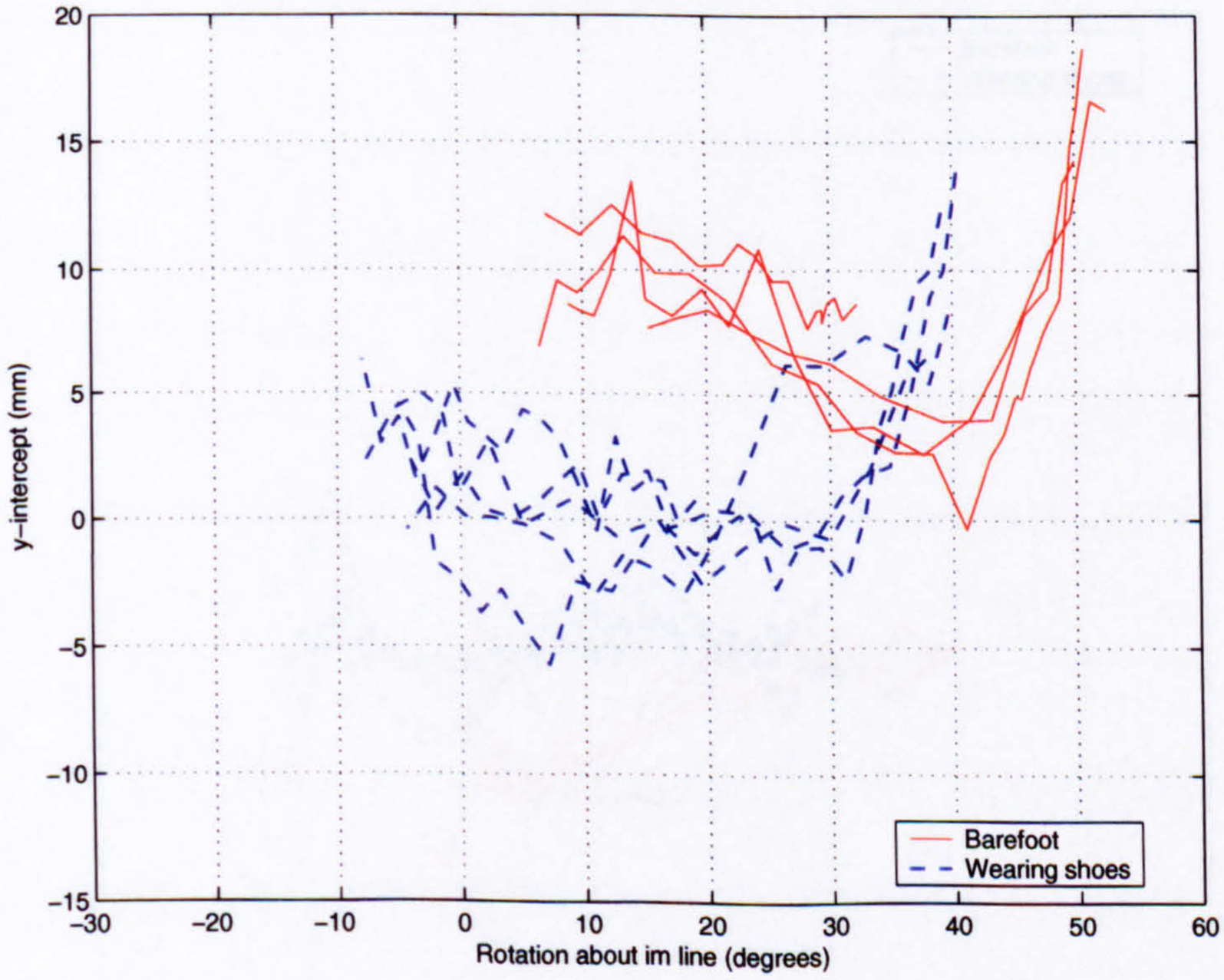

Figure 4.36: y-coordinate of point of intersection of axis with MM plane plotted against angle of rotation about IM line for Subject 2.

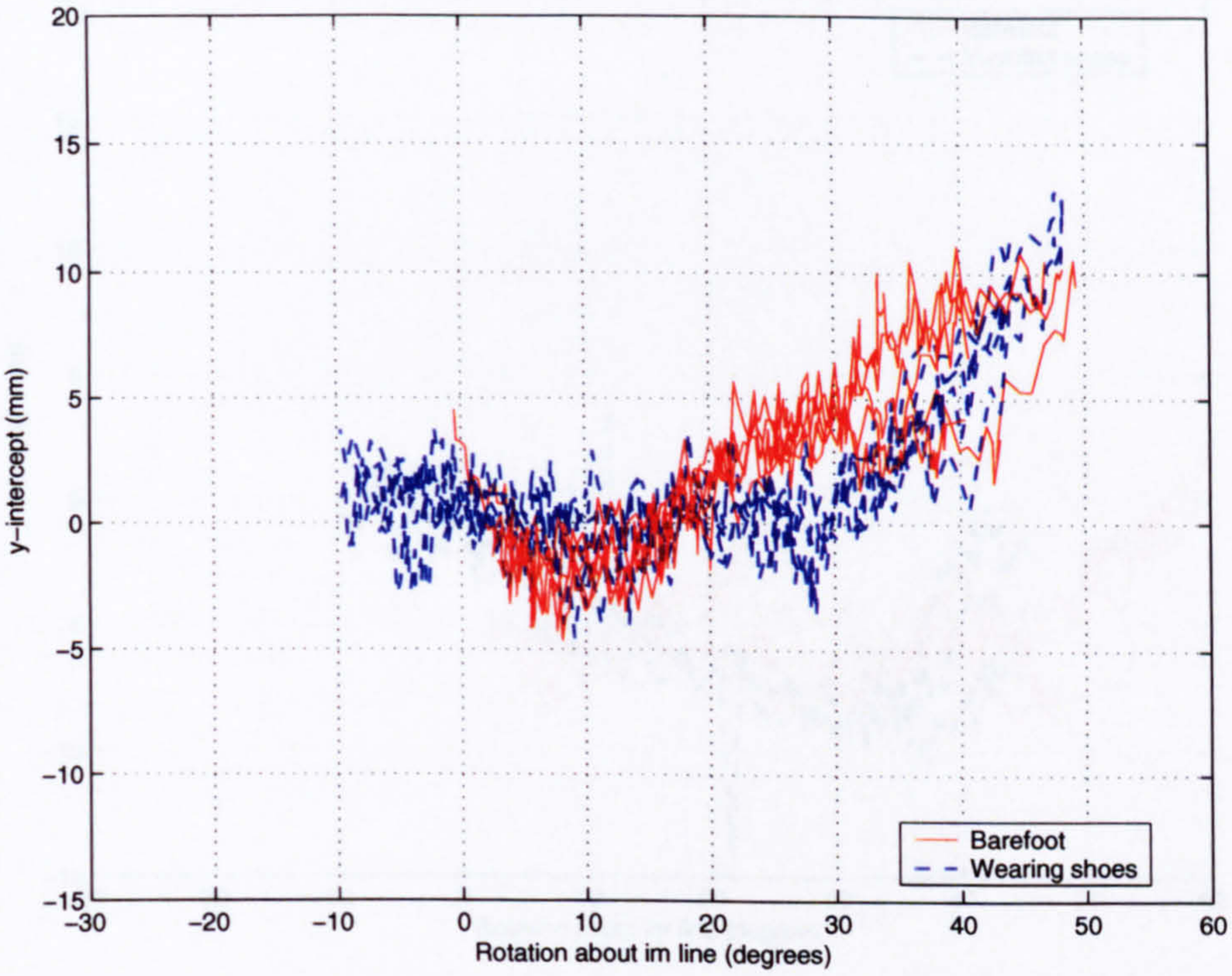

Figure 4.37: y-coordinate of point of intersection of axis with MM plane plotted against angle of rotation about IM line for Subject 3.

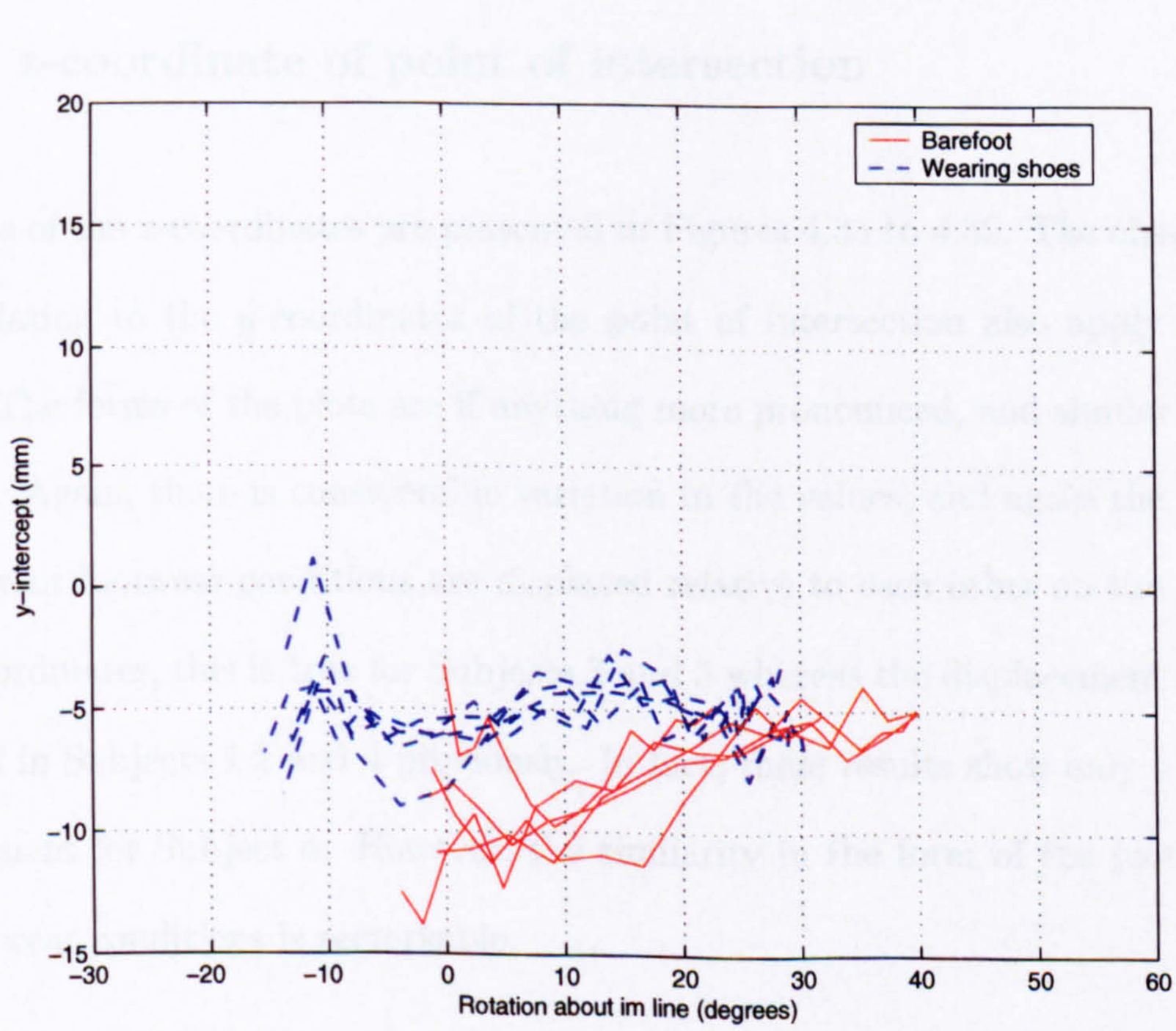

Figure 4.38: y-coordinate of point of intersection of axis with MM plane plotted against angle of rotation about IM line for Subject 4.

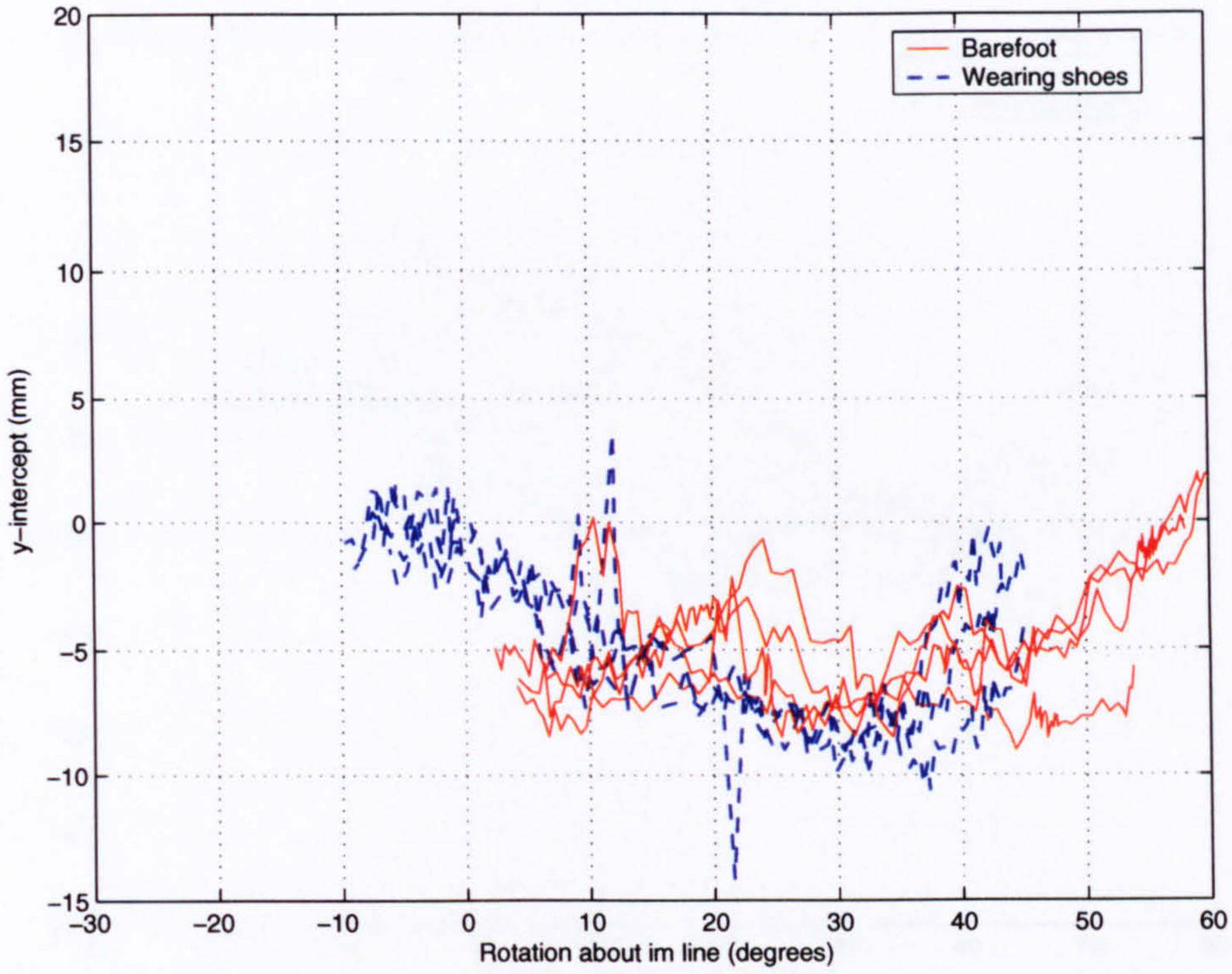

Figure 4.39: y-coordinate of point of intersection of axis with MM plane plotted against angle of rotation about IM line for Subject 5.

4.4.7 z-coordinate of point of intersection

The plots of the z-coordinates are presented in Figures 4.35 to 4.39. The observations made relating to the y-coordinates of the point of intersection also apply to these results. The forms of the plots are if anything more pronounced, and similar between subjects. Again, there is considerable variation in the values, and again the plots for the different footwear conditions are displaced relative to each other on the axes; for the z-coordinates, this is true for Subjects 3 and 5 whereas the displacement was only observed in Subjects 1,2 and 4 previously. In fact, these results show only a minimal displacement for Subject 4. However, the similarity in the form of the plots for the two footwear conditions is remarkable.

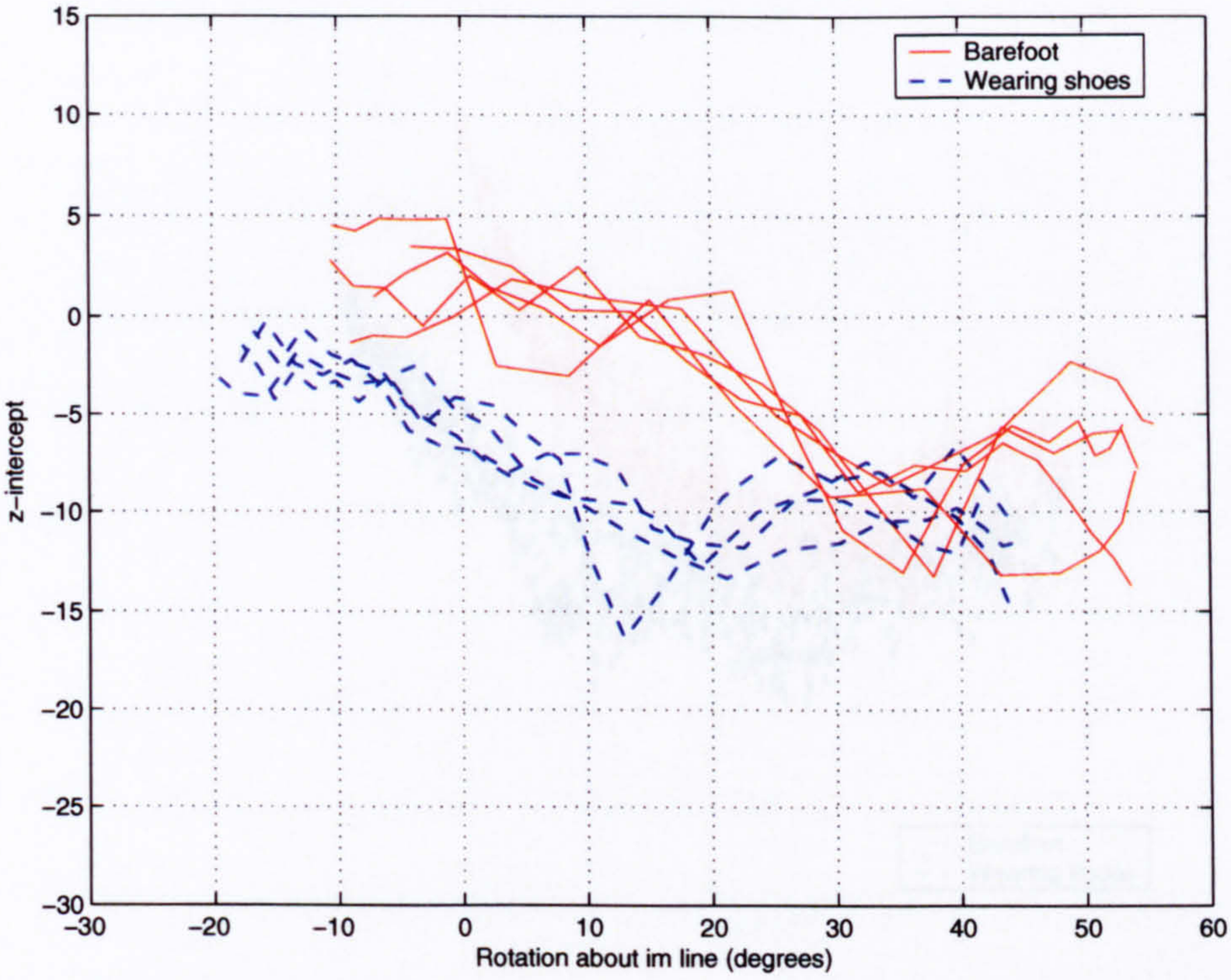

Figure 4.40: z-coordinate of point of intersection of axis with MM plane plotted against angle of rotation about IM line for Subject 1.

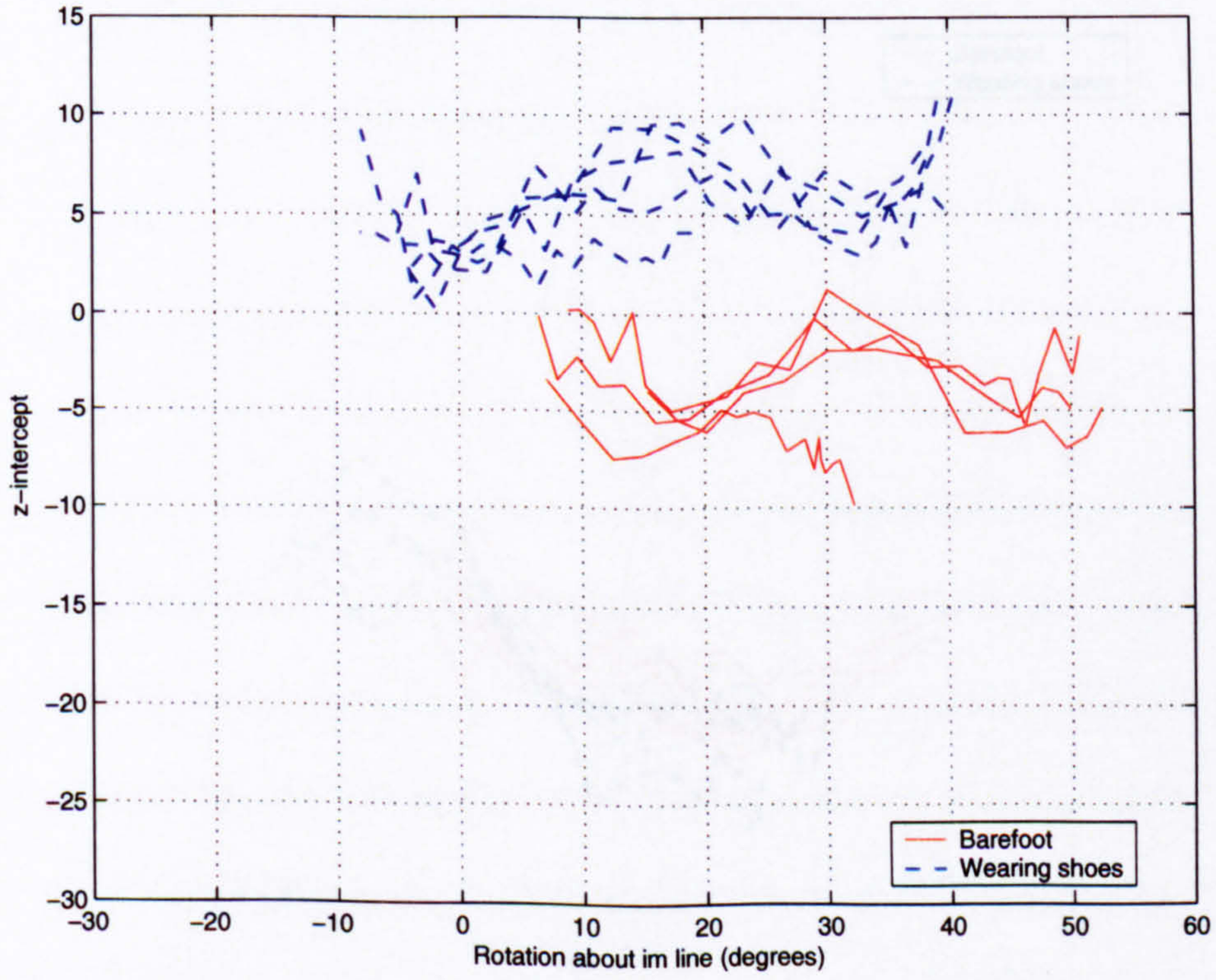

Figure 4.41: z-coordinate of point of intersection of axis with MM plane plotted against angle of rotation about IM line for Subject 2.

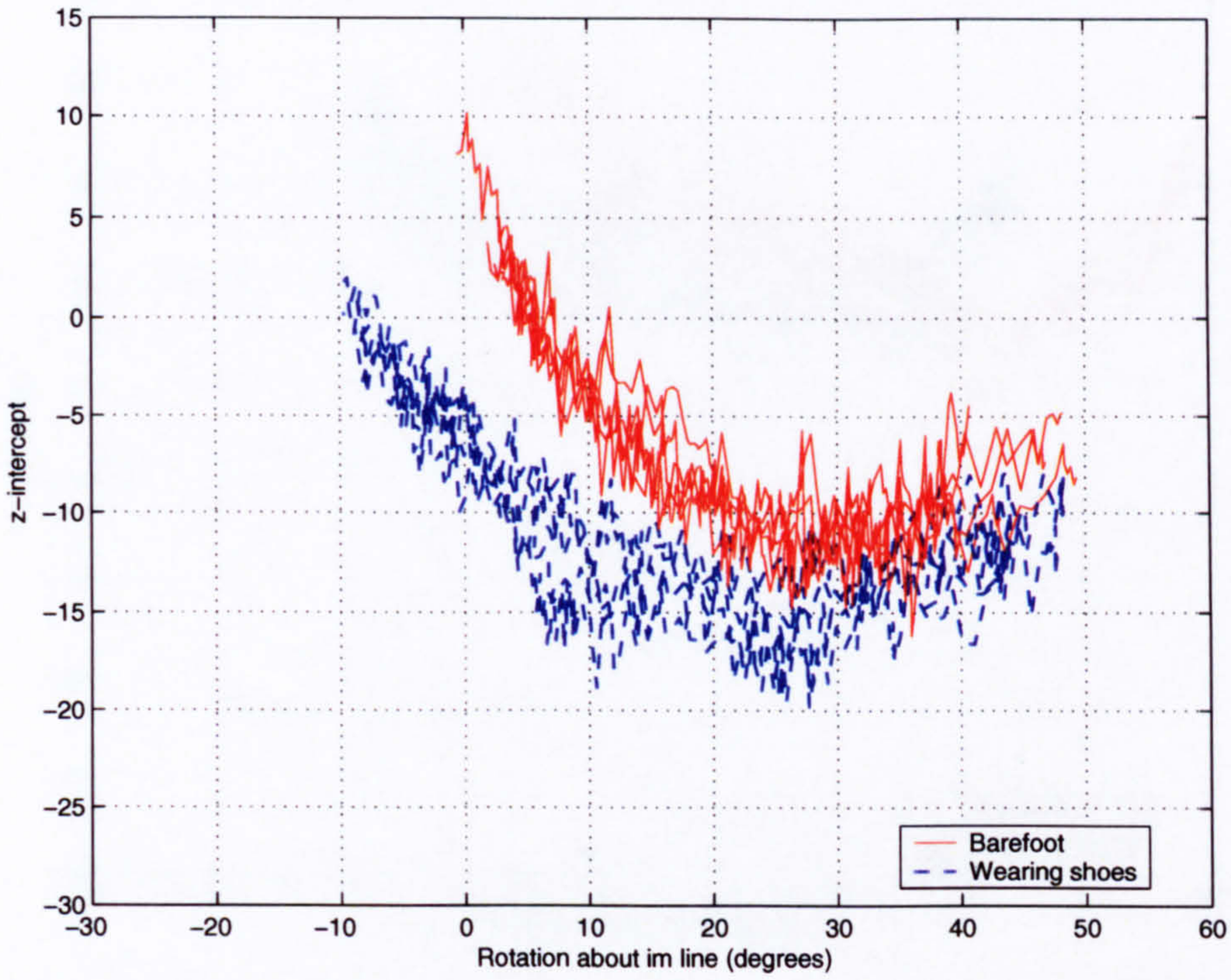

Figure 4.42: z-coordinate of point of intersection of axis with MM plane plotted against angle of rotation about IM line for Subject 3.

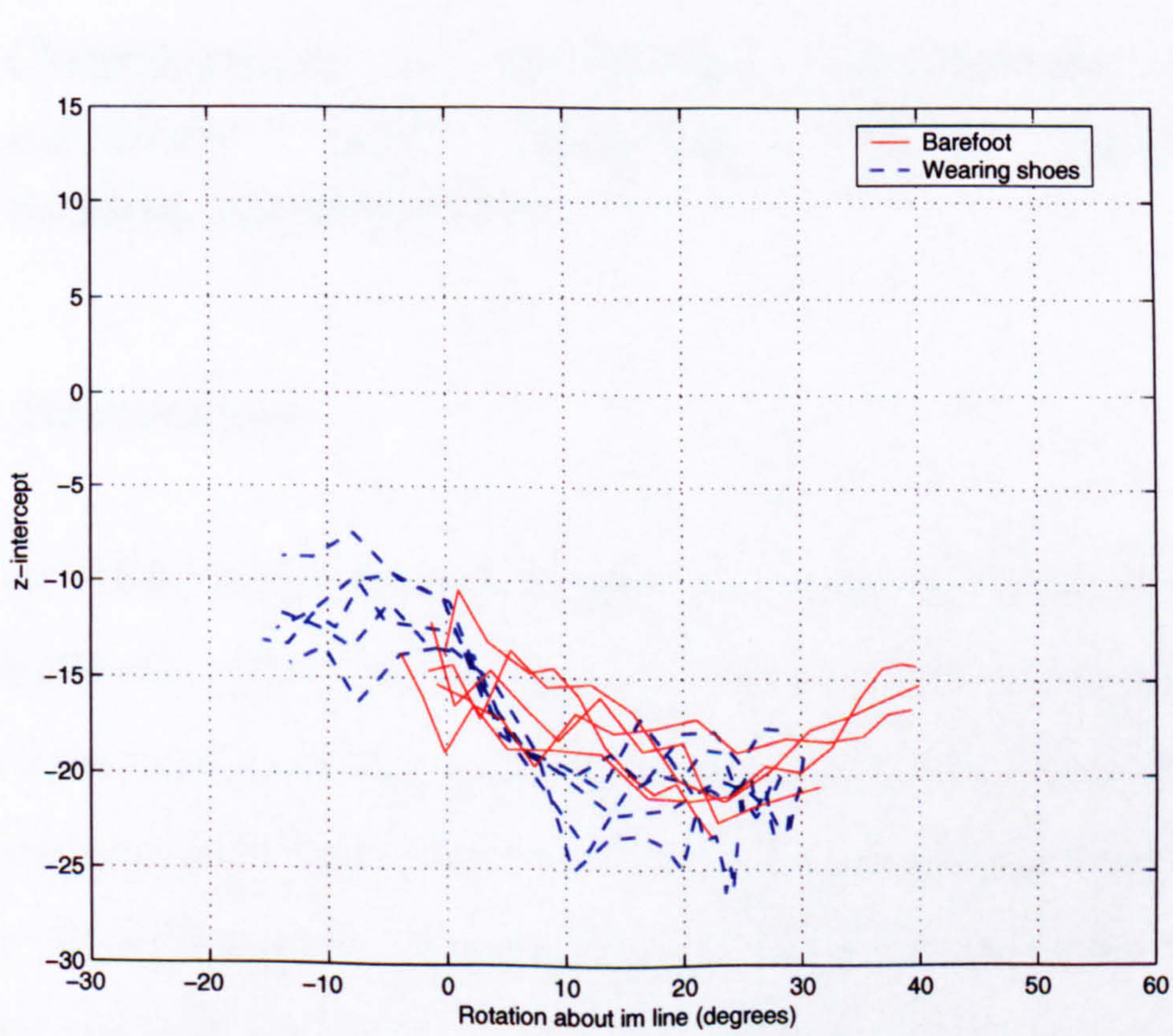

Figure 4.43: z-coordinate of point of intersection of axis with MM plane plotted against angle of rotation about IM line for Subject 4.

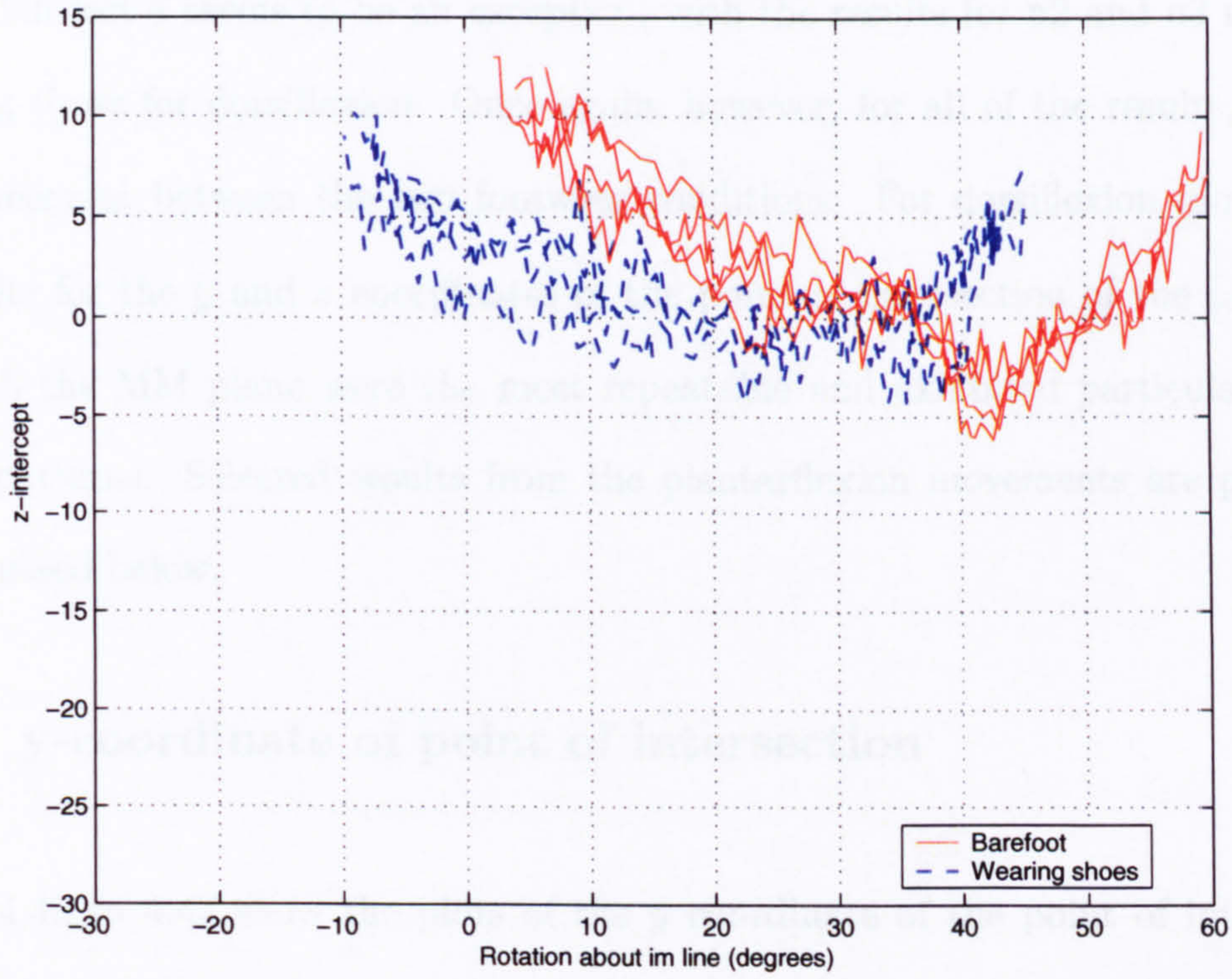

Figure 4.44: z-coordinate of point of intersection of axis with MM plane plotted against angle of rotation about IM line for Subject 5.

4.5 Comparison of unloaded movements made barefoot and wearing shoes (plantarflexion movements)

4.5.1 Introduction

A set of plots of the same parameters presented in the previous Section was produced for the corresponding plantarflexion movements. The angle-time and direction vector results will not be presented here as there is considerable overlap with those already discussed in detail for the dorsiflexion movements. However, there are some observations that are worth making. The spikes in the n1, n2 and n3 results for one of the dorsiflexion traces for Subject 5 also appear in one of the plantarflexion traces. The signs of the values of n1, n2 and n3 are reversed, as expected, due to the change in direction of rotation. However, in the majority of cases the magnitude remains very

similar. Subject 4 seems to be an exception, with the results for n2 and n3 not quite mirroring those for dorsiflexion. Once again, however, for all of the results, there is close agreement between the two footwear conditions. For dorsiflexion movements, the results for the y and z coordinates of the point of intersection of the calculated axes with the MM plane were the most repeatable and exhibited particularly well-defined patterns. Selected results from the plantarflexion movements are presented and discussed below.

4.5.2 y-coordinate of point of intersection

Figures 4.45 to 4.47 show the plots of the y coordinate of the point of intersection against θ for plantarflexion movements for Subjects 2, 3 and 4, respectively. In terms of the shape of the plots, these are very similar to the corresponding dorsiflexion plots (Figures 4.36 to 4.38). Although there are some variations in the actual values, these results add to the evidence to support repeatable patterns for a given subject and even similarities between subjects. These results also continue to indicate that there is no fundamental difference between results from subjects tested barefoot or wearing shoes.

4.5.3 z-coordinate of point of intersection

The results for the z-coordinate lead to similar conclusions to those drawn from the y-coordinate results. There is an exception here, which is that for Subject 4 (Figure 4.50) the slope of the plots is reversed between the dorsiflexion and plantarflexion results. It may be worthy of note that Subject 4 also exhibited the greatest variations in n2 and n3 results between dorsiflexion and plantarflexion. For completeness, plantarflexion y-coordinate plots are presented in Figures 4.48 and 4.49.

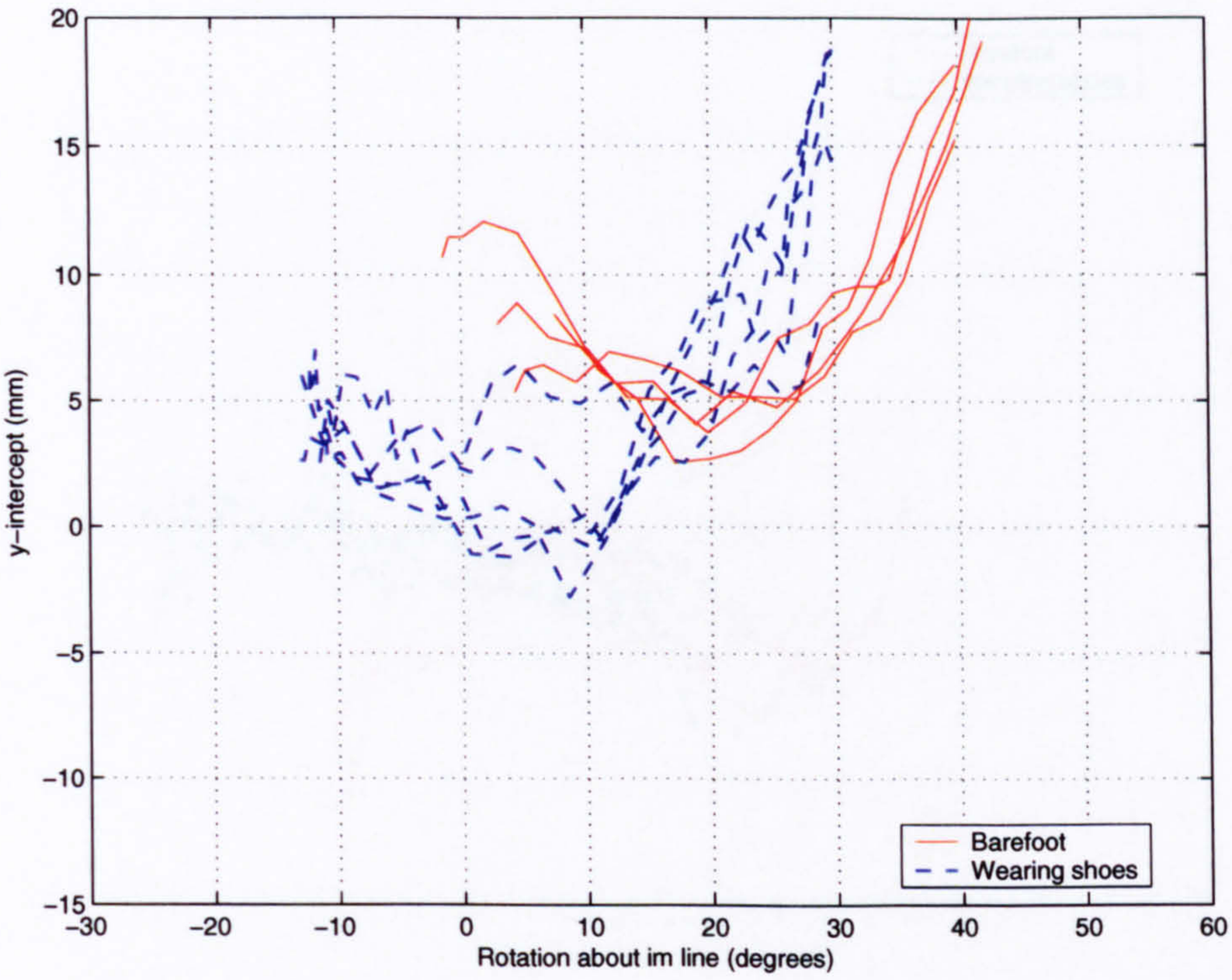

Figure 4.45: y-coordinate of point of intersection of axis with MM plane plotted against angle of rotation about IM line for Subject 2, plantarflexion movements.

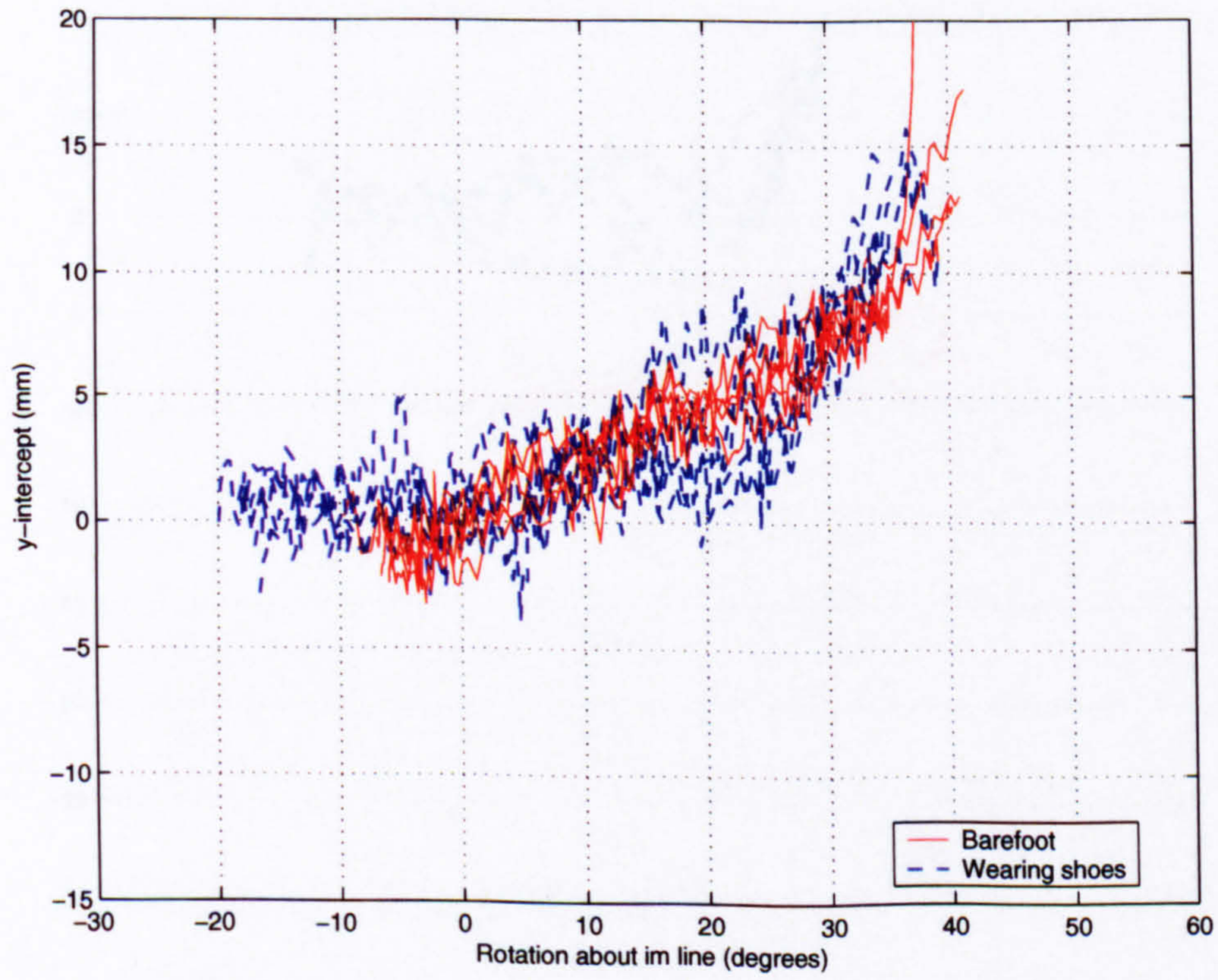

Figure 4.46: y-coordinate of point of intersection of axis with MM plane plotted against angle of rotation about IM line for Subject 3, plantarflexion movements.

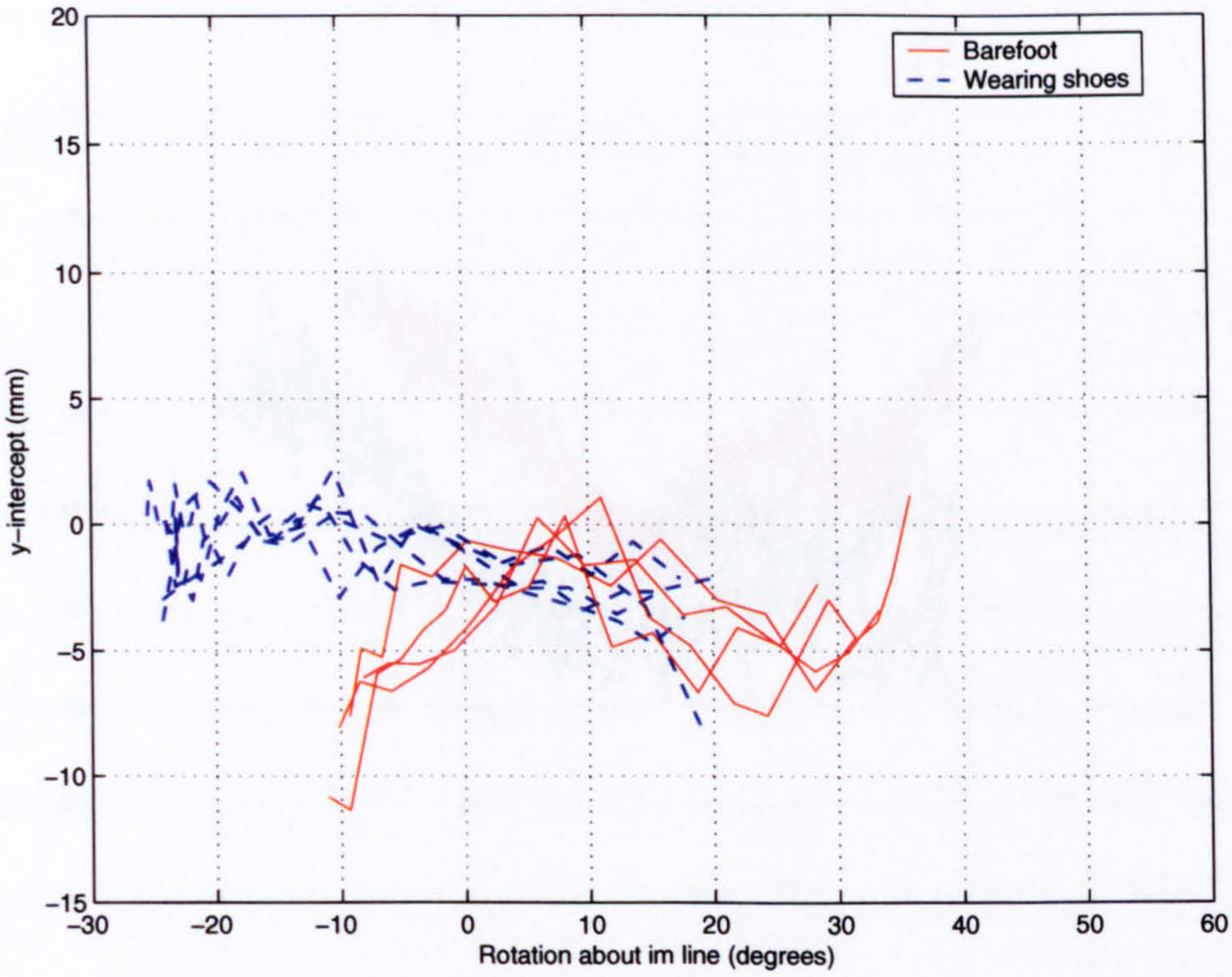

Figure 4.47: y-coordinate of point of intersection of axis with MM plane plotted against angle of rotation about IM line for Subject 4, plantarflexion movements.

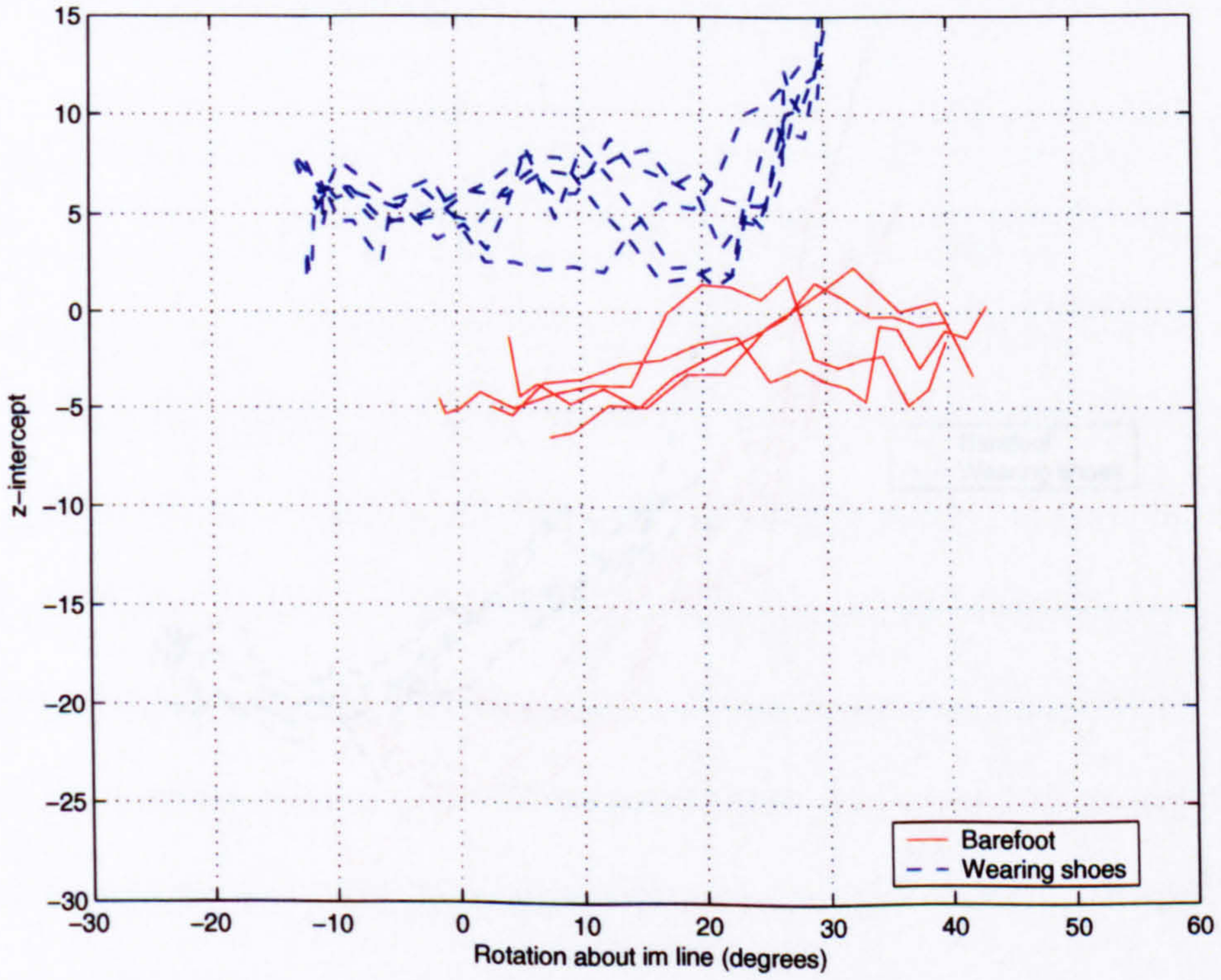

Figure 4.48: z-coordinate of point of intersection of axis with MM plane plotted against angle of rotation about IM line for Subject 2, plantarflexion movements.

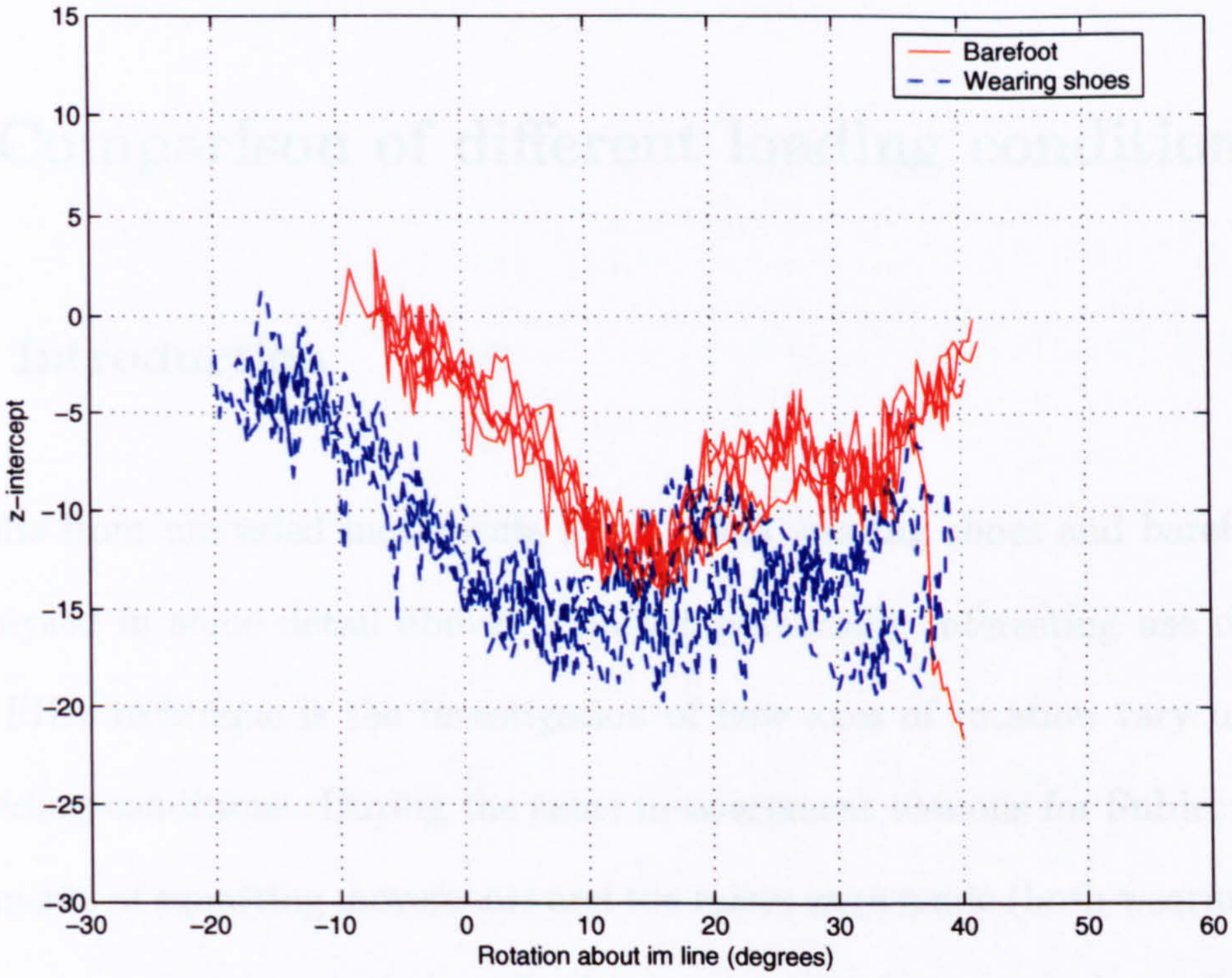

Figure 4.49: z-coordinate of point of intersection of axis with MM plane plotted against angle of rotation about IM line for Subject 3, plantarflexion movements.

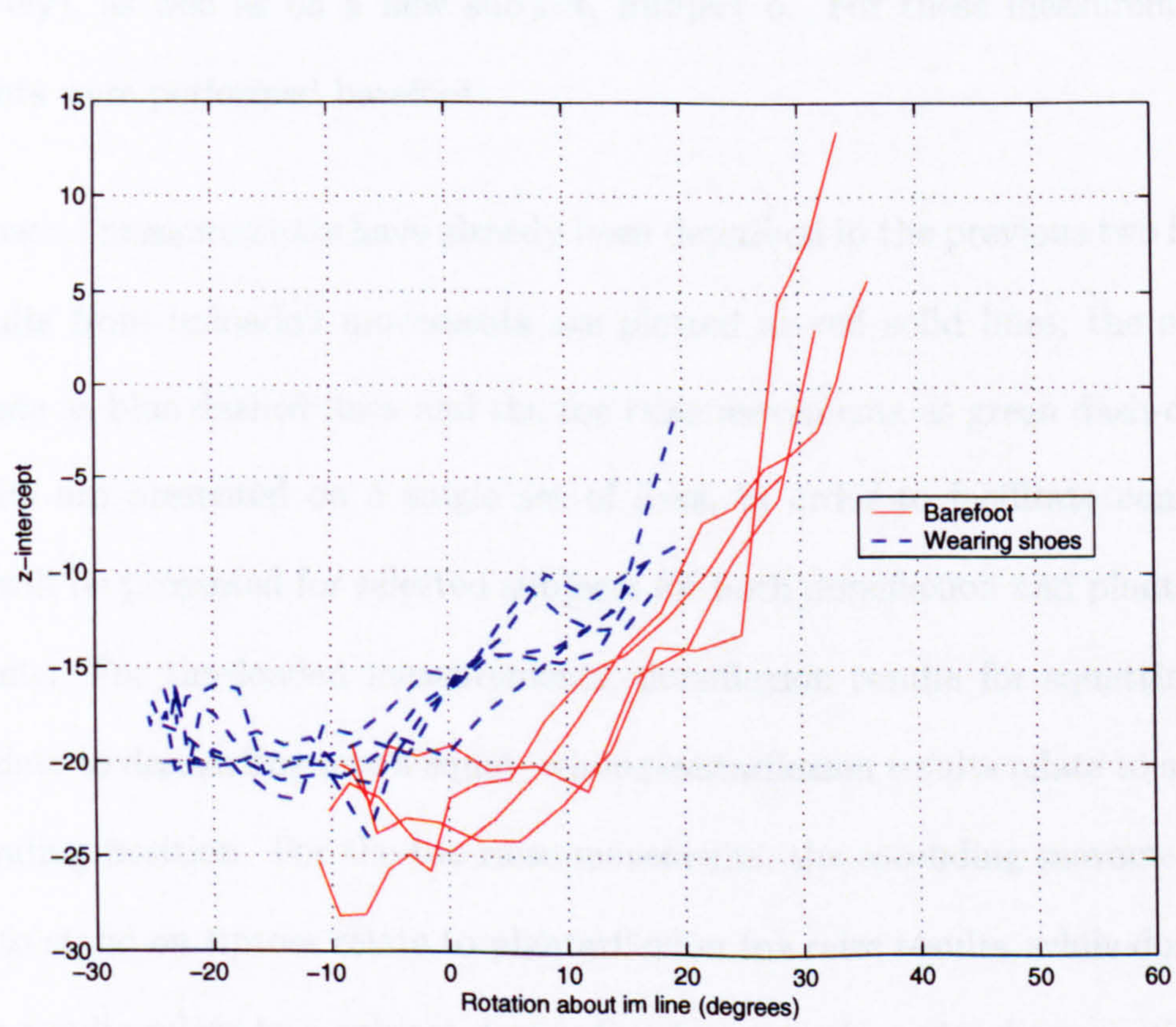

Figure 4.50: z-coordinate of point of intersection of axis with MM plane plotted against angle of rotation about IM line for Subject 4, plantarflexion movements.

4.6 Comparison of different loading conditions

4.6.1 Introduction

The results from unloaded movements for subjects wearing shoes and barefoot have been analysed in some detail above. Another potentially interesting use of the sequential FHA technique is the investigation of how axes of rotation vary under different loading conditions. During the same measurement sessions for Subjects 1 to 5, measurements of squatting movements and toe raises were made (both wearing shoes). In a separate measurement session, further measurements were made on Subjects 4 and 5 (these will be referred to as Subject 4, Session 2 and Subject 5, Session 2, respectively), as well as on a new subject, Subject 6. For these measurements, all movements were performed barefoot.

The unloaded measurements have already been described in the previous two Sections. The results from unloaded movements are plotted as red solid lines, the squatting movements as blue dashed lines and the toe raise movements as green dash-dot lines. All results are presented on a single set of axes, in order to facilitate comparison. Results will be presented for selected subjects for both dorsiflexion and plantarflexion movements. For the loaded measurements, dorsiflexion results for squatting movements relate to descending into a squat, while plantarflexion results relate to ascending to a standing position. For the toe raise movements, the ascending movement of the subject to stand on tiptoes relate to plantarflexion toe raise results, while dorsiflexion toe raise results relate to a subject descending to return to a standing position.

4.6.2 Theta vs time

The plots of θ against time for dorsiflexion and plantarflexion movements for Subject 2 (Figures 4.52 and 4.51), Subject 3 (Figures 4.54 and 4.53) and Subject 6 (Figures 4.56 and 4.55) respectively. These have been selected as representative of the results obtained.

The unloaded movements for Subjects 2 and 3 have already been discussed. For Subject 6, it is interesting to note the narrow range of movement (approximately 40^o) which is seen both in dorsiflexion and plantarflexion. In fact, Subject 6 is the only case where the range of the toe raise movements is greater than that of the unloaded movements. For Subjects 2 and 3, the range of the unloaded measurements is approximately 20^o greater than that of the toe raises, although in all cases the ranges overlap. For all subjects, there is little if any overlap between the results from the squatting movements and the unloaded and toe raise movements. This is explained by the fact that when squatting, the subject's weight forces a more dorsiflexed orientation than is achieved in a comfortable, unloaded movement. The lack of overlap between the squatting and toe raise movements is explained by the fact that the startpoint of the dorsiflexion squat is the same as the endpoint of the dorsiflexion toe raise, i.e. comfortable standing. It has been noted previously that a comfortable standing position is in a slight degree of dorsiflexion. The time taken for the squatting and toe raise movements is significantly longer for Subject 3 than for Subjects 2 and 6, as expected. The jerky nature of the unloaded and toe raise movements is absent from the squatting movement.

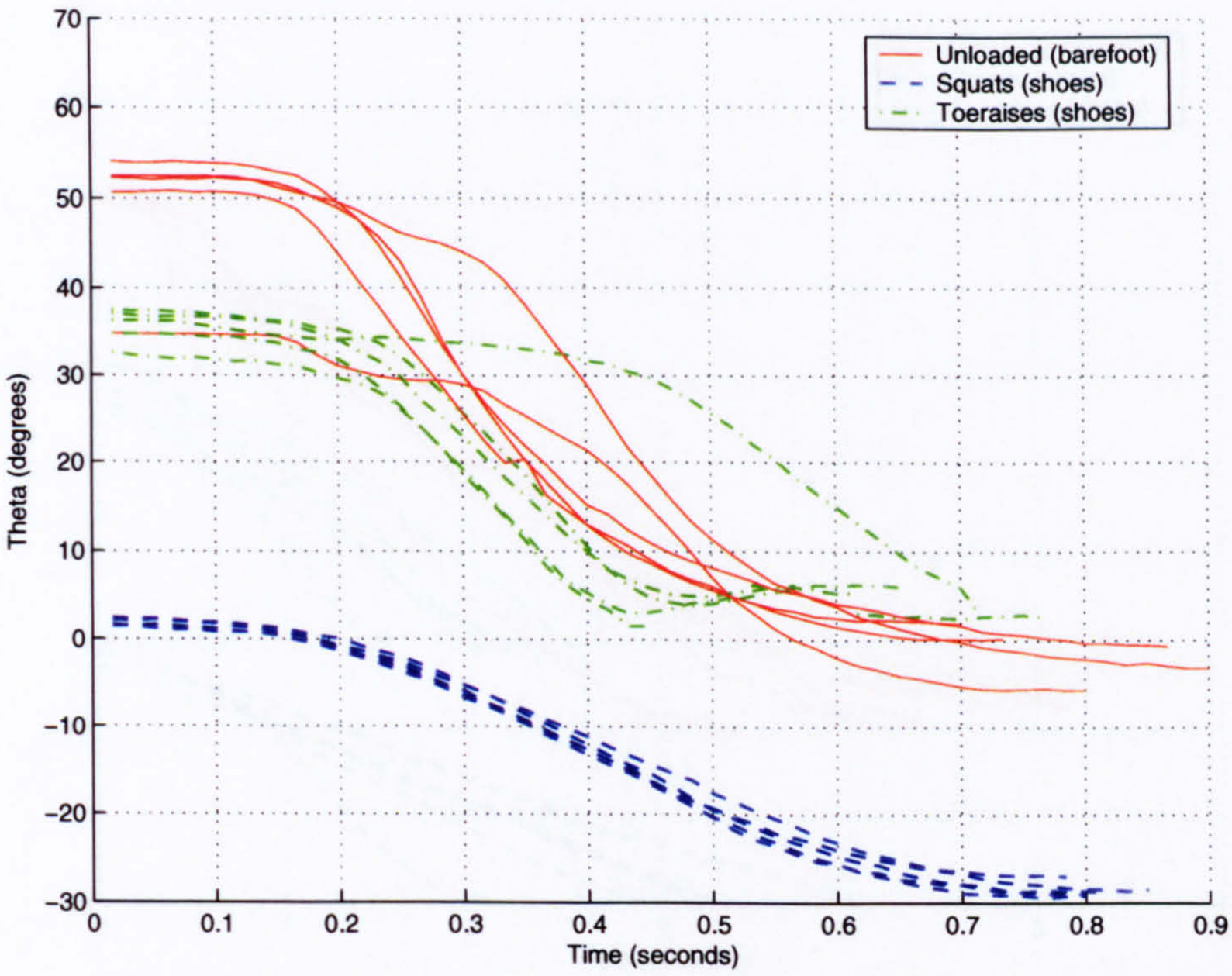

Figure 4.51: Angle of rotation about IM line (theta) plotted against time for Subject 2 (dorsiflexion movements).

Figure 4.52: Angle of rotation about IM line (theta) plotted against time for Subject 2 (plantarflexion movements).

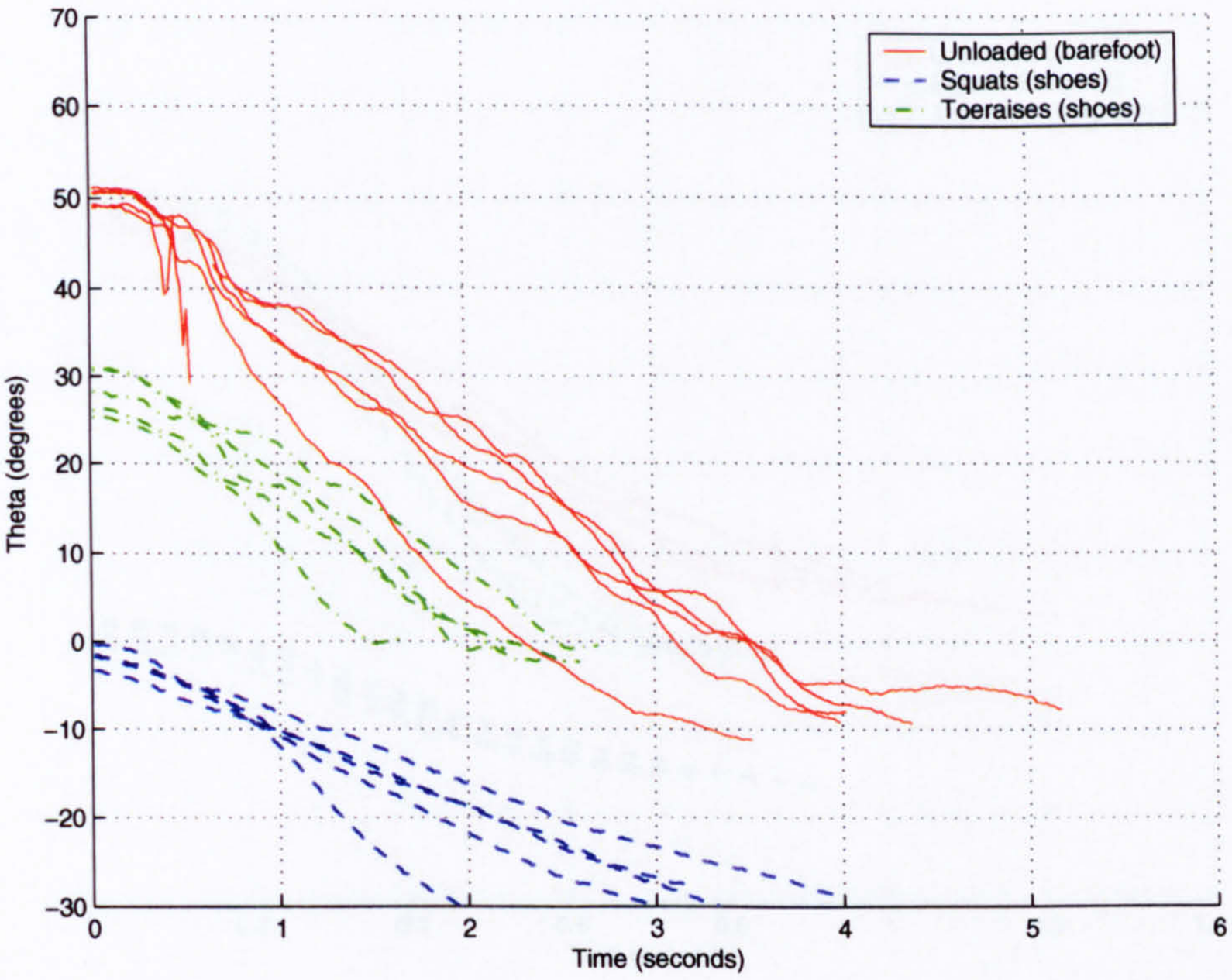

Figure 4.53: Angle of rotation about IM line (theta) plotted against time for Subject 3 (dorsiflexion movements).

Figure 4.54: Angle of rotation about IM line (theta) plotted against time for Subject 3 (plantarflexion movements).

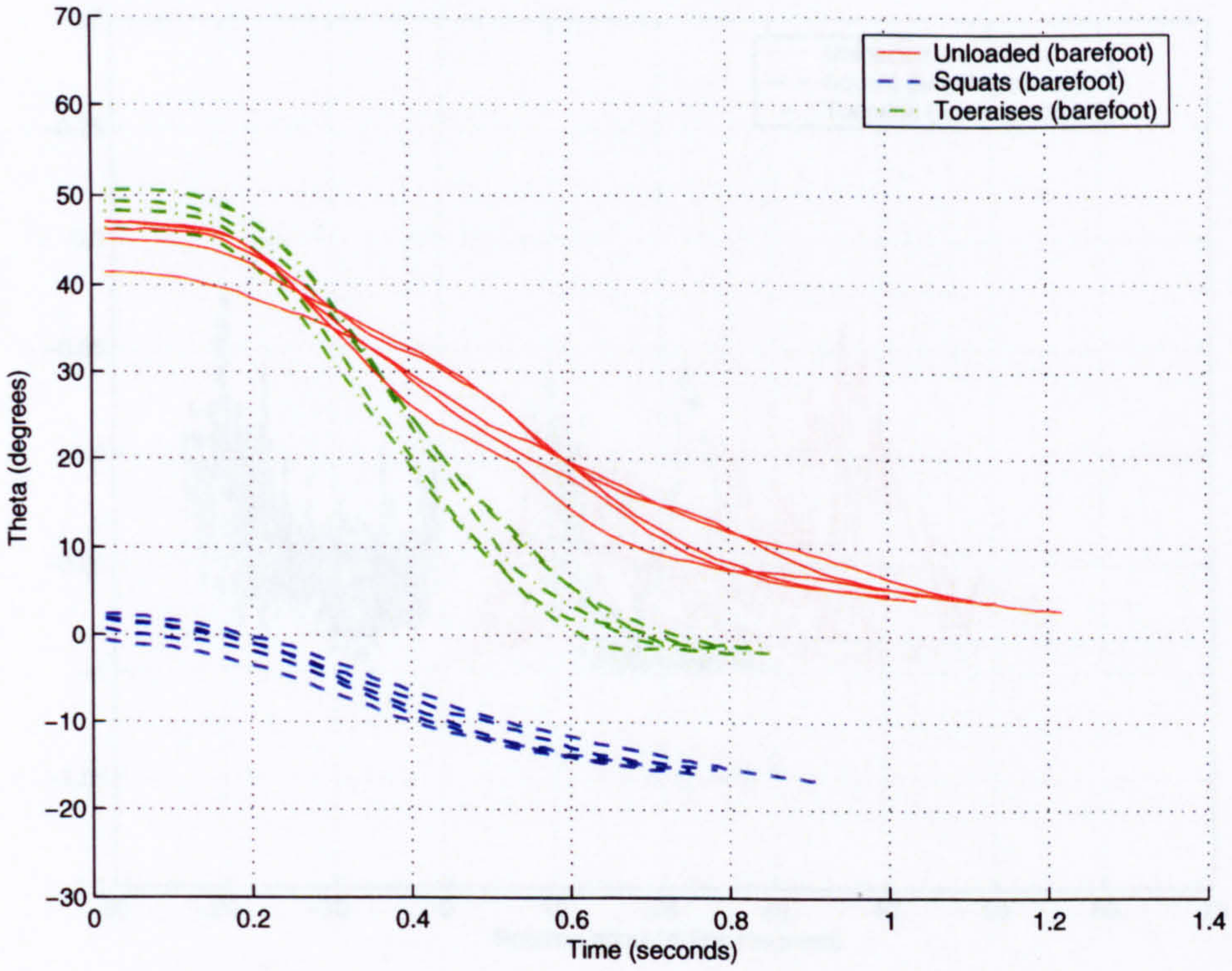

Figure 4.55: Angle of rotation about IM line (theta) plotted against time for Subject 6 (dorsiflexion movements).

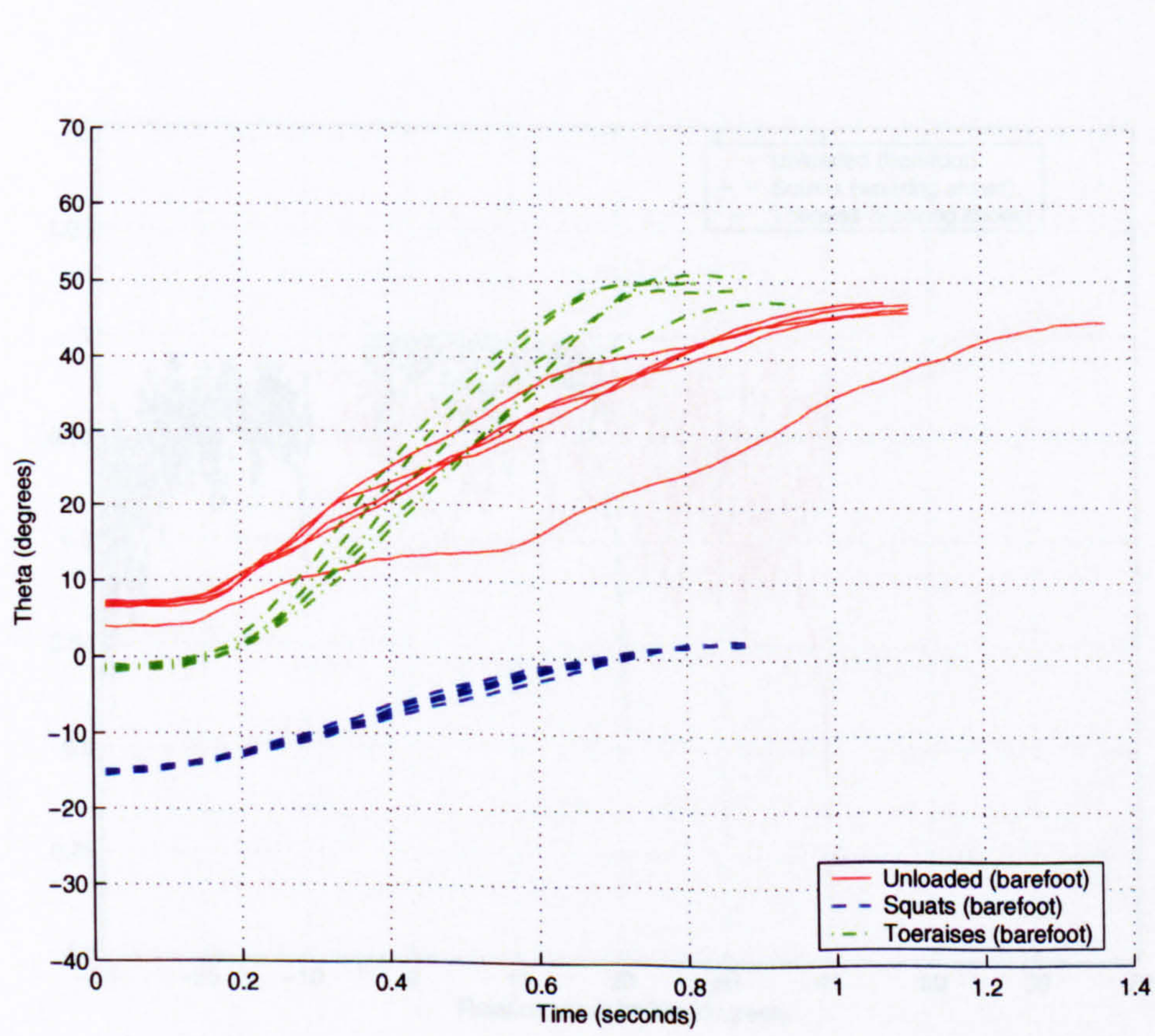

Figure 4.56: Angle of rotation about IM line (theta) plotted against time for Subject 6 (plantarflexion movements).

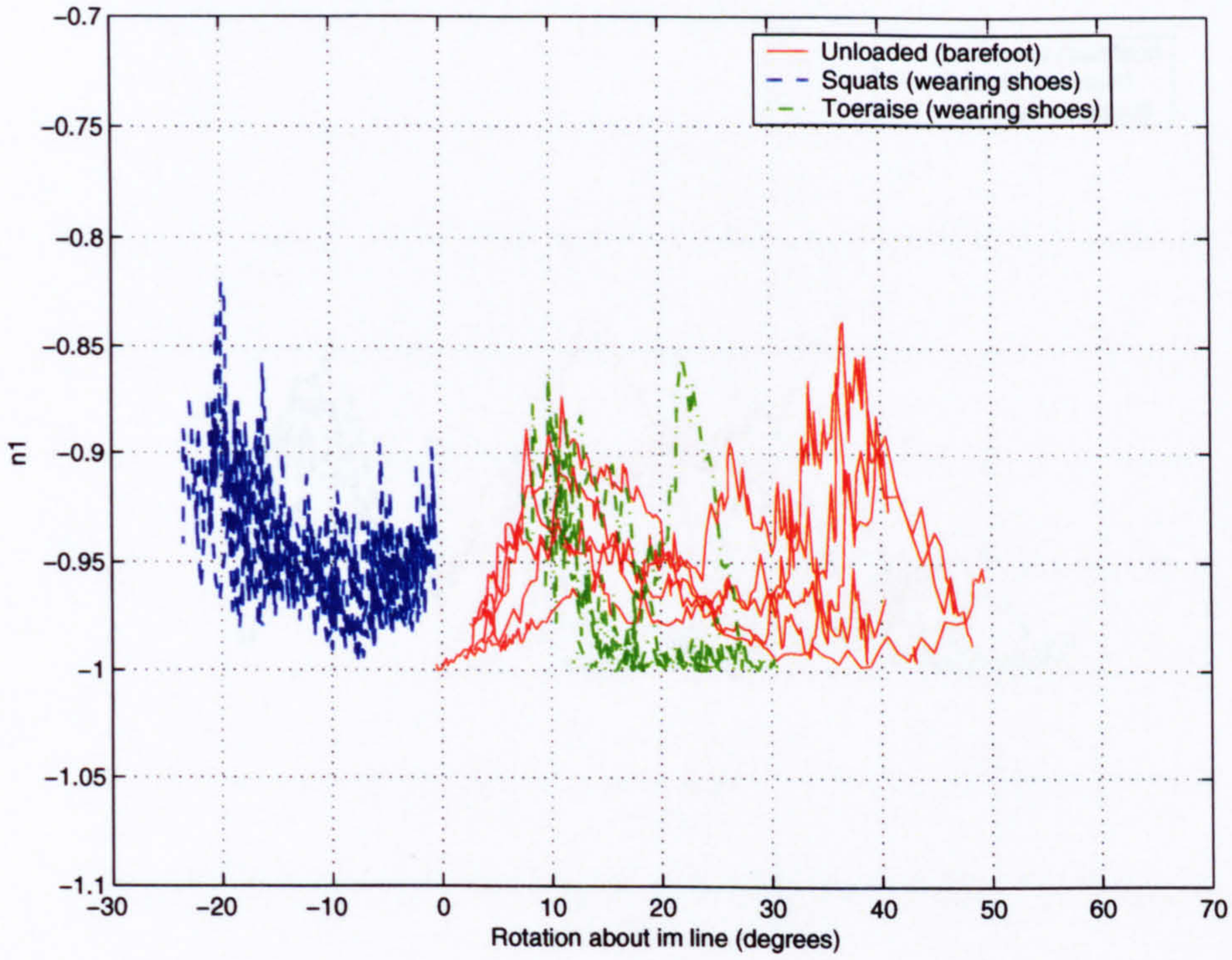

Figure 4.57: First component of direction vector (n1) plotted against angle of rotation about IM line for Subject 3 (dorsiflexion movements).

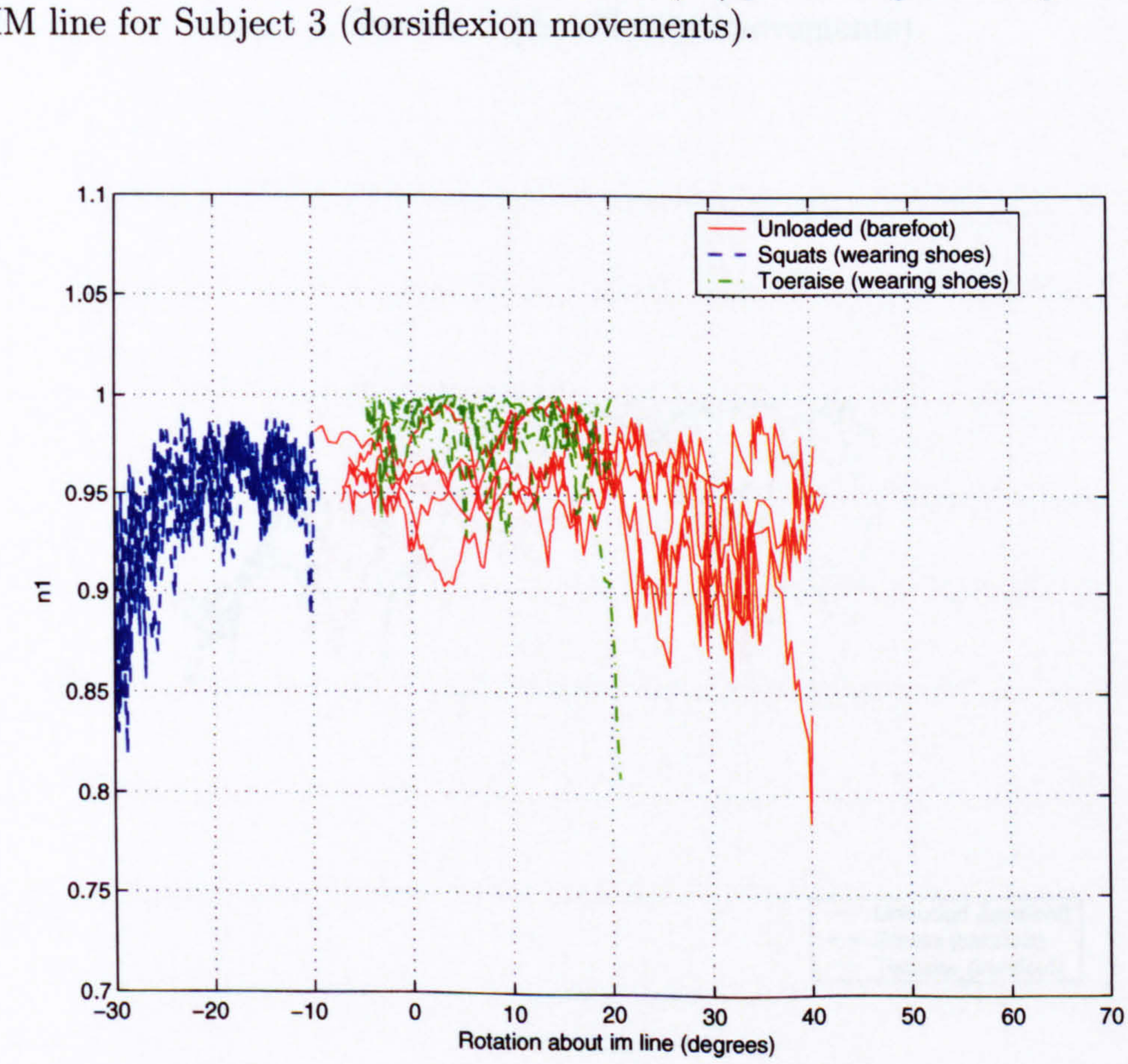

Figure 4.58: First component of direction vector (n1) plotted against angle of rotation about IM line for Subject 3 (plantarflexion movements).

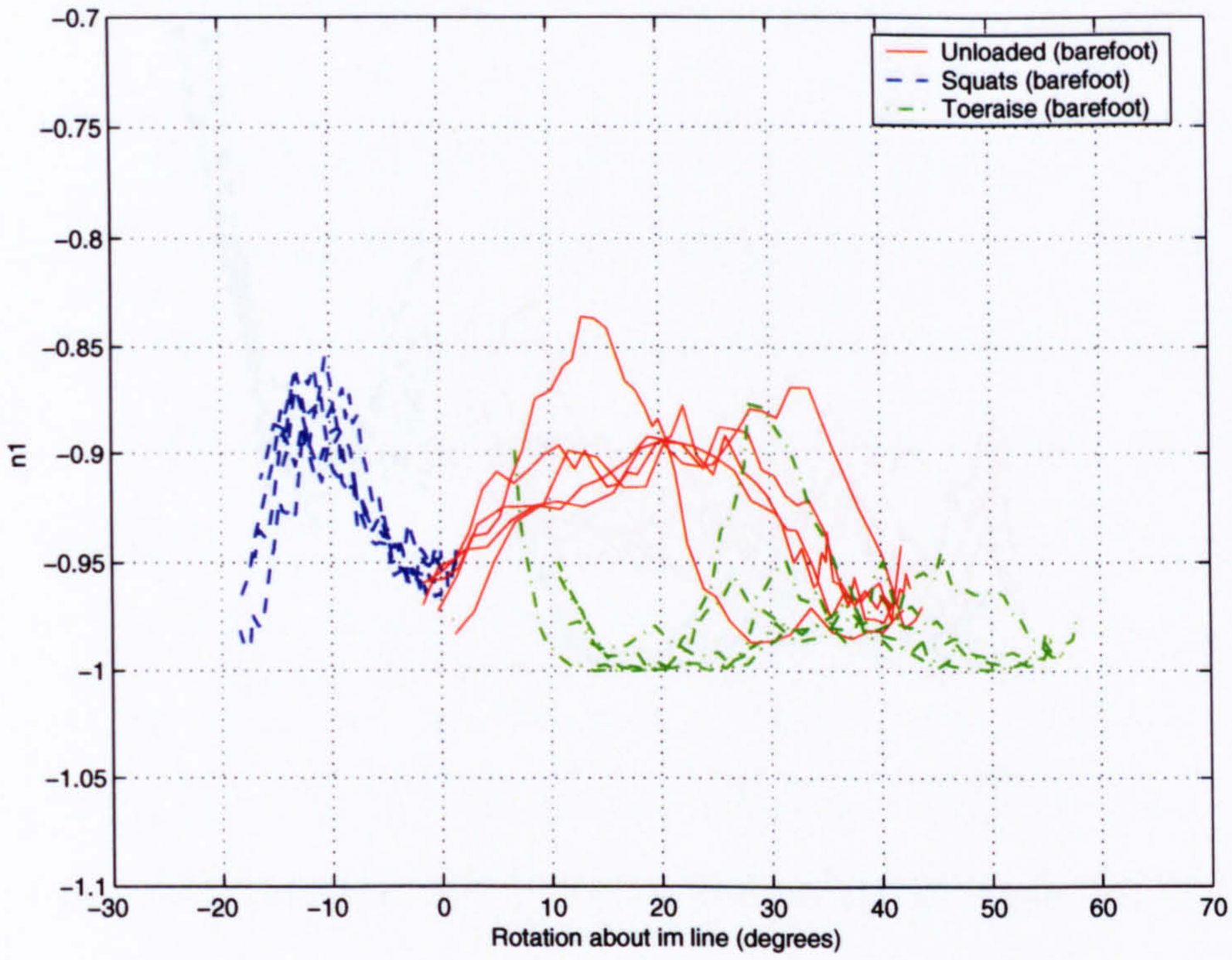

Figure 4.59: First component of direction vector (n1) plotted against angle of rotation about IM line for Subject 4, Session 2 (dorsiflexion movements).

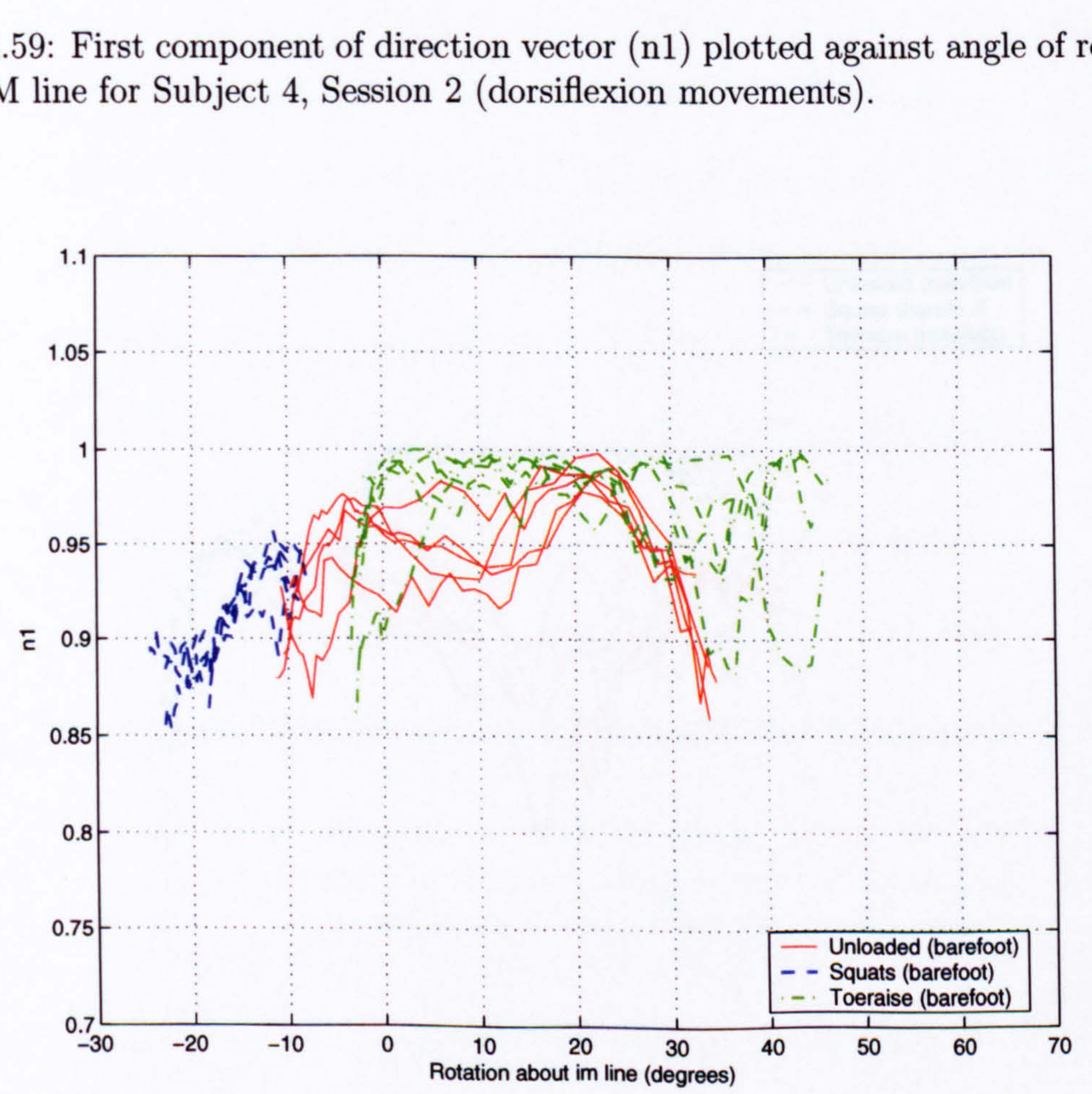

Figure 4.60: First component of direction vector (n1) plotted against angle of rotation about IM line for Subject 4, Session 2 (plantarflexion movements).

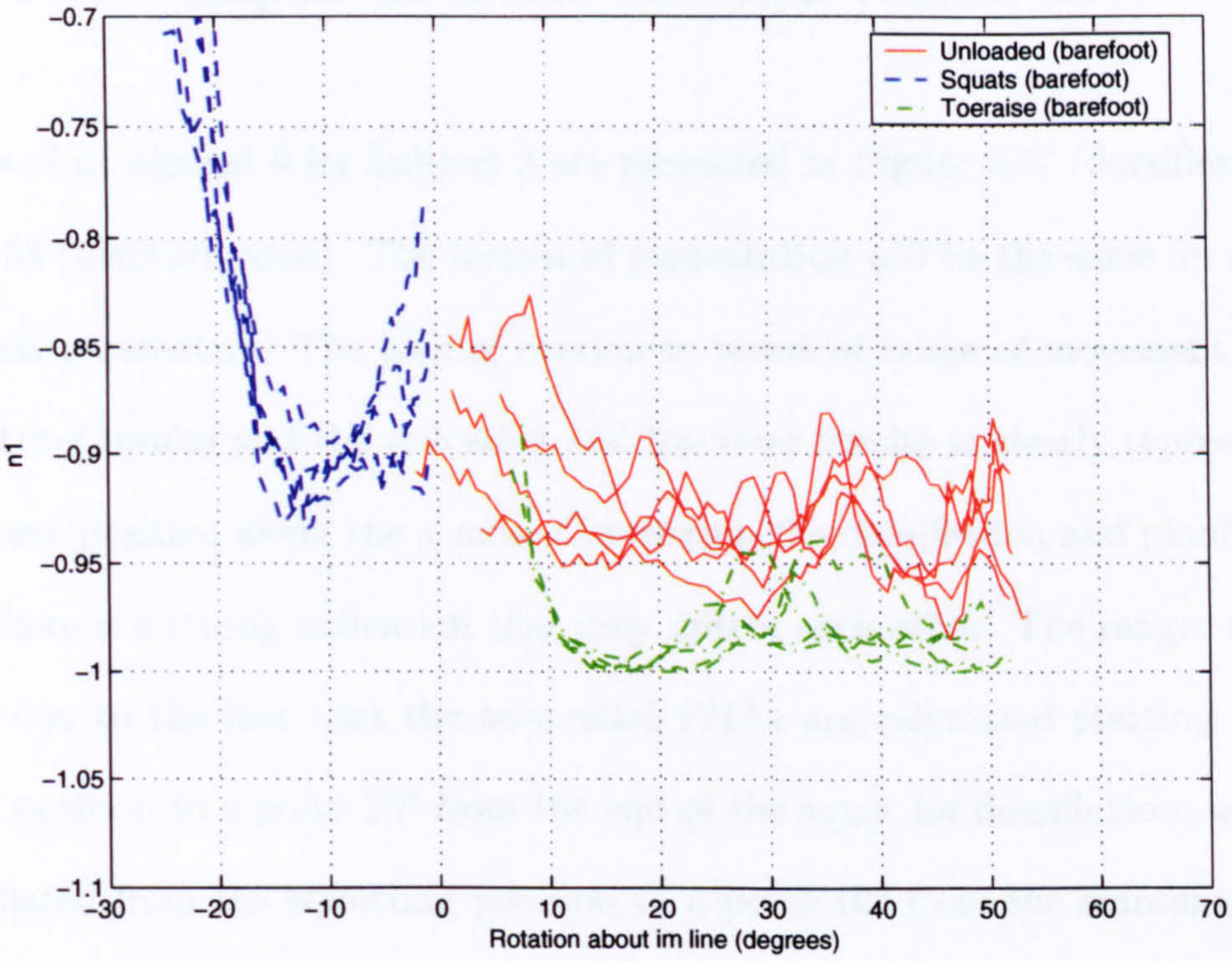

Figure 4.61: First component of direction vector (n1) plotted against angle of rotation about IM line for Subject 5, Session 2 (dorsiflexion movements).

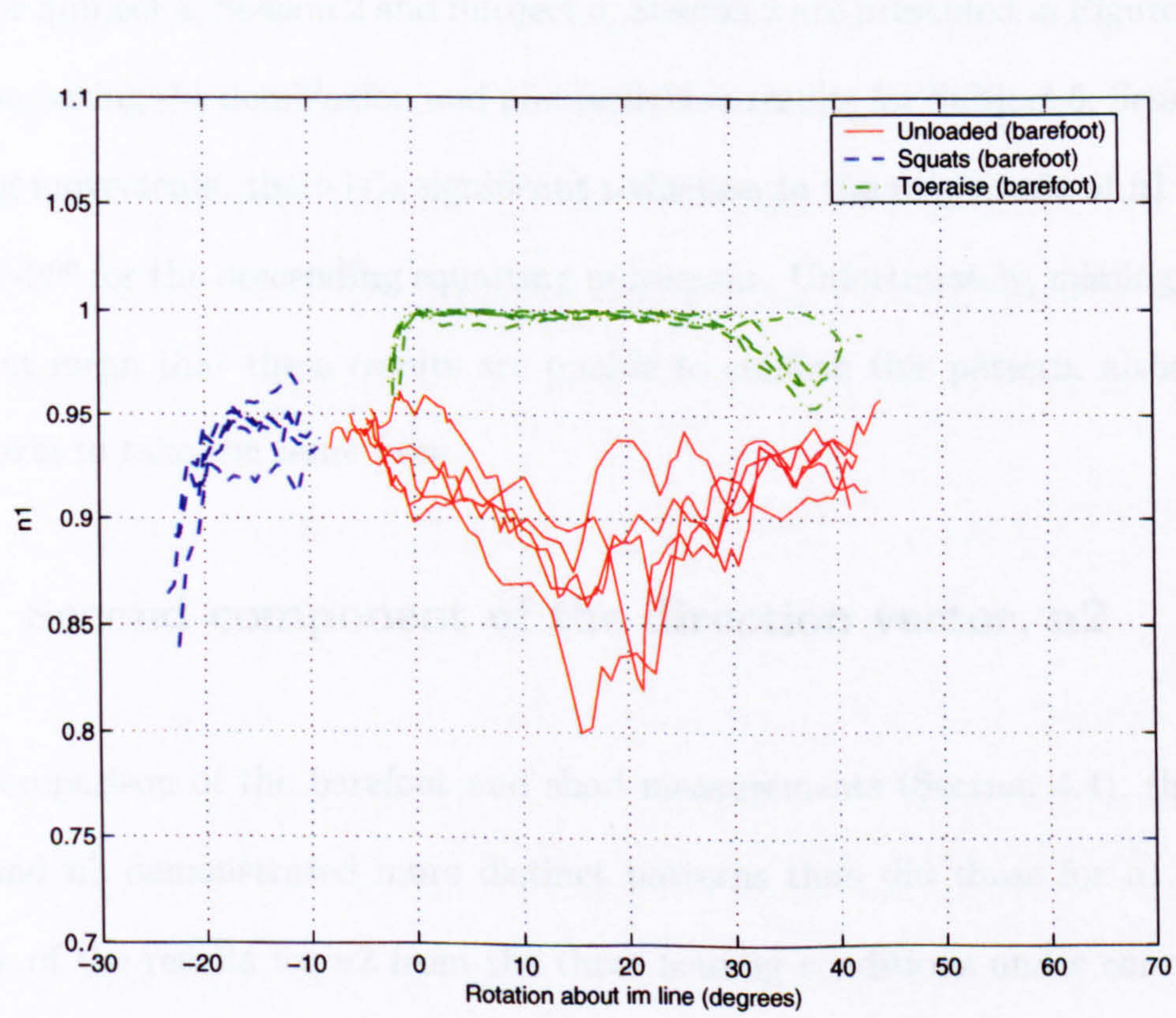

Figure 4.62: First component of direction vector (n1) plotted against angle of rotation about IM line for Subject 5, Session 2 (plantarflexion movements).

4.6.3 First component of the direction vector, n1

The plots of n1 against θ for Subject 3 are presented in Figure 4.57 (dorsiflexion) and Figure 4.58 (plantarflexion). The format of presentation will be the same for all of the helical axis parameters. The lack of overlap in terms of range of movement between the squatting results and the unloaded and toe raise results is clearly represented by the different position along the x-axis. Comparing the dorsiflexion and plantarflexion results, there is a strong indication that they mirror each other. The ranges are again different due to the fact that the sequential FHAs are calculated starting from the standing position to a point 10^o from the end of the squat for dorsiflexion, while they are calculated from the squatting position to a point 10^o from the standing position for plantarflexion. This is the same effect previously discussed when analysing the unloaded movements, and is also present in the toe raise movements. The equivalent results for Subject 4, Session 2 and Subject 5, Session 2 are presented in Figures 4.59 to 4.62. Comparing the dorsiflexion and plantarflexion results for Subject 5, Session 2 for squatting movements, there is a significant reduction in the magnitude of n1 between -30^o and -20^o for the descending squatting movement. Unfortunately, missing data for the ascent mean that these results are unable to confirm this pattern, although the curve starts to take the same form.

4.6.4 Second component of the direction vector, n2

In the comparison of the barefoot and shod measurements (Section 4.4), the results for n2 and n3 demonstrated more distinct patterns than did those for n1. This is also true of the results for n2 from the three loading conditions under consideration here. These distinct patterns allow comparison between dorsiflexion and plantarflexion movements, between subjects, and finally intrasubject comparisons.

Figures 4.63 to 4.68 show the results from Subjects 1, 2 and Subject 4 Session 2 for dorsiflexion and plantarflexion movements. Again, although it is by no means perfect, the way in which the results mirror each other is quite remarkable.

Comparing the dorsiflexion results from Subject 1 (4.63), Subject 4 Session 2 (4.67) and Subject 5 Session 2 (4.69), it is apparent that there is at least some degree of commonality in the patterns of the plots for the different loading conditions between subjects. This is also apparent for the other subjects, but to a lesser extent.

As there are two sets of measurements for Subjects 4 and 5, it is possible to investigate intra-subject variations. The two sessions were separated by approximately four months, and the squats and toe raises were performed barefoot in the second session compared with wearing shoes in the first session. The results for plantarflexion movements for Subject 4 are presented in Figure 4.70 (Session 1) and Figure 4.68 (Session 2), while those for Subject 5 are presented in Figure 4.71 (Session 1) and Figure 4.72 (Session 2). There is certainly some variation, but any differences are overshadowed by the extent to which similar patterns are followed. This is a strong indication that the patterns of axes as described by the individual parameters are reproducible for a given subject, irrespective of footwear, and possibly are reproducible between subjects.

4.6.5 Third component of the direction vector, n3

The plots of n3 against θ largely confirm the observations made regarding the n2 values. In terms of the plantarflexion results being a mirror image of the dorsiflexion results, Figures 4.73 to 4.76 demonstrate this effect for Subject 3 and Subject 4, Session 2. One important difference is the intra-subject variation seen for Subject 5 (Figures 4.77 and 4.78 for the dorsiflexion squatting movements. The slope of the line changes from a positive to a negative gradient. This effect is not seen for the corresponding

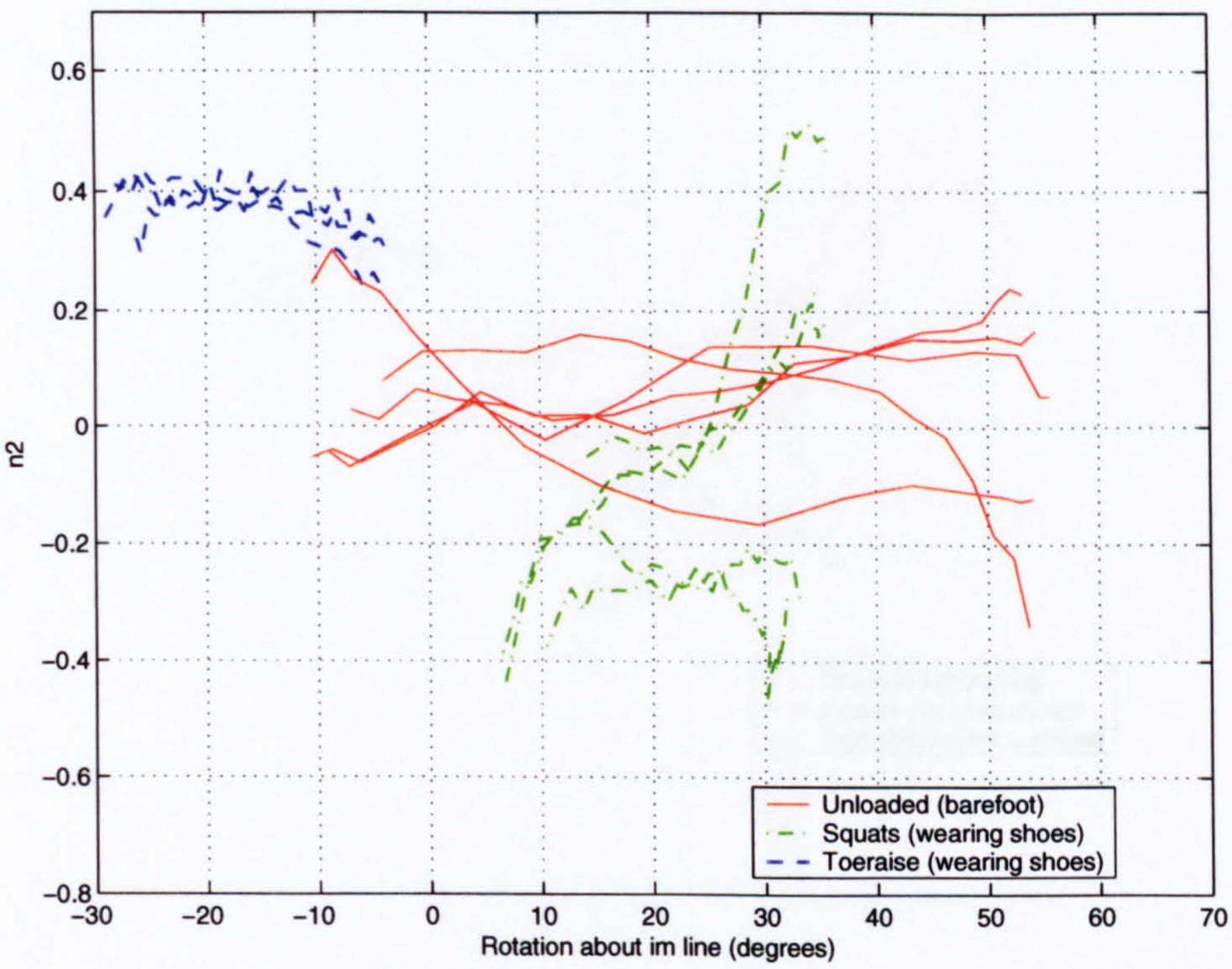

Figure 4.63: Second component of direction vector (n2) plotted against angle of rotation about IM line for Subject 1 (dorsiflexion movements).

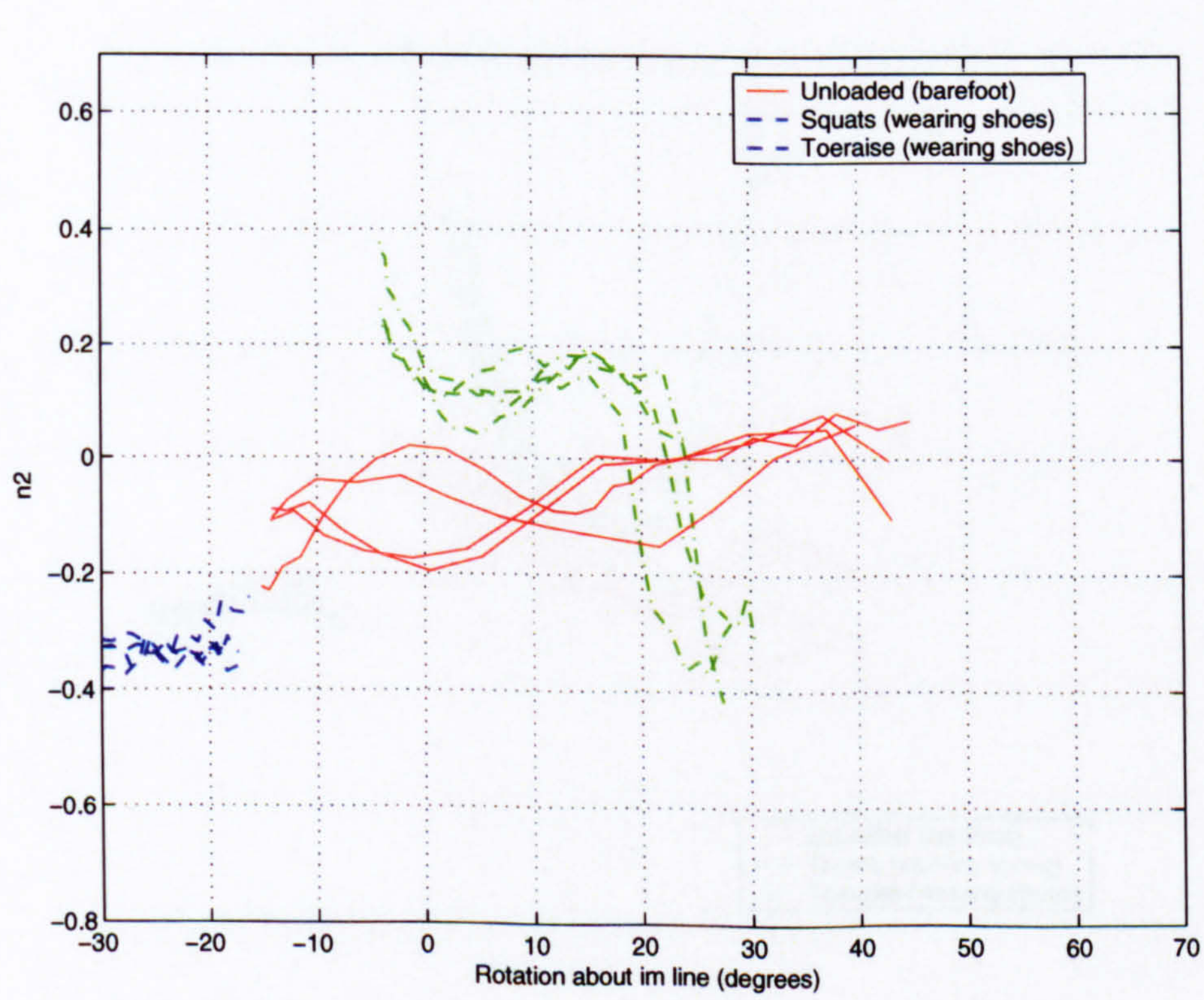

Figure 4.64: Second component of direction vector (n2) plotted against angle of rotation about IM line for Subject 1 (plantarflexion movements).

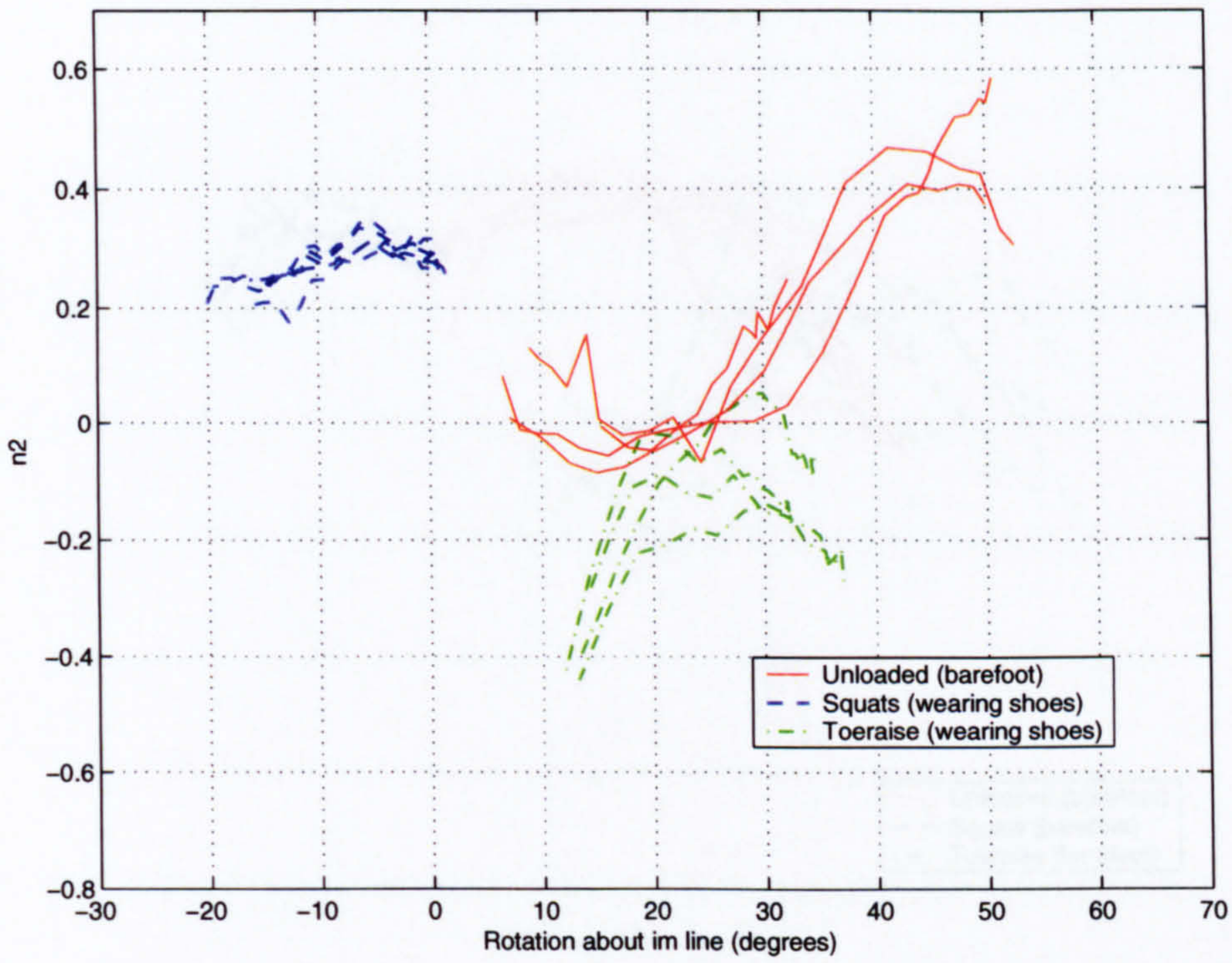

Figure 4.65: Second component of direction vector (n2) plotted against angle of rotation about IM line for Subject 2 (dorsiflexion movements).

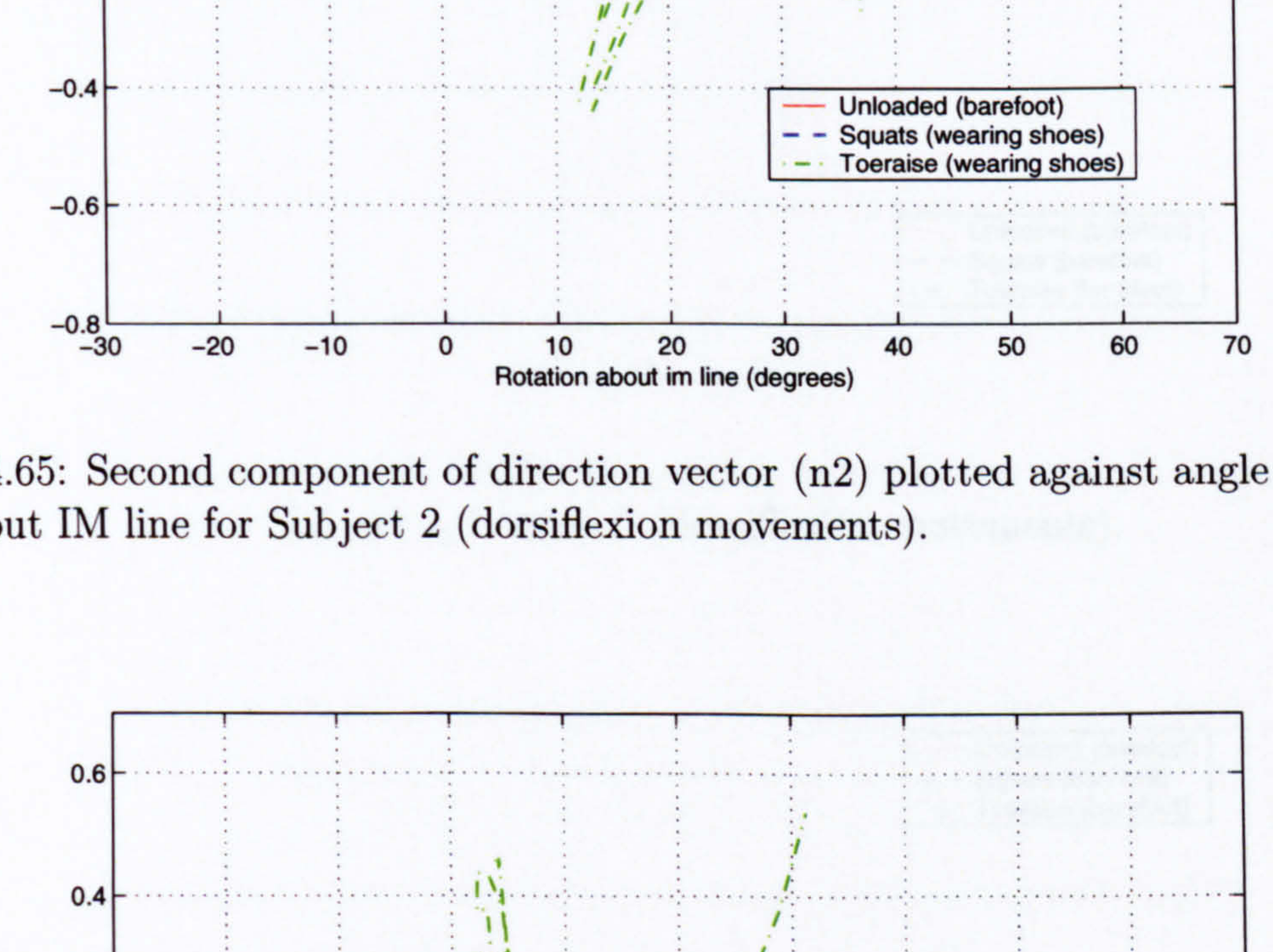

Figure 4.66: Second component of direction vector (n2) plotted against angle of rotation about IM line for Subject 2 (plantarflexion movements).

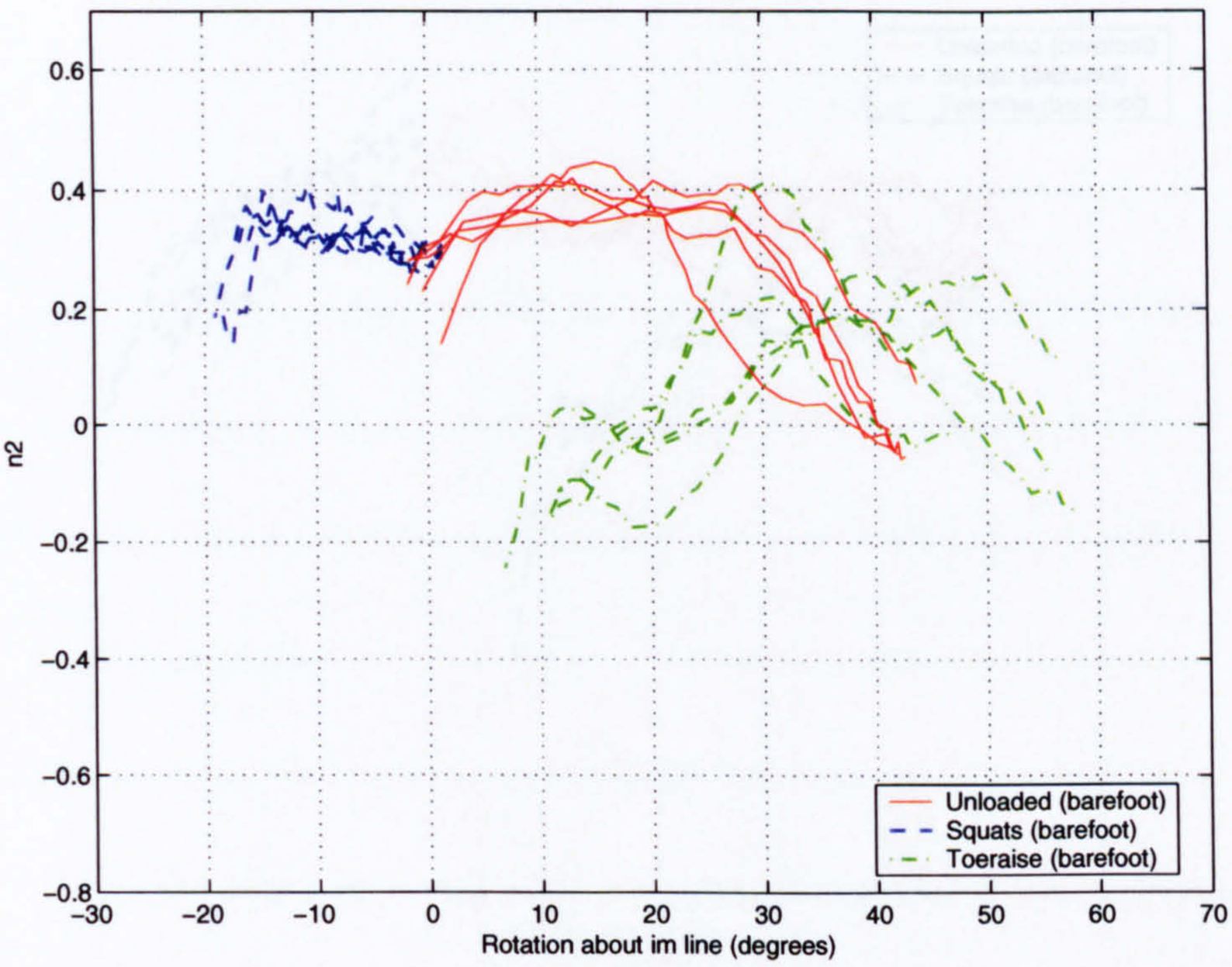

Figure 4.67: Second component of direction vector (n2) plotted against angle of rotation about IM line for Subject 4, Session 2 (dorsiflexion movements).

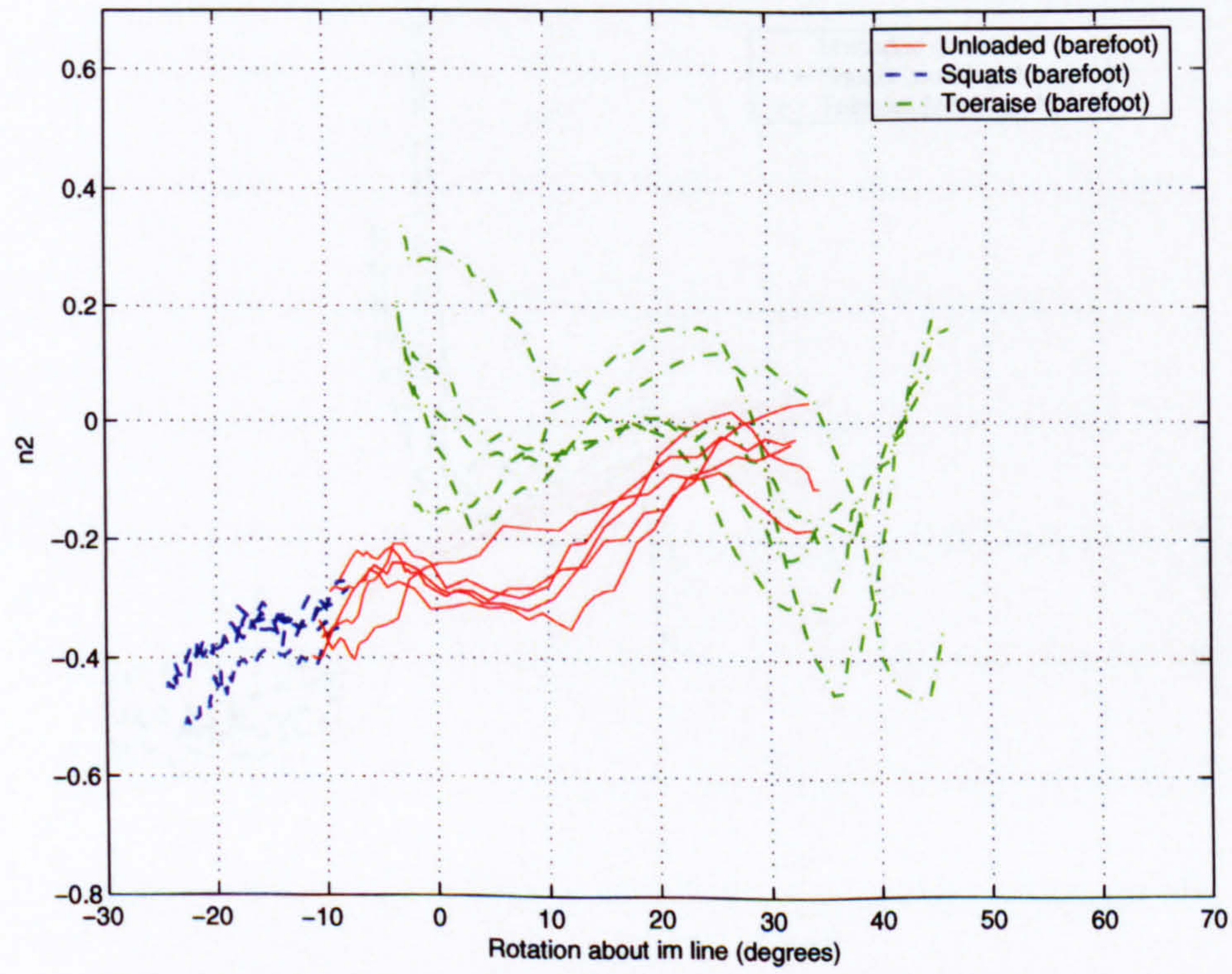

Figure 4.68: Second component of direction vector (n2) plotted against angle of rotation about IM line for Subject 4, Session 2 (plantarflexion movements).

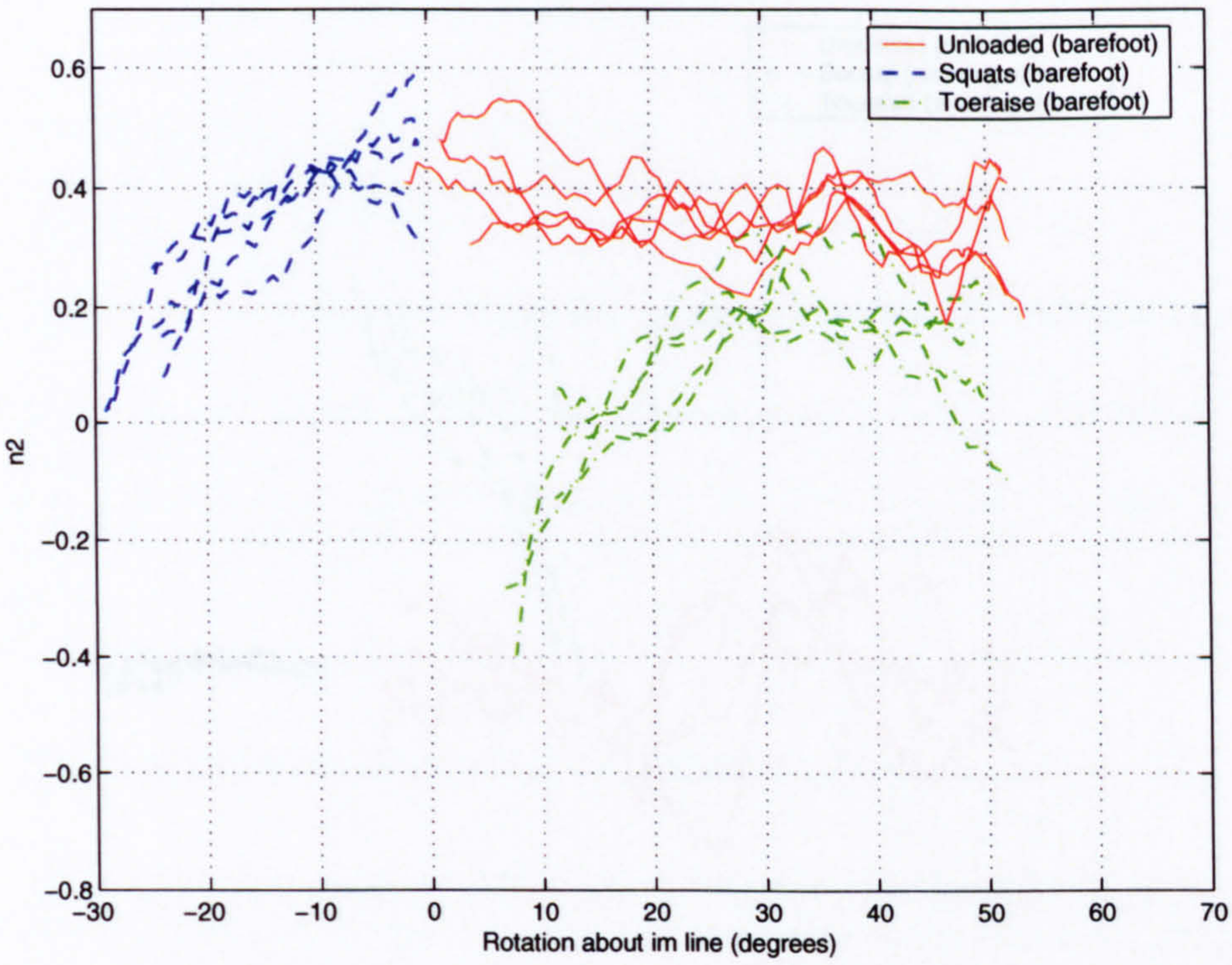

Figure 4.69: Second component of direction vector (n2) plotted against angle of rotation about IM line for Subject 5, Session 2 (dorsiflexion movements).

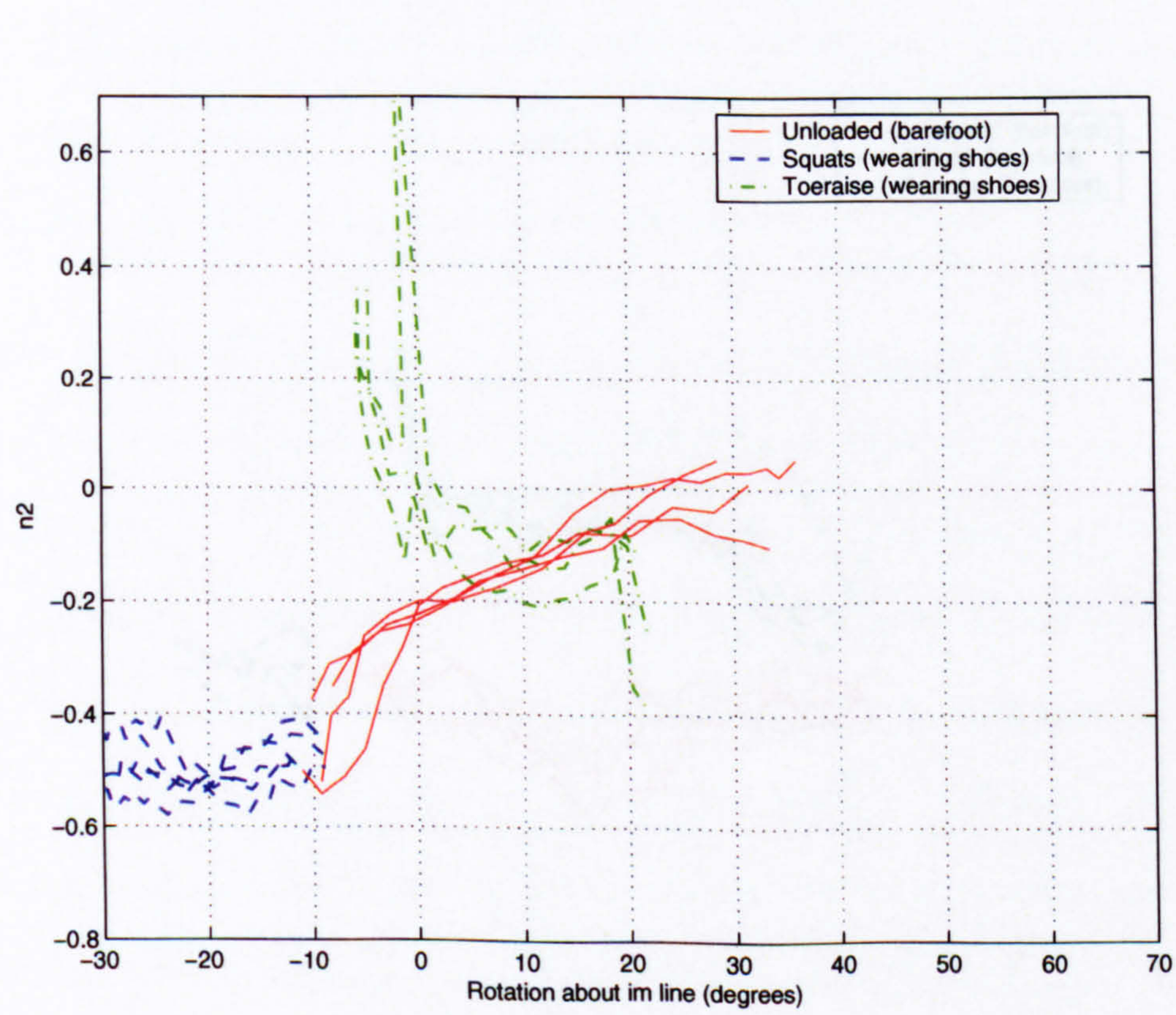

Figure 4.70: Second component of direction vector (n2) plotted against angle of rotation about IM line for Subject 4, Session 1 (plantarflexion movements).

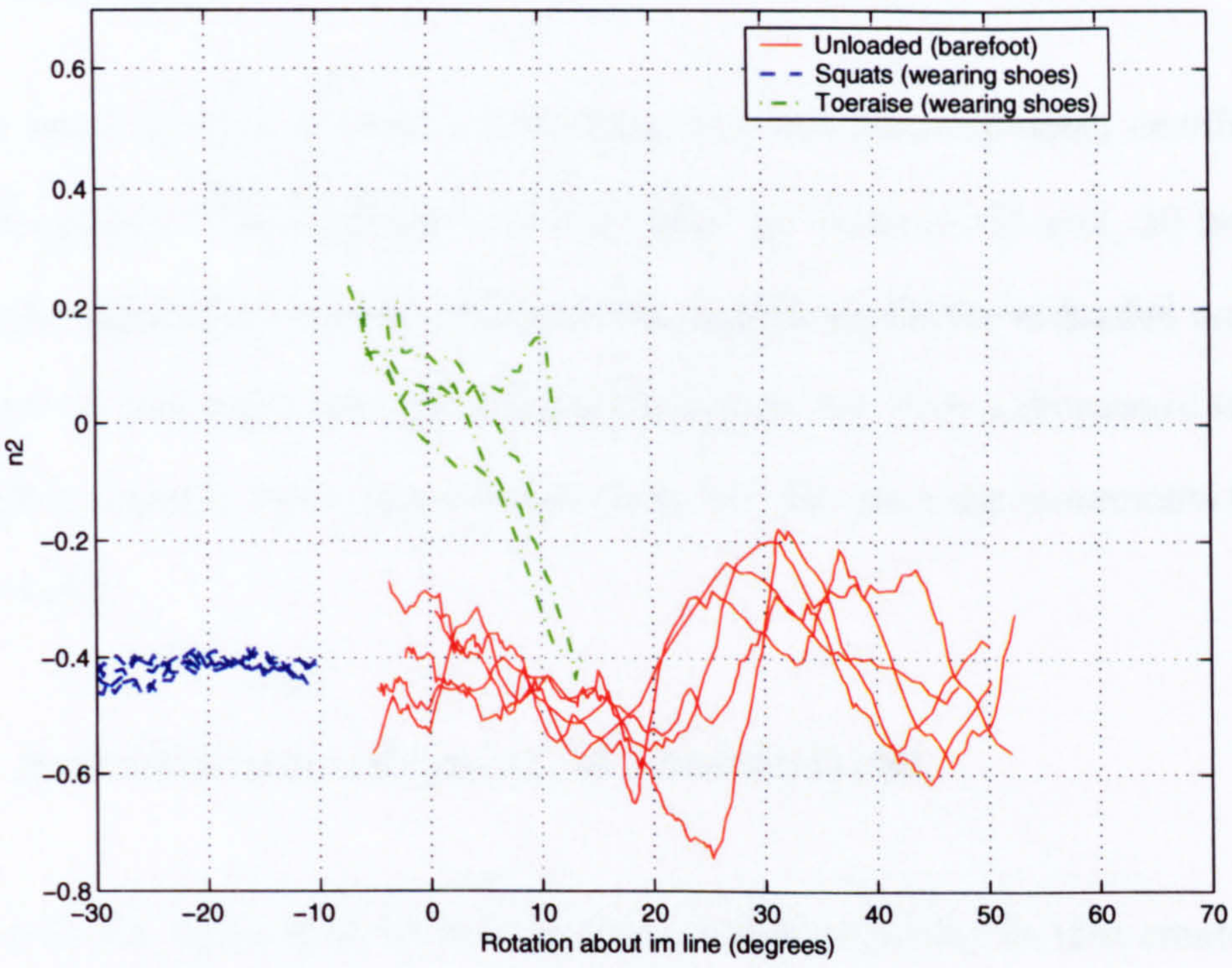

Figure 4.71: Second component of direction vector (n2) plotted against angle of rotation about IM line for Subject 5 (plantarflexion movements).

Figure 4.72: Second component of direction vector (n2) plotted against angle of rotation about IM line for Subject 5, Session 2 (plantarflexion movements).

plantarflexion results.

From the point of view of the z coordinates, the variations between conditions are again not marked. The results for the toe raises lie between -25 and -10 mm, while those for the squats lie between -18 and 0 mm, and those for the unloaded movements lie between -15 mm and 5 mm. The unloaded movements show a downward trend, the squats follow a gentle, fairly symmetrical curve and the toe raise movements follow an upwards trend.

4.6.6 y-coordinate of point of intersection

Moving on to the location of the axes in space, a similar picture to that created by the orientation parameters emerges. Overall, there is close agreement between dorsiflexion and plantarflexion results; unlike in the case of the orientation parameters there is no inversion of the results due to direction of rotation. Results from Subjects 2 and 3 and Subject 5, Session 2 are presented in Figures 4.79 to 4.84 to illustrate this. There are also some aspects of the patterns of the results that seem to repeat between subjects.

However, there are also variations, in terms of how the results of the different loading conditions relate to each other. In particular, for the barefoot measurements (Session 2) for Subjects 4 and 5, the y-coordinate of the point of intersection plot is more positive than the unloaded curve, while the opposite is true for the same movements wearing shoes. Figures 4.85 and 4.86 show the relatively poor agreement between Session 1 and Session 2 plantarflexion results from Subject 4; Figures 4.87 and 4.83 on the other hand show quite good agreement for dorsiflexion squatting and unloaded measurements between Session 1 and Session 2 measurements for Subject 5.

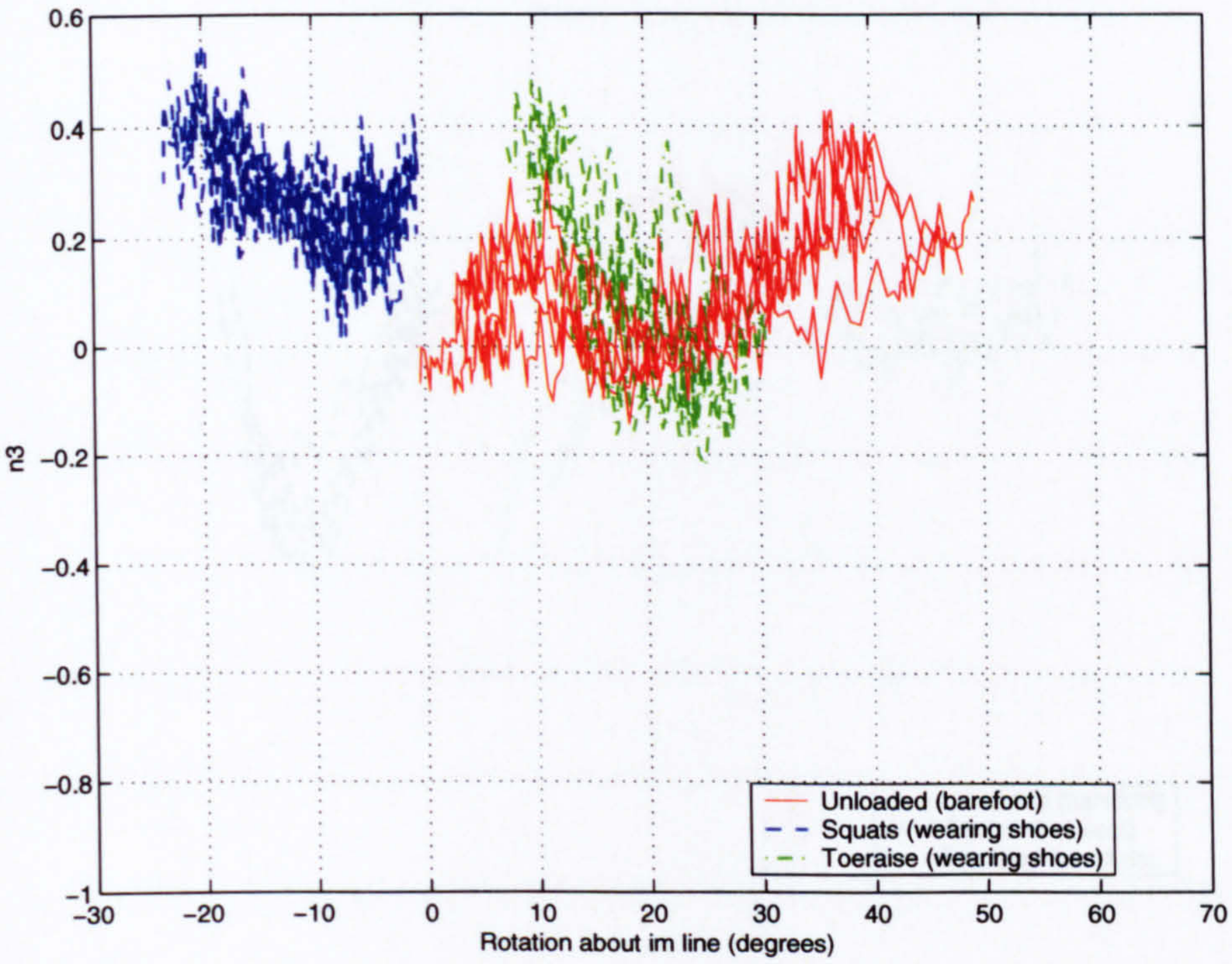

Figure 4.73: Third component of direction vector (n3) plotted against angle of rotation about IM line for Subject 3 (dorsiflexion results).

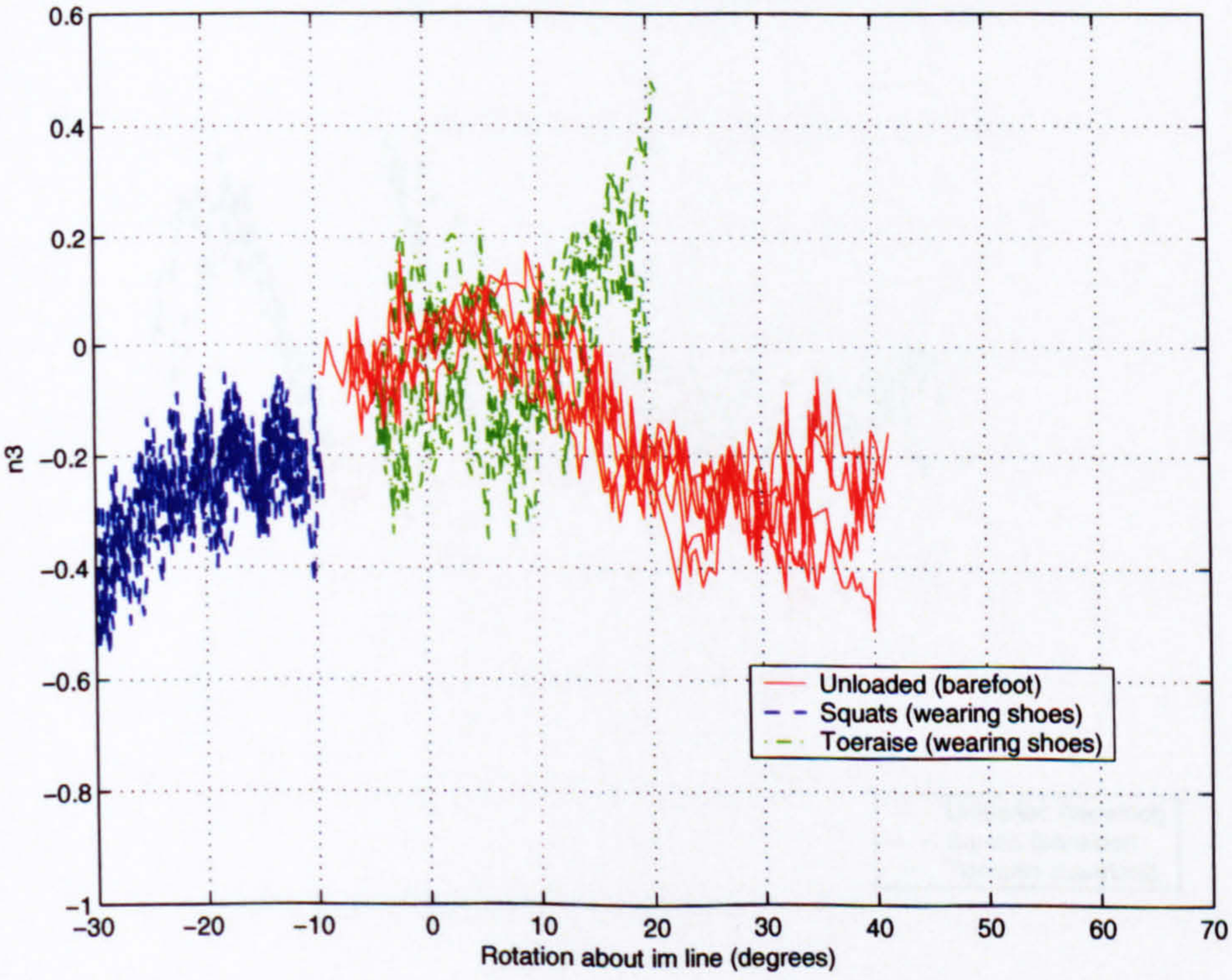

Figure 4.74: Third component of direction vector (n3) plotted against angle of rotation about IM line for Subject 3 (plantarflexion results).

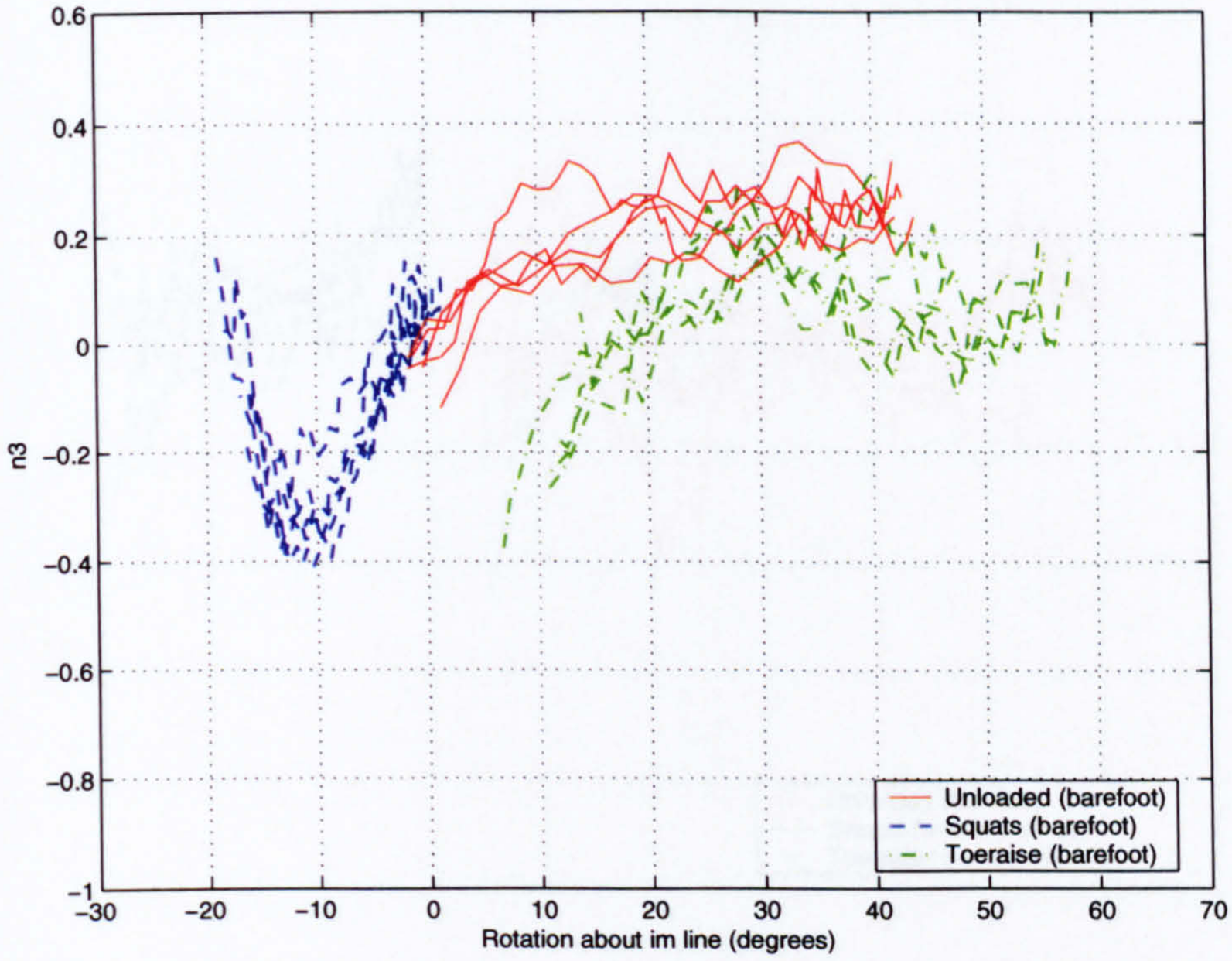

Figure 4.75: Third component of direction vector (n3) plotted against angle of rotation about IM line for Subject 4, Session 2 (dorsiflexion results).

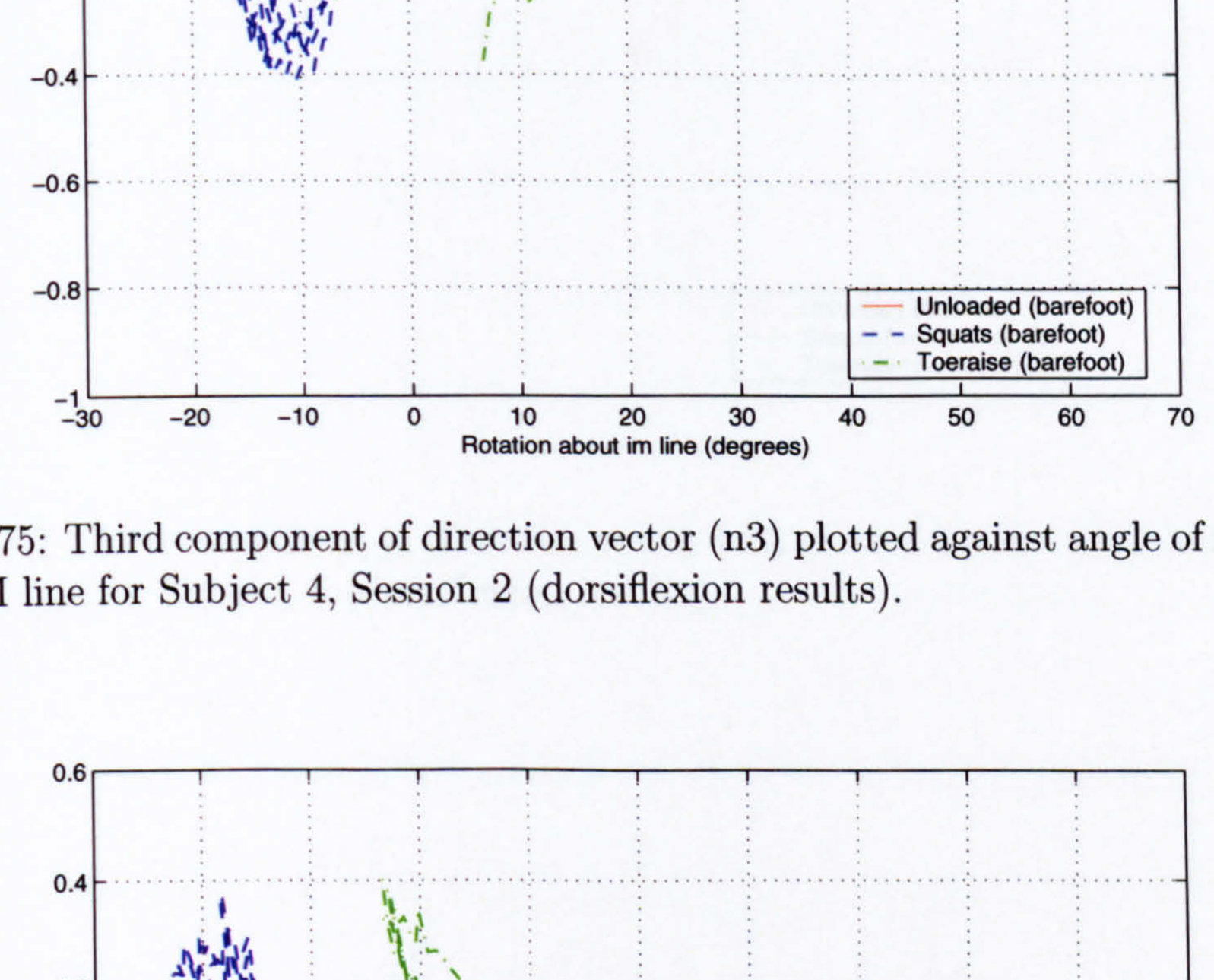

Figure 4.76: Third component of direction vector (n3) plotted against angle of rotation about IM line for Subject 4, Session 2 (plantarflexion results).

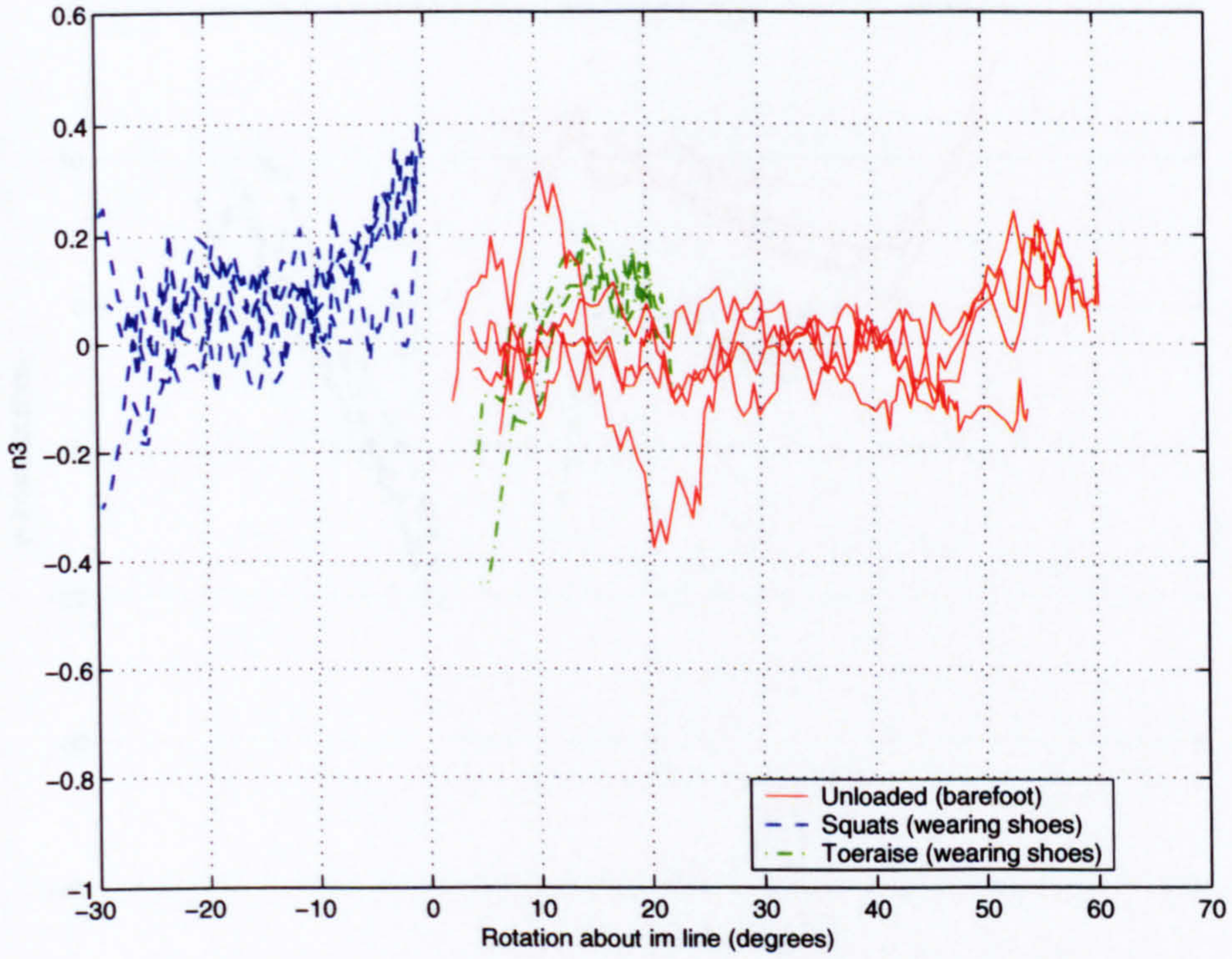

Figure 4.77: Third component of direction vector (n3) plotted against angle of rotation about IM line for Subject 5 (dorsiflexion results).

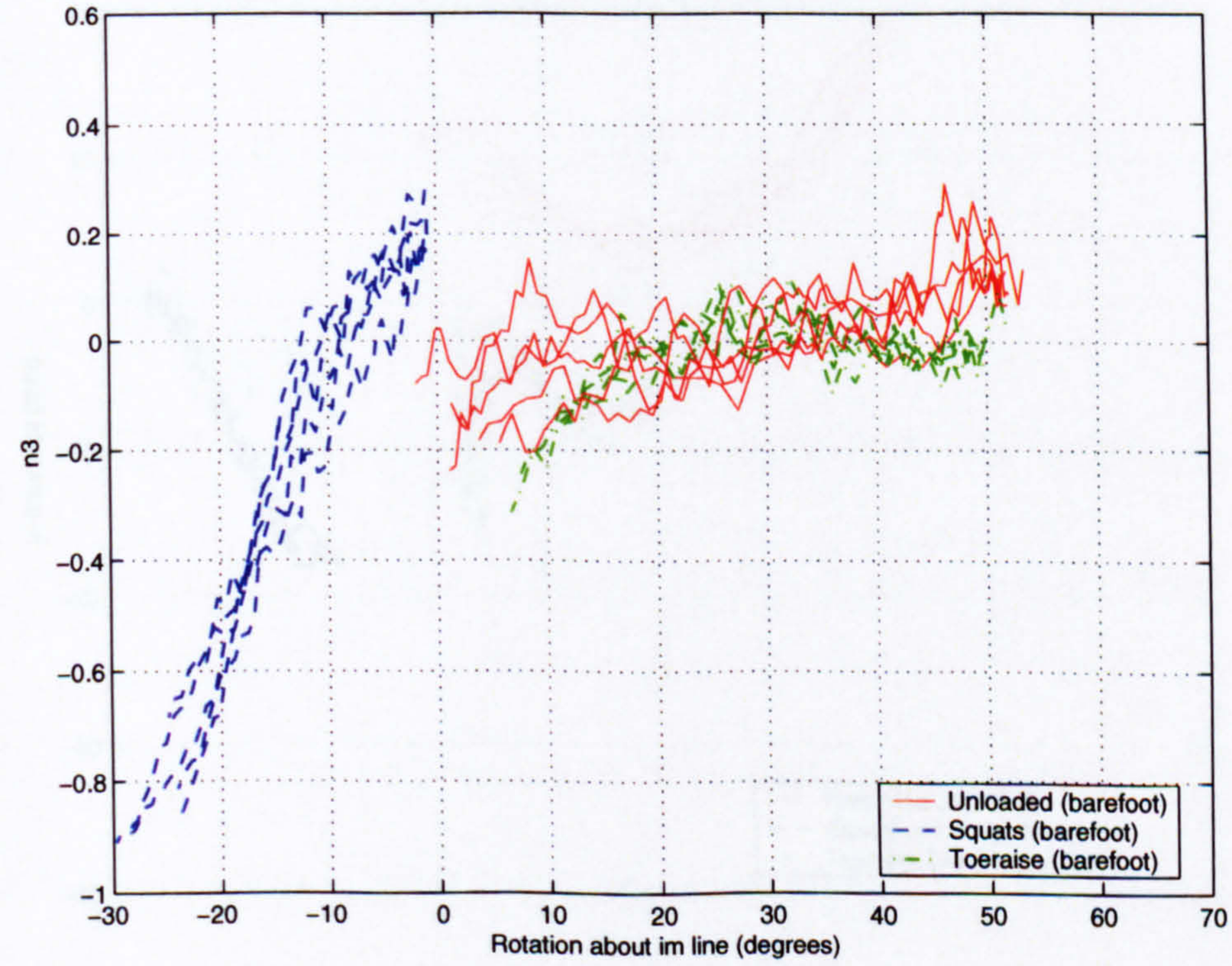

Figure 4.78: Third component of direction vector (n3) plotted against angle of rotation about IM line for Subject 5, Session 2 (dorsiflexion results).

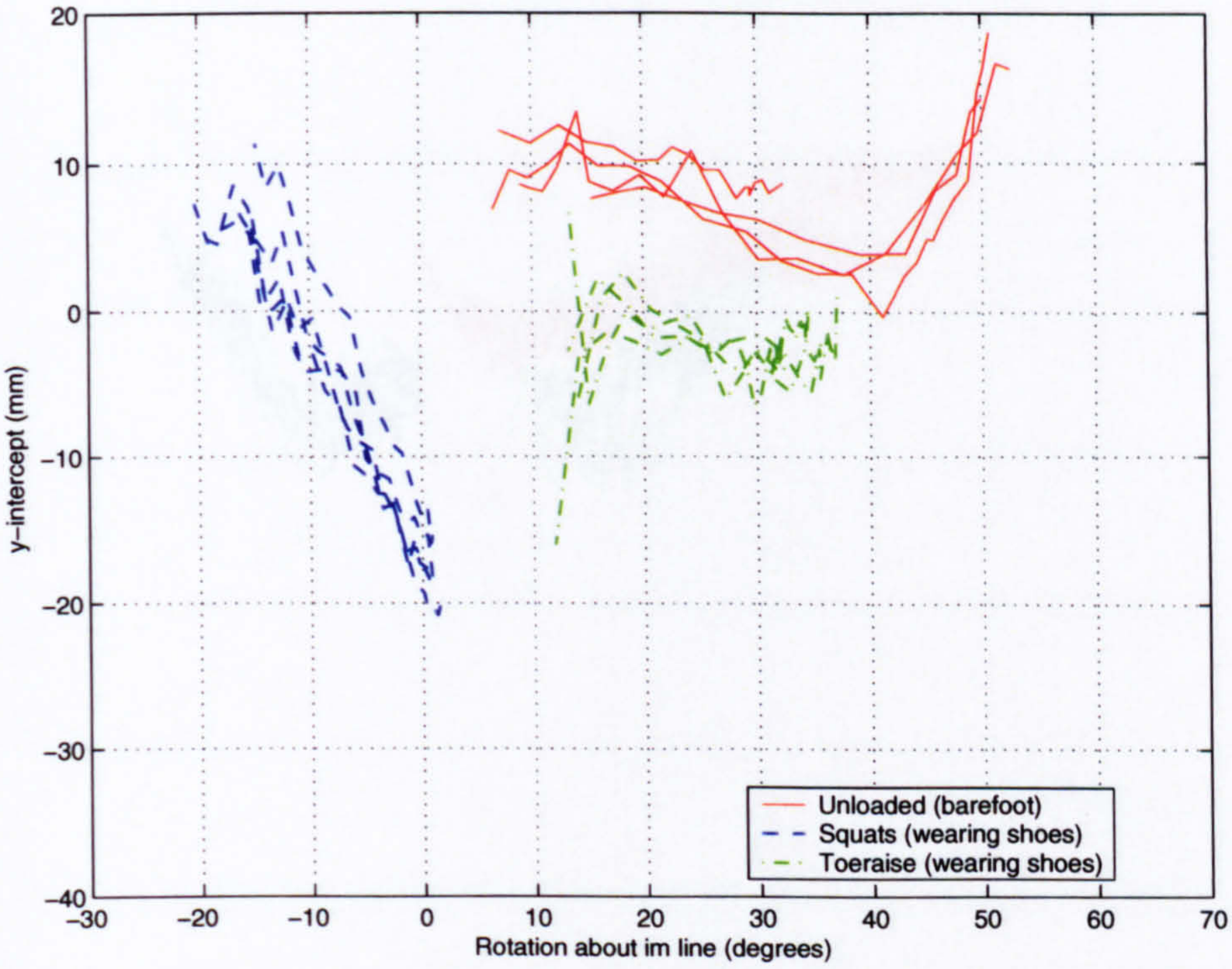

Figure 4.79: y-coordinate of point of intersection of axis with MM plane plotted against angle of rotation about IM line for Subject 2 (dorsiflexion movements).

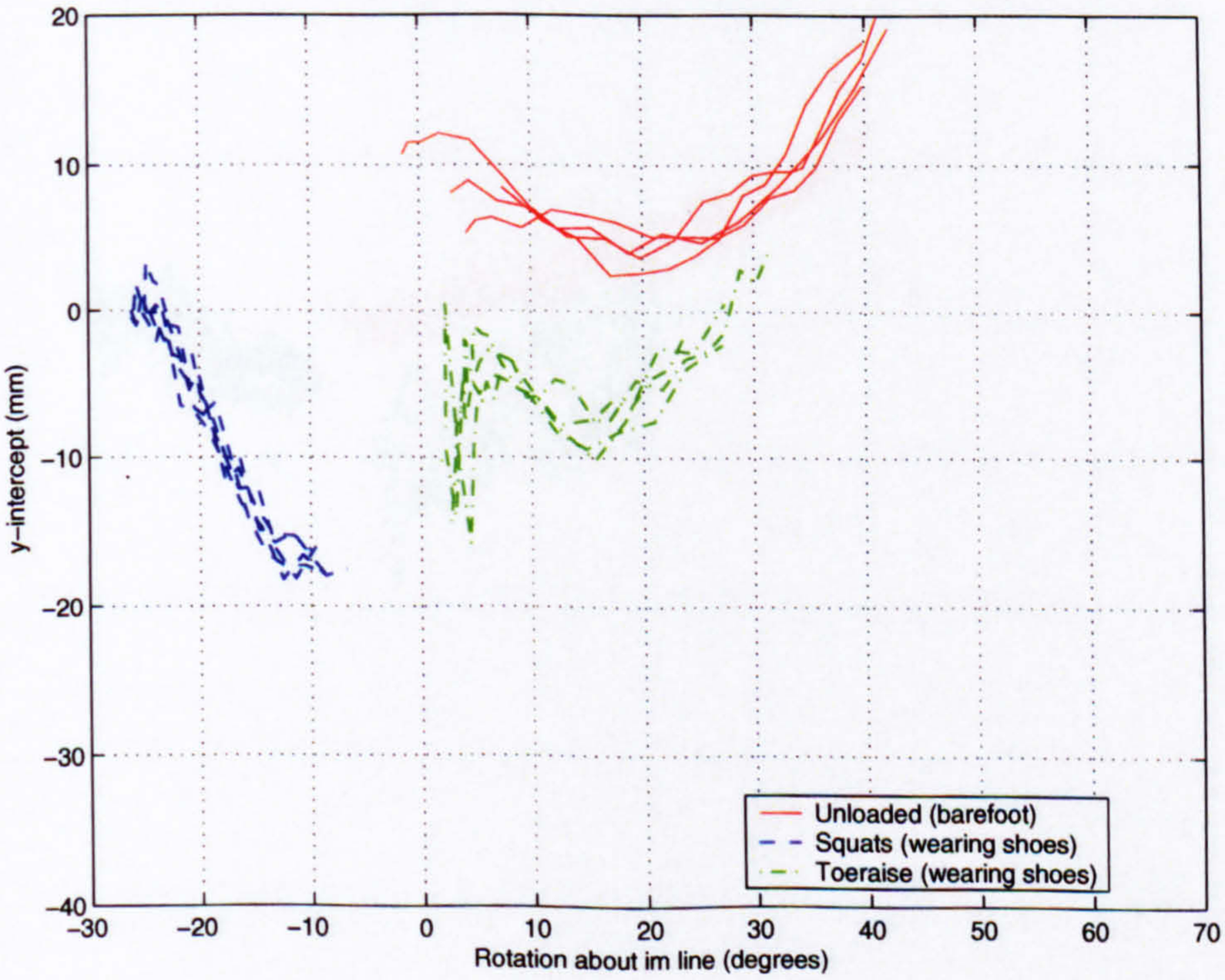

Figure 4.80: y-coordinate of point of intersection of axis with MM plane plotted against angle of rotation about IM line for Subject 2 (plantarflexion movements).

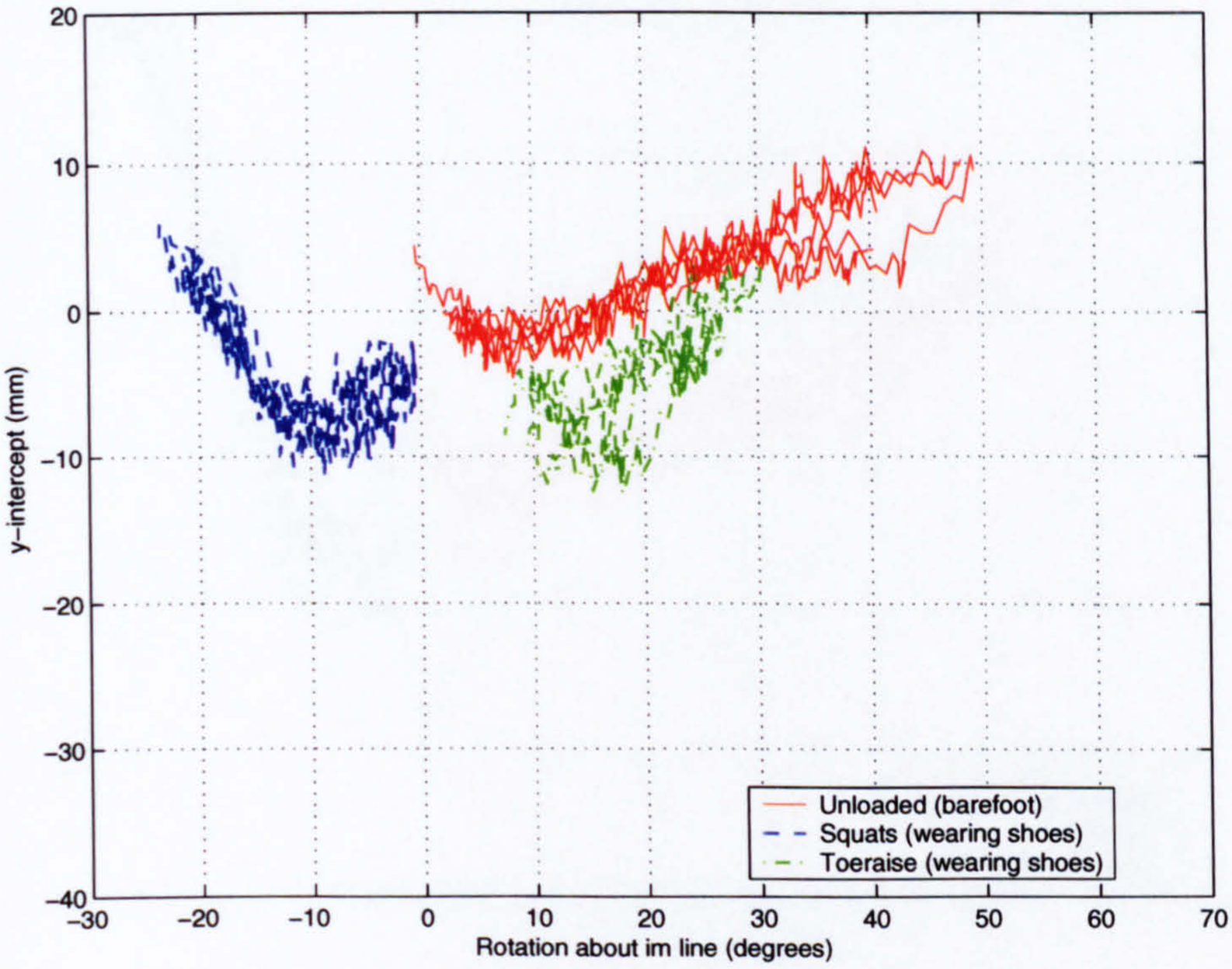

Figure 4.81: y-coordinate of point of intersection of axis with MM plane plotted against angle of rotation about IM line for Subject 3 (dorsiflexion movements).

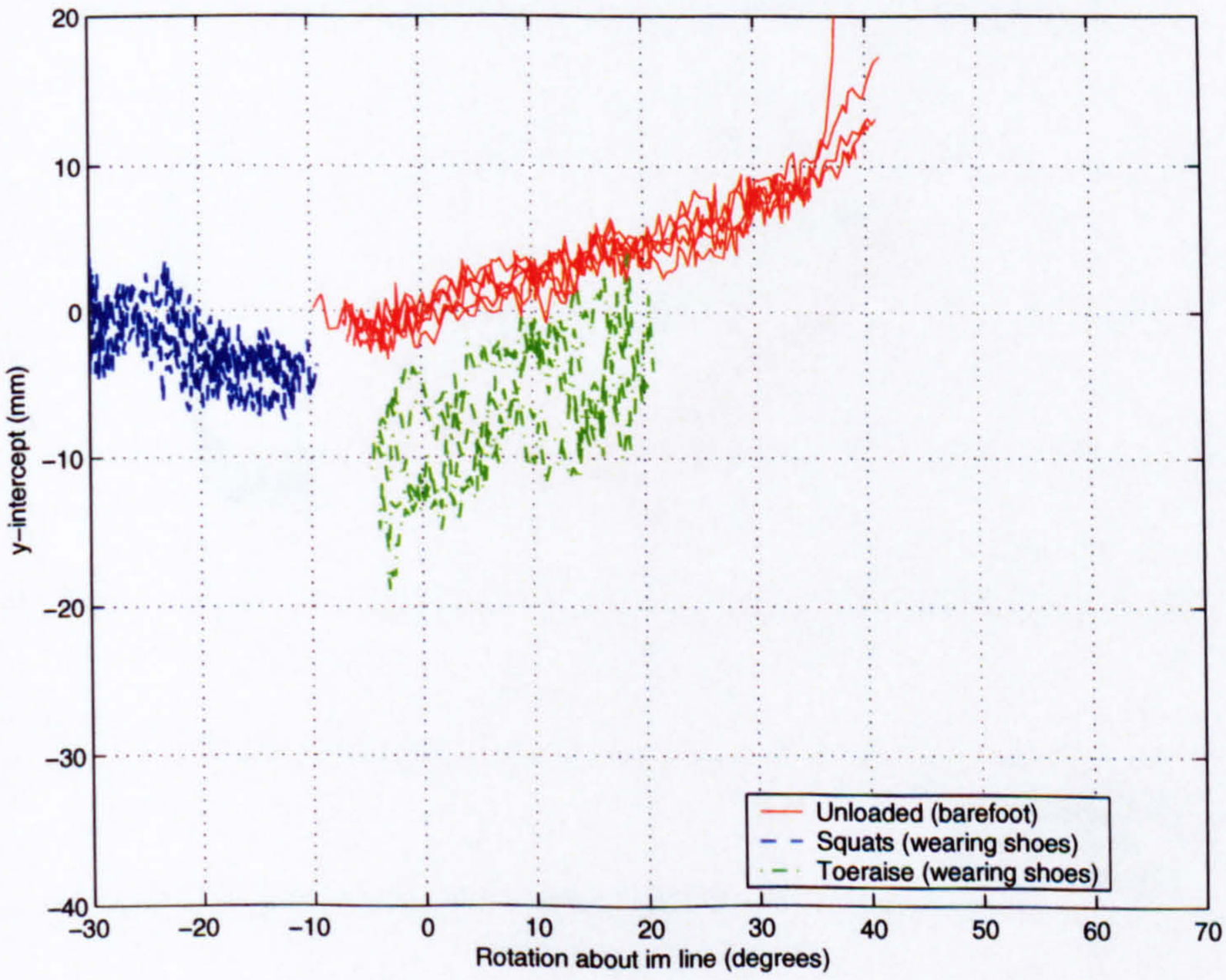

Figure 4.82: y-coordinate of point of intersection of axis with MM plane plotted against angle of rotation about IM line for Subject 3 (plantarflexion movements).

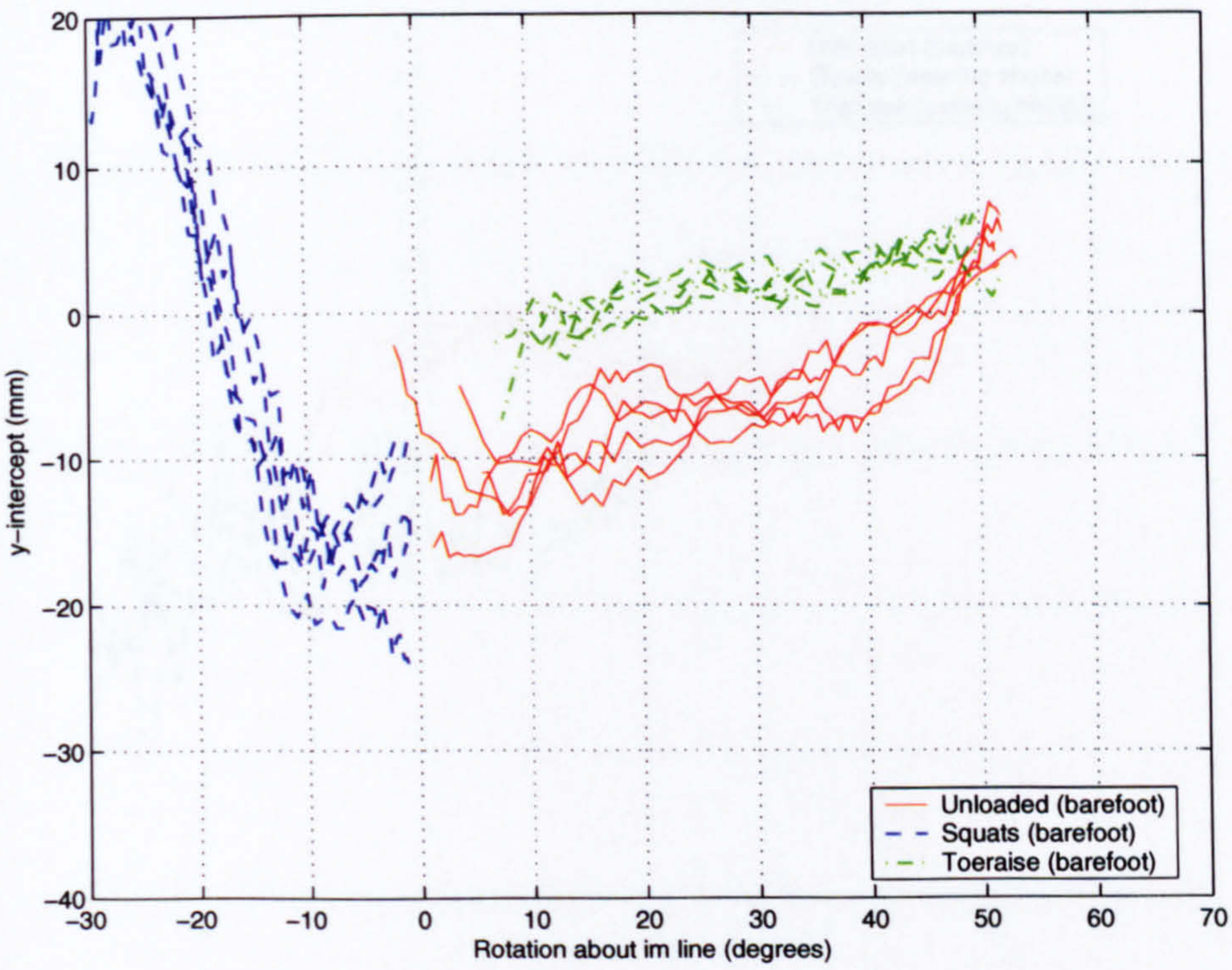

Figure 4.83: y-coordinate of point of intersection of axis with MM plane plotted against angle of rotation about IM line for Subject 5, Session 2 (dorsiflexion movements).

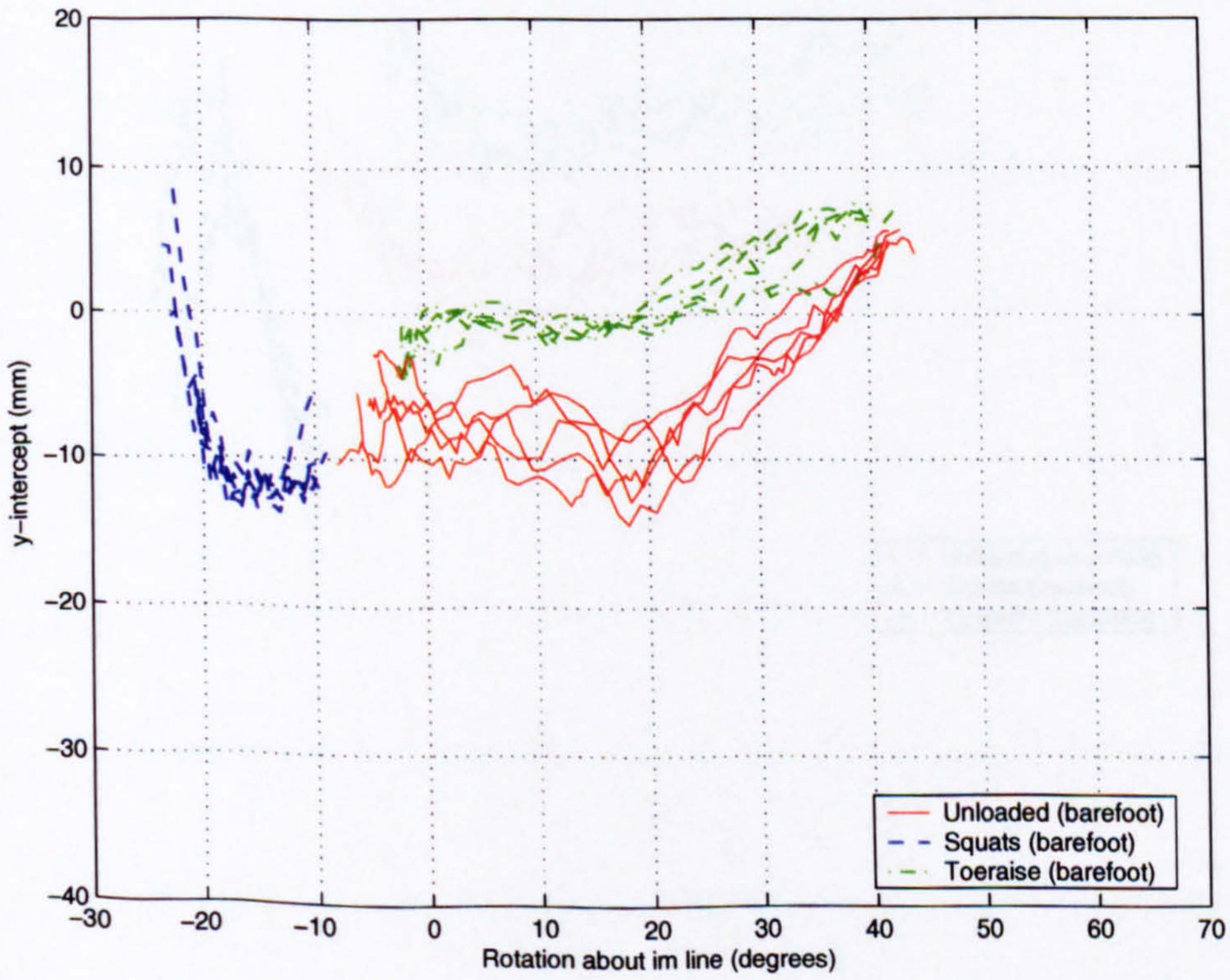

Figure 4.84: y-coordinate of point of intersection of axis with MM plane plotted against angle of rotation about IM line for Subject 5, Session 2 (plantarflexion movements).

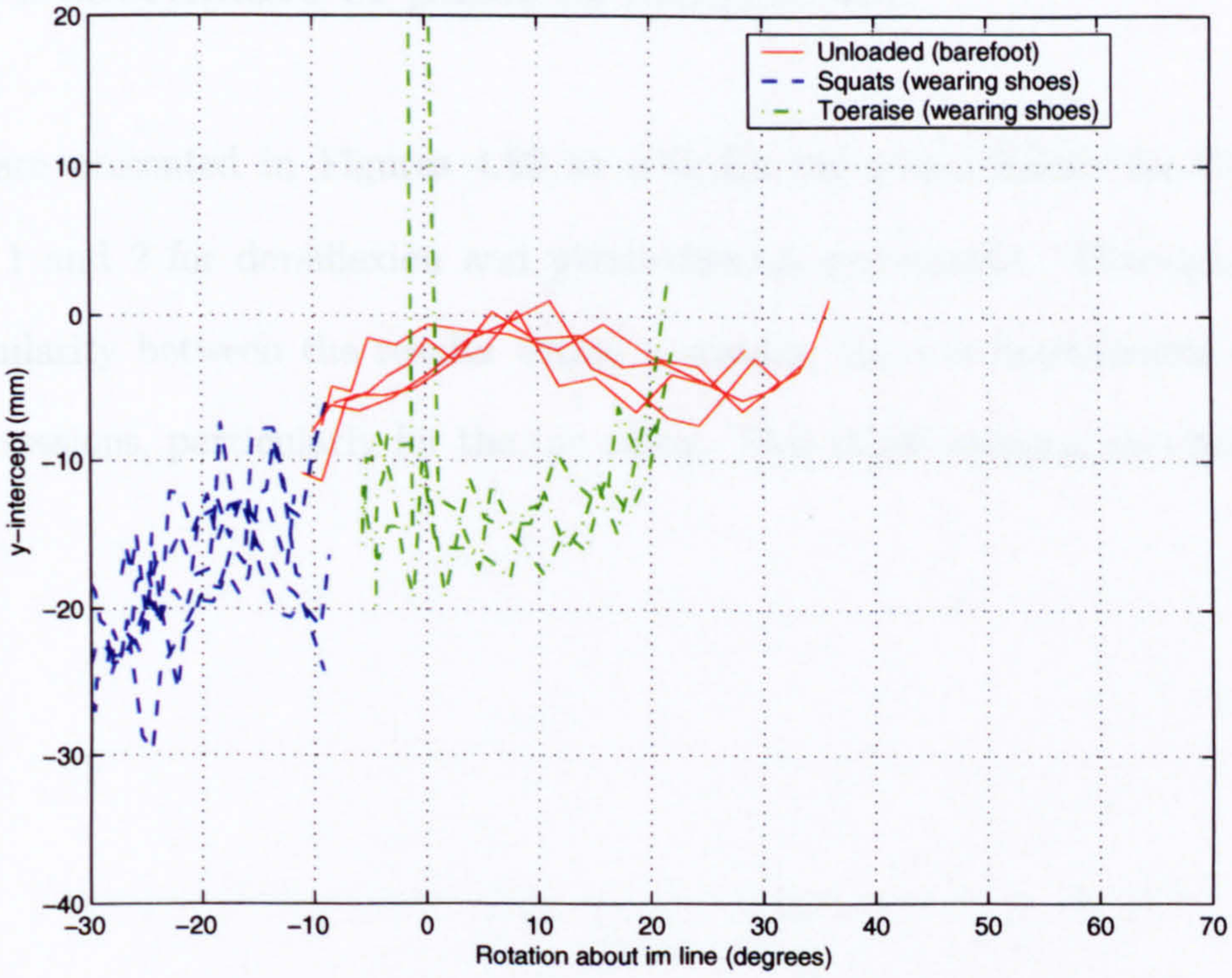

Figure 4.85: y-coordinate of point of intersection of axis with MM plane plotted against angle of rotation about IM line for Subject 4 (plantarflexion movements).

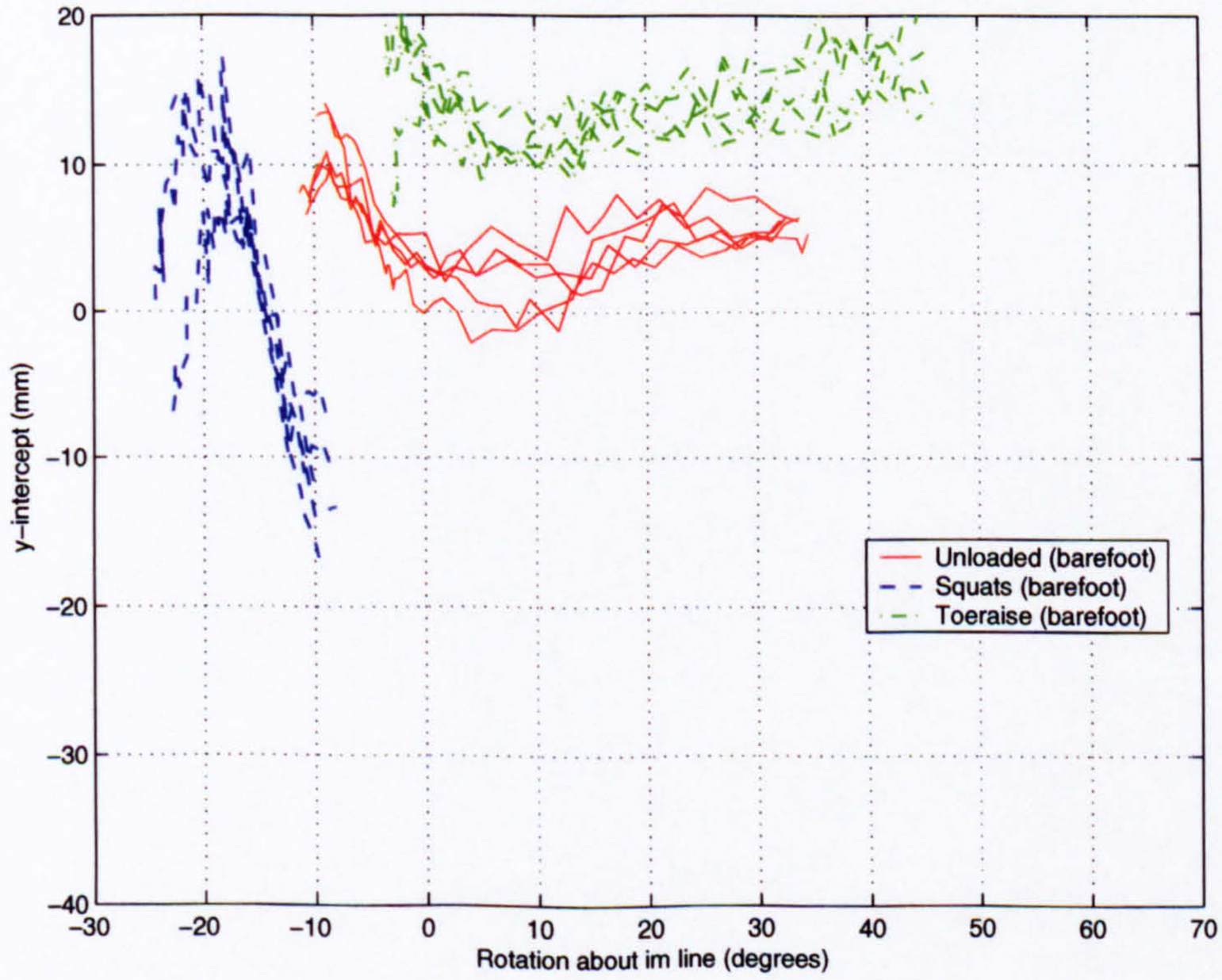

Figure 4.86: y-coordinate of point of intersection of axis with MM plane plotted against angle of rotation about IM line for Subject 4, Session 2 (plantarflexion movements).

4.6.7 z-coordinate of point of intersection

Results are presented in Figures 4.88 to 4.91 for the z-coordinates for Subject 5, Sessions 1 and 2 for dorsiflexion and plantarflexion movements. Although there is some similarity between the results within a session, there is considerable variation between sessions, particularly for the toe raises. This might indicate an effect due to footwear.

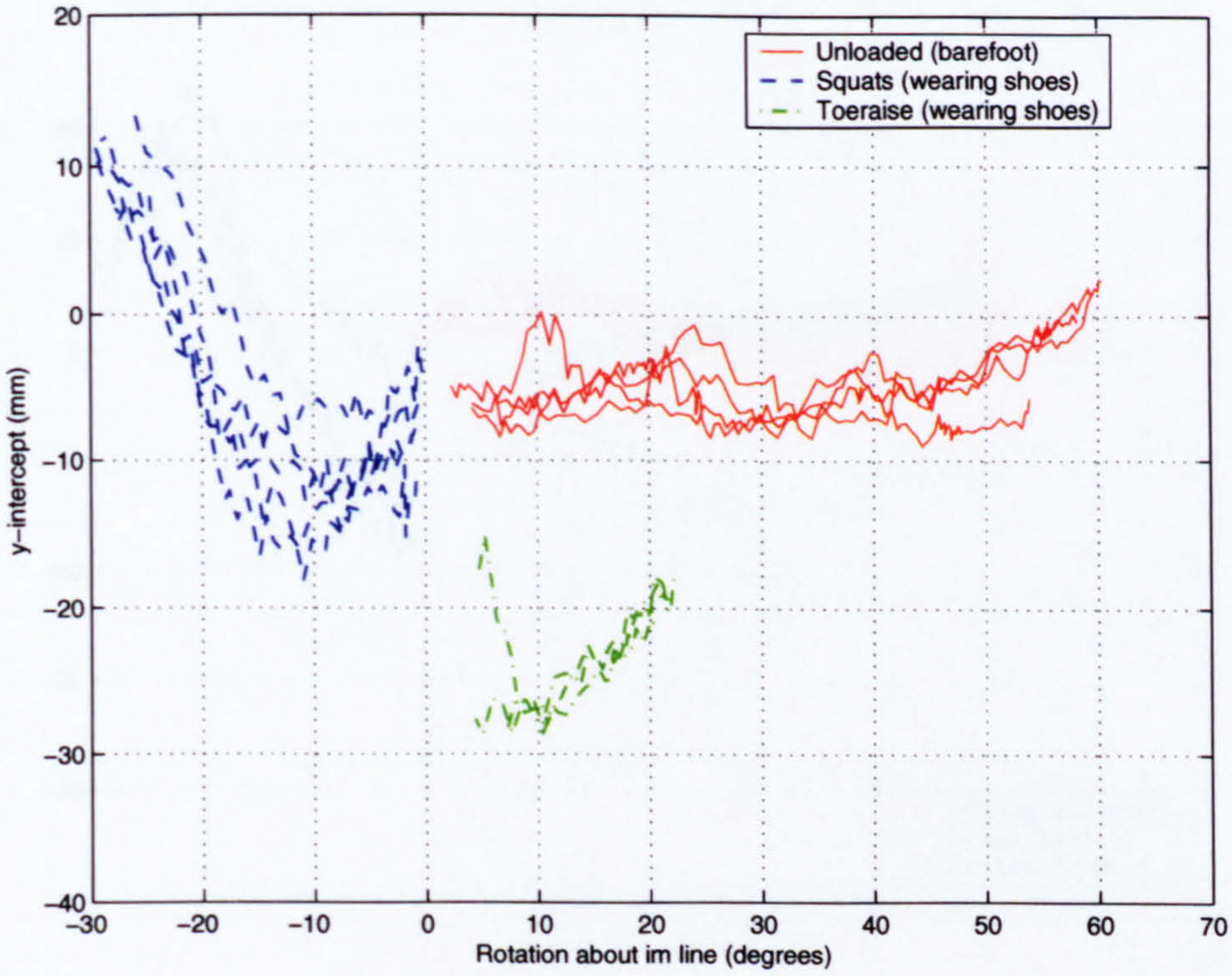

Figure 4.87: y-coordinate of point of intersection of axis with MM plane plotted against angle of rotation about IM line for Subject 5 (dorsiflexion movements).

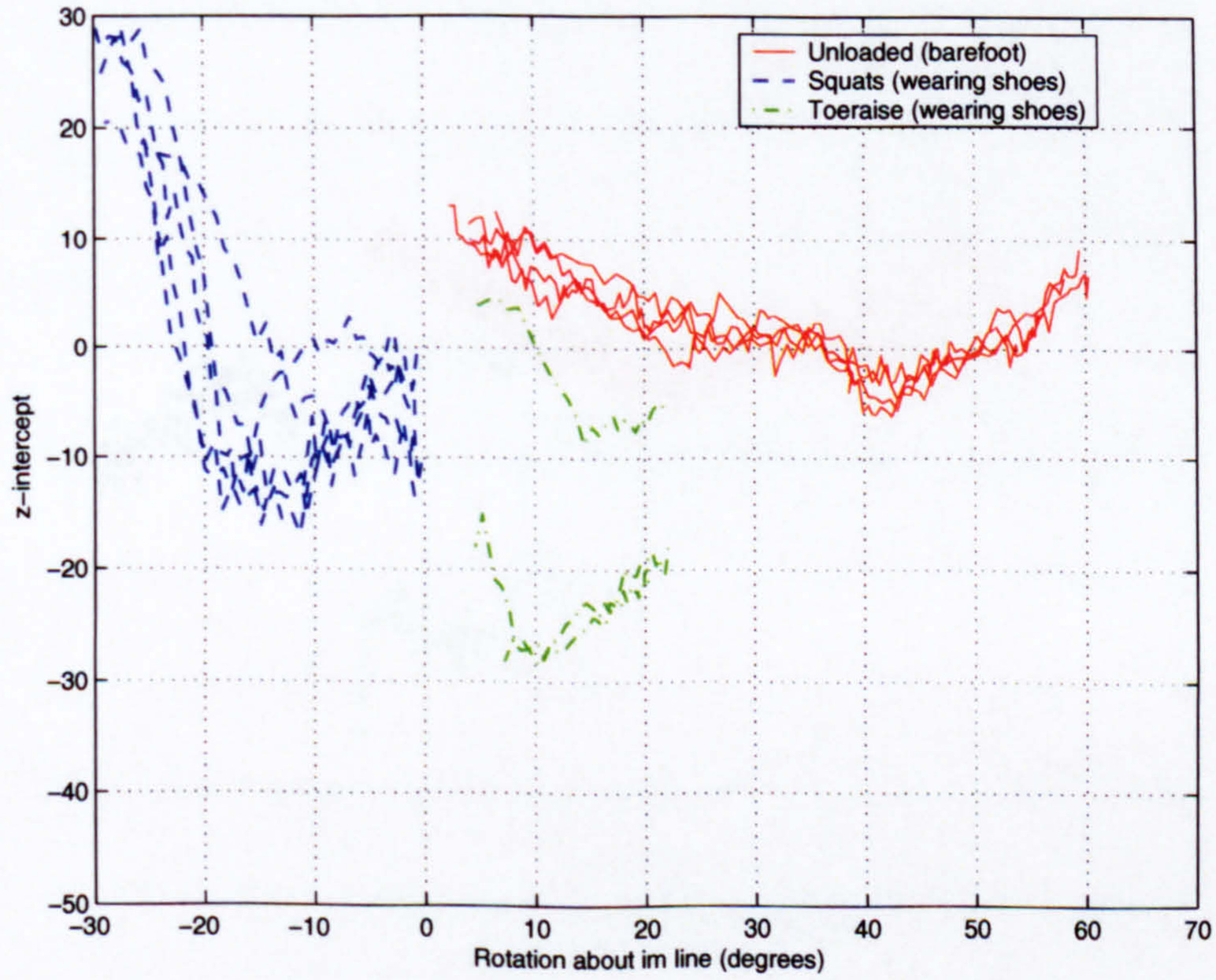

Figure 4.88: z-coordinate of point of intersection of axis with MM plane plotted against angle of rotation about IM line for Subject 5 (dorsiflexion movements).

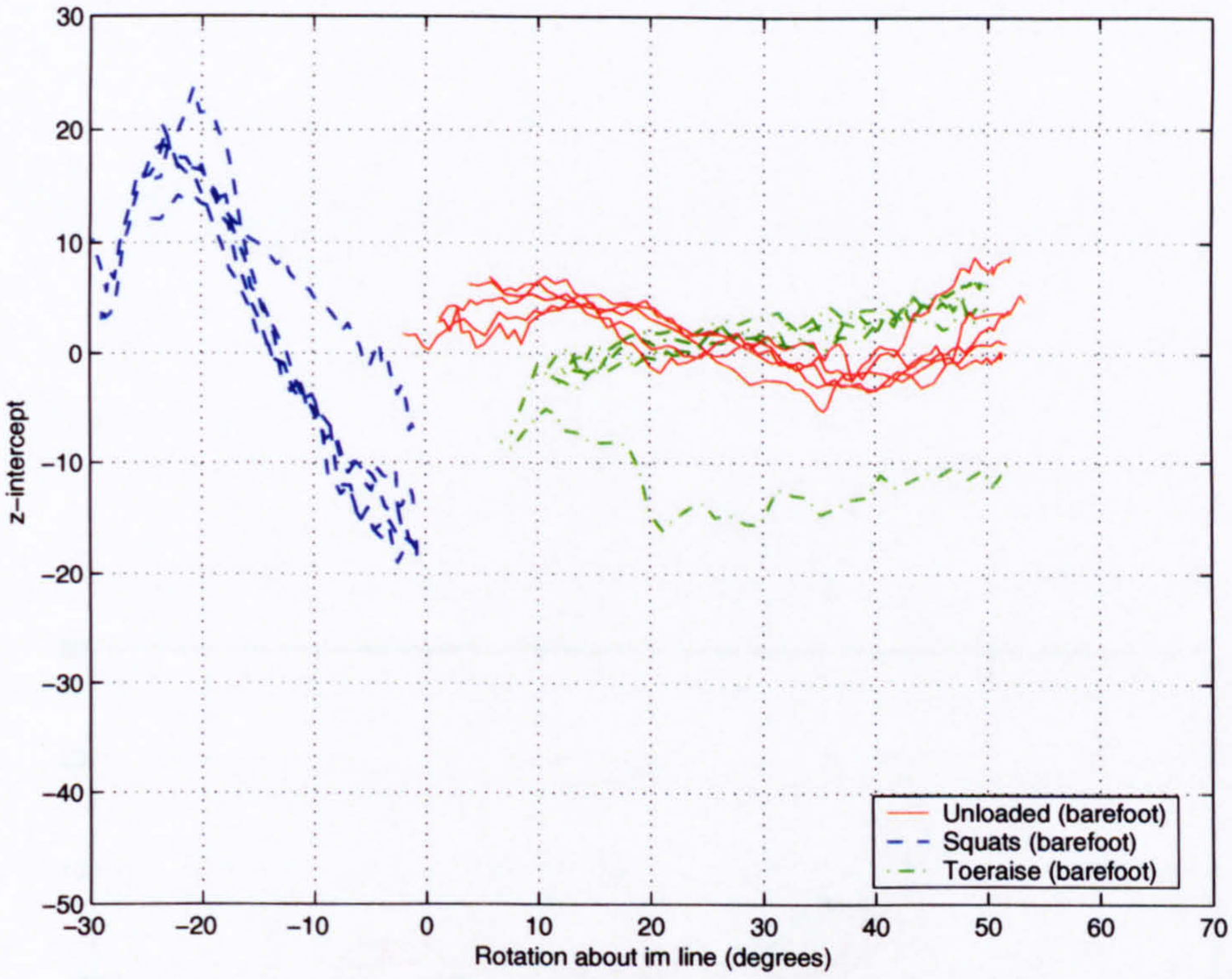

Figure 4.89: z-coordinate of point of intersection of axis with MM plane plotted against angle of rotation about IM line for Subject 5, Session 2 (dorsiflexion movements).

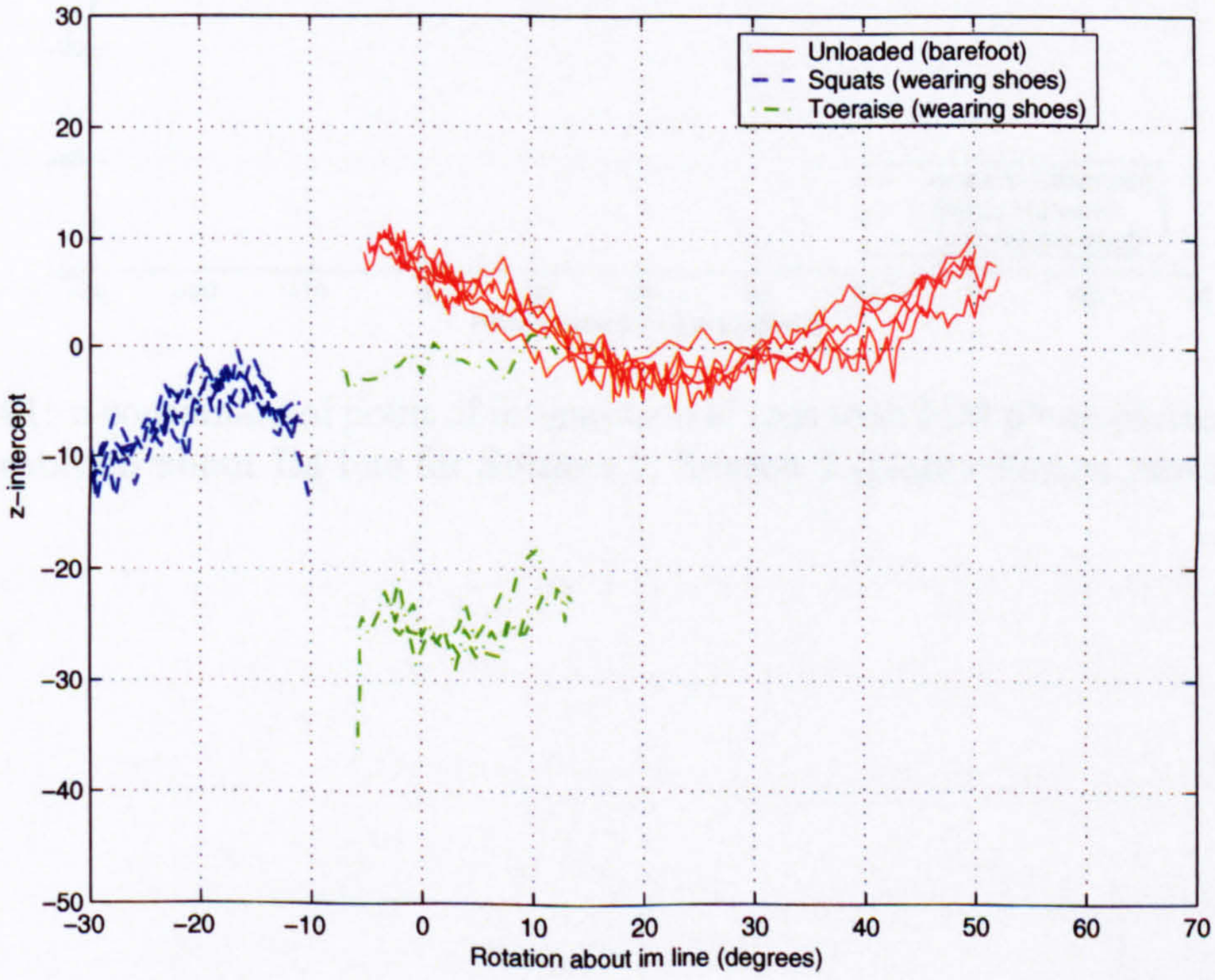

Figure 4.90: z-coordinate of point of intersection of axis with MM plane plotted against angle of rotation about IM line for Subject 5 (plantarflexion movements).

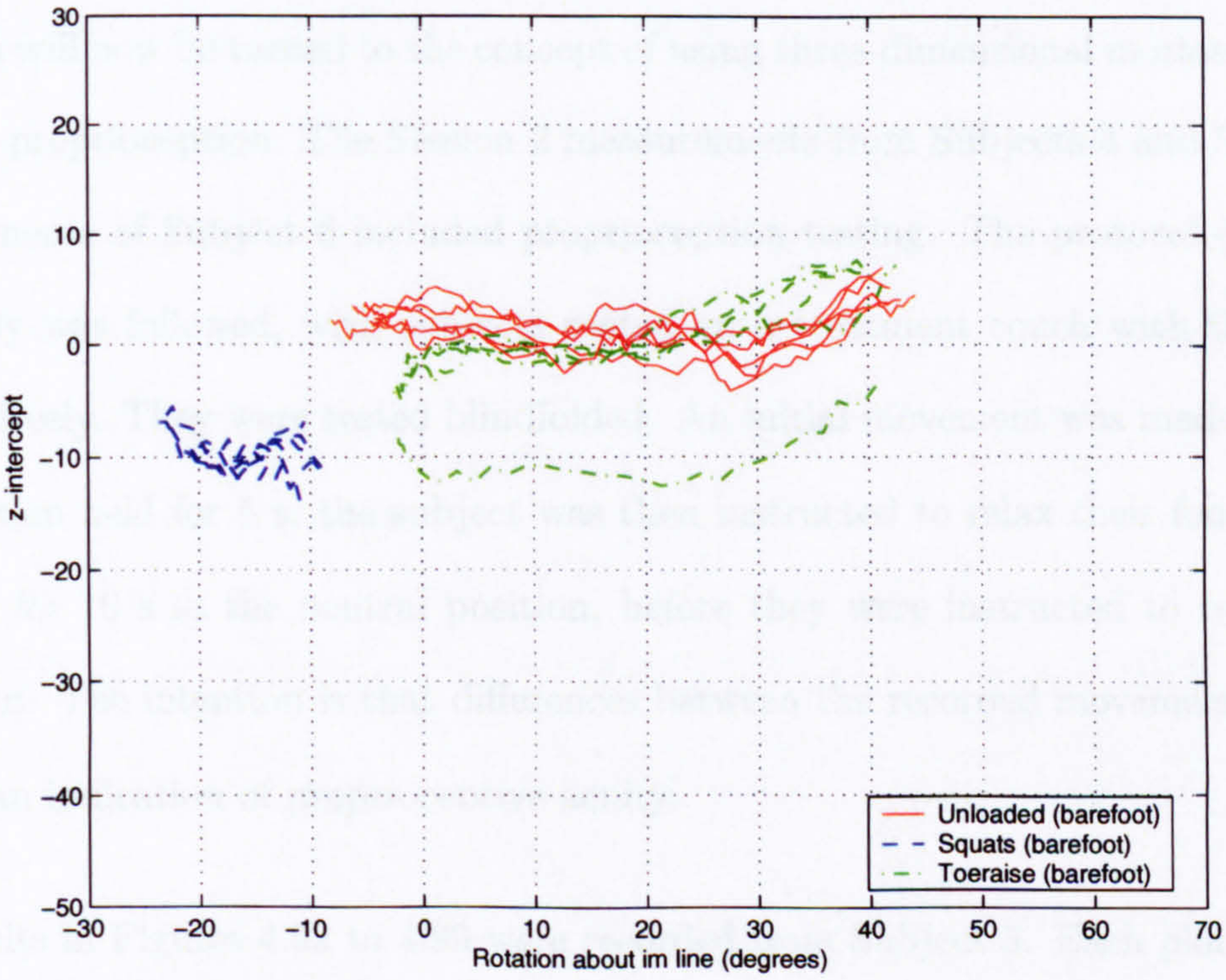

Figure 4.91: z-coordinate of point of intersection of axis with MM plane plotted against angle of rotation about IM line for Subject 5, Session 2 (plantarflexion movements).

4.7 Proprioception

4.7.1 Overview

Having concentrated so far on the variation in the axes measured during movements, attention will now be turned to the concept of using three-dimensional motion analysis to assess proprioception. The Session 2 measurements from Subjects 4 and 5 and the measurements of Subject 6 included proprioception testing. The protocol described previously was followed, with subjects seated on a treatment couch with the shank hanging freely. They were tested blindfolded. An initial movement was made and the end position held for 5 s, the subject was then instructed to relax their foot so that it rested for 10 s in the neutral position, before they were instructed to repeat the movement. The intention is that differences between the recorded movements can be used as an indication of proprioceptive acuity.

The results in Figures 4.92 to 4.99 were recorded from Subject 5. Each plot includes two initial and two repeated movements, as well as the five plots of barefoot dorsiflexion movements that have been presented previously. These are represented by dotted lines as they are included only for comparative purposes. Figures 4.92 to 4.94 show the three Euler angles describing the rotation of the shank ARF relative to the foot tool. The first of these, rotation about the IM line, has been used throughout this chapter. The other two angles, rotations about the y and z axes of the shank ARF, respectively, have not been considered before. They are included here to allow a more complete comparison of the movements. Figure 4.92 shows reasonably good agreement between initial and repeated movements, which is less varied than the barefoot

measurements. The reduced range is due to the fact that the proprioception measurements started from a relaxed neutral position rather than a maximally plantarflexed position. Variations in the other two angles are more pronounced for the first matching movements than for the second. The rotation about the y axis flattens off in a way that the results from the non-proprioception measurements do not.

Moving on to the helical axis parameters, clear patterns are apparent for n1, n2 and n3. These results are presented in Figures 4.95 to 4.97. While the n3 results follow very closely the results from non-targeted movements, the n1 and n2 parameters differ considerably. Although within similar ranges to the non-targeted movements, both follow a parabolic curve and exhibit much less variability. The y and z coordinate results (Figures 4.98 and 4.99) exhibit quite striking linearity. Again, although not dissimilar in terms of range of values to the non-directed movements, there is less variation and a clearer pattern.

For this subject, it would seem reasonable to conclude that the proprioception measurements are better controlled and more repeatable than the non-directed movements.

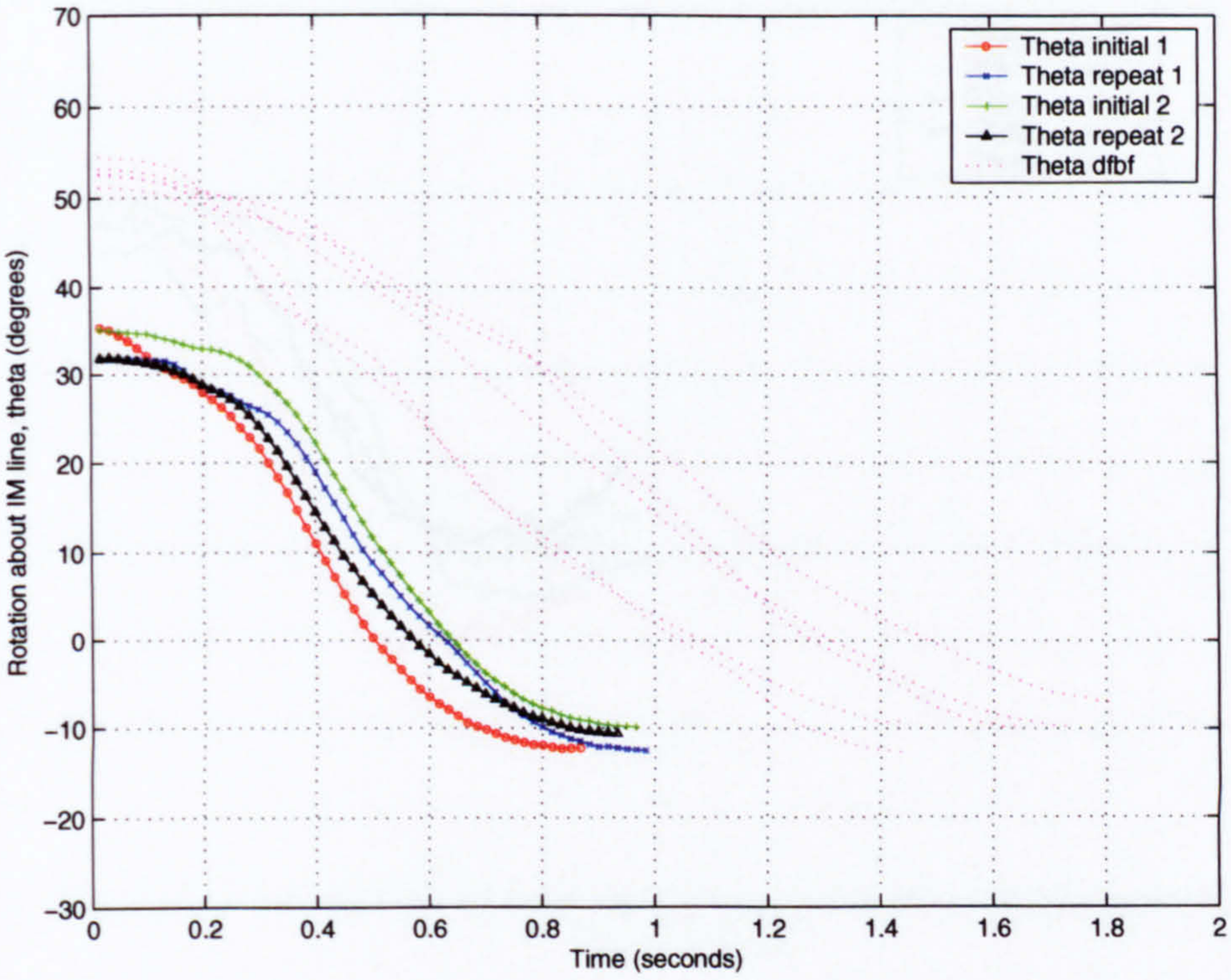

Figure 4.92: Subject 5 Session 2. Plots of theta vs time for 2 proprioception tests.

Figure 4.93: Subject 5 Session 2. Plots of theta2 vs time for 2 proprioception tests.

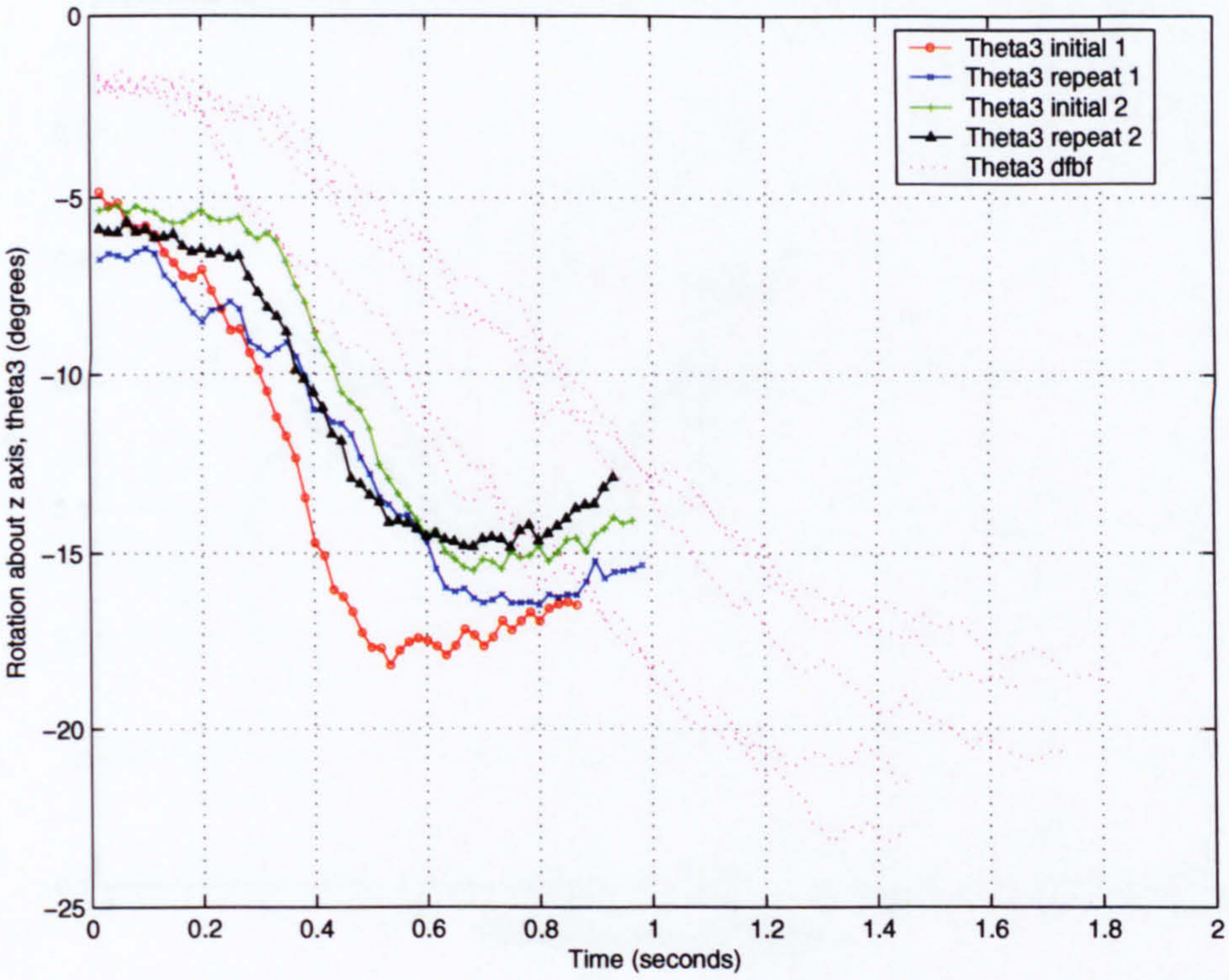

Figure 4.94: Subject 5 Session 2. Plots of theta3 vs time for 2 proprioception tests.

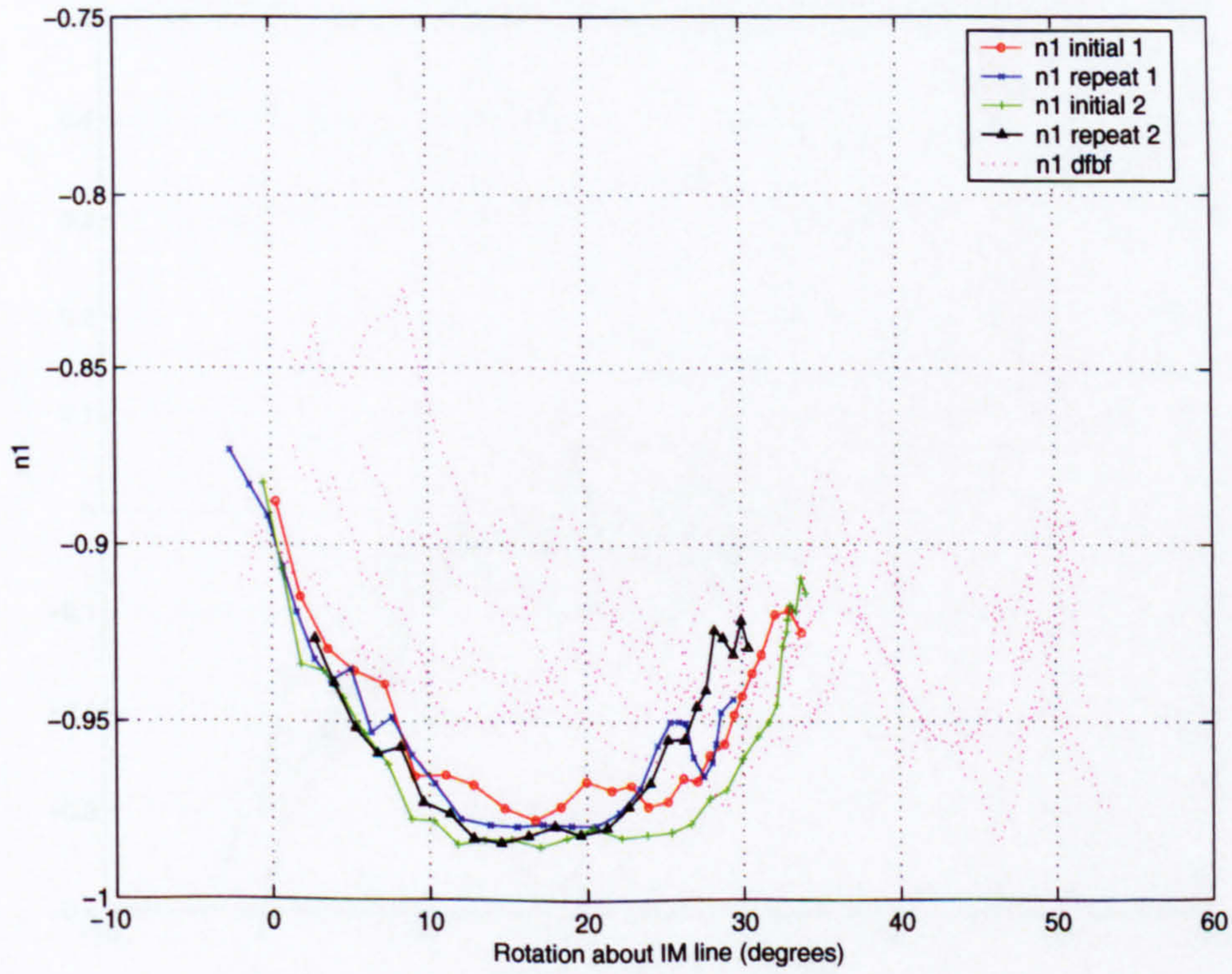

Figure 4.95: Subject 5 Session 2. Plots of n1 vs angle of rotation about IM line for 2 proprioception tests.

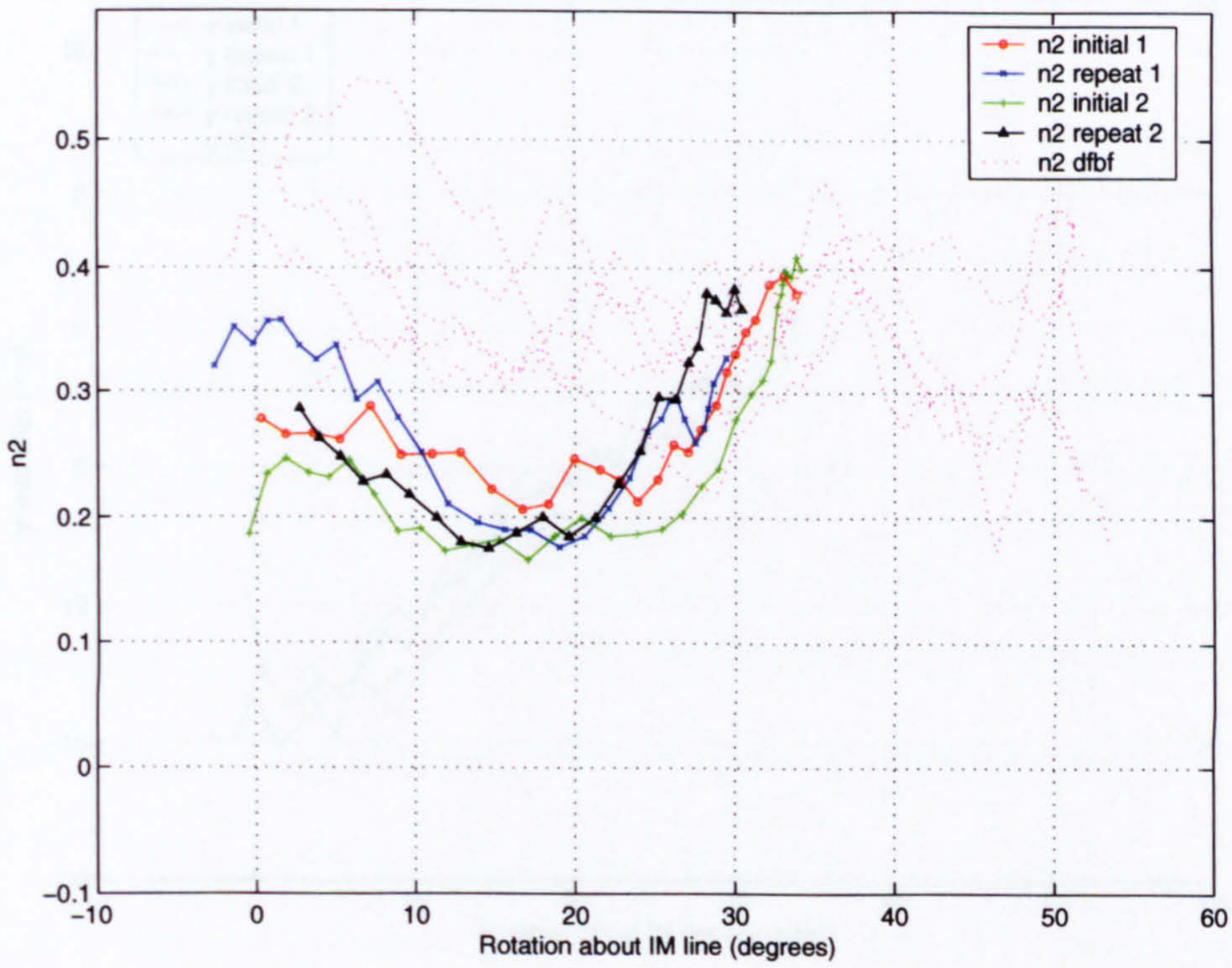

Figure 4.96: Subject 5 Session 2. Plots of n2 vs angle of rotation about IM line for 2 proprioception tests.

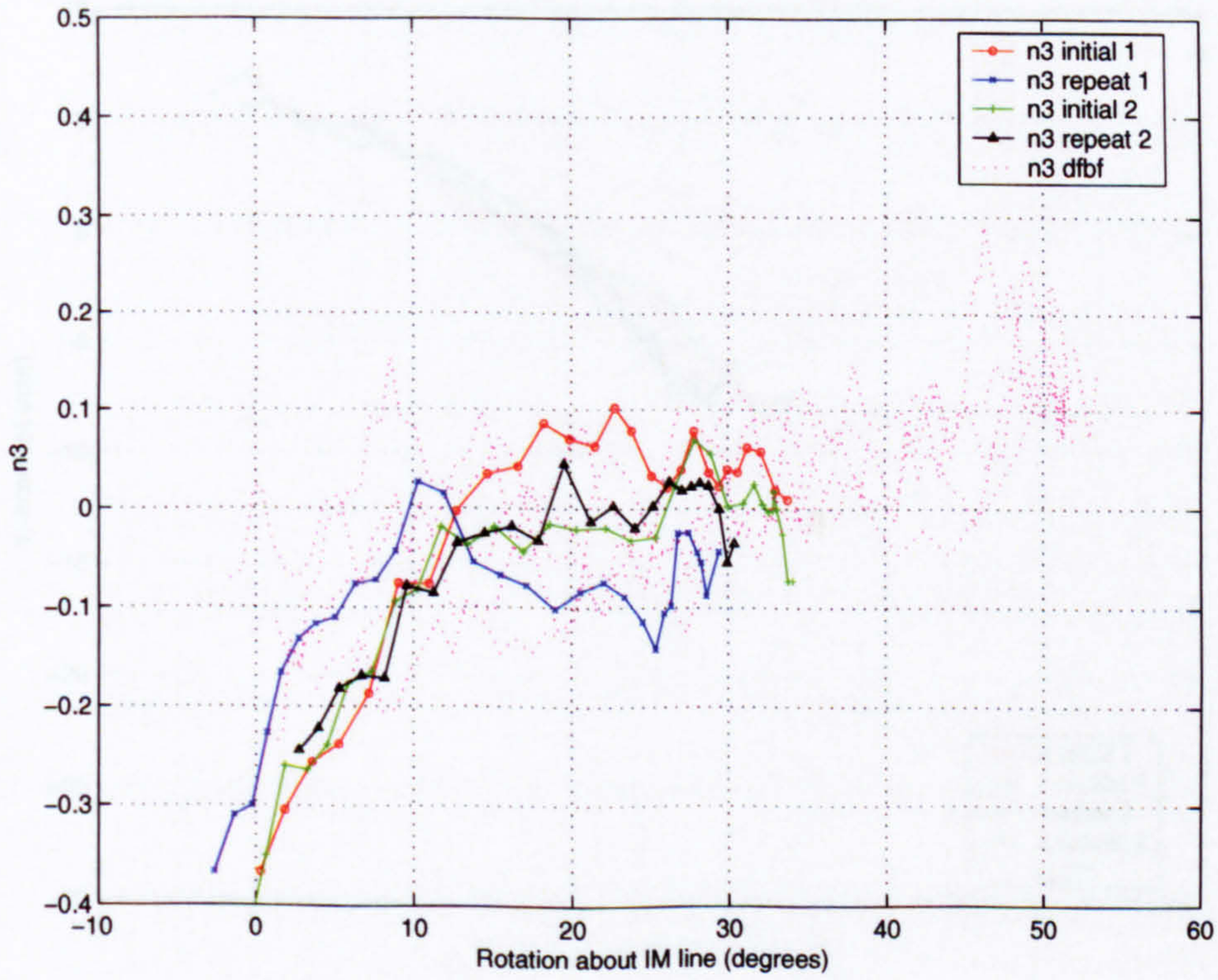

Figure 4.97: Subject 5 Session 2. Plots of n3 vs angle of rotation about IM line for 2 proprioception tests.

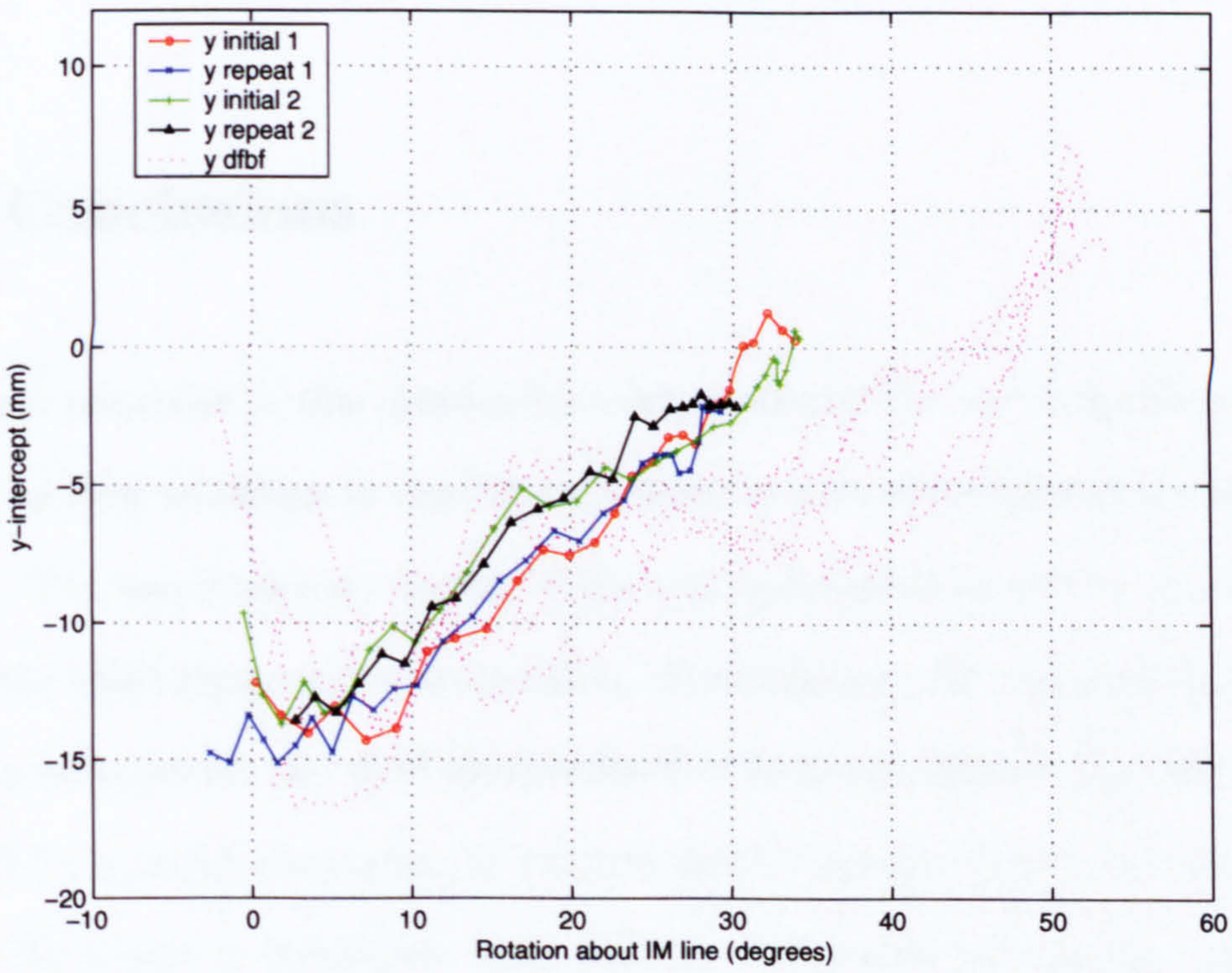

Figure 4.98: Subject 5 Session 2. Plots of y intercept vs angle of rotation about IM line for 2 proprioception tests.

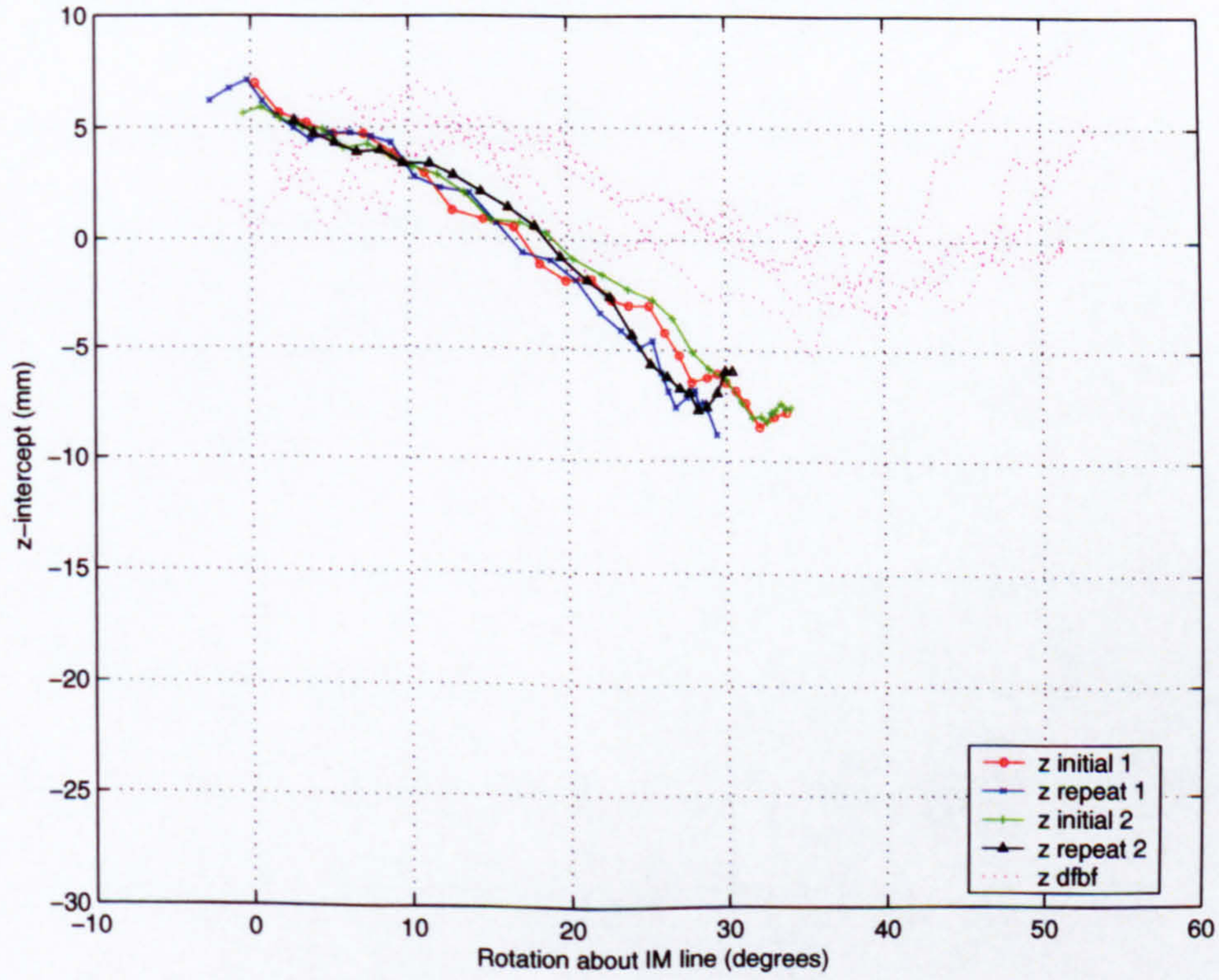

Figure 4.99: Subject 5 Session 2. Plots of z intercept vs angle of rotation about IM line for 2 proprioception tests.

4.8 Conclusions

The results presented in this chapter have demonstrated the use of the Sequential Finite Helical Axis technique to describe variations in axes of rotation of the ankle joint complex. The non-stationary nature of the axis apparent in all of the measurements justifies the close examination undertaken. Furthermore, the apparent repeatability of these measurements and their independence of footwear suggests that the approach may well be a useful alternative to current three-dimensional motion analysis techniques. The ability to investigate how axes vary under different loading conditions is an attractive feature, and the use of seqFHAs to assess proprioception has also been demonstrated. In the following chapter the implications of the results presented above, and a consideration of the future applications will be discussed.

Chapter 5

Discussion

5.1 Introduction

The development of the Sequential Finite Helical Axis (seqFHA) technique that allows the variation in axes of rotation of a joint to be assessed for unconstrained movement measured *in vivo* has been described. The technique can be employed to analyse any motion analysis data that is available in the form of transformation matrices; Chapter 4 includes a series of results obtained by applying this technique to the ankle joint complex under different loading conditions. The original motivation for the development of the seqFHA approach was the need to describe unconstrained repositioning movements in order to assess proprioception. The protocol for the assessment of proprioception that was developed as part of this work was employed to collect data, which was analysed using the seqFHA approach. Again, the results are presented in Chapter 4. This chapter will concentrate on evaluating the approaches taken to the assessment of proprioception and to the analysis of three-dimensional motion.

5.2 The evolution of the project

The original focus of the work was the investigation of factors influencing proprioception at the ankle joint complex. Such an investigation necessarily required both proprioception and the ankle joint complex to be clearly defined. This done, the natural first step was to review previous work that considered the assessment of proprioception, both at the ankle and at a variety of other joints. The key criticisms of the work reviewed were the lack of a consistent methodology, and the tendency to constrain movement, often so that it could be described in two dimensions. Leading directly on from this, a protocol for assessing proprioception at the ankle joint that allowed natural, unconstrained movements was proposed. Such a protocol requires the use of three-dimensional motion analysis in order to fully describe the complex movement patterns at the ankle; having identified the need for three-dimensional motion analysis, the question of which specific technique to use to describe the motion arose. Various options were considered, and the helical axis technique was identified as the most applicable to dorsiflexion-plantarflexion movements, with the attractive quality that it allows axes of rotation to be identified. The established limitation of the helical axis approach, namely that the parameters calculated are ill-defined for small rotations, was demonstrated. In order to address this limitation, a novel approach was developed that is not only applicable to the assessment of proprioception, but also allows an estimation of the continuous variation in location and orientation of the axis of rotation throughout movement. The novel approach was used to investigate patterns of variation in the axes under different loading conditions, before applying the technique to the assessment of proprioception.

Having considered how the project evolved over time, each of the steps outlined above will now be described in more detail. This will allow the justification for the approach

adopted to be evaluated.

5.3 Definitions

The lack of clear definitions of the ankle joint complex and proprioception was surprising. In order to communicate as clearly and unambiguously as possible the details of the investigations undertaken, working definitions were adopted at an early stage.

5.3.1 Ankle joint complex

In terms of bony anatomy, the ankle joint complex includes the distal ends of the tibia and fibula, the talus, calcaneus and the navicular bones. There is a wide variety in the terms used to refer to the different articulations between the bones within this complex, which are discussed in Section 2.3. For this work, it was decided to describe the ankle joint complex by linking movements to articulations. Therefore, adopting for these purposes a model of the ankle joint as a two-axis system (van den Bogert et al., 1994), dorsiflexion and plantarflexion were considered to describe movements that were composed primarily of rotations at the tibio-talar articulation, while inversion and eversion described those movements composed primarily of rotations at the talo-calcaneal joint. These are not intended to be definitive solutions to the problem of describing ankle joint motion; rather they are an attempt to avoid the confusion identified in a recent Biomch-l survey of what researchers and clinicians in the field understand by various common terms.

5.3.2 Proprioception

Although proprioception is referred to extensively in the literature, there is a distinct lack of a common accepted definition. The working definition adopted is as follows:

Proprioception is the sense of position and movement of parts of the body, based solely on neural input from mechanoreceptors in the joint capsules, ligaments, muscles, tendons and skin.

It is apparent that this definition refers in any detail only to the peripheral sources of afferent proprioceptive neural input. It does not consider how such information is processed centrally to achieve the sense of position and movement that is referred to; this is held to be outside the scope of this work. The way in which proprioceptive information is used will be considered in greater detail later.

5.4 Protocol for the assessment of proprioception

The review of the literature presented in Section 2.4 provides little evidence of a well-considered, intelligently argued and widely adopted approach to the assessment of proprioception. Let us briefly review the protocol developed here. Subjects were seated, blindfold, with their shanks hanging freely in space. They were barefoot, so that the ankle joint complex is unloaded except for distraction of the joint due to the weight of the foot. They are asked to relax so that the foot hangs in a slightly plantarflexed orientation. They are then asked to either dorsiflex or plantarflex their foot to a position of their own selection, and to hold that position for 5 s. The subject then returns their foot to the relaxed, neutral position for 10 s before being instructed to repeat the movement they have just made. The matching movement is then compared to the initial movement.

By ensuring that the subject is seated and blindfold, the visual and vestibular systems are isolated from movement at the ankle. Therefore, the only sensory input available to determine the position of the foot at a given point in time is that issuing from mechanoreceptors in the joint capsules, ligaments, muscles, tendons and skin. Therefore, if we accept the definition of proprioception given above, the subjects are being assessed for their ability to repeat a movement which must provide a measure of their proprioception.

The argument for the use of active initial and repeat movements is based on the fact that the firing pattern of muscle spindles is different in a contracting muscle to a muscle that is being stretched, or indeed one that is relaxed. Given that the impulses from the muscle spindles are assumed to contribute to proprioceptive acuity, it is reasonable to endeavour to ensure that the same muscle activity can be involved in the initial and repeat movements. Therefore, either passive/passive or active/active movement matching is required. The argument against passive/passive is that by manipulating the foot, a pattern of movement is imposed, and it is virtually impossible to ensure that it is repeated in exactly the same way. Furthermore, there is greater interest in proprioceptive acuity during active movements than passive movements.

5.5 Choice of 3D motion analysis technique

Considerable effort has been concentrated on the development of a novel technique to describe motion. Given that there are a number of established techniques that could have been adopted, it is important to question whether or not it was necessary to develop another one. Section 3.5 includes details of the various options, and their limitations. The central criticism relates to the fact that all approaches other than the helical axis approach impose stationary axes. The limitation of the helical axis

technique is that helical axes are ill-defined for small rotations - the seqFHA approach solves this. The use of seqFHAs is a significant departure from standard methods in that it describes how the axis of rotation varies throughout motion. So movement at a joint is represented by the movement of the axis of rotation. The results presented here are referenced to an Euler angle of rotation about the intermalleolar line. This gives an indication of where the ankle joint is in its range of motion. It is important to consider why the axis of rotation of the ankle joint is so important. The reasons given by various authors in Section 2.6 relate either to the calculation of joint moments or to the design of prostheses. It is the former that has the most wide-ranging implications. Throughout this work the focus has been clearly on voluntary, unconstrained movement. Voluntary movements are a result of joint moments created by muscles acting about a joint. Joint moments are the most important kinetic parameter, and it is nonsensical to consider moments without describing the related axis of rotation.

Returning to the aim of allowing unconstrained motion, unconstrained relates to artificial constraint. All movements are constrained by the morphology of the joint, and contact or support surfaces, for example the ground in standing or walking. However, imposing an artificial constraint such as a hinged footplate is a convenience to the investigator that is used to simplify movement and therefore the description of motion. Rather than constrain movement to something that is easy to measure, the approach adopted here is to develop a technique that is capable of describing complex motion. This is possible using Euler or Cardan angles, but the approach adopted is only capable of describing the motion in terms of a series of three rotations about axes selected for convenience rather than anatomical or physiological relevance. Again, the movement is being tailored to a means of describing it, rather than the other way around. The Joint Coordinate System is a considerable improvement, in that it allows two of the three axes to be selected on the basis of an individual's anatomy. However, it is

still limited to stationary axes. The description in Section 3.7.3 of the construction of a JCS based on functional axes is a further useful development, but it still imposes stationary axes. If one accepts the importance of axes of rotation, then the appeal of the helical axis approach is clear, and the seqFHA technique goes some way to address the limited resolution.

5.6 Limitations of the seqFHA technique

The seqFHA approach does not describe instantaneous axes of rotation. Rather, it allows an axis of rotation to be associated with each frame of data. For the method of calculation described here, this is only possible for a given frame if there is a subsequent frame of data that describes a transformation of a helical rotation of at least 10^o relative to that frame. Therefore, for any given rotation, seqFHAs cannot be calculated for the last 10^o of the movement. Also, seqFHAs are sensitive to changes in direction of rotation, such as may occur if a subject hesitates or makes a jerky movement. However, such measurements can be identified and subsequently excluded from the calculations by inspecting the angle-time graph. There is no direct description of rotation about each helical axis that is calculated; this is why the axis parameters are plotted relative to the angle of rotation about the IM line. Also, the method of describing the helical axes requires comparison of five separate parameters, although the author believes that with practice the orientation and location in space may become quite intuitive. It is important to note that the helical axis approach again represents the actual movement using a mathematical abstraction. However, the mathematical abstraction provides a representation of how the axis varies in space, and is particularly suited to hinge-type joints such as the ankle.

5.6.1 Sources of error

Before proceeding to discuss the conclusions that can be drawn from the results presented in Chapter 4, it is important to consider sources of error in the measurements. The effect of skin movement is difficult to measure; however, the ability to compare results from the same subject performing the same movements barefoot and then wearing shoes allows some appreciation of the impact that this has. This is discussed in greater detail below. There are several sources of error in the digitisation of the bony landmarks to create the Anatomical Reference Frame (ARF). This is clearly important because all of the results considered are presented in the axes of the ARF. The sources of error include error in the tracking of the pointer tool, error in the calculation of the tip offset, error in the palpation of the bony landmarks by the investigator and error in holding the pointer in place while the necessary frames of data are recorded to digitise a point. Of these, the latter two are likely to be the major contributors to the overall error. The ease with which the tips of the malleoli, for example, can be identified with good repeatability varies considerably from one individual to another. In order to evaluate the overall variation, the length of the intermalleolar line was calculated from the digitised medial and lateral malleoli for different measurement sessions for Subjects 4 and 5. There are four measurements for Subject 4, and seven for Subject 5, three of which were recorded from measurement sessions not described elsewhere. The results are presented in Table 5.1. It is clear that there is considerable variation. When comparing results based on ARFs calculated from a different set of digitised landmarks, the importance of this variation must be considered. For future work, it is recommended that several measurements are made and averages taken, to reduce this variability.

Table 5.1: Table of calculated lengths of intermalleolar line, in mm, for Subject 4 and Subject 5

	Subject 4	Subject 5
Measurement 1	78.5	67.2
Measurement 2	78.4	67.0
Measurement 3	79.9	70.1
Measurement 4	82.9	67.1
Measurement 5	X	66.9
Measurement 6	X	61.8
Measurement 7	X	66.7
Mean (range)	79.9 (4.5)	66.7 (8.3)

5.7 Conclusions drawn from axes results

The results obtained from applying the seqFHA technique to data collected from subjects under a range of loading conditions are presented in Sections 4.4, 4.5 and 4.6. To the author's knowledge, axes of rotation of the ankle joint complex have not previously been investigated for *in vivo*, continuous movements. Although it is important to bear in mind the limitations of the seqFHA technique outlined in Section 5.6 above, the following conclusions can be drawn.

The axis of the ankle joint complex is non-stationary Although the seqFHAs calculated for any given movement cannot describe the instantaneous axis, the fact that there is any variation in the parameters throughout the range of motion demonstrates that the axis of rotation is non-stationary. The results from a mechanical, single axis system obtained using the same technique are presented in Section 4.3.3. It is clear that none of the results calculated from the subject measurements exhibit the same degree of stability across all parameters. If there were significant errors in the definition of the ARF, this would simply impose an offset on the values of the parameters; they would still be constant if the axis were stationary. Therefore, there is compelling evidence that, for the movements investigated, the axis of the ankle joint complex is non-stationary.

The seqFHA parameters vary between subjects For voluntary movements, the location and orientation of seqFHAs will depend upon joint morphology, the orientation and mechanical properties of the ligaments of the ankle joint and muscle action about the joint. Each of these factors is dependent on the individual, so it follows that the seqFHAs will vary according to the individual; this was confirmed by the data collected.

5.7.1 Observations

There are a number of interesting observations that arise from the analysis of the results presented relating to the patterns of variation of the seqFHA parameters. The small number of subjects investigated and the nature of the data collected limit the extrapolation of these findings to all subjects, but they serve as useful indications of inter-subject similarities that deserve further investigation.

There is no overall dependence on footwear The results presented in Sections 4.4 and 4.5 indicate that movement of the markers relative to the underlying bony anatomy does not significantly affect the patterns of variation in the seqFHA parameters. It is highly unlikely that the movement of the Polaris tools relative to the bony anatomy would be the same when the tool was attached directly to the foot as when the tool was attached to a subject's shoe. There are several examples of a significant offset - this is believed to be due to inconsistencies in digitisation of the bony landmarks required to construct the ARF, in addition to any effect that wearing shoes might have on a subject's relaxed standing position, which would change the reference orientation of the foot relative to the shank.

Direction of movement does not seem to have an effect Dorsiflexion and plantarflexion are used to describe directions of rotation. Therefore, the

seqFHA parameters relating to orientation have an opposite sign for the two movements. However, for the majority of subjects, the absolute values are very similar. This is seen in the way the dorsiflexion and plantarflexion results for a given subject mirror each other. The y and z coordinates are generally very similar. It was considered possible that, due to different muscle activation patterns for the two movements, the axes of rotation might vary. There is no clear evidence to support the different pattern of axes described for dorsiflexion and plantarflexion by Lundberg et al. (1989b).

There is evidence of repeatable patterns Although the values of the parameters vary, in many cases there are indications of similarities in the pattern of variation of the seqFHA parameters between subjects. These observations require further measurements in order to investigate their validity.

The effect of the loading conditions varies The different loading conditions investigated allow results from the full range of movement to be described. In some subjects, the results from one loading condition seem continuous with the results for adjacent or overlapping ranges recorded from different movements, while for other subjects there is a sharp discontinuity.

The points of intersection are reasonably contained Across all subjects, the y and z coordinates of the point of intersection of the axis with the MM plane lie within a circle of radius 30mm centred at the origin of the shank ARF, which is coincident with the origin of the MM plane. The error in digitising the bony landmarks required for the construction of the MM plane must be considered, as it may distort the true variation.

5.7.2 Is the variation in the axis important?

Having identified variations in the axis of rotation of the ankle joint, it is reasonable to query the relevance of these variations. There is an inherent interest in describing the patterns of variation of the axis because it gives an insight into the physiology of the joint, and may allow ankle pathologies to be investigated. However, in terms of the kinetics of the joint, if the variations in the axis do not significantly affect calculations, then it may be reasonable to resort to the use of the IM line as an approximation. With the data that has been collected, it is not possible to calculate kinematic parameters. However, for illustrative purposes, it is possible to calculate an effective moment arm for the weight of the foot acting about the calculated axis for a frame, and that about the intermalleolar line. In order to do this, a vertical reference tool was tracked in addition to the foot and the shank tools. The centre of mass of the foot is estimated to be one third of the length of the foot from the rearmost point of the calcaneus; a point on the dorsum of the foot was digitised approximately this distance from the calcaneus. Although the centre of mass of the foot is clearly not on the dorsal surface, this approximation was adopted.

In order to calculate effective moment arms, the approximate foot *COM* was transformed to the shank ARF. Simultaneous equations were used to identify the point of intersection of a line perpendicular to the calculated axis, passing through the foot COM, with the calculated axis itself. The length of this line, which will be referred to as the COM line, could then be calculated. The vertical reference gives the line of action of the weight of the foot. The dot product of the vertical direction vector and a direction vector perpendicular to the COM line was calculated and the cosine of the angle (γ) between the two derived. The effective moment arm was calculated as the product of the length of the COM line and the cosine of γ. The moment of the weight of the foot about the axis would be calculated by multiplying the weight

of the foot by the effective moment arm. This series of calculations was repeated for the IM line. For a given weight of foot, the difference in the moments calculated will be proportional to the difference in effective moment arms.

Figures 5.1 and 5.2 show effective moment arms calculated from the data collected from unloaded, barefoot movements during the second session for Subjects 4 and 5. It is apparent that over the range of movement, there is considerable variation between the calculations based on the seqFHA and those based on the IM line. This is only an illustrative example, however it does indicate that the variations in the seqFHAs that have been identified may have important implications for the kinetics of motion at the joint.

5.8 Observations on proprioception results

The results from assessment of proprioception of Subject 5 are presented in Section 4.7 in the previous chapter. In general, the seqFHA parameters exhibit better repeatability between initial and repeated movements than those calculated from the dorsiflexion movements conducted to investigate axes of rotation. It is interesting to note that for all of the parameters, the proprioceptive results are within the variation of the non-proprioception results. This is to be expected. In particular, the coordinates of the point of intersection of the seqFHAs with the MM plane are very well controlled and highly repeatable; there is greater variability in the orientation parameters. Although the results are not presented here, this is also seen in the data collected from Subject 4, which is the only other complete proprioceptive data available. The three Cardan angles are included in order to demonstrate that there is some variability in these; if there were changes in orientation of the seqFHAs that were not reflected in changes in these angles there would be cause for concern over the seqFHA approach. The ability

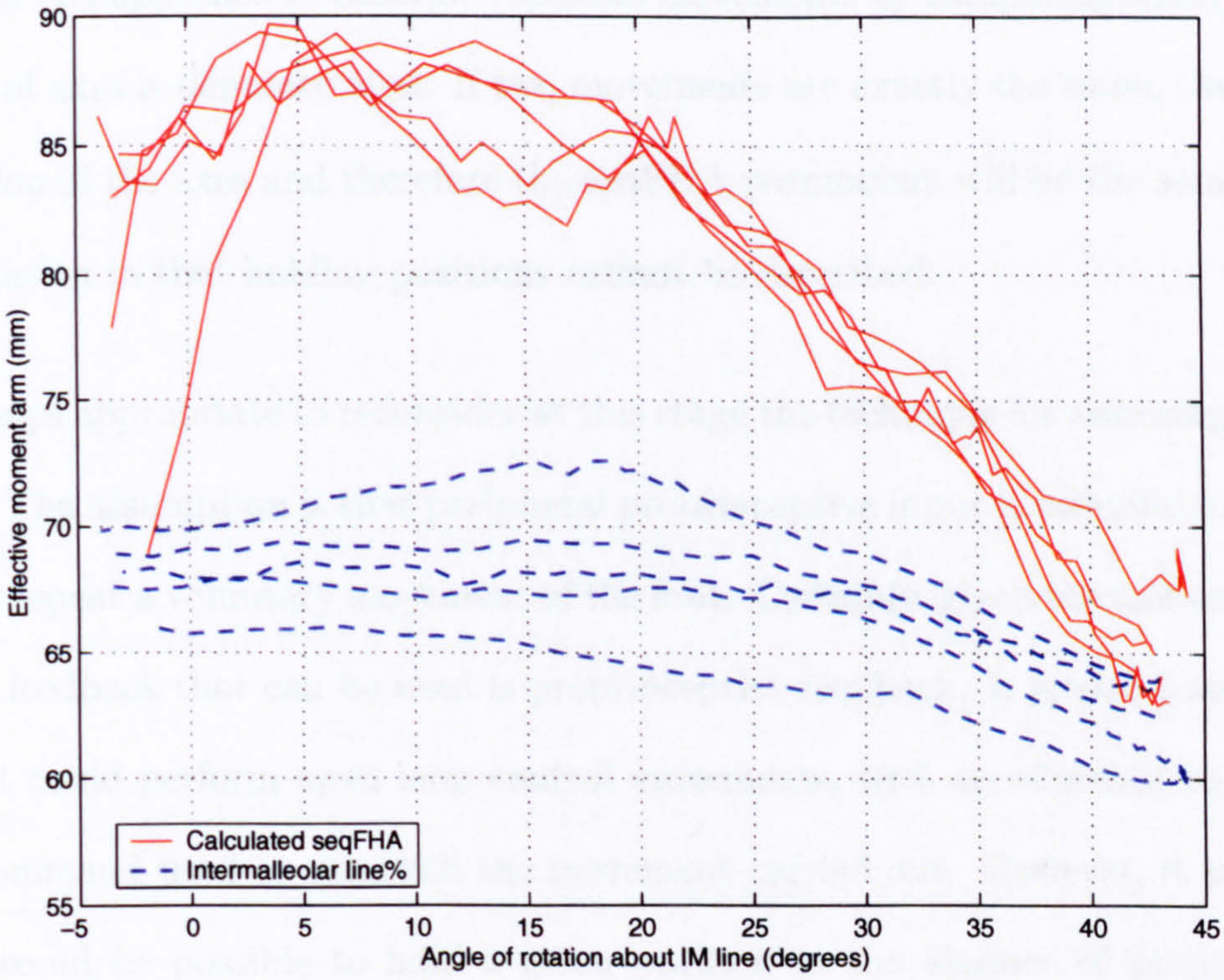

Figure 5.1: Subject 4, Session 2. Effective moment arms calculated for unloaded, barefoot, dorsiflexion movements

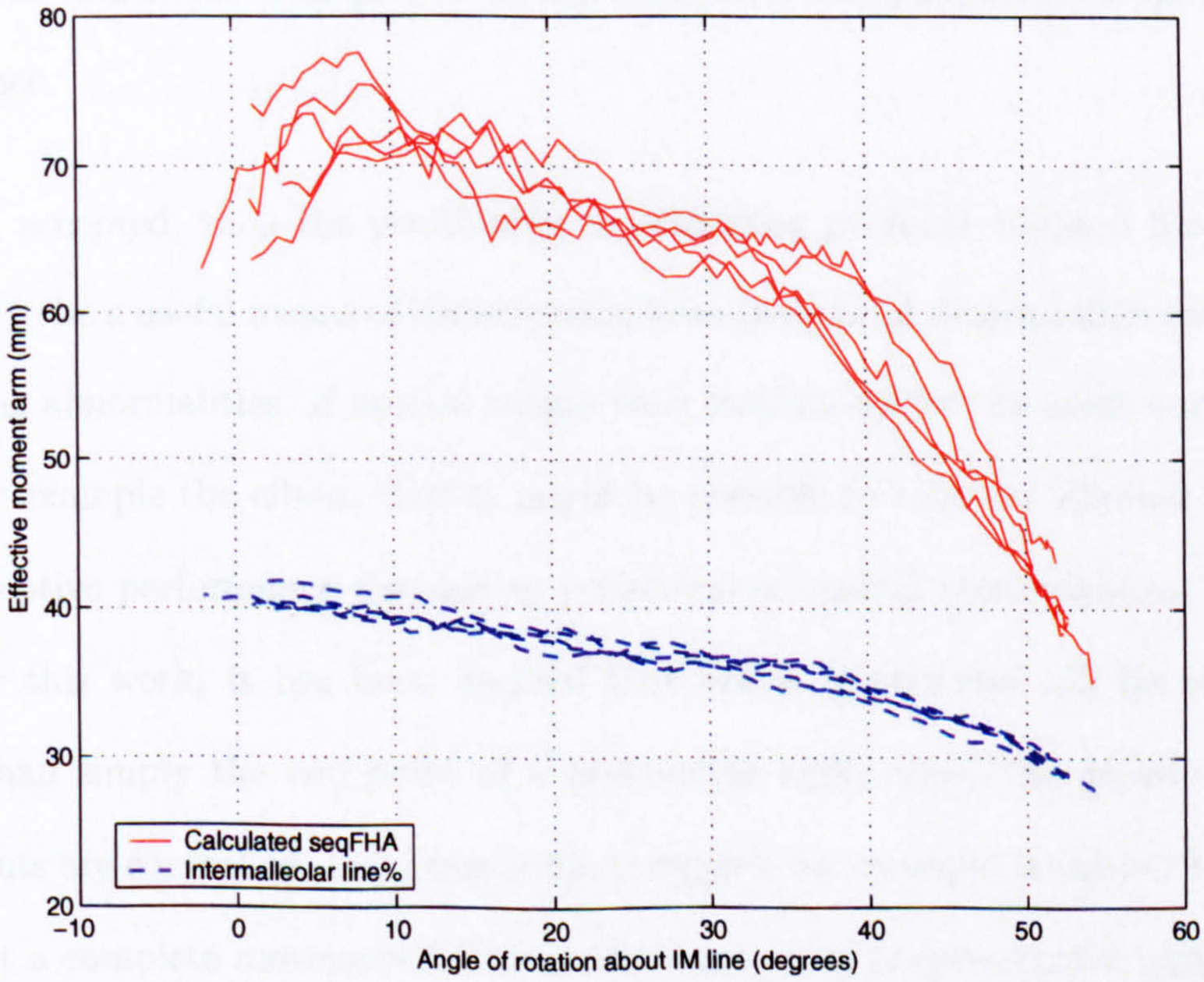

Figure 5.2: Subject 5, Session 2. Effective moment arms calculated for unloaded, barefoot, dorsiflexion movements

of the seqFHA approach to describe repeated movements by comparing changes in the patterns of axes is demonstrated. If two movements are exactly the same, the pattern of variation of the axes and therefore the seqFHA parameters will be the same. There is a limitation in that holding positions cannot be described.

It is perhaps appropriate to reconsider at this stage the technique for assessing proprioception. The assumption is that peripheral proprioceptive input is essential in order to precisely repeat a voluntary movement of the foot. Certainly, given the test conditions, the only feedback that can be used is proprioceptive feedback. It is also possible that a subject could perform open loop control movements, with an efference copy of the motor command used to establish the movement carried out. However, it is unlikely that it would be possible to hold a given position in the absence of proprioceptive feedback. The work carried out by Goodwin et al. (1972) indicates that perturbation of the peripheral mechanoreceptors by applying tendon vibrations results in distorted perceptions of motion. This gives a strong indication that peripheral receptors are of importance.

If this is accepted, then the positioning-repositioning protocol adopted here can be assumed to be a useful means of investigating both peripheral neuropathies and central processing abnormalities. If normal ranges were established for the ankle and another joint, for example the elbow, then it might be possible to indicate whether impaired proprioceptive performance was due to peripheral or central abnormalities. The fact that, for this work, it has been decided that entire movements will be compared, rather than simply the end point of a positioning task, raises the question of how movements are controlled. Is it reasonable to expect, for example, a subject to be able to repeat a complete movement? This would imply that proprioceptive input is used throughout the movement to match the original movement. The indication from the results presented is that when a subject is asked to perform two matched movements,

there is less variability between them than between a series of movements where a subject is simply asked to move the foot up and down. It would seem reasonable to hypothesise that it is possible to consciously use peripheral proprioceptive input to modify a more general movement pattern, that may possibly be generated by a pattern generator in the brain. This theory may be extended to a general consideration of movements - there are gross motor patterns that are employed by lower brain centres but these can be consciously modified using available inputs. This would indicate that *the protocol described here is appropriate. However, it does not shed any light on* to what degree, if at all, complex movement patterns are pre-programmed, or how multi-joint, targeted movements are made given the infinite number of combinations of joint angles that can achieve the same end position.

5.9 Further work

There are a number of ways in which the investigations presented here can be extended. One obvious area for further work is the application of the technique to other joints. In the same way as the technique offers an indication of how far the ankle joint deviates from a simple hinge, it is possible that the technique could be used to investigate to what degree the shoulder and hip joint deviate from spherical joints, by investigating the point of intersection of the seqFHAs. The areas of further work relating directly to the investigations performed thus far are presented below.

5.9.1 Collection of normative data

The results presented in this thesis only provide an indication of how the various parameters vary between subjects. Further subject testing is required in order to es-

tablish normal ranges for the seqFHA parameters. Such results would also allow the repeatability of patterns between subjects to be investigated in greater detail. The recommendation has already been made that the digitisation of the bony landmarks be repeated more than once and then averaged in order to reduce the variability of these measurements. Intra-subject repeatability also requires investigation. In order to facilitate comparison between different sets of results for the same subject, an Anatomical Reference Frame for the foot could be employed in the same way as that for the shank. This would require digitisation of three bony landmarks on the foot. The problem of different standing orientations creating an offset in the results would thus be avoided. In addition to the activities described, it would also be interesting to investigate how seqFHAs vary in repeated movements such as walking and cycling. Similar investigations of normal ranges and inter- and intra-subject repeatability are also required for the application of the seqFHA technique to the assessment of proprioception. Finally, the technique could easily be applied to investigate inversion and eversion in addition to dorsiflexion and plantarflexion.

5.9.2 Investigation of ankle pathologies and neuropathies

Once a body of normative data is available, patients presenting with ankle pathologies could be investigated. For example, it would be possible to investigate whether a damaged ligament resulted in greater variation in the seqFHAs, as one might expect. This could be done by comparison between damaged and intact joints for unilateral injuries. The value of the technique in quantifying improvements during the process of rehabilitation could also be established. The application of the protocol described for the assessment of proprioception could be used to investigate the same patients presenting with mechanical ankle injuries, as well as patients presenting with peripheral neuropathies.

5.9.3 Calculation and presentation of results

The results presented here have been calculated from raw motion analysis data from Polaris. It is possible that filtering of the data would reduce the angular separation required to calculate well-defined seqFHAs. This might enable a more accurate description of how the axis varies, but could also introduce further problems. The justification for using a separation angle of 10° has been presented in Section 3.7.1. This has allowed the technique to be applied in order to obtain the results presented. However, it is possible that this could be improved by calculating axes from a given frame until a stable axis is achieved, assessed by monitoring the variation of the various parameters.

Finally, the cumbersome nature of considering the variation in five separate parameters has previously been noted. The potential for the surface swept by the seqFHAs calculated for a movement to be described mathematically required investigation. If this could be done in a concise manner, it might facilitate comparison of different results.

5.10 Conclusions

The potential value of the seqFHA technique is apparent from the consideration of further work above. The development of a protocol for the assessment of proprioception that is thoroughly justified also offers an opportunity to consider a standardised approach to such testing. The work described above has enabled the *in vivo* investigation of axes of rotation of the ankle joint for continuous movements and across different loading conditions. This enabled the conclusions that the axis of the ankle joint is non-stationary, and that locations and orientations of axes vary between subjects, to

be drawn. Furthermore, the implementation of the proposed protocol for the assessment of proprioception has demonstrated how complete movements may be compared to allow a more sensitive assessment of an individual's proprioception than a comparison of endpoints of movements allows. Throughout this work, there has been a focus on axes of rotation of the ankle joint complex. The author believes that the intimate relationship between joint moments and axes of rotation justifies this approach. If the further work suggested is carried out, the seqFHA technique and the protocol for the assessment of proprioception have the potential to contribute valuable knowledge to the biomechanics community.

Bibliography

R J Abboud, Agarwal S K, Rendall G C, and Rowley D I. A direct method for quantitative measurement of ankle proprioception. *The Foot*, 9(1):27–30, 1999.

R L Barrack, H B Skinner, M E Brunet, and R J Haddad Jr. Functional performance of the knee after intraarticular anaesthesia. *American Journal of Sports Medicine*, 11(4):258–261, 1983.

D S Barrett, A G Gobb, and G Bentley. Joint proprioception in normal, osteoarthritic and replaced knees. *Journal of Bone and Joint Surgery Series B*, 73(1):53–56, 1991.

R A Berenberg, J M Shefner, and J J Sabol Jr. Quantitative assessment of position sense at the ankle: A functional approach. *Neurology*, 37(1):89–93, 1987.

J N Bernier and D H Perrin. Effect of coordination training on proprioception of the functionally unstable ankle. *Journal of Orthopaedic and Sports Physical Therapy*, 27(4):264–275, 1998.

L Blankevoort, R Huiskes, and A de Lange. Helical axes of passive knee joint motions. *Journal of Biomechanics*, 23(12):1219–1229, 1990.

J Boyle and V Negus. Joint position sense in the recurrently sprained ankle. *Australian Journal of Physiotherapy*, 44(3):159–163, 1998.

P R Burgess, J Y Wei, F J Clark, and J Simon. Signalling of kinaesthetic information by peripheral sensory receptors. *Annual Reviews in Neuroscience*, 5:171–187, 1982.

D Burke, K-E Hagbarth, L Löfstedt, and B G Wallin. The responses of human muscle spindle endings to vibration of non-contracting muscles. *Journal of Physiology*, 261: 673–693, 1976.

A Cappozzo, F Catani, U Della Croce, and A Leardini. Position and orientation in space of bones during movement: anatomical frame definition and determination. *Clinical Biomechanics*, 10(4):171–178, 1995.

L Cheze, BJ Fregly, and J Dimnet. Determination of joint functional axes from noisy marker data using the finite helical axis. *Human Movement Science*, 17:1–15, 1998.

DM Demarais, RA Bachschmidt, and GF Harris. The instantaneous axis of rotation (iaor) of the foot and ankle: A self-determining system with implications for rehabilitation medicine application. *IEEE Transactions on Neural Systems and Rehabilitation Engineering*, 10(4):232–238, 2002.

R A Donatelli. *The Biomechanics of the Foot and Ankle.* F. A. Davis, second edition, 1996.

J W Feuerbach, M D Grabiner, T J Koh, and G G Weiker. Effect of an ankle orthosis and ankle ligament anaesthesia on ankle joint proprioception. *American Journal of Sports Medicine*, 22(2):223–229, 1994.

M G Gilsing, C G Van den Bosch, S G Lee, J A Ashton Miller, and N B Alexander. Association of age with the threshold for detecting ankle inversion and eversion in upright stance. *Age and Ageing*, 24(1):58–66, 1995.

G M Goodwin, McCloskey D I, and P B Matthews. The contribution of muscle afferents to kinaesthesia shown by vibration induced illusions of movement and by the effects of paralysing joint afferents. *Brain*, 95(4):705–748, 1972.

D S Gordan. Pedal goniometer to assess ankle proprioception. *Archives of Physical Medicine and Rehabilitation*, 69(6):461–462, 1988.

H Gray. *Anatomy, Descriptive and Surgical.* Bounty Books, 1977.

P Grigg, G A Finerman, and L H Riley. Joint position sense after total hip replacement. *Journal of Bone and Joint Surgery Series A*, 55(5):1016–1025, 1973.

ES Grood and WJ Suntay. A joint coordinate system for the clinical description of three-dimensional motions: Application to the knee. *Transactions of the ASME*, 105:136–144, 1983.

M T Gross. Effects of recurrent lateral ankle sprains in active and passive judgements of joint position. *Physical Therapy*, 67:1505–1509, 1987.

P W Hamer, A M Munt, C D Harris, and N C James. The influence of ankle strapping on wobbleboard performance, before and after exercise. *Australian Journal of Physiotherapy*, 38(2):85–92, 1992.

E J Heit, S M Lephart, and S L Rozzi. The effect of ankle bracing and taping on joint position sense in the stable ankle. *Journal of Sport and Rehabilitation*, 5(3): 206–213, 1996.

J N Hertel, K M Guskiewicz, D W Kahler, and D H Perrin. Effect of lateral ankle joint anaesthesia on centre of balance, postural sway and joint position sense. *Journal of Sport and Rehabilitation*, 5(2):111–119, 1996.

T Hogervorst. Mechanoreceptors in joint function. *Journal of Bone and Joint Surgery Series A*, 80(9):1365–1378, 1998.

D Hopper, D Whittington, and J Davies. Does ice immersion influence ankle joint position sense? *Physiotherapy Research International*, 2(4):223–236, 1997.

V T Inman. *The Joints of the Ankle.* Baltimore: Williams and Wilkins, 1976.

E R Kandel, J H Schwartz, and T M Jessell. *Principles of Neural Science.* Appleton and Lange, third edition, 1991.

L Konradesen, J B Ravn, and A I Sørensen. Proprioception at the ankle: The effect of anaesthetic blockade of ligament receptors. *Journal of Bone and Joint Surgery Series B*, 75B:433–436, 1993.

L Konradsen, S Olesen, and H M Hansen. Ankle sensorimotor control and eversion strength after acute ankle inversion injuries. *American Journal of Sports Medicine*, 26(1):72–77, 1998.

A Leardini, JJ O'Connor, F Catani, and S Giannini. Kinematics of the human ankle complex in passive flexion; a single degree of freedom system. *Journal of Biomechanics*, 32:111–118, 1999.

A Leardini, R Stagni, and JJ O'Connor. Mobility of the subtalar joint in the intact ankle complex. *Journal of Biomechanics*, 34:805–809, 2001.

A Lundberg, O K Svensson, G Nemeth, and G Selvik. The axis of rotation of the ankle joint. *Journal of Bone and Joint Surgery*, 71B:94–99, 1989a.

A Lundberg, OK Svensson, G Nemeth, and G Selvik. The axis of rotation of the ankle joint. *Journal of Bone and Joint Surgery*, 71B:94–99, 1989b.

P B C Matthews. Where does Sherrington's "muscular sense" originate? muscles, joints, corollary discharges? *Annual Reviews of Neuroscience*, 5(189-218), 1982.

J D Michelson and C Hutchins. Mechanoreceptors in human ankle ligaments. *Journal of Bone and Joint Surgery Series B*, 77B:219–224, 1995.

K A Payne, K Berg, and R W Latin. Ankle injuries and ankle strength, flexibility, and proprioception in college basketball players. *Journal of Athletic Training*, 32 (3):221–225, 1997.

R J Petrella, P J Lattanzio, and M G Nelson. Effect of age and activity on knee joint

proprioception. *American Journal of Physical Medicine and Rehabilitation*, 76(3): 235–241, 1997.

S Robbins, E Waked, and J McClaran. Proprioception and stability: Foot position awareness as a function of age and footwear. *Age and Ageing*, 24(1):67–72, 1995.

M J Rowinski. Afferent neurobiology of the joint. In J A Gould, editor, *Orthopaedic and Sports Physical Therapy*, pages 49–63. St. Louis: C.V. Mosby, 1990.

G G Simoneau, R M Degner, C A Kramper, and K H Kittleson. Changes in ankle joint proprioception resulting from strips of athletic tape applied over the skin. *Journal of Athletic Training*, 32(2):141–147, 1997.

G G Simoneau, J A Derr, J S Ulbrecht, M B Becker, and P R Cavanagh. Diabetic sensory neuropathy effect on ankle joint movement perception. *Archives of Physical Medicine and Rehabilitation*, 77(5):453–460, 1996.

H B Skinner, R L Barrack, and S D Cook. Age-related decline in proprioception. *Clinical Orthopaedics and Related Research*, 184:208–211, 1984.

CW Spoor and FE Veldpaus. Rigid body motion calculated from spatial co-ordinates of markers. *Journal of Biomechanics*, 13:391–393, 1980.

G J Steele, R A Harter, and A J Ting. Comparison of functional ability following percutaneous and open surgical repairs of acutely ruptured achilles tendons. *Journal of Sport and Rehabilitation*, 2(2):115–127, 1993.

M Stokdijk, CGM Meskers, HEJ Veeger, YA de Boer, and PM Rozing. Determination of the optimal elbow axis for evaluation of placement of prostheses. *Clinical Biomechanics*, 14:177–184, 1999.

M Stokdijk, J Nagels, and PM Rozing. The glenohumeral joint rotation centre in vivo. *Journal of Biomechanics*, 33:1629–1636, 2000.

D G Thelen, C Brockmiller, J A Ashton Miller, A B Schultz, and N B Alexander. Thresholds for sensing foot dorsi- and plantarflexion during upright stance: Effects of age and velocity. *Journal of Gerontology*, 53(1):M33–38, 1998.

H A Thieme, C D Ingersoll, K L Knight, and J C Ozmun. Cooling does not affect knee proprioception. *Journal of Athletic Training*, 31(1):8–11, 1996.

G J Tortora and S R Grabowski. *Principles of Anatomy and Physiology*. HarperCollins, eigth edition, 1996.

AJ van den Bogert, GD Smith, and BM Nigg. *In vivo* determination of the anatomical axes of the ankle joint complex: An optimization approach. *Journal of Biomechanics*, 27(12):1477–1488, 1994.

C G Van den Bosch, M G Gilsing, S G Lee, J K Richardson, and J A Ashton Miller. Peripheral neuropathy effect on ankle inversion and eversion detection thresholds. *Archives of Physical Medicine and Rehabilitation*, 76(9):850–856, 1995.

HEJ Veeger. The position of the rotation center of the glenohumeral joint. *Journal of Biomechanics*, 33:1711–1715, 2000.

FE Veldpaus, HJ Woltring, and LJMG Dortmans. A least-squares algorithm for the equiform transformation from spatial marker co-ordinates. *Journal of Biomechanics*, 21(1):45–54, 1988.

G B Wilkerson and A J Nitz. Dynamic ankle stability: Mechanical and neuromuscular interrelationships. *Journal of Sport and Rehabilitation*, 3(1):43–57, 1994.

HJ Woltring. 3-d attitude representation of human joints: a standardisation proposal. *Journal of Biomechanics*, 27(12):1399–1414, 1994.

G Wu, P Allard, C Kirtley, A Leardini, D Rosenbaum, M Whittle, D D'Lima, L Cristofolini, H Witte, O Schmid, and I Stokes. Letter to the editor. ISB recommendation

on definitions of joint coordinate system of various joints for the reporting of human joint motion - part i: ankle, hip and spine. *Journal of Biomechanics*, 35:543–548, 2002.

B Wyke. Articular neurology - a review. *Physiotherapy*, pages 94–99, 1972.

B D Wyke. The neurology of joints. *Annals of the Royal College of Surgeons of England*, 41:25–50, 1967.

VM Zatsiorsky. *Kinematics of Human Motion.* Human Kinetics, 1998.